Controlling polymer architectures : high-throughput experimentation, tailor-made macromolecules and glycopolymers via "click" reactions

Controlling Polymer Architectures

High-throughput experimentation, tailor-made macromolecules and glycopolymers via "click" reactions

PROEFSCHRIFT

ter verkrijging van de graad van doctor aan de Technische Universiteit Eindhoven, op gezag van de Rector Magnificus, prof.dr.ir. C.J. van Duijn, voor een commissie aangewezen door het College voor Promoties in het openbaar te verdedigen op donderdag 25 juni 2009 om 16.00 uur

door

Caglar Remzi Becer

geboren te Izmir, Turkije

Dit proefschrift is goedgekeurd door de promotoren:

prof.dr. U.S. Schubert
en
prof.dr. J.-F. Gohy

Copromotor:
dr.ir. R. Hoogenboom

Kerncommisie:	prof.dr. U.S. Schubert (Eindhoven University of Technology) prof.dr. J.-F. Gohy (Eindhoven University of Technology) dr.ir. R. Hoogenboom (DWI an RWTH Aachen) prof.dr. M. Sawamoto (Kyoto University)
Overige commissieleden:	prof.dr. S. Kusefoglu (Bogazici University) prof.dr. P.J. Lemstra (Eindhoven University of Technology) dr. M. Schneider (Chemspeed Technologies)

This research has been financially supported by the Dutch Polymer Institute
(DPI project # 502).

Omslagontwerp: C. Remzi Becer and Ayse S. Gursoy Becer
Druk: PrintPartners Ipskamp, Enschede, The Netherlands

Controlling polymer architectures: High-throughput experimentation, tailor-made macromolecules and glycopolymers via “click” reactions / by C. Remzi Becer

A catalogue record is available from the Eindhoven University of Technology Library

ISBN: 978-90-386-1872-2

Controlling Polymer Architectures

High-throughput experimentation, tailor-made macromolecules and glycopolymers via "click" reactions

Aysem'e hediyem.

Table of contents

Chapter 1

Introduction to high–throughput experimentation, tailor made macromolecules and "click" reactions

Abstract

Tailor–made polymers that are designed for a specific function to be used in fields such as nanotechnology and biomaterials require a deep fundamental understanding and knowledge on the structure–property relationships. The use of controlled/"living" polymerization techniques in combination with highly efficient "click" reactions provides an access to well–defined functional macromolecules. These techniques require intensive optimization reactions. Therefore, high–throughput experimentation tools were utilized in order to accelerate the research. Besides, the automated parallel synthesizers are inevitable tools for the preparation of systematic copolymer libraries. In this chapter, an overview on controlled/"living" polymerization techniques, "click" chemistry, and high–throughput experimentation is provided.

Parts of this chapter have been published as review articles: C. R. Becer, U. S. Schubert, *Adv. Polym. Sci.* **2009**, in press; C. R. Becer, R. Hoogenboom, U. S. Schubert, *Angew. Chem. Int. Ed.* **2009**, DOI: 10.1002/anie.200900755.

1.1 Polymer science in the 21st century

Polymers evolved into superb alternative materials to glass, metal, and wood. In the last decades, polymers have not only been used as industrial bulk material but also have attracted great attention in high technology fields, *e.g.* nanotechnology, optics, and biomaterials.[1] Therefore, the syntheses of tailor–made macromolecules with desired molecular design and, consequently, the understanding of the quantitative structure–property relationships (QSPR) have become main focus areas for synthetic chemists. However, if one considers that every single small molecule exhibits different properties depending on their atomic structure, then an enormous number of different micro or macro configurations can be expected in the case of macromolecules. Some important structural parameters can be listed as the monomer composition, chain length, chain ends and side chain functionalities, topology, and architecture. The absolute control over the micro structure of the macromolecules requires the development of well–established synthesis methodologies and exhaustive research to optimize the reaction conditions specific to each monomer, initiator, solvent, or catalyst.

The discovery of controlled/"living" polymerization (CLP) techniques has been realized in the second half of the 20th century. The invention of living anionic polymerization has been reported by Szwarc *et al.* in 1956.[2] This enabled polymer chemist for the first time to gain control over the degree of polymerization (DP), molar mass (M_n), and polydispersity index (PDI). Due to exclusion of the termination process, block copolymers became accessible upon addition of the second monomer after the full consumption of the first monomer batch. In our days, the most complicated structures, *e.g.* pentablock quintopolymers, can be synthesized by living anionic polymerization.[3] Similarly, the cationic polymerization technique was developed and employed for several monomers.[4] The demanding requirements to conduct ionic polymerizations directed synthetic chemists to focus on radical polymerizations. Thus, controlled/"living" radical polymerization (CRP) techniques have been reported in the late 1990s and attracted great attention in different research fields. As illustrated in Figure 1.1, researchers reflected their great interest with the enormous number of publications (>5000) with more than 100,000 citations in less than two decades for the three main CRP techniques, namely, atom transfer radical polymerization (ATRP), nitroxide mediated polymerization (NMP), and reversible addition fragmentation chain transfer polymerization (RAFT).[5]

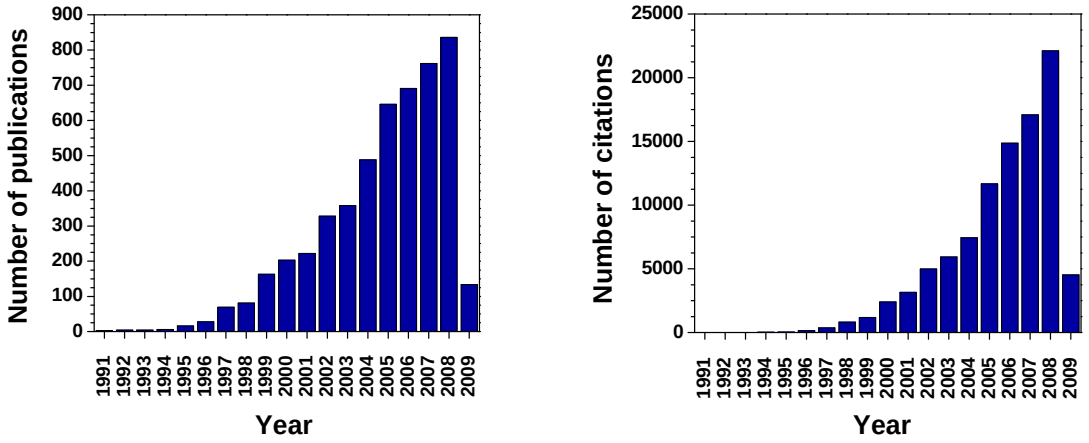

Figure 1.1. Number of publications (*left*) and citations (*right*) in each year for the three main controlled/"living" radical polymerization techniques.[5]

In principle, CRP techniques are based on the delicate balance between dormant and active species. A large variety of different controlling agents or catalysts have been used for every monomer or initiator to obtain well–defined macromolecules. Therefore, intensive optimization reactions need to be performed for each CRP method. Almost all chemical companies established or have access to high–throughput experimentation centers. Nonetheless, in academia only a few polymer laboratories utilize automated parallel synthesizers for the rapid screening and optimization of reactions. The parallel synthesis robots not only accelerate the research speed, but also allow researchers to prepare libraries of compounds under the same experimental conditions with the same handling errors, if there are any. In addition, the analytical instruments developed rapidly in the last decades, enabling fast and accurate analysis of polymers in detail.

Controlling polymer architectures allow to synthesize macromolecules with specific functionalities on the predetermined positions of the chains by using functional initiators, functional monomers, and end cappers. Post polymerization modification reactions are also considered as a successful tool for the synthesis of functional macromolecules that can be reacted with small organic molecules such as proteins or drugs, and also with other macromolecules to yield block copolymers or star–shaped copolymers. There is an enormous interest in the use of these macromolecules not only in the biological applications but also in electronics, and nanotechnology.

In 2001, Sharpless received the Nobel Prize in Chemistry for his work on chirally catalyzed oxidation reactions.[6] In addition, he has introduced the concept of "click" chemistry that is based on highly efficient organic reactions in between two easily accessible functional groups, *e.g.* azides and alkynes. Following this concept, several "click" reactions have been

described in the literature which are employed in medicinal chemistry, biochemistry and materials science. There is no doubt that the growing interest in "click" chemistry will lead researchers to efficiently functionalize their desired tailor–made macromolecules for advanced applications.

The investigations of the latest trends in polymer science form the basis of this thesis. Therefore, we have discussed in the following sections several aspects of CLP techniques including both controlled radical and ionic polymerizations, HTE methodologies applied for the optimization of the polymerization parameters and the synthesis of polymer libraries as well as application of "click" reactions to macromolecules.

1.2 Controlled/"living" polymerization techniques

Starting from 1956, living ionic polymerizations received major interest for the synthesis of well–defined polymers. Szwarc reported that in the anionic polymerizations of styrene the polymer chains grew until all the monomer was consumed; the chains continued to grow upon addition of more monomer.[7] According to the IUPAC definition, ionic polymerization is a type of chain polymerization where the kinetic–chain carriers are ions or ion pairs.[8] However, these techniques have some limitations such as the necessity of extreme purity of the chemicals and the reaction medium, incompatibility between the reactive centers and monomers, and the sensitivity to certain chemical functionalities that limits the monomer selection.

These challenges stimulated researchers to discover or develop alternative polymerization techniques. One of the alternative polymerization routes is radical polymerization since it is less discriminating regarding the types of polymerizable vinyl monomers and more tolerant to several functionalities. The most common method is the free radical polymerization, which results in polymers with broad molar mass distributions. Indeed, polymers with relatively high polydispersity indices may be of advantage in industrial processing. For instance, low molar mass polymer chains in polymers with broad molar mass distributions provide a plasticizing effect during processing. However, these ill–defined polymers are not suited for advanced applications and might complicate the development of structure–property relationships.

As a consequence of the free radical polymerization kinetics, the termination rates are extremely fast in comparison to the slow initiation rates. This results in the formation of high molar mass chains at the initial stage of the polymerization and decreasing molar masses in the latter stages due to the decrease in the monomer concentration. Under these circumstances

broad molar mass distributions are inevitable. There were several attempts to gain better control on the free radical polymerization process.[9,10] One of these methods was named as "iniferter" method. The compounds used in this technique can serve as *ini*tiator, trans*fer* agent and *ter*minating agent.[11–13] Another technique is based on the use of bulky organic compounds such as diaryl or triarylmethyl derivatives.[14–16] The main disadvantages of these systems include slow initiation, slow exchange, direct reaction of counter radicals with monomers, and their thermal decomposition. Therefore, these techniques did not offer the desired level of control over the polymerization processes.

Relatively new controlled radical polymerization methods, which were discovered in the mid 1990's, focused on establishing a precise equilibrium between active and dormant species. Three approaches, namely atom transfer radical polymerization (ATRP),[21,22] nitroxide mediated radical polymerization (NMP)[17,18] and reversible addition fragmentation chain transfer polymerization (RAFT),[19,20] out of several others, have attracted the most attention due to their relative simplicity and their success to introduce relatively stable chain end functionalities that can be reactivated for subsequent block copolymerizations or post polymerization modifications.

1.2.1. Atom transfer radical polymerization

ATRP has become the most widely applied CRP technique due to the simple synthetic procedure and commercially available reagents. This technique was first reported by both Sawamoto and Matyjaszewski in 1995.[21,22] The polymerization mechanism is based on the reversible redox reaction between alkyl halides and transition metal complexes.

The ATRP proceeds via reversible activation of carbon–halogen terminals by a metal complex, where the metal center undergoes a redox reaction via interaction with the halogen atom at the polymer terminal, as depicted in Scheme 1.1. The reaction is usually initiated by the activation of the carbon–halogen bond of an appropriate alkyl halide (R–X) in form of a homolytic cleavage via one–electron oxidation of the metal center (M_t^n/Ligand) to yield an initiating radical species (R·) and an oxidized metal compound (M_t^{n+1}/Ligand). The radical reacts with the halogen on the oxidized metal complex to regenerate R–X or adds to the monomer to generate oligomeric structures. Depending on the deactivation rates, after a short period of time the radical is transformed into a dormant species via abstraction of a halogen atom from M_t^{n+1}/Ligand. The carbon–halogen bond of the dormant species is subsequently activated by the metal complex, similarly to R–X, to result in a similar carbon–halogen bond at the polymer terminal via a repetitive set of the reactions. The key factors for these reactions are the low concentration of the radical intermediates at a given time and their fast but

reversible transformation into the dormant species before undergoing successive addition to monomers.

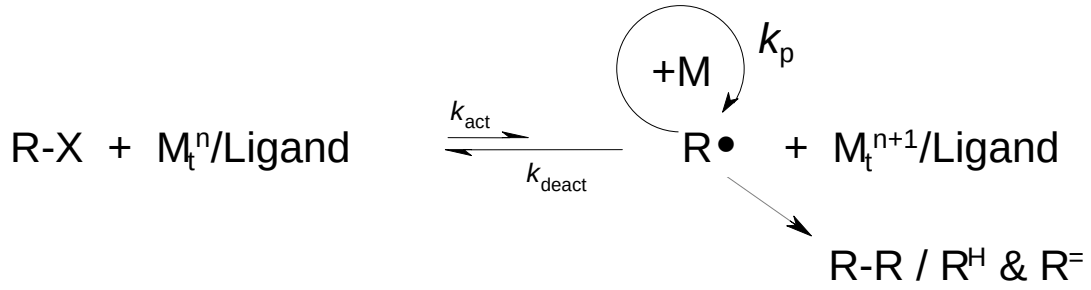

Scheme 1.1. Proposed mechanism for atom transfer radical polymerization.

The rate of ATRP depends on the value of the ATRP constants for activation and deactivation (eq 1). The polydispersity index (M_w/M_n) of the polymers obtained depends on the ratio of the propagation rate constant (k_p) to the deactivation rate constant (k_{deact}), the concentration of the deactivator X–$Cu^{II}Y/L_n$ (denoted as [Cu^{II}]), the concentration of the initiator ([RX]), monomer conversion (p), and the targeted degree of polymerization (DP_n) (eq 2). The activation rate constant (k_{act}) has been extensively examined in the literature.[23–36] Direct determination of k_{deact} is more challenging. On the other hand, values of k_{deact} can be calculated from the equation $k_{deact} = k_{act}/k_{ATRP}$ if values of both k_{act} and k_{ATRP} are known. Therefore, the determination of the k_{ATRP} values is very crucial. The rate of polymerization of a given monomer depends on the value of kp and on the radical concentration ([Pm·]), which is determined by k_{ATRP}. Thus, the evaluation of k_{ATRP} is crucial for a deeper understanding of this catalytic system and for optimal catalyst selection, in particular for newly developed ATRP systems that use low concentrations of the catalyst Cu^IY/L_n, *e.g.* [Cu^I] on the order of ppm.

$$\ln\left(\frac{[M]_0}{[M]_t}\right) = \frac{k_p\, k_{ATRP}[P_mX][Cu^I]}{[Cu^{II}]}t \qquad (1)$$

$$\frac{M_w}{M_n} = 1 + \frac{1}{DP_n} + \left(\frac{k_p([RX]_0 - [RX])}{k_{deact}[Cu^{II}]}\right)\left(\frac{2}{p} - 1\right) \qquad (2)$$

Ligands that are used to stabilize the metal salt have a critical importance in ATRP. Therefore, a comparison chart for the nitrogen based ligands has been reported by Matyjaszewski *et al.*[30] Activation rate constants (k_{act}) with EtBriB are shown in Figure 1.2. These values were measured directly or extrapolated and arranged in a logarithmic scale for a better comparison of activities of Cu complexes with various ligands. It should be noted that

extrapolated values may underestimate the values of k_{act} for active complexes. Indeed, the catalysts become more active when its Cu(II) state is better stabilized by the ligand, according to electrochemical studies.[37,38] In general, tetradentate ligands form the most active complexes, in particular Cyclam–B, in which the ethylene linkage further stabilizes the Cu(II) complex. Complexes with branched tetradentate ligands produce the most active catalysts; *e.g.*, Cu(I)Br/Me_6TREN, Cu(I)Br/Me_6TPMA, and also Cu(I)Br/Cyclam–B are the three most active complexes in Figure 1.2. This maybe associated with a small entropic penalty in ligand rearrangement from Cu(I) to Cu(II) state.[39] Cyclic ligands are located in the middle of the scale, indicating normal activities when forming a Cu complex. Most of the linear tetradentate ligands are placed at the left side of the scale, except BPED. Tridentate ligands, *e.g.* PMDETA and BPMPA, form fairly active complex. All bidentate ligands are located at the left side of the scale, forming the least active ATRP complexes.

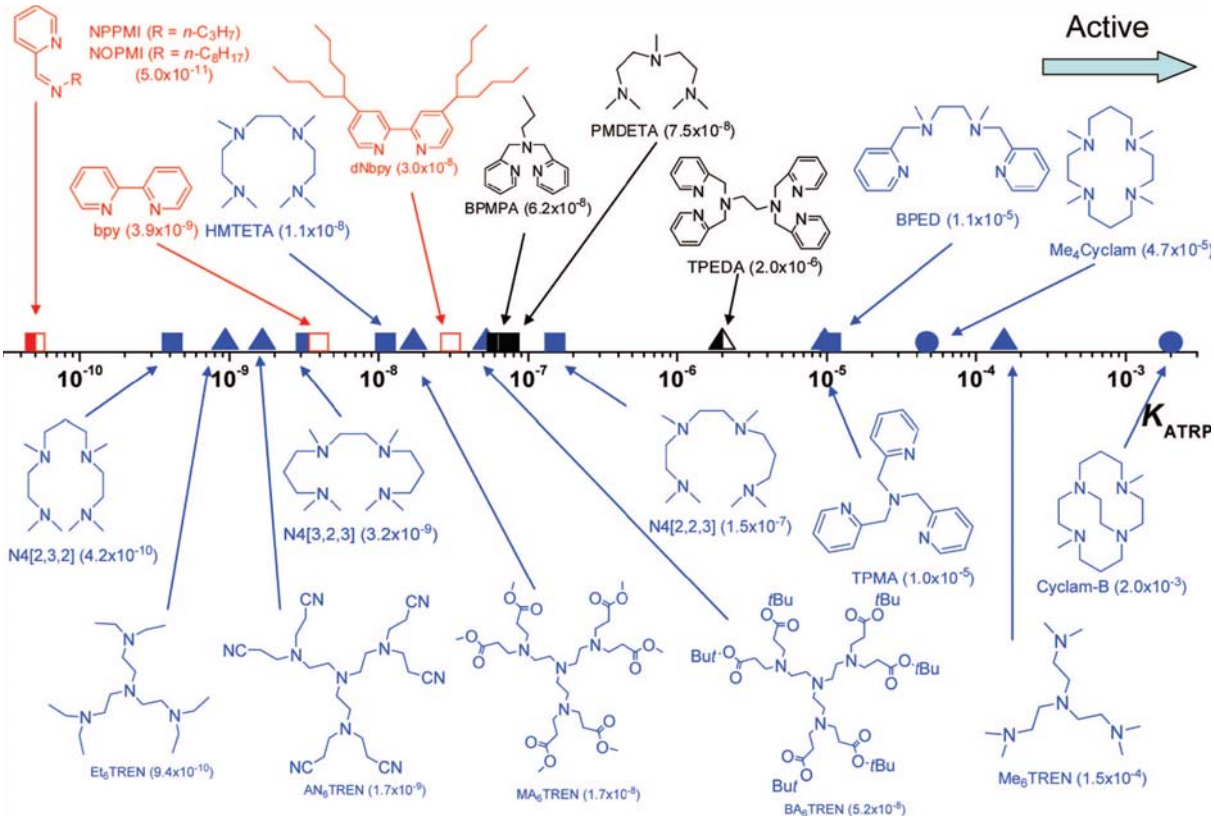

Figure 1.2. ATRP activation rate constants for various ligands with EtBriB in the presence of $Cu^{I}Y$ (Y = Br or Cl) in MeCN at 35 °C: N2, red; N3, black; N4, blue; amine/imine, solid; pyridine, open. Mixed, left–half solid; linear, □; branched, ▲; cyclic, ● (Reprinted from reference 30).

The differences in activity for the resulting complexes exceed 1 million times. The general order of activities of Cu complexes is related to their structure and follows the following order: tetradentate (cyclic–bridged) > tetradentate (branched) > tetradentate (cyclic) > tridentate > tetradentate (linear) > bidentate ligands. The nature of the N atoms is also

important and follows the order pyridine ≥ aliphatic amine > imine. Ethylene is a better linkage for N atoms in the ligand than propylene. The activities of the Cu complexes strongly depend on the ligand structures, and even small structural changes may lead to large differences in their activity.

The interest to develop more active or functional catalysts led us to conduct a piece of work in this field. We have introduced a pegylated tetradentate amine ligand (*N,N,N′,N″,N‴,N‴*,–hexaoligo(ethylene glycol) triethylenetetramine, HOEGTETA) for the ATRP of methyl methacrylate. The initial motivation was the solubility difference between the ligand and the obtained polymer due to the oligo(ethylene glycol) substituents. Unexpected results were obtained during the examination of different ratios of CuBr and $CuBr_2$, which are discussed in Chapter 4.

ATRP is a versatile method which is widely applied in solution as well as on surfaces. Growing well–defined polymer brushes that are tethered on the surface is not a challenge anymore. We have contributed in the nanotechnology field by synthesizing polystyrene brushes on electrochemically patterned surfaces (Chapter 4). "Grafting from" the chemically active surface templates was performed using HOEGTETA as ligand. Moreover, block copolymerization using *tert*–butyl acrylate as the second monomer was demonstrated.

1.2.2. Nitroxide mediated radical polymerization

Nitroxide mediated radical polymerization (NMP) is one of the most environmentally friendly CRP techniques and has a relatively simple polymerization mechanism since there is no need for a catalyst. Solomon, Rizzardo and Moad have demonstrated the reaction between 2,2,6,6–tetramethylpiperidinyloxy (TEMPO) and vinyl monomers in the range of the free radical polymerization temperature (40 to 60 ºC).[40] Since then, two different NMP concepts have been developed, namely the bimolecular and the unimolecular process, respectively. Georges *et al.* described the bimolecular process for the preparation of low PDI value polystyrenes initiated by benzoylperoxide and mediated by TEMPO.[41] The bimolecular process is based on a radical source, *e.g.* peroxides, azo initiators or photo initiators, and mediating nitroxide compounds. Following to that, unimolecular initiators have been developed that have a similar concept to well–defined initiators in living anionic and cationic procedures.[42] In unimolecular processes, both the initiator and the mediator are combined in a single molecule (*e.g.* alkoxyamines) that also simplifies the polymerization kinetics. In general the initiating group of the alkoxyamine is identical to the monomer structure. Hawker and his coworkers exploited this method and named the compounds as "unimer" to describe these initiators.[43] The difference between the rates of initiation and propagation is minimized,

which greatly affects the overall kinetics of the polymerization. Therefore, the use of alkoxyamines allows the greatest degree of control over the final polymeric structure with well–defined functional end groups.

The investigation on stable free nitroxide compounds were started with TEMPO and extended to several different types of nitroxide containing compounds, such as phosphonate derivatives[44] or arenes.[45] However, TEMPO is among the first cyclic counter radicals and it is efficient for styrene polymerization at elevated temperatures (*e.g.* 120 °C). Later, a new type of non cyclic β–hydrogenated nitroxides, called SG1, was introduced by Tordo.[46] These new radicals controlled the polymerization of styrene and acrylate monomers at temperatures above 80 °C. The reaction of SG1 and acrylic acid results in the formation of very efficient alkoxyamine called Bloc Builder™, which is currently a commercial initiator from Arkema.[47] The structures of Bloc Builder™, SG1 and the proposed unimolecular NMP process are illustrated in Scheme 1.2.

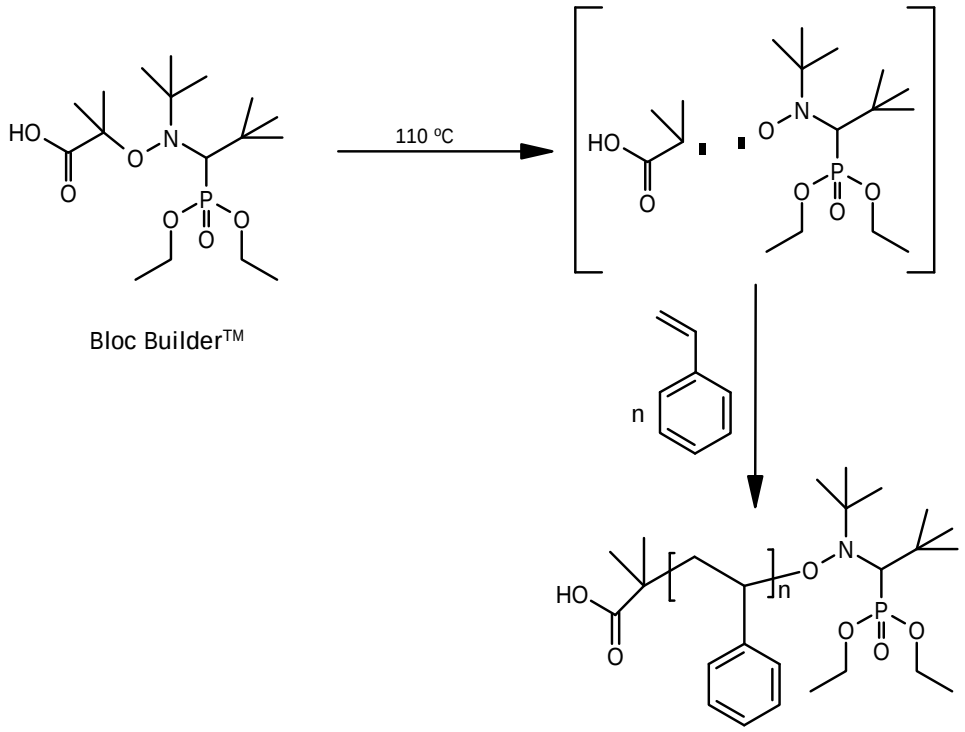

Scheme 1.2. Schematic representation of the proposed mechanism of the unimolecular NMP of styrene initiated by Bloc Builder™.

Polymerization of methacrylates was only possible using the selected nitroxide compounds exclusively devoted to methacrylates.[48] However, SG1–mediated polymerization of methyl methacrylate (MMA) and methacrylic acid (MAA) has been reported in the presence of small amounts of styrene (<10%).[49–51] High conversions could be reached by using Bloc Builder as initiator. Addition of styrene resulted in a dramatic reduction of the

concentration of propagating radicals leading to a decrease of the irreversible termination rate. This method favored the formation of a methacrylate–styrene–SG1 terminal sequence that is able to dissociate into a propagating radical and a free nitroxide at low temperatures (<90 °C). Moreover, Nicolas *et al.* reported the synthesis of poly(oligo(ethylene glycol) methacrylate)s in ethanol by addition of styrene (8.8 mol %).[52]

In this thesis, we have investigated the effect of some important reaction parameters on the NMP of various monomers. For instance, we have screened the effect of polymerization temperature for styrene (St) as well as *tert*–butyl acrylate (*t*–BA) and accordingly optimized the concentration of additional SG1. Following to these rapid optimization reactions, we have prepared a small library (3×3) of St and *t*–BA block copolymers, which is explained in more detail in Chapter 2.

We have also focused on the preparation of thermoresponsive copolymer libraries based on hydroxypropyl acrylate. For this purpose, we utilized an automated parallel synthesizer for optimizing the homopolymerizations of 2–hydroxypropyl acrylate (HPA), *N*–acryloyl morpholine (Amor), and *N,N*–dimethyl acrylamide (DMAc). Optimum reaction parameters were determined for all three monomers. Libraries of p(Amor–*stat*–HPA) and p(DMAc–*stat*–HPA) were synthesized with 0 to 100 mol % HPA with 10 mol % HPA increments using the optimized conditions obtained from the homopolymerizations. Additionally, thermal properties and solution properties of these copolymer libraries were investigated in detail (Chapter 2).

1.2.3. Reversible addition–fragmentation chain transfer polymerization

The first RAFT polymerization using thiocarbonylthio compounds was reported by the Common Wealth Scientific and Industrial Research Organization (CSIRO) in 1998.[20] Subsequently, another group reported a similar mechanism using xanthate RAFT agents; they named this technique as MADIX.[53,54] The RAFT polymerization has several advantages over other CRP techniques. The most significant advantage is the compatibility of the technique with a wide range of monomers, such as styrene, acrylates, methacrylates and derivatives. This large number of monomers provides the opportunity of creating well–defined polymer libraries by the combination of different monomeric units.

The mechanism of the RAFT polymerization comprises a sequence of addition–fragmentation processes as shown in Scheme 1.3. The initiation and radical–radical termination reactions occur as in conventional free radical polymerization. This is followed by the addition of the propagating species (A) to the chain transfer agent (CTA), which leads to the formation of an intermediate species (B). Subsequently, a new radical (D) can be released

to form new propagating chains (E). In step IV, rapid equilibrium between active propagating radicals and the corresponding dormant species provides equal probability for all chains to grow and allows for the preparation of polymers with low PDI values. Termination reactions occur via combination or disproportionation (step V) to some extent, but can be largely eliminated by maintaining appropriate conditions that control the apparent radical concentration.

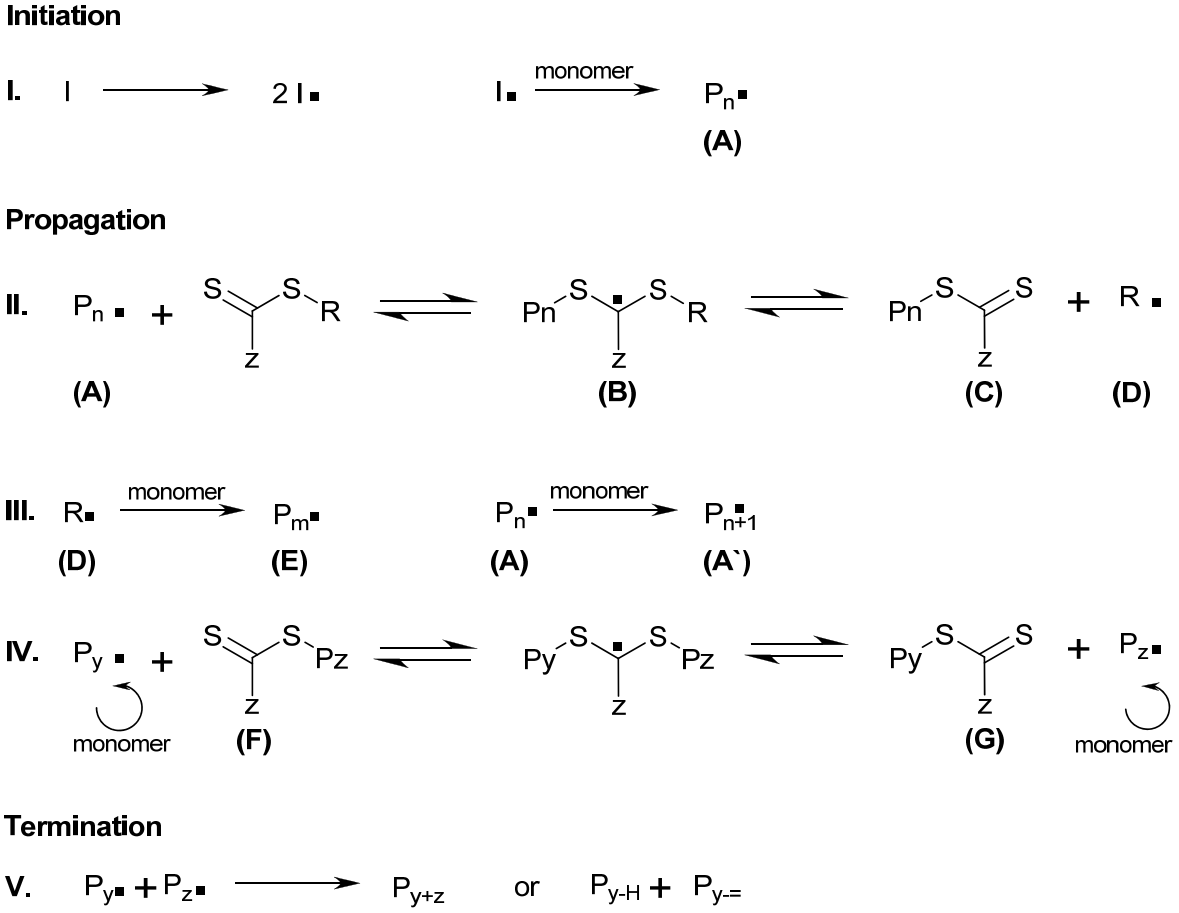

Scheme 1.3. Schematic representation of the mechanism of the RAFT polymerization.

RAFT polymerizations can be performed for a wide range of monomers in a large variety of solvents.[55–56] In comparison to other radical polymerization processes, RAFT is highly tolerant to functional groups. Furthermore, functional end groups can be introduced by incorporation in either the initiator moiety or in the RAFT agent. The latter methodology can have some limitations, since the nature of the functional groups substantially influences the stability of the dithioester radical intermediate. Strong radical stabilizing groups will favor the formation of this dithioester radical intermediate, which enhances the reactivity of the S=C bond toward radical addition. However, the stability of the intermediate requires adjustment to promote fragmentation that liberates the reinitiation group.

We have used the RAFT polymerization technique to synthesize methacrylic acid and oligo(ethylene glycol) methacrylate containing thermoresponsive homopolymer and copolymer libraries. Therefore, the Chemspeed Accelerator SLT106™ was utilized for the rapid synthesis of libraries of polymers. Subsequently, turbidimetry measurements were performed in parallel to screen the aqueous phase transition behavior of polymers upon the temperature change at different pH values. Not only the lower critical solution temperature (LCST) behavior of the polymers but also the water uptake behaviors of various classes of hydrophilic polymers were investigated in detail. As expected, thermoresponsive polymers exhibited hydrophilic behavior below their LCST and hydrophobic behavior above their LCST.

RAFT polymerization of various monomers has been performed in automated parallel synthesizers for several years in our group. By taking the advantage of this experience, we have developed a standard protocol for the parallel optimization of RAFT polymerization conditions using an automated parallel synthesizer. We believe this protocol will provide the basic knowledge to start the HTE cycle; moreover, it discusses the typical limitations and considerations that one should take into account before hand. These investigations form the basis of Chapter 3.

1.2.4. Cationic ring opening polymerization

The living cationic ring–opening polymerization (CROP) of 2–ethyl–2oxazoline (EtOx) was first described in literature in 1966.[57–59] Ever since, the biocompatible and hydrophilic poly(2–ethyl–2–oxazoline)s have been used for a broad range of applications.[60,61] The living character of the polymerization provides easy access to block copolymers by sequential addition of different monomers and functional end–groups by using functional initiators or terminating agents.[62] By chain extending the hydrophilic poly(2–ethyl–2–oxazoline) (P(EtOx)) with a hydrophobic block, amphiphilic structures can be obtained.[63–67]

The acetyl halide initiated reaction mechanism for the cationic ring–opening polymerization of 2–ethyl–2–oxazoline is depicted in Scheme 1.4. The polymerization is initiated by the electrophilic acetyl halide forming the cationic oxazolinium ring. The C–O bond in the oxazolinium ring is weakened and the polymerization propagates by nucleophilic attack of the next monomer onto this carbon atom. Block copolymers can be potentially synthesized by adding a second monomer when all initial monomer is consumed or the polymerization can be terminated by adding a nucleophile (terminating agent). If chain transfer and chain termination can be excluded, the polymerization proceeds in a living

manner. In this case, the concentration of propagating species is constant and the polymerization should proceed via first order kinetics.

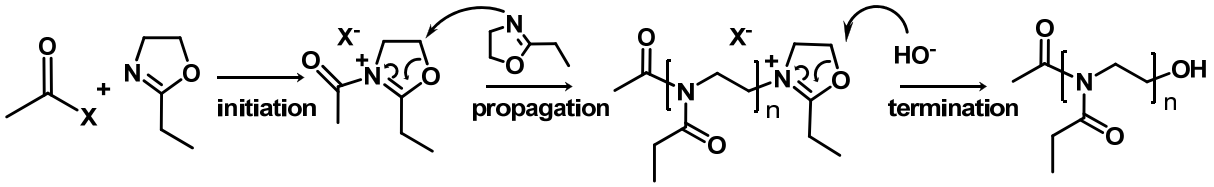

Scheme 1.4. Schematic representation of the acetyl halide initiated CROP of 2–ethyl–2–oxazoline.

The polymerization kinetics for the cationic ring–opening polymerization of 2–oxazolines with many initiators were already investigated by a number of groups.[68– 73] Most commonly, tosylate and triflate derivatives are used as initiators.[74] Moreover, some research groups focused on using bifunctional and multifunctional initiators in order to combine CROP of oxazolines with nitroxide mediated radical polymerization, with anionic ring opening polymerization or with other radical polymerization techniques.[75,76] The use of acetyl chloride and methacryloyl chloride as initiator for the CROP of 2–methyl–2–oxazoline and 2–phenyl–2–oxazoline was demonstrated with and without addition of silver triflate or potassium iodide to accelerate the polymerizations.[77] However, the use of different acetyl halides as initiators for the CROP of 2–oxazolines has not been reported to the best of our knowledge.

We have performed kinetic investigations on the cationic ring–opening polymerization of 2–ethyl–2–oxazoline using acetyl chloride, acetyl bromide, and acetyl iodide as initiators. Various polymerization temperatures ranging from 80 °C to 220 °C were applied under microwave irradiation. The resulting polymerization mixtures were characterized with gas chromatography (GC) and gel permeation chromatography (GPC) for the determination of monomer conversion and molar mass distribution, respectively. Well–defined polymers with narrow molar mass distributions were obtained with all three initiators. Moreover, the polymerization rates (k_p) for the cationic ring–opening polymerization of 2–ethyl–2–oxazoline were compared using the three different halides as counter ion. These investigations on the CROP of EtOx will be discussed in detail in Chapter 5.

1.3 High–throughput experimentation in polymer science

The growing economies and developments in the communication and marketing fields expanded the market demand for novel materials with superb properties. Both chemical companies and scientists of universities should intensify their research to accelerate new inventions and products. The research and development departments of large companies

started up their own high–throughput experimentation (HTE) research centers or got access to contract based HTE centers.[78] Commercialization of automated synthesis platforms enabled the academic research groups to conduct accelerated research as well.[79]

CRP techniques provide successful synthesis of well–defined polymers with different compositions, topologies, and architectures. However, the polymerization parameters need to be optimized to obtain the desired structures. Therefore, screening different reaction parameters, while keeping the rest of the conditions constant, is crucial for understanding the reaction kinetics and investigating structure–property relationships. For these purposes, Chemspeed automated parallel synthesis robots were utilized extensively during this Ph.D. thesis. As depicted in Figure 1.3, the Chemspeed Accelerator™ SLT106 has a very flexible working platform. It contains modular units, *e.g.* parallel reactors, sample racks, stock solution racks, reservoir bottles, which can be positioned according to the needs. Besides, the robotic arm can operate different modules, *e.g.* a 4–needle head (4–NH) and a solid dosing unit (SDU), to handle transfers with high operation speed and accuracy. Different types of reactor blocks, *e.g.* an individually heatable reactor block, or a pressure reactor block, enable to conduct reactions at different reaction temperatures in each reactor or under pressurized conditions.

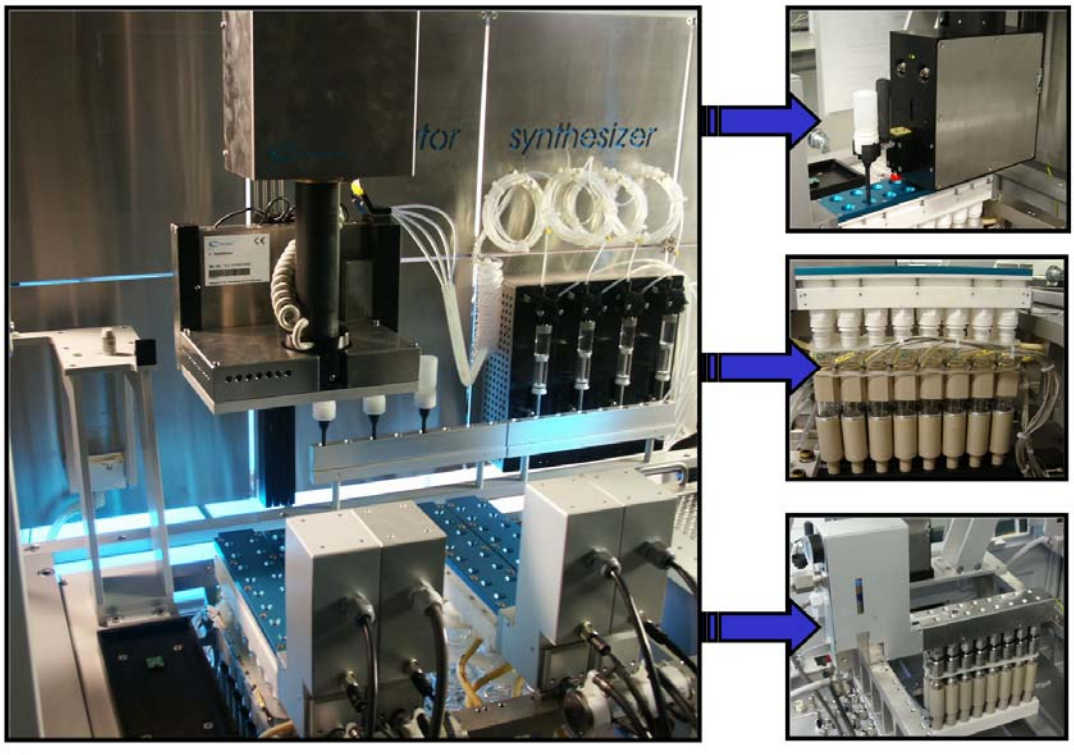

Figure 1.3. Chemspeed Accelerator SLT106™ parallel synthesis robot. Solid dosing unit, individual heater reactor block and pressure reactor block (from right top to bottom).

Researchers have already invested several decades to elucidate the effect of input variables on the polymerization kinetics and the resulting polymer structures. Many research groups devoted their resources to obtaining reproducible data on polymerization kinetics. One of the methods to achieve that is to conduct several experiments in parallel to keep most reaction inputs constant and to minimize unpredictable environmental effects. In this regard, it appeared to be necessary to apply automated parallel synthesis platforms and standardized experimental protocols in order to provide extended and comparable data sets within a short period of time. Controlled radical polymerizations, including reversible addition fragmentation chain transfer (RAFT) polymerization,[20,80] atom transfer radical polymerization (ATRP)[21,81] and nitroxide–mediated radical polymerizations (NMP), were performed successfully in a high–throughput manner.

1.3.1 HTE applied to controlled radical polymerizations

The current simplicity of the controlled polymerization reactions are the result of intense research carried out by several groups on the importance and the fundamentals of each parameter. In particular, Matyjaszewski *et al.* have spent great effort on the construction of numerous comparison charts on the activity of initiators and ligands that are used in ATRP.[82,83] These published comparison tables represent the summary of hundreds of single experiments and represent now a very important and reliable source of data for the ATRP technique. However, this amount of data could also be obtained in relatively shorter time periods using HTE tools. In the case of NMP, several groups investigated the mechanism and the use of different nitroxide compounds. The most cited up to date review on NMP is published by Hawker *et al.* in 2001.[17] Besides, Benoit and Hawker *et al.* developed one of the most efficient free nitroxide compounds, namely TIPNO.[45] Moreover, Braslau *et al.* had an important contribution on the nitroxide decomposition and design.[84] The RAFT polymerization technique has been developed in CSIRO by Moad, Rizzardo, Thang and their co–workers. They have performed the polymerization of various monomers in both organic and aqueous medium with several dedicated RAFT agents. In the following of this section, only a few selected examples will be highlighted rather than providing a complete overview of HTE in controlled radical polymerizations.

One representative example on the high–throughput screening of ATRP parameters was reported by Schubert *et al.* [85] ATRP of methyl methacrylate was successfully applied for the rapid screening and optimization of a range of reaction conditions. A set of 108 different reactions was designed for this purpose. Different initiators and different metal salts have been used, namely ethyl–2–bromo–isobutyrate, methyl–2–bromopropionate, (1–bromoethyl)

benzene, and *p*–toluene–sulfonylchloride, and CuBr, CuCl, CuSCN, $FeBr_2$, and $FeCl_2$, respectively. 2,2`–Bipyridine and its derivatives were used as ligands. The high–throughput experimentation of ATRP of MMA was carried out in a Chemspeed ASW2000 automated synthesizer to rapidly screen and to optimize the reaction conditions. Two reactor blocks were used in parallel and each block consisted of 16 reaction vessels equipped with a double jacket heater. The typical layout of the automated synthesis platform is illustrated in Figure 1.4. There are several locations for the reactor blocks in the platform and most commonly one or two blocks are used in parallel in order to keep the high–throughput workflow running without any bottle–necks. The stock solution rack is equipped with an argon inlet to keep the stock solutions under inert conditions. A solid phase extraction (SPE) unit, which is equipped with alumina oxide columns, is used to remove the metal salt from the aliquots. The samples intended for characterization are transferred into small vials arranged in racks and the racks are transferred to the autosampler of the analytical instruments, such as gas chromatography (GC) or gas chromatography coupled with mass spectrometry (GC–MS), or size exclusion chromatography (SEC). In addition, there is an injection port for online SEC measurements. The technical details and further explanation on the automated parallel synthesizer can be found in several reviews.[86 –91]

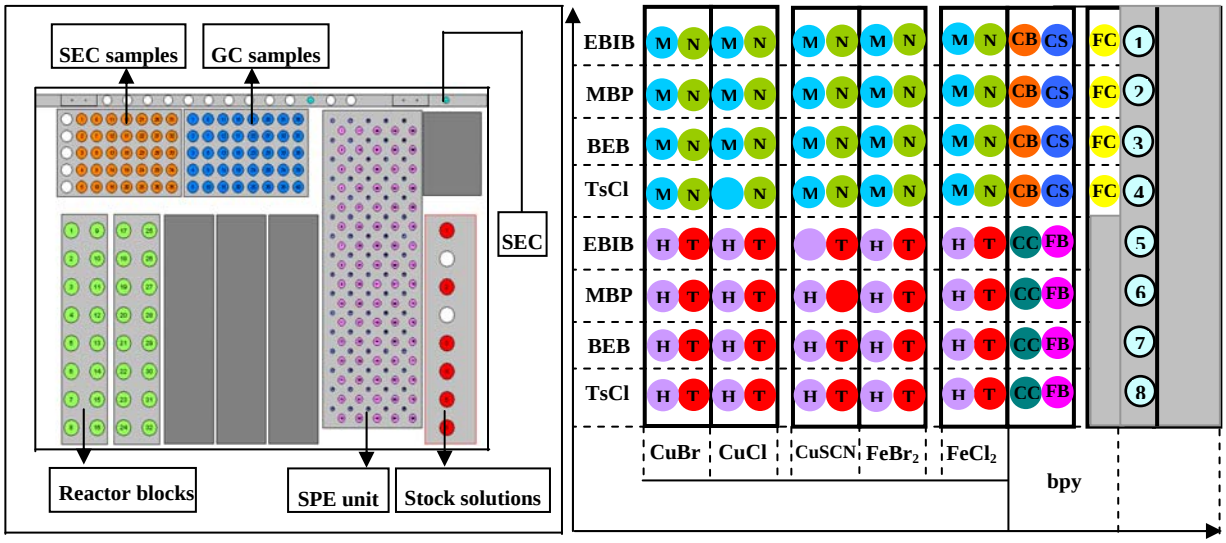

Figure 1.4. Representation of the automated synthesizer and combinations of metal salts, initiators and ligands used in this study. The symbols used in this figure are as follows: dMbpy, M; dHbpy, N; dTbpy, T; CuBr, CB; CuCl, CC; CuSCN, CS; $FeBr_2$, FB; $FeCl_2$, FC; CuBr + ligand + TsCl (ligand = 4,5'–dMbpy, 1; 5,5'–dMbpy, 2; 4Mbpy, 3; and 6Mbpy, 4), and CuCl + ligand + TsCl (ligand = 4,5'–dMbpy, 5; 5,5'–dMbpy, 6; 4Mbpy, 7; and 6Mbpy, 8).

It should be noted that the computer–based planning and robotic performing of the reactions as well as the utilization of fast characterization techniques dramatically decreased the required research time for the designed library from several months to two weeks. The

obtained experimental results could be compared and used for elucidation of structure–property relationships of monomer, initiator, and catalytic systems since all the reactions were carried under the same conditions.

Three main parameters were used to evaluate the efficiency of the polymerization, namely monomer conversion (C_{MMA}), initiation efficiency of the reaction ($f = M_{n,theo}/M_{n,SEC}$), and polydispersity index. These results are depicted in Figure 1.5. It is obvious that the Cu(I)–catalyzed systems are more effective than the Fe(II)–catalyzed systems under the studied conditions. It was concluded that a bipyridine based ligand with a critical length of the substituted alkyl group (*e.g.*, dHbpy) shows the best performance in Cu(I)–mediated systems. Besides, Cu(I) halide–mediated ATRP with 4,5'–Mbpy as the ligand and TsCl as the initiator was better controlled than that with dMbpy as the ligand, and polymers with much lower PDI values were obtained in the former case.

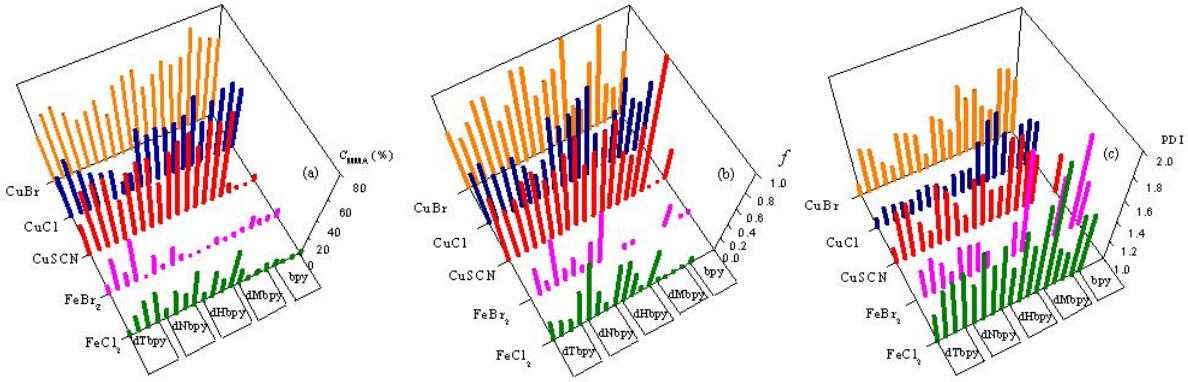

Figure 1.5 Effects of metal salts, ligands and initiators on (*left*) C_{MMA}'s, (*middle*) *f*, (*right*) PDI values of the polymers in the ATRP of MMA in *p*–xylene at 90 °C. $[MMA]_0$:$[initiator]_0$:$[metal\ salt]_0$:$[ligand]_0$ = 150:1:1:2, MMA/*p*–xylene = 1:2 v/v. EBIB, MBP, BEB, and TsCl were used as initiator from right to left in each ligand column, respectively (reprinted from reference 85).

Some of the most important critical points in RAFT polymerizations are the relative concentrations of the free radical initiator, the chain transfer agent, and the monomer, since these will establish the delicate balance between the dormant and active species. However, initially the reproducibility of the RAFT polymerization in an automated synthesizer was investigated.[92] Therefore, the same polymerization was performed in 16 reactors in parallel. The characterization of the obtained polymers was performed by SEC as well as MALDI TOF MS and revealed comparable results. The polymers had narrow polydispersity indices with the predetermined molar masses. Besides, the end group characterization of the polymers was performed by automated MALDI TOF MS measurements and confirmed the presence of dormant polymer chains. This is also clearly demonstrated by chain extension reactions. Following to that, temperature optimization reactions were performed utilizing an individually

heatable reactor block. Acrylate and methacrylate derivatives can be successfully polymerized using 2–cyano–2–butyl dithiobenzoate (CBDB) as a CTA. However, the amount of free radical initiator (azobisisobutyronitrile (AIBN) is used in general) to CTA determines the control over the polymerization. Schubert *et al.* reported the RAFT polymerization of 8 different acrylates or methacrylates with different ratios of CTA to AIBN.[93] The structures of the monomers and the design of the experiment are shown in Figure 1.6. A reactor block consisting of 16 reactors was divided into four zones with four different CTA to initiator ratios, and four different acrylates or methacrylates were used in each set of experiment. The polymerization of *tert*–butyl methacrylate was repeated four times to demonstrate the reproducibility of the polymerization in an automated parallel synthesizer. Structural analysis of the polymers revealed that there was less than 10% deviation in the number average molar mass and the PDI values.

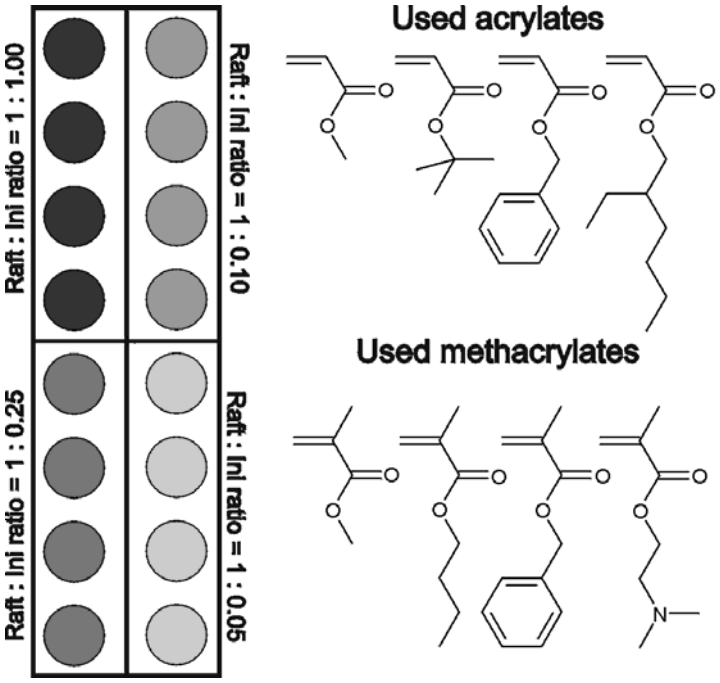

Figure 1.6. Schematic representation of the design of experiment and the structures of the used (meth)acrylates (reprinted from reference 93).

The polymerization of four different acrylates at four different CTA to initiator ratios are shown in Figure 1.7 as representative example. The increased ratio of CTA to AIBN resulted in improved PDI values; however, there is a decrease observed in the number average molar masses of the polymers. All polymerizations were conducted at 70 °C for 10 hours. Due to the different initiator concentrations the rate of polymerization differs and a significant decrease occurs in the molar mass for a certain reaction time. Nevertheless, this systematic study not only proved the reproducibility of the RAFT polymerization of several

(meth)acrylates but also provided the optimum ratio of CTA to initiator to be used in further reactions.

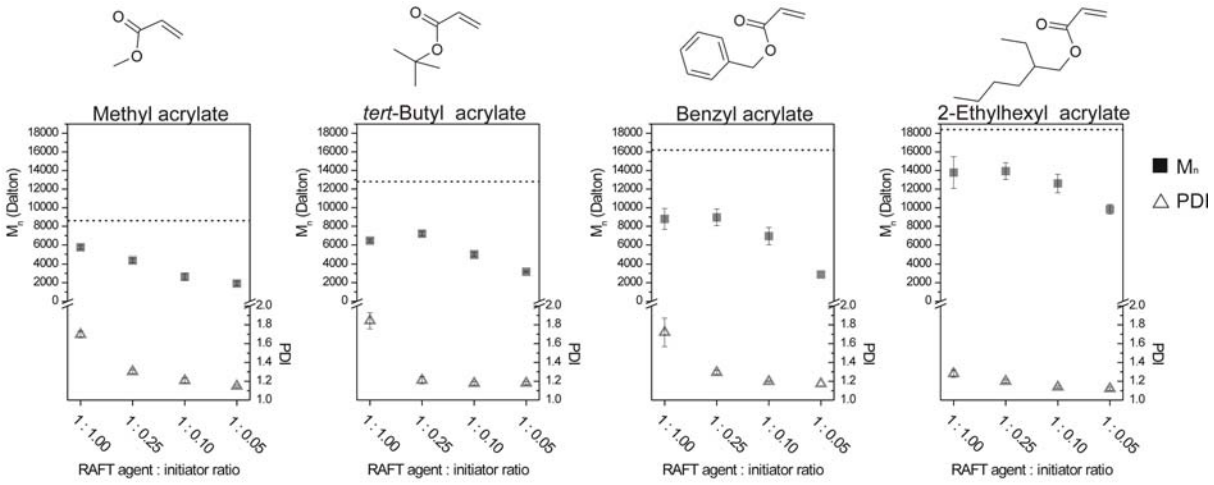

Figure 1.7. M_n and PDI values *versus* CTA to AIBN ratio plots for different acrylates (reprinted from reference 93).

1.3.2 HTE applied for the cationic ring opening polymerization

The alkyl group attached at the 2 position of 2–oxazoline provides extraordinary possibilities for variations in the polymer structure and the properties. This monomer family is a good candidate for high–throughput experimentation and allows creating different copolymer libraries by a combination of 2–oxazolines with different side groups. However, the typical required polymerization times for this type of monomer were previously in the range of 10 to 20 hours. Nevertheless, the reaction time for 2–ethyl–2–oxazoline in acetonitrile could be reduced from 6 hours under standard conditions (oil bath heating, reflux at 82 °C) to less than 1 minute (at 200 °C) under microwave irradiation. Thus, a high–throughput experimentation workflow could be applied for the CROP of 2–oxazolines. Several reaction parameters, such as temperature, pressure, and solvent were investigated under microwave irradiation and using automated parallel synthesizers.[94 –97]

The living CROP of 2–methyl, 2–ethyl, 2–nonyl, and 2–phenyl–2–oxazolines were investigated at different temperatures in the range of 80 to 200 °C using a single mode microwave synthesizer.[98] The reaction rates were enhanced by a factor of up to 400. The livingness of the polymerization over the whole range of polymerization temperatures was examined by following the first–order kinetics of the monomer consumption. The semi–logarithmic kinetic plots for MeOx, EtOx, NonOx and PhOx are shown in Figure 1.8. All reactions show a linear increase, which is an indication of a living polymerization.

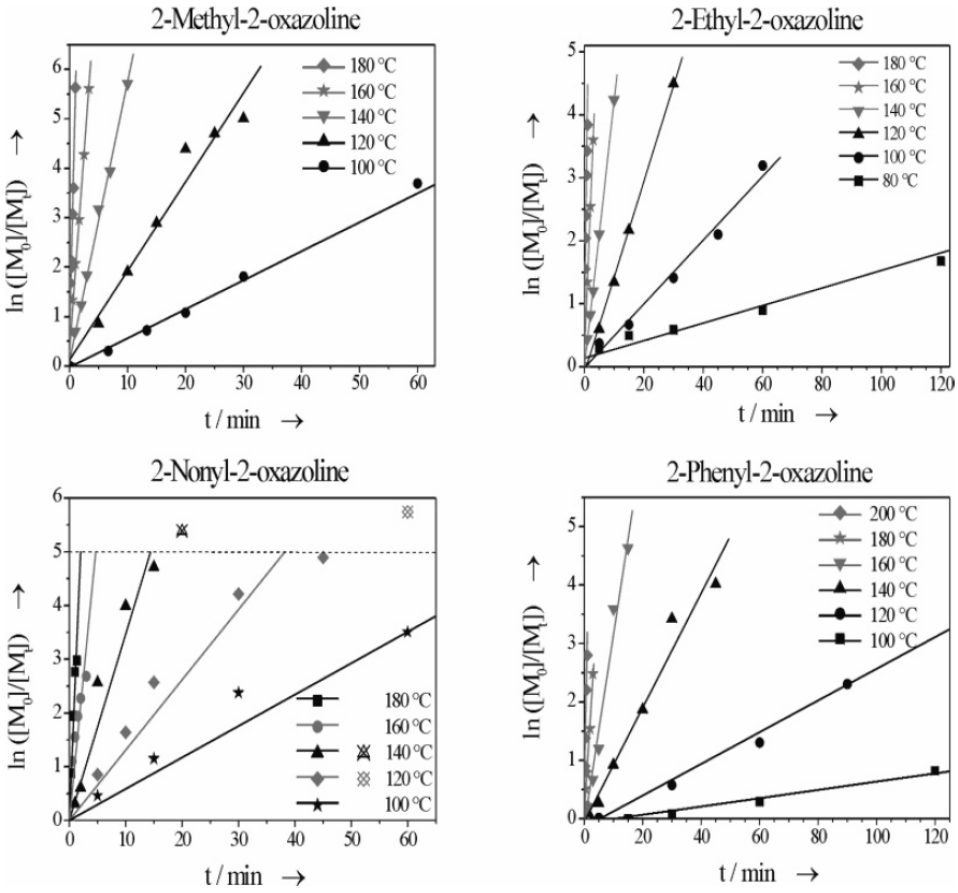

Figure 1.8. Semi–logarithmic kinetic plots for different 2–oxazolines at various temperatures (reprinted from reference 98).

1.4 "Click" reactions in polymer science

The "click" chemistry concept has been introduced by Sharpless *et al.* in 2001.[99] Selected reactions were classified as "click" chemistry when they are modular, stereospecific, wide in scope, result in high yields, and generate only inoffensive byproducts. Besides, the reaction must proceed with simple reaction conditions, readily available starting materials and without any solvent or in a benign solvent. The purification process of these reactions is expected to be as easy as the synthesis process. Therefore, nonchromatographic methods, *e.g.* crystallization or distillation, are preferred for simple product isolation.

There is a variety of "click" reactions existing in organic chemistry. However, the Huisgen 1,3–dipolar cycloaddition of azides and alkynes (CuAAC) is highlighted as the "cream of the crop", which has evolved into a common coupling procedure in all chemical disciplines within a few years.[100 –104] This chemistry has been neglected for a long time because of safety concerns about the azide moiety. Despite its potentially explosive character, azide moieties have superb properties such as stability against dimerization or hydrolysis in comparison to most other functional groups. The reaction rate of the Huisgen 1,3–dipolar

cycloaddition of azides and alkynes is dramatically increased in the presence of an appropriate catalyst such as transition metal ions which, at the same time, provide stereospecificity, making this cycloaddition compatible with the "click" chemistry requirements. This reaction is commonly performed in the presence of copper ions and nitrogen based ligands. However, concerns on the cytotoxicity of copper directed researchers to investigate other types of catalysts. Different ligands (PMDETA, bipyridine derivatives, terpyridine derivatives, and Me_6Tren) and transition metal ions (Ru, Ni, Pd, Pt, and Fe) have been examined to widen the scope of the copper–catalyzed cycloaddition reaction.[105 –110]

In the last couple of years there has been a significant interest to develop alternative "click" reactions that do not require any metal catalyst and perform as good as the copper–catalyzed azide–alkyne click reaction, *e.g.* fulfill all the requirements of "click" chemistry. In a recent highlight paper, Lutz provided an excellent overview of metal–free azide–alkyne cycloadditions.[111] However, "click" chemistry is not limited to cycloadditions and can be extended to other highly efficient reactions, such as nucleophilic substitution, radical addition, Michael addition as well as Diels–Alder and retro–Diels Alder reactions. The common advantage of these alternative reactions is that they commonly proceed in the absence of metal catalysts and they are schematically illustrated in Figure 1.9.

Figure 1.9. Schematic representation of different types of "click" reactions.

The potential toxicity of metal catalysts used in organic synthesis is a major issue when the products are designed to be used in biological applications.[112,113] Similarly, even though it is possible to synthesize a wide variety of compounds by employing the copper(I)

catalyzed azide–alkyne cycloaddition, the copper salt, used as a catalyst in the reaction, may still remain in the product at least in ppm levels after purification. Therefore, there has been a significant interest to develop alternative "click" reactions that do not require any metal–catalyst.

The free–radical addition of thiols onto double bonds is a highly efficient tool used for polymerizations, curing reactions, and for the modification of polymers.[114–116] Schlaad *et al.* demonstrated a post–polymerization modification of a well–defined poly[2–(3–butenyl)–2–oxazoline], which was polymerized by a CROP process. Various mercaptans, *e.g.* fluorinated thiols, acetylated glucose thiols, and dihydroxy functionalized thiols, were used as model reactions. "Thio–click" reactions were performed under inert atmosphere and exposed to UV light for 24 hours.[117] Furthermore, Schlaad *et al.* performed the "thio–click" reaction for poly(butadiene) modification under direct sunlight, since the thiol–ene photoaddition reaction can proceed at near–visible wavelengths (λ = 365 – 405 nm).[118] Another example was reported by Hawker *et al.* that was a robust, efficient, and orthogonal synthesis of 4th generation dendrimers using thiol–ene "click" reactions.[119] The solvent free reaction between alkene and thiol was performed at room temperature, without deoxygenation, by irradiation for 30 min with a hand–held UV–lamp (λ = 365 nm). Additionally, trace amounts of photoinitiator were used to increase the radical concentration and, thus, the reaction rate.

One elegant approach was first reported by Bertozzi and her co–workers where they have reacted azides with cyclooctyne derivatives.[120–125] This reaction is called *strain promoted [3+2] azide alkyne cycloaddition* (SPAAC) reaction and developed from the initial work of Wittig and Krebs.[126,127] However, SPAAC reactions with the first generation of cyclooctyne **1** exhibited relatively slow reaction rates in comparison to the corresponding CuAAC reactions. Therefore, mono–fluorinated (2nd generation) and difluorinated (3rd generation) derivatives of cyclooctynes have been synthesized to decrease the LUMO level of the alkyne by introducing electron–withdrawing groups to its neighbor resulting in increased second order rate constants.[128] The corresponding relative second–order rate constants ($M^{-1}s^{-1}$) of cyclooctynes are reported as 1.0, 1.8 and 31.8 for **1**, **2**, and **3**, respectively. The representative schematic structures of cyclooctynes and the SPAAC "click" reaction scheme are shown in Scheme 1.5.

Selective labeling of biomolecules has been successfully performed using difluorinated cyclooctyne (DIFO) derivatives in SPAAC reactions. Recently, Yin *et al.* reported the use of biotin conjugated DIFO derivatives for SPAAC with an azide substituted substrate attached to a peptidyl carrier protein (PCP).[129] Boons and his co–workers developed

an active cyclooctyne by introducing benzyl groups to increase the ring strain.[130] Thus, they have used 4–dibenzocyclooctynols for labeling living cells with azides.

The SPAAC reaction clearly fulfils many requirements of "click" chemistry. However, the demanding organic synthesis of cyclooctyne derivatives needs to be improved in order to be used not only in chemical biology but also in the other fields of chemistry. Alternatively, the commercial availability of **3** would significantly improve the scope and applicability of this reaction.

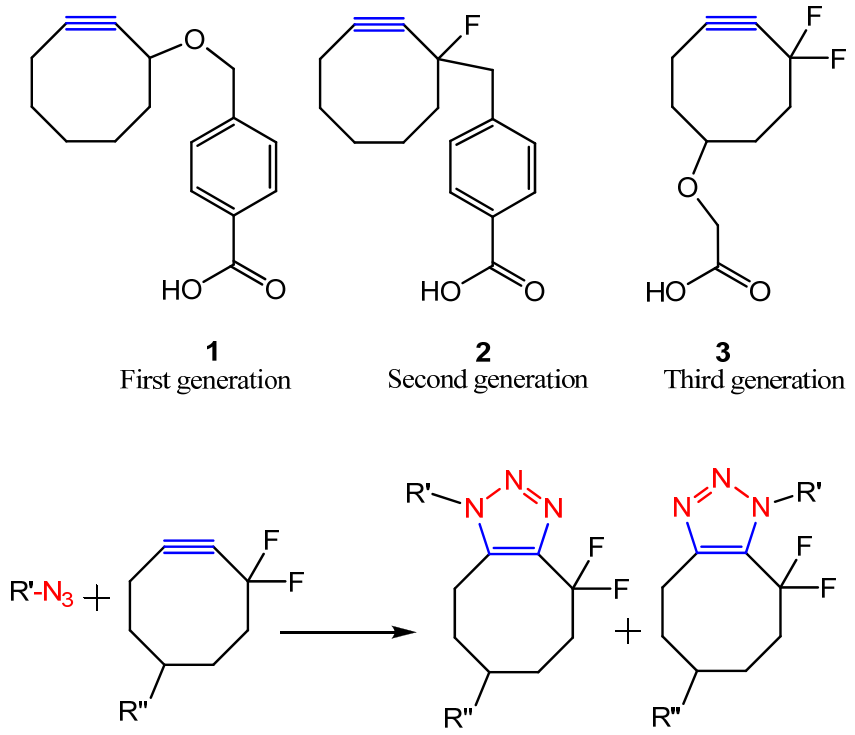

Scheme 1.5. *Top:* Schematic representation of the structures of cyclooctyne derivatives with different substituents. *Bottom:* Schematic representation of the SPAAC "click" reaction.

The beauty and popularity of azide–alkyne cycloaddition lies in the simple, readily available building blocks, whereas most of the metal–free alternative "click" reactions involve rather large complicated reactive groups such as cyclooctyne, pentafluorostyrene, dipyridyltetrazine and anthracene. In addition, the large, when compared to 1,2,3–triazole, resulting 'coupling units' are disadvantageous for most applications. As such, it is believed that most of the hitherto reported metal free "click" reactions will remain beautiful scientific examples rather than broadly applied methods.

The only distinctly simpler metal free "click" reaction is the thiol–ene radical addition. The introduction of terminal alkene and thiol groups into a large variety of structures is straightforward while the resulting thio–ether bond is even smaller in size than the 1,2,3–triazole that results from azide–alkyne cycloaddition. Furthermore, the coupling procedure is

even simpler than the CuAAC since no catalysts are required other than UV–light. As such, it is believed that thiol–ene "click" chemistry has the potential to become as broadly applied as CuAAC.

In the last Chapter, we have discussed a metal–free "click" reaction concept using thiols and pentafluorophenyl functionalities. A series of well–defined glycopolymers was prepared by employing the thiol–*para*–fluoro "click" reaction on polymers that were synthesized by NMP. The versatility and efficiency of amine or thiol substitution to the *para* position of C_6F_5 have been demonstrated to comply with most of the "click" chemistry requirements. In addition, a wide range of primary amines and thiols are commercially available. However, the accessibility of C_6F_5 groups is rather limited obstructing the scope and modularity of the reaction.

1.5 Aim of the thesis

The area of polymer science is moving from macro to nano scales, which requires absolute control over the molecular architectures and also fundamental knowledge on the structure–property relationships. Development of CLP techniques and "click" reactions allow researchers to synthesize well–defined tailor–made macromolecules. However, these polymerization techniques require a delicate selection of the appropriate catalyst, initiator, and solvent at a certain polymerization temperature and period for each type of monomer. Therefore, high–throughput experimentation tools and techniques are required to screen the effect of reaction parameters in relatively short times.

Consequently, performing controlled/"living" polymerizations in an automated parallel synthesizer were intended in this thesis not only for the optimization of the polymerization parameters but also for the preparation of polymer libraries with systematical variations. The investigation of the structure–property relationships based on several polymer libraries has been investigated. Namely, lower critical solution temperature (LCST) behavior of the polymer libraries was examined using parallel synthesis and characterization instruments.

The synthesis of tailor–made macromolecules may require the combination of different polymerization mechanisms to combine different types of monomers in the same polymer chain. Therefore, the use of heterobifunctional initiators was of significant interest of this thesis. The synthesis of amphiphilic block copolymers was also targeted by combination of hydrophilic and hydrophobic monomeric units.

Furthermore, the utilization of "click" reactions in particular in the polymer field has been examined and an alternative "click" reaction that does not require any metal catalyst has

been developed. Thus, the preparation of well–defined glycopolymers was achieved by combination of controlled living polymerization techniques and a metal–free "click" reaction.

1.6 Outline of the thesis

Controlled/living polymerization techniques have attracted great attention in the last decade. These techniques opened avenues to the synthesis of tailor–made macromolecules. In the major part of this thesis, we have focused on the optimization, combination, and utilization of these CLP techniques using HTE approaches.

We describe in the second Chapter the optimization of the NMP of St and *t*–BA utilizing an automated synthesis platform and, subsequently, the preparation of a 3×3 block copolymer library. Besides, thermoresponsive polymer libraries comprising of HPA and DMAc or Amor were prepared in an automated fashion using NMP.

In Chapter 3, we focused on the ATRP of MMA in solution and St on surfaces using a new ligand, HOETETA. Following the optimization reactions of HOETETA, the ATRP of St was conducted on the electrochemically patterned surface bearing initiator functionalities.

Chapter 4 describes the use of the RAFT polymerization technique to synthesize MAA and OEGMA containing thermoresponsive homopolymer and copolymer libraries. The LCST behavior and also the water uptake behavior of various classes of polymers were investigated in details. Additionally, we report a standard protocol for the parallel optimization of RAFT polymerization conditions using an automated parallel synthesizer.

The combination of different polymerization techniques has critical importance for the synthesis of block copolymers consisting of monomers that can only polymerize with different methods. For instance, the combination of the cationic ring opening polymerization of 2–ethyl–2–oxazolines and the ATRP of styrene is described in Chapter 5 by employing a commercially available heterobifunctional initiator. Besides, optimization reactions for the CROP of EtOx are presented using different acetyl halide initiators.

The last Chapter of the thesis is mainly focused on the synthesis of well–defined glycopolymers by a combination of NMP of styrenics and the thio–*para* fluoro "click reaction". We have introduced this type of click reaction in the polymer field for the first time and it has a significant potential for applications in the field of biopolymers since it does not require any metal catalyst.

1.7. References and Notes

(1) R. Ruiz, H. M. Kang, F. A. Detcheverry, E. Dobisz, D. S. Keercher, T. R. Albrect, J. J. de Pablo, P. F. Nealey, *Science* **2008**, *321*, 936–939.
(2) M. Szwarc, M. Levy, R. Milkovich, *J. Am. Chem. Soc.* **1956**, *78*, 2656–2657.
(3) P. Fragouli, H. Iatrou, D. J. Lohse, N. Hadjichristidis, *J. Polym. Sci., Part A: Polym. Chem.* **2008**, *46*, 3938–3946.
(4) M. Sawamoto, *Prog. Polym. Sci.* **1991**, *16*, 111–172.
(5) Web of science search was performed with keywords of "Atom transfer radical polymerization" or "Nitroxide mediated polymerization" or "Reversible addition–fragmentation chain transfer" on March 20th, 2009.
(6) http://nobelprize.org/nobel_prizes/chemistry/laureates/2001/index.html.
(7) M. Szwarc, *Nature* **1956**, *178*, 1168–1169.
(8) http://goldbook.iupac.org/I03178.html (last accessed on March 20th, 2009).
(9) G. Moad, D. H. Solomon, **1995**, The chemistry of free radical polymerization. Elsevier Science, Bath.
(10) M. Sawamoto, M. Kamigaito, **1999**, In: D. Schlueter (ed) Synthesis of polymers. VCH, Weinheim.
(11) T. Otsu, A. Matsumoto, *Adv. Polym. Sci.* **1998**, *136*, 75–137.
(12) A. Ajayaghosh, R. Francis, *Macromolecules* **1998**, *31*, 1436–1438.
(13) A. Ajayaghosh, R. Francis, *J. Am. Chem. Soc.* **1999**, *121*, 6599–6606.
(14) E. Borsig, M. Lazar, M. Capla, *Makromol. Chem.* **1967**, *105*, 212–222.
(15) A. Sebenik, *Prog. Polym. Sci.* **1998**, *23*, 875–917.
(16) S. H. Qin, K. Y. Qiu, G. Swift, D. G. Westmoreland, S. Wu, *J. Polym. Sci., Part A: Polym. Chem.* **1999**, *37*, 4610–4615.
(17) C. J. Hawker, A. W. Bosman. E. Harth, *Chem. Rev.* **2001**, *101*, 3661–3688.
(18) G. Moad, E. Rizzardo, *Macromolecules* **1995**, *28*, 8772–8728.
(19) G. Moad, E. Rizzardo, S. H. Thang, *Acc. Chem. Res.* **2008**, *41*, 1133–1142.
(20) J. Chiefari, Y. K. Chong, F. Ercole, J. Krstina, J. Jeffery, T. P. T. Le, R. T. A. Mayadunne, G. F. Meijs, C. L. Moad, G. Moad, E. Rizzardo, S. H. Thang, *Macromolecules* **1998**, *31*, 5559–5562.
(21) J. S. Wang, K. Matyjaszewski, *J. Am. Chem. Soc.* **1995**, *117*, 5614–5615.
(22) M. Kato, M. Kamigaito, M. Sawamoto, T. Higashimura, *Macromolecules* **1995**, *28*, 1721–1723.
(23) T. Pintauer, P. Zhou, K. Matyjaszewski, *J. Am. Chem. Soc.* **2002**, *124*, 8196–8197.
(24) A. K. Nanda, K. Matyjaszewski, *Macromolecules* **2003**, *36*, 599–604.
(25) A. K. Nanda, K. Matyjaszewski, *Macromolecules* **2003**, *36*, 1487–1493.
(26) A. K. Nanda, K. Matyjaszewski, *Macromolecules* **2003**, *36*, 8222–8224.
(27) T. Pintauer, W. Braunecker, E. Collange, R. Poli, K. Matyjaszewski, *Macromolecules* **2004**, *37*, 2679–2682.
(28) K. Matyjaszewski, A. K. Nanda, W. Tang, *Macromolecules* **2005**, *38*, 2015–2018.
(29) W. Tang, A. K. Nanda, K. Matyjaszewski, *Macromol. Chem. Phys.* **2005**, *206*, 1171–1177.
(30) W. Tang, K. Matyjaszewski, *Macromolecules* **2006**, *39*, 4953–4959.
(31) W. Tang, K. Matyjaszewski, *Macromolecules* **2007**, *40*, 1858–1863.
(32) G. Chambard, B. Klumperman, A. L. German, *Macromolecules* **2000**, *33*, 4417–4421.
(33) A. Goto, T. Fukuda, *Macromol. Rapid Commun.* **1999**, *20*, 633–636.
(34) K. Ohno, A. Goto, T. Fukuda, J. Xia, K. Matyjaszewski, *Macromolecules* **1998**, *31*, 2699–2701.
(35) M. A. J. Schellekens, F. de Wit, B. Klumperman, *Macromolecules* **2001**, *34*, 7961–7966.
(36) R. Venkatesh, F. Vergouwen, B. Klumperman, *Macromol. Chem. Phys.* **2005**, *206*, 547–552.
(37) K. Matyjaszewski, H. J. Paik, P. Zhou, S. J. Diamanti, *Macromolecules* **2001**, *34*, 5125–5131.
(38) D. B. Rorabacher, *Chem. Rev.* **2004**, *104*, 651–697.
(39) T. Pintauer, K. Matyjaszewski, *Coord. Chem. Rev.* **2005**, *249*, 1155–1184.
(40) G. Moad, E. Rizzardo, D. H. Solomon, *Macromolecules* **1982**, *15*, 909–914.
(41) M. K. Georges, R. P. N. Veregin, P. M. Kazmaier, G. K. Hamer, *Macromolecules* **1993**, *26*, 2987–2988.
(42) C. J. Hawker, *J. Am. Chem. Soc.* **1994**, *116*, 11185–11186.
(43) C. J. Hawker, G. G. Barclay, A. Orellana, J. Dao, W. Devonport, *Macromolecules* **1996**, *29*, 5245–5254.
(44) D. Benoit, S. Grimaldi, S. Robin, J. P. Finet, P. Tordo, Y. Gnanou, *J. Am. Chem. Soc.* **2000**, *122*, 5929–5939.
(45) D. Benoit, V. Chaplinski, R. Braslau, C. J. Hawker, *J. Am. Chem. Soc.* **1999**, *121*, 3904–3920.
(46) S. Grimaldi, F. Lemoigne, J. P. Finet, P. Tordo, P. Nicol, M. Plechot, Y. Gnanou, WO Patent, **1996**, *96*, 24620.
(47) www.blocbuilder.com.
(48) Y. Guillaneuf, D. Gigmes, S. R. A. Marque, P. Astolfi, L. Greci, P. Tordo, D. Bertin, S. Magnet, L. Couvreur, *Macromolecules* **2007**, *40*, 3108–3114.

(49) B. Charleux, J. Nicolas, O. Guerret, *Macromolecules* **2005**, *38*, 5485–5492.
(50) J. Nicolas, C. Dire, L. Mueller, J. Belleney, B. Charleux, S. R. A. Marque, D. Bertin, S. Magnet, L. Couvreur, *Macromolecules* **2006**, *39*, 8274–8282.
(51) C. Dire, B. Charleux, S. Magnet, L. Couvreur, *Macromolecules* **2007**, *40*, 1897–1903.
(52) J. Nicolas, P. Couvreur, B. Charleux, *Macromolecules* **2008**, *41*, 3758–3761.
(53) P. Corpart, D. Charmot, T. Biadatti, S. Z. Zard, D. Michelet **1998**, WO9858974 *Chem. Abstr. 130*, 82018.
(54) P. Chapon, C. Mignaud, G. Lizarraga, M. Destarac, *Macromol. Rapid Commun.* **2003**, *24*, 87–91.
(55) G. Moad, J. Chiefari, Y. K. Chong, J. Krstina, R. T. A. Mayadunne, A. Postma, E. Rizzardo, S. H. Thang, *Polym. Int.* **2000**, *49*, 993–1001.
(56) G. Moad, E. Rizzardo, S. H. Thang, *Aust. J. Chem.* **2006**, *59*, 669–692.
(57) D. A. Tomalia, D. P. Sheetz, *J. Polym. Sci., Part A: Polym. Chem.* **1966**, *4*, 2253–2265.
(58) W. Seeliger, E. Aufderhaar, W. Diepers, R. Feinauer, R. Nehring, W. Thier, H. Hellmann, *Angew. Chem.Int. Ed.* **1966**, *5*, 875–889.
(59) T. G. Bassiri, A. Levy, M. Litt, *Polym. Lett.* **1967**, *5*, 871–879.
(60) K. Aoi, M. Okada, *Prog. Polym. Sci.* **1996**, *21*, 151–208.
(61) S. Kobayashi, H. Uyama, *J. Polym. Sci., Part A: Polym. Chem.* **2002**, *40*, 192–209.
(62) O. W. Webster, *Science* **1991**, *496*, 887–893.
(63) S. Kobayashi, T. Igarashi, Y. Moriuchi, T. Saegusa, *Macromolecules* **1986**, *19*, 535–541.
(64) R.–H. Jin, *Adv. Mater.* **2002**, *14*, 889–892.
(65) R. Hoogenboom, F. Wiesbrock, H. Huang, M. A. M. Leenen, S. F. G. M. van Nispen, M. van der Loop, C.–A. Fustin, A. M. Jonas, J.–F. Gohy, U. S. Schubert, *Macromolecules* **2006**, *39*, 4719–4725.
(66) R. Hoogenboom, F. Wiesbrock, M. A. M. Leenen, H. M. L. Thijs, H. Huang, C. A. Fustin, P. Guillet, J.–F. Gohy, U. S. Schubert, *Macromolecules* **2007**, *40*, 2837–2843.
(67) H. Huang, R. Hoogenboom, M. A. M. Leenen, P. Guillet, A. M. Jonas, U. S. Schubert, J.–F.Gohy, *J. Am. Chem. Soc.* **2006**, *128*, 3784–3788.
(68) R. Hoogenboom, M. W. M. Fijten, U. S. Schubert, *J. Polym. Sci., Part A: Polym. Chem.* **2004**, *42*, 1830–1840.
(69) T. Saegusa, H. Ikeda, *Macromolecules* **1973**, *6*, 808–811.
(70) T. Saegusa, H. Ikeda, H. Fujii, *Macromolecules* **1972**, *5*, 359–362.
(71) T. Saegusa, H. Ikeda, H. Fujii, *Macromolecules* **1973**, *6*, 315–319.
(72) Q. Lui, M. Konnas, J. S. Riffle, *Macromolecules* **1993**, *26*, 5572–5576.
(73) A. Dworak, *Macromol. Chem. Phys.* **1998**, *199*, 1843–1849.
(74) M. Einzmann, W. H. Binder, *J. Polym. Sci., Part A: Polym. Chem.* **2001**, *39*, 2821–2831.
(75) R. D. Puts, D. Y. Sogah, *Macromolecules* **1997**, *30*, 7050–7055.
(76) Y. Wang, W. J. Brittain, *Macromol. Rapid Commun.* **2007**, *28*, 811–815.
(77) A. Dworak, *Polym. Bull.* **1997**, *38*, 7–13.
(78) www.flamac.be; www.hte–company.com.
(79) www.chemspeed.com; www.symyx.com; www.boschrexroth.com; www.avantium.com.
(80) C. Barner–Kowollik, T. P. Davis, J. P. A. Heuts, M. H. Stenzel, P. Vana, M. Whittaker, *J. Polym. Sci., Part A: Polym. Chem.* **2003**, *41*, 365–375.
(81) K. Matyjaszewski, *Macromolecules* **1998**, *31*, 4710–4717.
(82) Y. Kwak, K. Matyjaszewski, *Macromolecules* **2008**, *41*, 6627–6635.
(83) W. Tang, Y. Kwak, W. Braunecker, N. V. Tsarevsky, M. L. Coote, K. Matyjaszewski, *J. Am. Chem. Soc.* **2008**, *130*, 10702–10713.
(84) A. Nilsen, R. Braslau, *J. Polym. Sci., Part A: Polym. Chem.* **2006**, *44*, 697–717.
(85) H. Q. Zhang, V. Marin, M. W. M. Fijten, U. S. Schubert, *J. Polym. Sci., Part A: Polym. Chem.* **2004**, *42*, 1876–1885.
(86) M. A. R. Meier, U. S. Schubert, *Soft Matter* **2006**, *2*, 371–376.
(87) M. A. R. Meier, R. Hoogenboom, U. S. Schubert, *Macromol. Rapid Commun.* **2004**, *25*, 21–33.
(88) R. Hoogenboom, M. A. R. Meier, U. S. Schubert, *Macromol. Rapid Commun.* **2003**, *24*, 15–32.
(89) M. A. R. Meier, U. S. Schubert, *J. Mater. Chem.* ***2004***, *14*, 3289–3299.
(90) H. Q. Zhang, R. Hoogenboom, M. A. R. Meier, U. S. Schubert, *Meas. Sci. Technol.* **2005**, *16*, 203–211.
(91) C. Guerrero–Sanchez, R. M. Paulus, M. W. M. Fijten, M. J. de la Mar, R. Hoogenboom, U. S. Schubert, *Appl. Surf. Sci.* **2006**, *252*, 2555–2561.
(92) M. W. M. Fijten, M. A. R. Meier, R. Hoogenboom, U. S. Schubert, *J. Polym. Sci., Part A: Polym. Chem.* **2004**, *42*, 5775–5783.
(93) M. W. M. Fijten, R. M. Paulus, U. S. Schubert, *J. Polym. Sci., Part A: Polym. Chem.* **2005**, *43*, 3831–3839.
(94) R. Hoogenboom, M. W. M. Fijten, R. M. Paulus, U. S. Schubert, *Polymer* **2006**, *47*, 75–84.
(95) R. Hoogenboom, M. W. M. Fijten, U. S. Schubert, *Macromol. Rapid Commun.* **2004**, *25*, 339–343.

(96) R. Hoogenboom, F. Wiesbrock, M. A. M. Leenen, U. S. Schubert, *J. Comb. Chem.* **2005**, *7*, 10–13.
(97) R. Hoogenboom, R. M. Paulus, M. W. M. Fijten, U. S. Schubert, *J. Polym. Sci., Part A: Polym. Chem.* **2005**, *43*, 1487–1497.
(98) F. Wiesbrock, R. Hoogenboom, M. A. M. Leenen, M. A. R. Meier, U. S. Schubert, *Macromolecules* **2005**, *38*, 5025–5034.
(99) H. C. Kolb, M. G. Finn, K. B. Sharpless, *Angew. Chem. Int. Ed.* **2001**, *40*, 2004–2021.
(100) C. J. Hawker, K. L. Wooley, *Science* **2005**, *309*, 1200–1205.
(101) W. H. Binder, R. Sachsenhofer, *Macromol. Rapid Commun.* **2007**, *28*, 15–54.
(102) D. Fournier, R. Hoogenboom, U. S. Schubert, *Chem. Soc. Rev.* **2007**, *36*, 1369–1380.
(103) H. C. Kolb, K. B. Sharpless, *Drug Discovery Today* **2003**, *8*, 1128–1137.
(104) V. D. Bock, H. Hiemstra, J. H. van Maarseveen, *Eur. J. Org. Chem.* **2006**, *1*, 51–68.
(105) V. O. Rodionov, V. V. Fokin, M. G. Finn, *Angew. Chem. Int. Ed.* **2005**, *44*, 2210–2215.
(106) P. L. Golas, N. V. Tsarevsky, B. S. Sumerlin, K. Matyjaszewski, *Macromolecules* **2006**, *39*, 6451–6457.
(107) C. N. Urbani, C. A. Bell, M. R. Whittaker, M. J. Monteiro, *Macromolecules* **2008**, *41*, 1057–1060.
(108) S. Chassaing, A. S. S. Sido, A. Alix, M. Kumarraja, P. Pale, J. Sommer, *Chem. Eur. J.* **2008**, *14*, 6713–6721.
(109) B. C. Boren, S. Narayan, L. K. Rasmussen, L. Zhang, H. Zhao, Z. Lin, G. Jia, V. V. Fokin, *J. Am. Chem. Soc.* **2008**, *130*, 8923–8930.
(110) B. Saba, S. Sharma, D. Sawant, B. Kundu, *Synlett* **2007**, *10*, 1591–1594.
(111) J. F. Lutz, *Angew. Chem. Int. Ed.* **2008**, *47*, 2182–2184.
(112) Q. Wang, T. R. Chan, R. Hilgraf, V. V. Fokin, K. B. Sharpless, M. G. Finn, *J. Am. Chem. Soc.* **2003**, *135*, 3192–3193.
(113) J. Gierlich, G. A. Burley, P. M. E. Gramlich, D. M. Hammond, T. Carell, *Org. Lett.* **2006**, *8*, 3639–3642.
(114) R. L. A. David, J. A. Kornfield, *Macromolecules* **2008**, *41*, 1151–1161.
(115) C. Nilsson, N. Simpson, M. Malkoch, M. Johansson, E. Malmstrom, *J. Polym. Sci. Part A: Polym. Chem.* **2008**, *46*, 1339–1348.
(116) A. Dondoni, *Angew. Chem. Int. Ed.* **2008**, *47*, 8995–8997.
(117) A. Gress, A. Volkel, H. Schlaad, *Macromolecules* **2007**, *40*, 7928–7933.
(118) N. ten Brummelhuis, C. Diehl, H. Schlaad, *Macromolecules* **2008**, *41*, 9946–9947.
(119) K. L. Killops, L. M. Campos, C. J. Hawker, *J. Am. Chem. Soc.* **2008**, *130*, 5062–5064.
(120) J. M. Baskin, J. A. Prescher, S. T. Laughlin, N. J. Agard, P. V. Chang, I. A. Miller, A. Lo, J. A. Codelli, C. R. Bertozzi, *Proc. Nat. Acad. Sci. U.S.A.* **2007**, *104*, 16793–16797.
(121) S. T. Laughlin, J. M. Baskin, S. L. Amacher, C. R. Bertozzi, *Science* **2008**, *320*, 664–667.
(122) J. A. Johnson, J. M. Baskin, C. R. Bertozzi, J. F. Koberstein, N. J. Turro, *Chem. Commun.* **2008**, 3064–3066.
(123) J. A. Codelli, J. M. Baskin, N. J. Agard, C. R. Bertozzi, *J. Am. Chem. Soc.* **2008**, *130*, 11486–11493.
(124) E. M. Sletten, C. R. Bertozzi, *Org. Lett.* **2008**, *10*, 3097–3099.
(125) J. M. Baskin, C. R. Bertozzi, *QSAR Comb. Sci.* **2007**, *26*, 1211–1219.
(126) G. Wittig, A. Krebs, *Chem. Ber. Recl.* **1961**, *94*, 3260–3275.
(127) A. T. Blomquist, L. H. Liu, *J. Am. Chem. Soc.* **1953**, *75*, 2153–2154.
(128) D. H. Ess, G. O. Jones, K. N. Houk, *Org. Lett.* **2008**, *10*, 1633–1636.
(129) Y. Zou, J. Yin, *Bioorg. Med. Chem. Lett.* **2008**, *18*, 5664–5667.
(130) X. Ning, J. Guo, M. A. Wolfert, G. J. Boons, *Angew. Chem. Int. Ed.* **2008**, *47*, 2253–2255.

Chapter 2

Nitroxide mediated radical polymerization

Abstract

Nitroxide mediated radical polymerization is one of the most widely applied controlled radical polymerization techniques and does not require any catalyst or transfer agents. Besides, the development of efficient nitroxide compounds expanded the applicability of this polymerization process to a wide range of monomers. Therefore, we have performed a series of automated parallel optimization experiments to understand the effect of polymerization temperature and concentration of free nitroxide on the polymerization rates, molar masses and polydispersity indices. The optimization reactions based on styrene and tert–butyl acrylate allowed the preparation of a small block copolymer library of those monomers. Intensive screening was conducted for the polymerization of 2–hydroxypropyl acrylate, N–acryoyl morpholine and N,N–dimethyl acrylamide in order to identify the optimum reaction conditions. According to the obtained results, statistical copolymer libraries of these monomers were prepared with a systematical variation of the composition. Moreover, these copolymer libraries were investigated in detail for their thermal properties and phase transition behaviors.

Parts of this chapter have been published: C. R. Becer, R. M. Paulus, R. Hoogenboom, U. S. Schubert, *J. Polym. Sci., Part A: Polym. Chem.* **2006**, *44*, 6202–6213; T. M. Eggenhuisen, C. R. Becer, M. W. M. Fijten, R. Eckardt, R. Hoogenboom, U. S. Schubert, *Macromolecules* **2008**, *41*, 5132–5140.

2.1 Introduction

The rapid development of controlled/"living" radical polymerization (CRP) techniques such as atom transfer radical polymerization (ATRP),[1,2] nitroxide mediated radical polymerization (NMP),[3,4] and reversible addition–fragmentation chain transfer polymerization (RAFT)[5,6] allowed the straightforward synthesis of well–defined polymers and copolymers with desired compositions, architectures and functionalities. All these CRP methods are based on a fast and reversible dynamic equilibrium between the dormant species and active species. The equilibrium constants, which are very low in these systems, keep the concentration of active radical species very low.[7] As a result, termination and transfer reactions are minimized and a controlled radical polymerization can be achieved under the appropriate polymerization conditions. However, a low radical concentration also complies with relatively long polymerization times. According to the mechanistic features both NMP and ATRP are controlled by the persistent radical effect,[8,9] whereas RAFT is based on a chain transfer mechanism. ATRP and RAFT have some advantages in comparison to NMP including better control for the synthesis of block copolymers and a wider range of monomers. Besides, the controlling agents such as metal ions or dithio compounds that are used in ATRP and RAFT limit their industrial applications. In contrast, there is no need to use metal or sulfur containing controlling agents for NMP and therefore NMP has attracted a lot of attention for its environmentally benign radical chemistry.[10]

The kinetic investigation on NMP of different kinds of monomers has been reported by various groups.[11– 17] Libraries of nitroxide compounds have been prepared to explore their effect on NMP of styrene or acrylates.[18] Besides, different polymerization temperatures were investigated for the polymerization of many kinds of monomers by using selected nitroxide compounds.[19] The NMP with various nitroxide compounds has been investigated in detail.[20–22] Fischer *et al.* reported that derivatives of β–phosphonylated nitroxide compounds allow to perform polymerizations at higher rates than the ones that can be achieved by using TEMPO derivatives by their high activation rates at low temperatures.[21] In addition, the alkoxyamine initiator that was used in this study bears a carboxylic acid functionality. This functionality could be used for post polymerization modifications while the nitroxide compound still provides the living feature on the other end of the polymer chain. The schematic representation of the structure of the Bloc Builder™ and the schematic representation of the NMP of St are shown in Scheme 2.1. Bloc Builder™ is an efficient alkoxyamine for styrenics as well as acrylates and commercially available from Arkema.

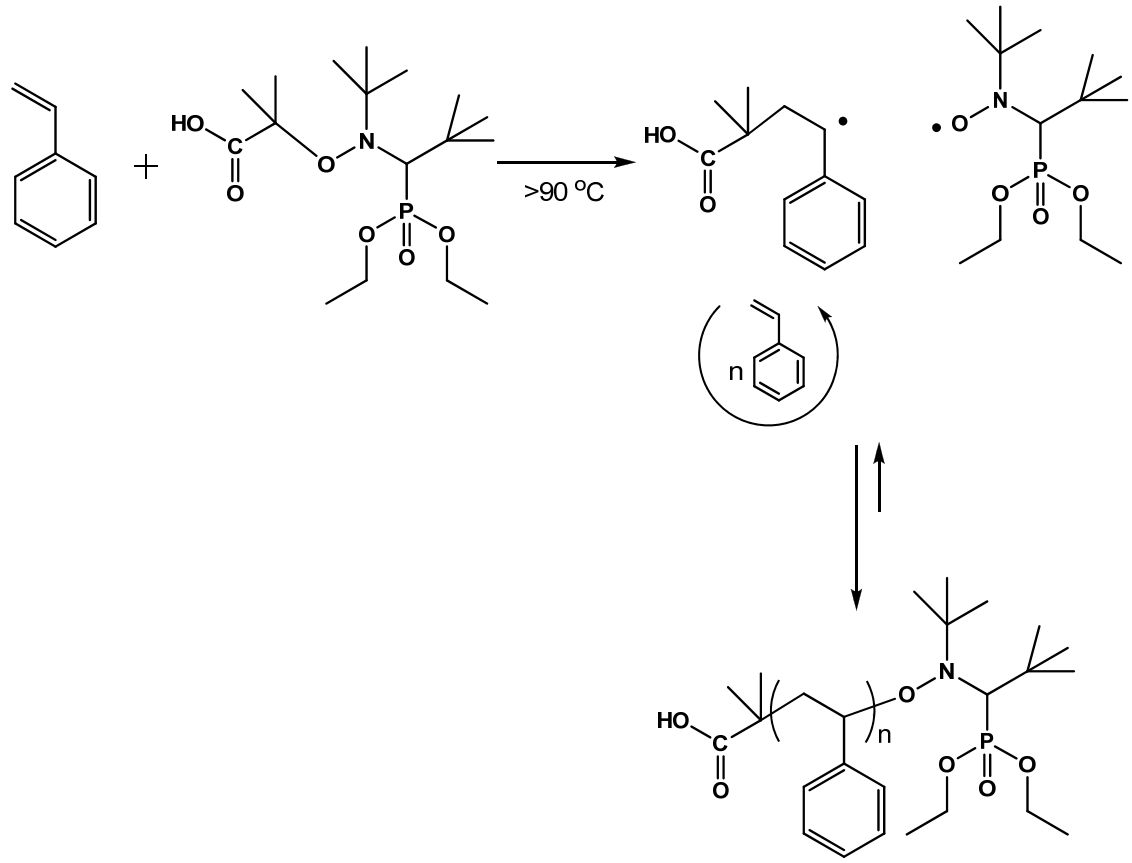

Scheme 2.1. Schematic representation of the NMP of St initiated by Bloc Builder™.

Some research groups investigated the effect of an excess of free nitroxide to the polymerization kinetics of styrene and acrylates as well.[23] However, these studies mainly focused on a few temperatures and none of them investigated the effect of free nitroxide in a series for homopolymerization of both styrene and *tert*–butyl acrylate. These separate investigations applying different conditions make a direct comparison very difficult. Therefore, we have utilized an automated parallel synthesizer to systematically investigate the effect of these important parameters on the properties of the obtained polymers. The polymerization temperature and the concentration of free–nitroxide were varied for various monomers, *e.g.* styrene (St), *tert*–butyl acrylate (*t*BA), 2–hydroxypropyl acrylate (HPA), *N*–acryoyl morpholine (Amor) and *N*,*N*–dimethyl acrylamide (DMA). Thus, a block copolymer library of St and *t*BA was synthesized and characterized. Moreover, statistical copolymer libraries of HPA/Amor and HPA/DMA were prepared by varying the monomer contents systematically. These libraries were not only screened by means of molecular characterization techniques but also their thermal properties and phase transition behaviors were investigated in details.

2.2 Optimization of polymerization parameters for styrene and *tert*–butyl acrylate

The objective of the current investigations was the optimization of the reaction temperature and the amount of free nitroxide for the nitroxide mediated radical polymerization of St and *t*BA to obtain the desired molar masses, while at the same time achieving reasonable rates of polymerization. Secondly, the optimized polymerization conditions will be applied for the synthesis of homopolymers or block copolymers with narrow molar mass distributions.

Therefore, we used an automated parallel synthesizer, a Chemspeed Accelerator™ SLT106, which allows to screen the effect of different parameters on the polymerization by conducting a large number of reactions under identical conditions and minimizing the handling errors. Previously, controlled and living radical polymerization systems i.e. ATRP, RAFT, NMP, cationic and anionic polymerizations (solvent based and emulsion polymerizations) were conducted successfully by the use of automated parallel synthesizers.[24– 28] In this study the automated parallel synthesizer platform was applied extensively to investigate the nitroxide mediated radical polymerization conditions.

The optimization reactions were conducted in solution to prevent high viscosities that would decrease the efficiency of automated sampling. Anisole was used as a solvent since it has a higher boiling point (154 °C) in comparison to toluene (111 °C). This enabled us to perform the polymerizations at higher temperatures. As a first step, the optimization of the reaction temperature for the NMP of St in anisole was performed in order to determine the most efficient polymerization temperature. A stock solution was prepared with a concentration of 2 M monomer in anisole, and the monomer to initiator ratio (M/I) was set to 100. Afterwards, 4 mL of this stock solution was transferred to seven different reactors. The individual ceramic heating mantels of the vessels were set to 90, 100, 110, 115, 120, 125, and 130 °C and several samples were withdrawn automatically in different time intervals. All samples were characterized with GC and SEC to determine the conversion of the monomer, the molar mass and molar mass distribution, respectively. As shown in Figure 2.1, higher polymerization rates were achieved for styrene with the elevated reaction temperatures as it was expected. The semi–logarithmic first order kinetic plots for the polymerizations of styrene at different reaction temperatures revealed a linear behavior for all polymerization temperatures. A large increase in the rate of polymerization was observed for styrene in between 110 °C and 115 °C. The reason for this may be the auto–initiation of styrene, which is becoming more evident at elevated temperatures. In general, molar masses were found

close to the theoretical line and the polydispersity indices were below 1.3 at moderate reaction temperatures. The experimental molar masses that are lower than the theoretical values for the polymerizations at 90 and 100 ºC are most likely due to a slower initial polymerization rate that results in a broader molar mass distribution and thus also results in lower molar mass values. It is obvious that the increase in the reaction temperature would result in an increase in the rate of polymerization. It is shown in Figure 2.1 that in the case of a polymerization temperature of 130 °C, molar masses were above the theoretical line and polydispersity indices were above 1.4. This deviation from the theoretical line shows a loss of control over the polymerization of St initiated by Bloc Builder™ at 130 °C. This is most likely due to a combination of increased termination reactions and also higher rates of autoinitiation of St.

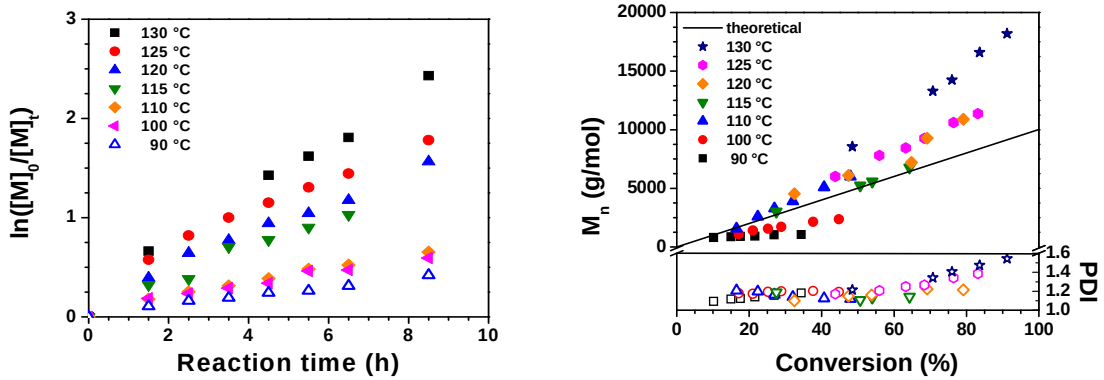

Figure 2.1. *Left:* First order kinetic plot for the polymerization of St in anisole at various polymerization temperatures. *Right:* Corresponding M_n and PDI values *versus* monomer conversion plot.

A second set of reactions was conducted in order to optimize the polymerization temperature of *t*BA at 2 M concentration in anisole with a M/I of 100. Four different reaction temperatures (90, 100, 120 and 130 °C) were examined as described above. The obtained kinetic data for the homopolymerization of *t*BA are shown as $\ln([M]_0/[M]_t)$ *versus* time plot in Figure 2.2. Faster polymerization rates were observed for the polymerization of *t*BA at elevated temperatures. Similar to the homopolymerization of St, the values for the *t*BA exhibit a linear behavior for all investigated temperatures. To calculate the number average molar masses of poly(*tert*–butyl acrylate) (P*t*BA), poly(styrene) (PS) standards for the SEC calibration were preferred compared to poly(methyl methacrylate) (PMMA) standards based on previous findings.[29] Nevertheless, the calculated molar masses are not close to the theoretical line, which is an indication of chain transfer reactions. In this case, hydrogen abstraction from the polymeric chain end as well as back–biting reactions might be the favored chain transfer processes resulting in a loss of control over the polydispersity indices, as depicted in Figure 2.2.

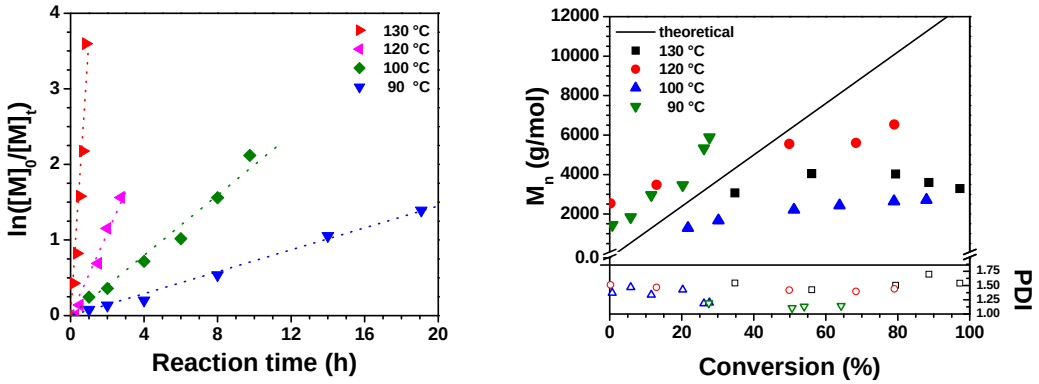

Figure 2.2. *Left:* First order kinetic plot for the polymerization of *t*BA in anisole at various polymerization temperatures. *Right:* Corresponding M_n and PDI values *versus* monomer conversion plot.

Based on the temperature optimization, Arrhenius plots were drawn for the NMP of St and *t*BA in order to calculate the activation energies, which are shown in Figure 2.3. The apparent propagation rates were calculated from the slopes of the semi–logarithmic kinetic plots. It is assumed that the ratio of dormant and active species, i.e. the concentration of propagating species, were constant at all temperatures. The apparent propagation rate for the NMP of St at 120 °C was found as 0.54×10^{-4} and for *t*BA as 1.52×10^{-4}. Activation energies for NMP of St and *t*BA were found to be 55 kJ/mol·K and 186 kJ/mol·K with regression coefficients of 0.9667 and 0.9862, respectively. Gnanou *et al.* reported the activation energies for the bulk polymerization of St and *t*BA using macroinitiators, i.e. PS_{35}–SG1 or P*t*BA_{35}–SG1, as 121 kJ/mol·K and 130 kJ/mol·K, respectively.[30] Although, it is obvious that the activation energy values reported by Gnanou *et al.* are different from the ones reported here, we do not know the exact reason for this discrepancy. A possible explanation for this observation might be the use of different polymerization media, namely bulk *versus* anisole.

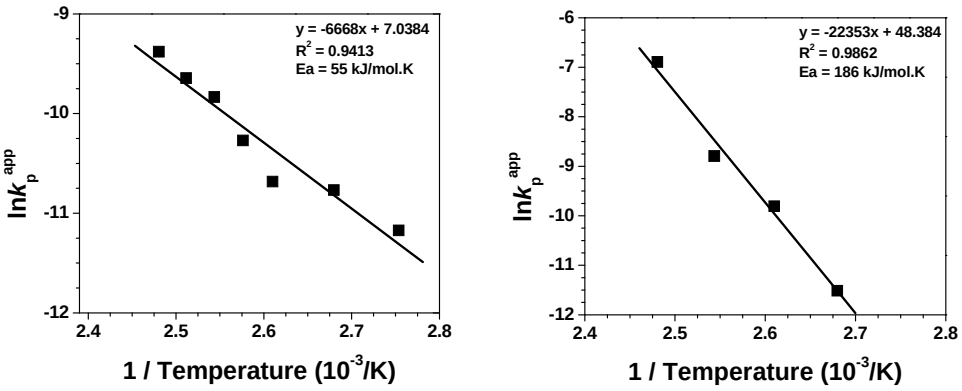

Figure 2.3. *Left:* Arrhenius plot for the Bloc Builder™ initiated polymerization of St in anisole. *Right:* Arrhenius plot for the Bloc Builder initiated™ polymerization of *t*BA in anisole.

Subsequently, the effect of the free nitroxide concentration for the polymerization of St in anisole was investigated at 110 °C. It was reported by Studer *et al.* that the conversion of the monomer is independent of the alkoxyamine concentration for the bulk polymerization of St.[31] In contrast, Yin *et al.* reported that the addition of free nitroxide to the bulk polymerization of St improves the control over the molar mass distribution, whereby lower polymerization rates were observed.[32] Therefore, we investigated the effect of free nitroxide on the NMP of both St and *t*BA in anisole. Eight different ratios of free nitroxide (SG1), from 0 to 10 mol percent (regarding to the amount of initiator), were used for both monomers. As it is shown in Figure 2.4 no significant effect of the addition of free nitroxide was observed on the rate of polymerization of St. In addition, there is no difference observed between the number average molar masses of the samples that all exhibit a linear increase with increasing conversion.

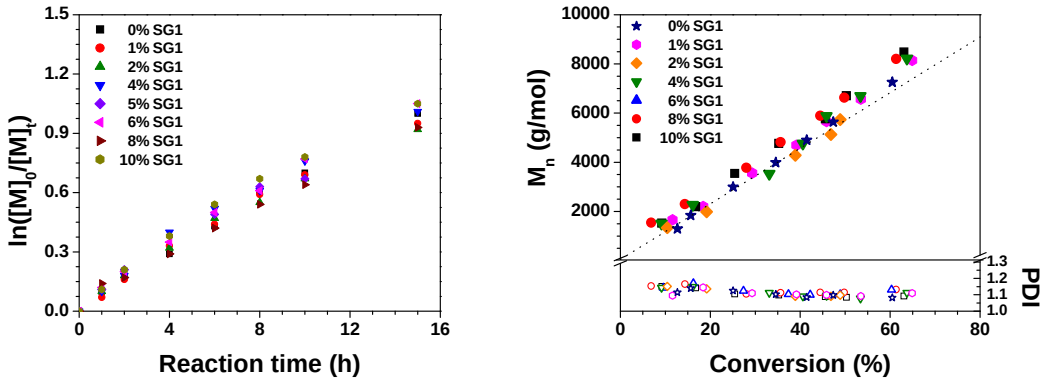

Figure 2.4. *Left:* First order kinetic plot for the polymerization of St in anisole with additional free–nitroxide at different concentrations. *Right:* Corresponding M_n and PDI values *versus* monomer conversion plot.

However, in the case of the NMP of *t*BA in anisole a significant decrease on the polymerization rates was observed with the addition of free nitroxide. The calculated apparent rates of polymerization for *t*BA at different concentrations of additional free nitroxide are listed in Table 2.1. Besides, the control over the molar mass distribution of P*t*BA was improved by introducing a slight excess of free nitroxide. The semi–logarithmic kinetic plot of NMP of *t*BA with different amounts of free nitroxide content is shown in Figure 2.5. The highest reaction rate was obtained in the absence of free nitroxide; however, the measured PDI value was over 1.5 which is a clear indication of an increased rate of side reactions. These side reactions were suppressed by addition of an excess of SG1. It can be concluded that the addition of 5 to 6% excess of SG1 (regarding to the amount of alkoxyamine initiator) to the polymerization medium of *t*BA improves the control over the molar mass distribution with reasonable polymerization periods.

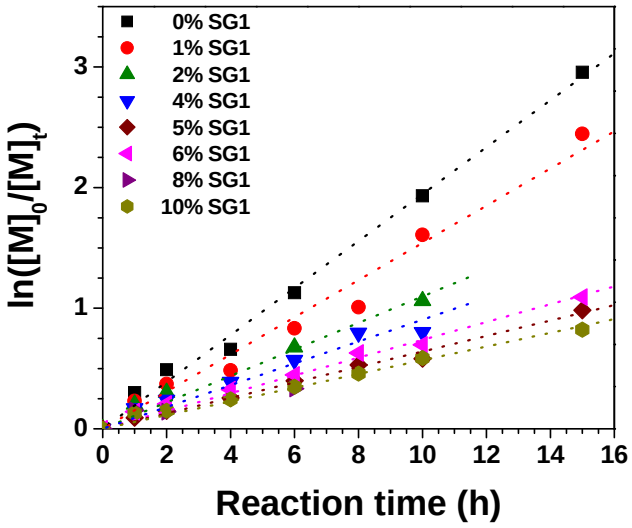

Figure 2.5. First order kinetic plot for the polymerization of *t*BA in anisole with additional free–nitroxide at different concentrations.

Table 2.1. Polymerization of *t*BA in anisole at different concentrations of free nitroxide.

Run	Ini:SG1	Time [hours]	Conv [%]	$M_{n,theo}$ [g/mol]	$M_{n,SEC}$ [g/mol]	PDI [M_w/M_n]	k_p^{app} [10^{-5} s^{-1}]
1	1:0.00	15	95	12,200	7,800	1.53	5.41
2	1:0.01	15	91	11,700	7,200	1.59	4.28
3	1:0.02	10	65	8,300	7,600	1.39	3.05
4	1:0.04	10	55	7,100	7,600	1.35	2.51
5	1:0.05	15	63	8,100	7,200	1.30	1.78
6	1:0.06	15	66	8,500	7,300	1.31	2.05
7	1:0.08	6	28	3,600	6,500	1.24	1.65
8	1:0.10	15	56	7,200	6,700	1.24	1.58

2.3 Synthesis of a 3×3 library of poly(styrene)–*b*–(*tert*–butyl acrylate) block copolymers

PS macroinitiators with three different chain lenght and a P*t*BA macroinitiator were synthesized according to the insights in the polymerization kinetics that were obtained from the parallel screening experiments. PS macroinitiators with narrow molar mass distributions as low as 1.08 were synthesized in anisole at 110 °C without any additional free nitroxide. These macroinitiators were intended for further use in the synthesis of PS–*b*–P*t*BA block copolymers. Before further use, the macroinitiators were characterized by SEC measurements. In addition, a P*t*BA macroinitiator with 65 repeating units was synthesized in anisole with an

additional 6% of SG1 at 110 °C and 12 hours of reaction time. The synthesis of these macroinitiators is described in further detail in the experimental part and the obtained results are summarized in Table 2.2.

Table 2.2. Synthesis of PS and P*t*BA macroinitiators initiated by Bloc Builder™ in anisole.

Run	Monomer	Mon:Ini	Additive [SG1]	Time [hours]	Conv [%]	$M_{n,\,theo}$ [g/mol]	$M_{n,\,SEC}$ [g/mol]	PDI [M_w/M_n]
1	St	100:1	–	5.5	70	7,300	5,200	1.08
2	St	120:1	–	6	67	8,400	8,200	1.13
3	St	200:1	–	6.5	70	14,600	12,500	1.11
4	*t*BA	200:1	0.06	12	50	12,800	8,300	1.25

Moreover, block copolymers of PS–*b*–P*t*BA were synthesized in the automated synthesizer by using different PS macroinitiators and characterized by GC and SEC. The reaction scheme is depicted in Scheme 2.2. Excess of SG1 (6%) was added and the reactions were performed at 110 °C for 20 hours and samples were withdrawn in different time intervals for GC and SEC analysis. The kinetic data of the block copolymerizations is illustrated in Figure 2.6 as a semilogarithmic kinetic plot.

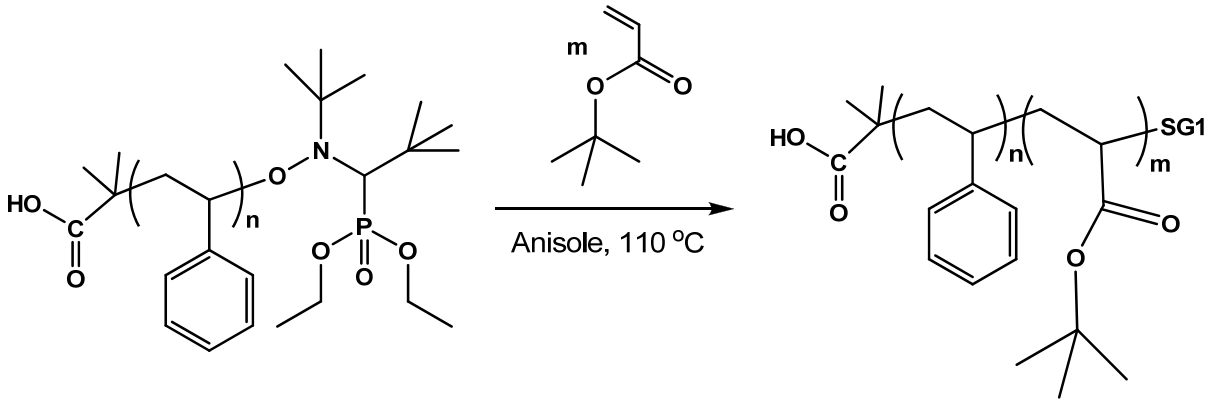

Scheme 2.2. Schematic representation of the nitroxide mediated block copolymerization of *t*BA initiated by the PS macroinitiator.

It was observed that the conversions of *t*BA are limited when the polymerization was initiated with a PS macroinitiator. The possible explanation for this behavior might be the hydrogen abstraction of the free nitroxide from the *t*BA monomers that will result in deactivated free nitroxide and an active radical chain end. Unfortunatelly, these active chain ends can easily undergo termination reactions and most likely disproportionation reaction would occur in the case of acrylate polymerization. Nevertheless, PS–*b*–P*t*BA block copolymers could be obtained with narrow molar mass distributions. The data obtained from this screening were summarized in Table 3.

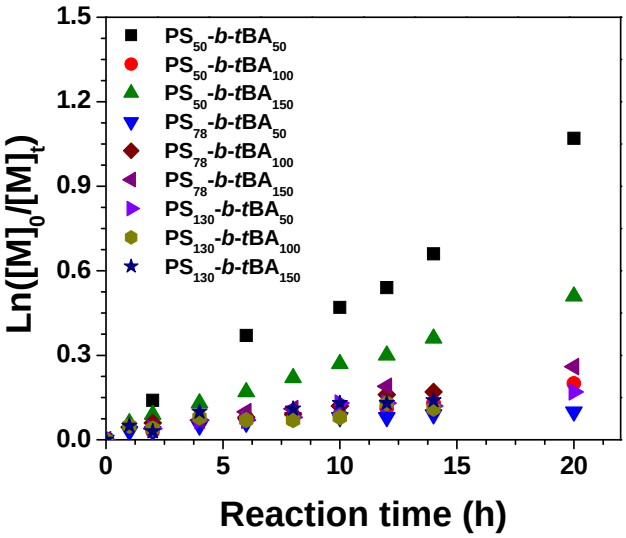

Figure 2.6. First order kinetic plot for the block polymerization of *t*BA initiated by various PS macroinitiators.

Table 2.3. PS_n–SG1 initiated block copolymerization of PS–*b*–P*t*BA at different macroinitiator to monomer ratios.

Run	PS_n [n]	Ini:*t*BA	Time [hours]	Conv [%]	$M_{n,theo}$ [g/mol]	$M_{n,SEC}$ [g/mol]	PDI [M_w/M_n]
1	50	1: 50	20	65	13,600	6,700	1.17
2	50	1:100	20	18	7,500	6,600	1.12
3	50	1:150	20	40	10,300	14,800	1.33
4	78	1: 50	20	10	9,400	8,900	1.10
5	78	1:100	14	15	10,200	9,900	1.09
6	78	1:150	20	23	11,100	11,100	1.15
7	120	1: 50	14	11	14,800	14,800	1.13
8	120	1:100	14	10	14,100	15,600	1.10
9	120	1:150	14	13	14,500	17,300	1.11

P*t*BA initiated block copolymerization of St was investigated to synthesize block copolymers with lower polydispersity indices at higher monomer conversions. Reactions were carried out at a monomer concentration of 2 M and 6% of excess of SG1, at 110 °C for 35 hours. It was obvious that the P*t*BA macroinitiator exhibits good initiation and revealed controlled polymerization of the second block as shown in Figure 2.7. The experimental and theoretical molar masses, PDI and conversion values are as follows: $M_{n,SEC}$ = 18,600 g/mol, $M_{n,theo}$ = 17,100 g/mol, PDI = 1.20, conversion = 84%. SEC traces of the block copolymers at different polymerization times are displayed in Figure 2.7.

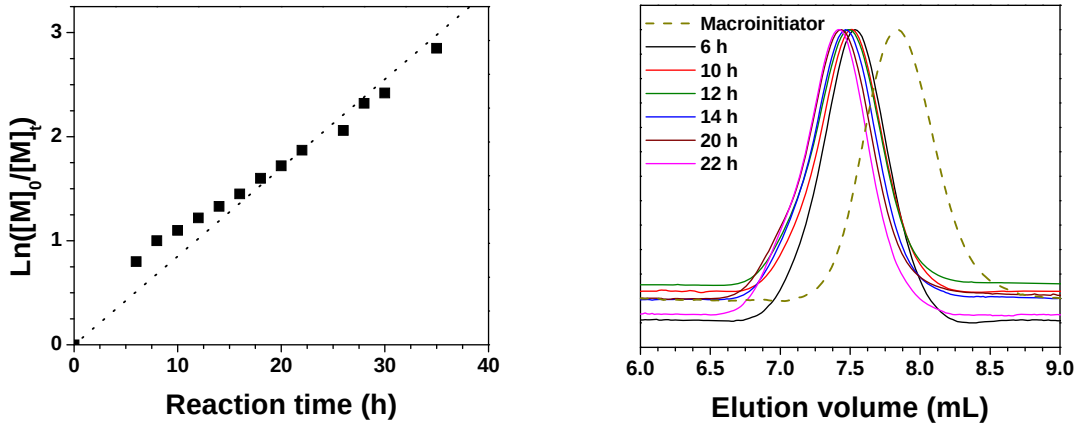

Figure 2.7. *Left:* First order kinetic plot for the block polymerization of St initiated by P*t*BA macroinitiator. *Right:* Corresponding SEC traces of the obtained block copolymers.

Finally, PS–*b*–P*t*BA and P*t*BA–*b*–PS block copolymers were synthesized with narrow molar mass distributions (PDI < 1.2) in the automated synthesizer and also characterized by GC and SEC in order to determine the monomer conversion and the molar masses. In conclusion, the synthesis of block copolymers consisting of St and *t*BA repeating units is more efficient and well–controlled by using P*t*BA macroinitiators in comparison to PS macroinitiators.

2.4 Synthesis of libraries of statistical hydroxypropyl containing copolymers

Smart materials with a stimuli responsive behavior have attracted great attention in the last decade. The responsive polymers exhibit a phase transition upon change in the temperature or pH value of the medium. A narrow molar mass distribution is an important prerequisite to create polymers with sharp lower critical solution temperature (LCST) transitions.[33] Controlled radical polymerization techniques provide access to a large collection of monomers that can be polymerized in a controlled manner.[34] NMP was chosen for the present study as the development of acyclic phosphonylated nitroxides like *N*–*tert*–butyl–*N*–(1'–diethylphosphono–2,2'–dimethylpropyl)–nitroxide (SG1)[35,36] and highly reactive alkoxyamine initiators, such as the Bloc Builder™ initiator[37] greatly improved the versatility, rate and efficiency of this polymerization method.[38–39] The polymerization rates of highly reactive monomers can be tuned using additional free nitroxide and controlled polymerization of styrenics, acrylates, and acrylamides was already demonstrated.[40,41]

In the framework of this Ph.D. thesis, we intended to access a new group of polymers with tunable LCST by copolymerizing HPA with Amor and DMA. The reported LCST value

for PHPA is 16.0 °C.[42] Therefore, incorporation of more hydrophilic monomers such as HPA to PAmor or PDMA allows to tune the LCST of the copolymers. In doing so, we would like to add HPA and Amor to the already vast collection of monomers that can be polymerized in a controlled manner using the Bloc Builder™ initiator in NMP. In order to facilitate kinetic investigations and to create copolymer libraries for studying structure–property relationships, a high–throughput experimentation set–up is used.[43] Scheme 2.3 displays the schematic representation of the structure of 2–hydroxypropyl acrylate (HPA) and the selected hydrophilic comonomers, *N*–acryloyl morpholine (Amor) and *N*,*N*–dimethylacrylamide (DMA). Although controlled radical polymerization of HPA *via* RAFT was reported recently, the NMP of HPA was not yet reported.[44] However, NMP of hydroxyethyl acrylate using SG1 has been described.[45,46] Amor has been reported as comonomer in LCST polymers using both free radical[47] and RAFT polymerization procedures.[48–50] NMP of Amor has only been described in a copolymerization with styrene using hydroxy–TEMPO, but the homopolymerization was uncontrolled.[51] DMA was added to the present library as it is a well–known comonomer for LCST applications in combination with acrylates,[52,53] St[54] and other acrylamides.[55–57] Controlled NMP of DMA has also been reported with various nitroxides[58] as well as with AIBN/SG–1[59,60] and Bloc Builder™/SG1.[61]

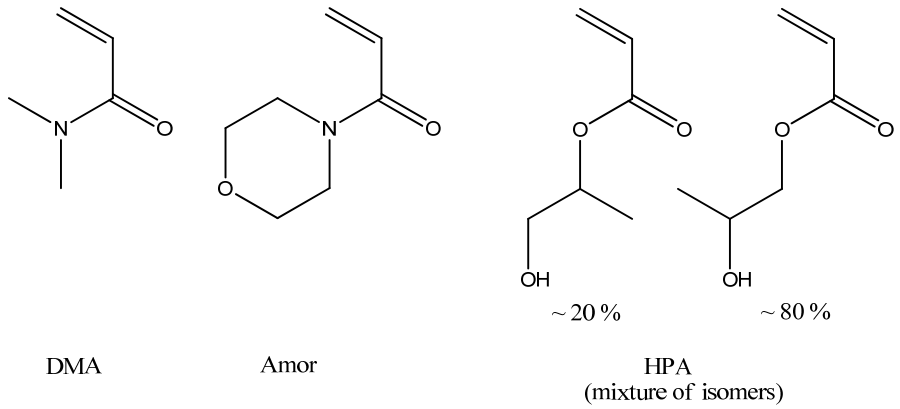

Scheme 2.3. Schematic representation of the monomers used for the synthesis of thermoresponsive copolymers.

In the present study, a kinetic investigation was conducted for the homopoly–merizations of Amor, DMA and HPA to establish optimal reaction conditions for the synthesis of statistical copolymers based on these monomers. The use of a Chemspeed ASW2000 synthesis robot allowed rapid screening of important reaction parameters, such as the solvent, temperature and free nitroxide concentration. The previously obtained optimal conditions for the NMP of *t*BA were taken as a starting point: toluene as solvent, 110 °C polymerization temperature and SG1 percentages up to 10% relative to the alkoxyamine initiator.[62] Since poly(*N*–acryoyl morpholine) (PAmor) is insoluble in toluene, *N*,*N*–

dimethylformamide (DMF) was taken as a more polar solvent, which is known to increase the polymerization rate in NMP.[63] Temperatures of 110 °C and 120 °C were tested with SG1 percentages up to 20%. Increased polymerization rates were obtained at 120 °C reducing the reaction times, but none of the polymerizations revealed good control at 120 °C, even with 20% additional SG1. Therefore, all further reactions were performed at 110 °C. Other reaction conditions were kept constant using a 2 M monomer concentration and a monomer/initiator ratio of 100 to 1. For the kinetic investigations, nine aliquots were withdrawn from the polymerization mixtures at set intervals during 15 hours to determine the monomer conversions, average molar masses and polydispersity indices.

The optimization of the additional SG–1 percentage at 110 °C in DMF for Amor is shown in Figure 2.8. Linear first order kinetics were observed for NMP of Amor at different SG1 percentages indicating a constant concentration of propagating radicals under these conditions. Amor revealed the highest polymerization rates without additional SG1, but the polydispersity indices demonstrated poorly controlled polymerization.

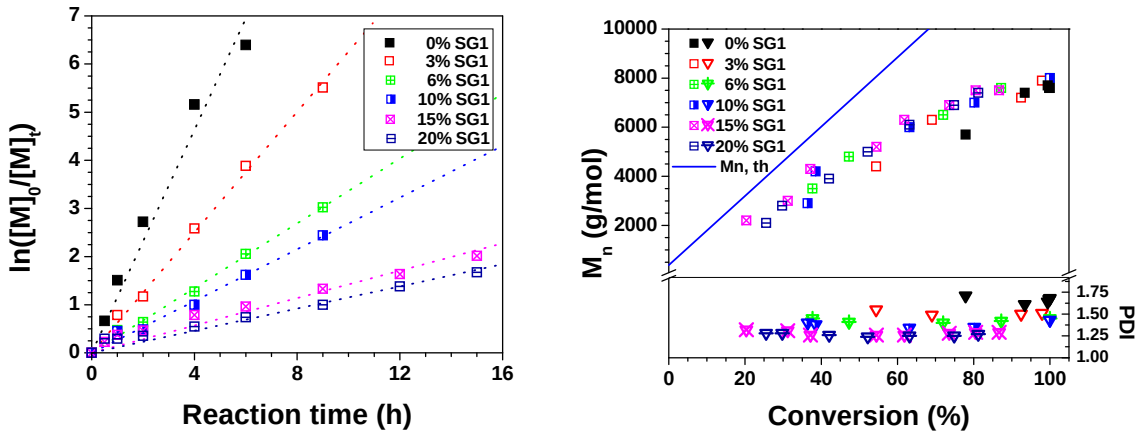

Figure 2.8. *Left:* First order kinetic plot for the polymerization of Amor in DMF at 110 °C with different concentrations of additional free–nitroxide. *Right:* Corresponding M_n and PDI values *versus* monomer conversion plot.

With the addition of free nitroxide, the polymerization rate decreased due to the presence of more dormant species and thus a lower free radical concentration. The lower concentration of free radicals results in less termination reactions leading to the necessary increase in control. With the addition of 20% SG1, PDI values in the range from 1.2 to 1.3 were obtained for a conversion up to 80%. For all investigated Amor polymerizations with additional SG1, the M_n increased linearly with the conversion with a lower slope than the theoretical M_n. In general, there is most likely a discrepancy between the hydrodynamic volume of PAmor and the PMMA calibration used for calculating the molar mass. In addition,

the occurrence of some chain transfer and/or auto–initiation reactions may result in lower molar mass than the expected values.

Similar to the results for Amor and to what has been reported in literature,[59–61] controlled polymerization of DMA was achieved by addition of SG1. Without the free nitroxide, a non–zero intercept in the semi–logarithmic plot and PDI values of ~1.6 were observed, indicating a relatively fast initiation and the occurrence of side reactions. Nonetheless, the desired level of control was obtained at 15% and 20% SG1 with PDI values in between 1.20 and 1.25. The M_n values increased linearly with conversion up to ~75%. The slightly lower slope than for the theoretical M_n may result from similar effects as discussed previously for PAmor. Addition of 20% SG1 resulted in improved control and PDI values in the range of 1.2 to 1.3 for conversions up to at least 60%. In the case of DMA, 20% SG1 resulted in similar control as 15%, while for the other two monomers an increase in control could still be observed. Nevertheless, 20% SG1 was taken as the maximum as it led to the desired control, while still a reasonable conversion could be obtained within 15 hours reaction time.

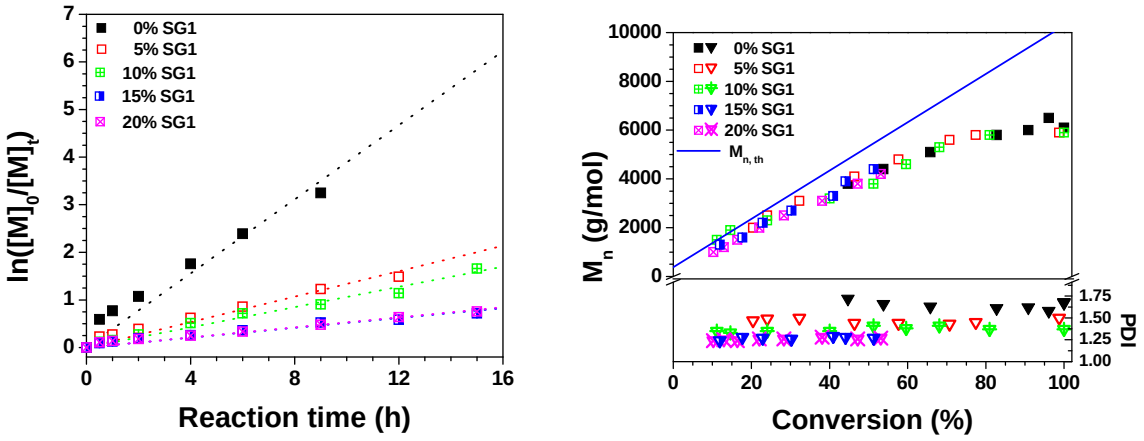

Figure 2.9. *Left:* First order kinetic plot for the polymerization of DMA in DMF at 110 °C with different concentrations of additional free–nitroxide. *Right:* Corresponding M_n and PDI values *versus* monomer conversion plot.

Reaction conditions of 110 °C and 20% additional SG1 also resulted in the best results for the homopolymerization of HPA. The M_n increased linearly with the conversion up to 60%, after which the M_n leveled off and the PDI values started to increase. Possible side reactions, such as chain transfer, autoinitiation, termination and nitroxide decomposition, may cause the increased PDI values at higher monomer conversions. Therefore, reaction times should be limited to aim for 60% conversion of HPA to ensure good control over the polymerization.

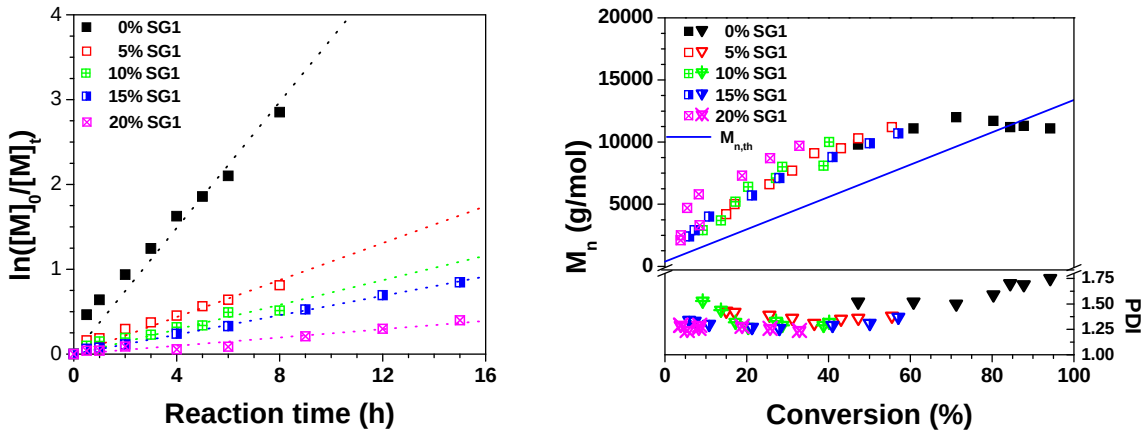

Figure 2.10. *Left:* First order kinetic plot for the polymerization of HPA in DMF at 110 °C with different concentrations of additional free–nitroxide. *Right:* Corresponding M_n and PDI values *versus* monomer conversion plot.

In addition, the M_n values obtained by SEC measurements seem to be overestimated using the PMMA calibration. Unfortunately, poly(2–hydroxypropyl acrylate) (PHPA) is not suitable for MALDI–TOF MS analysis and end group identification in ^{1}H NMR spectroscopy was not possible. However, the livingness of the polymerization was confirmed by the continuous progression of the SEC traces with time as presented in Figure 2.10. The monomer conversions were calculated as the sum of the two hydroxypropyl acrylate isomers. The increasing molar masses with conversion and progression of the monomodal SEC traces in time further confirmed the control over the polymerizations of all three monomers.

The two hydrophilic monomers, Amor and DMA, were copolymerized with HPA to create two libraries with tunable LCST properties. The reaction conditions were chosen based on the kinetic investigation of the homopolymerizations. For all three monomers good control was obtained for 2 M DMF solutions at 110 °C and with 20% additional SG1. Statistical copolymers of Amor with HPA and DMA with HPA were synthesized with varying monomer feed ratios from 0 to 100 mol% HPA with intervals of 10 mol% for both combinations. To achieve well–defined materials with narrow molar mass distributions and thus sharp LCST transitions, reaction times of 8 hours and 15 hours were used for the Amor and DMA library, respectively.

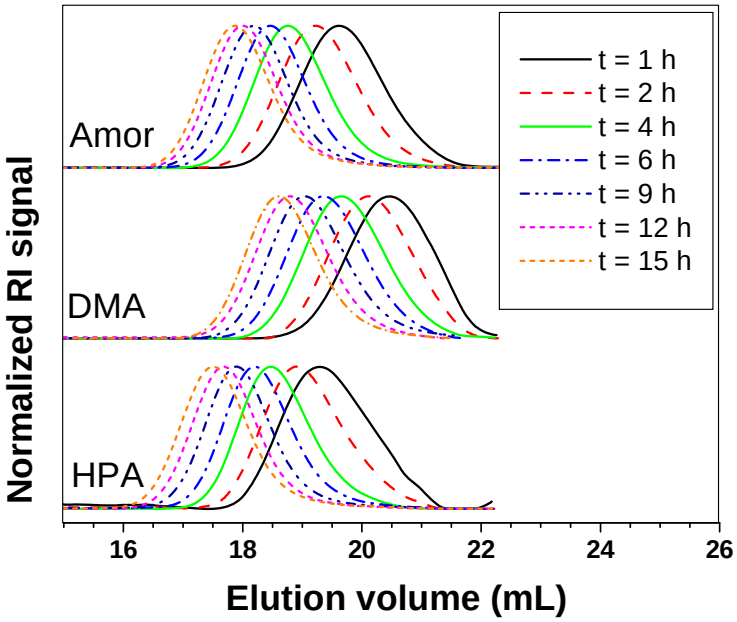

Figure 2.11. SEC traces of the obtained homopolymers at different reaction times.

The copolymers obtained for the PAmor–*stat*–PHPA library revealed relatively low polydispersity indices in the range from 1.16 to 1.32 and increasing M_n values with increasing HPA content (Table 2.4). This is in contradiction with the lower molar mass of HPA and the lower conversions observed for the polymerizations with higher HPA contents in the monomer feed.

However, this can be ascribed to the use of the PMMA calibration in the SEC measurements and corresponds to the difficulties already encountered for the determination of the M_n of the homopolymers. The SEC traces show a constant progression of M_n with time as depicted in Figure 2.12. The monomer conversions appear to be dependent on the composition of the monomer mixture. The observed polymerization rates for both monomers decreased with increasing HPA content. Apparently, the polymerization rate is dominated by the slower HPA–SG1 dissociation and association kinetics. For A100 in Table 2.4, the conversion is calculated by ^{1}H NMR spectroscopy.

Copolymer compositions could be calculated from the GC conversion as well as by using ^{1}H NMR spectroscopy of the precipitated polymers. However, the latter method was complicated due to overlapping signals of the Amor side group (–C*H*$_2$–, δ = 3.1–3.9 ppm) and HPA signals (–C*H*$_2$– and C*H*, δ = 3.4–4.2 ppm). Nevertheless, in both methods similar compositions were obtained and the ^{1}H NMR compositions were used to determine structure–property relationships for this library.

Table 2.4. Copolymerization results of the PAmor–*stat*–PHPA library.

Name [a]	Conversion [b] [%] Amor / HPA	M_n [c] [g/mol]	PDI [c]	Composition GC [b] [mol%] Amor / HPA	Composition NMR [d] [mol%] Amor / HPA
A100	70 / 0 [e]	6,900	1.32	100 / 0	100 / 0
A90H10	63 / 69	7,700	1.27	89 / 11	90 / 10
A80H20	48 / 51	7,200	1.22	79 / 21	78 / 22
A70H30	56 / 53	8,300	1.26	71 / 29	68 / 32
A60H40	45 / 38	8,100	1.21	64 / 36	58 / 42
A50H50	45 / 42	8,500	1.23	52 / 48	47 / 53
A40H60	37 / 28	8,300	1.20	47 / 53	38 / 62
A30H70	37 / 31	8,800	1.20	34 / 66	29 / 72
A20H80	34 / 28	8,400	1.20	23 / 77	18 / 82
A10H90	28 / 20	8,100	1.16	13 / 87	7 / 93
H100	0 / 22	8,200	1.16	0 / 100	0 / 100

[a] Names indicate monomer feed: A50H50 = $PAmor_{50}$–*stat*–$PHPA_{50}$, [b] calculated by GC using monomer/DMF ratios, [c] of the precipitated polymer, determined by SEC in DMAc using PMMA calibration, [d] ^{1}H NMR spectra were recorded in $CDCl_3$, [e] conversions calculated by ^{1}H NMR spectroscopy.

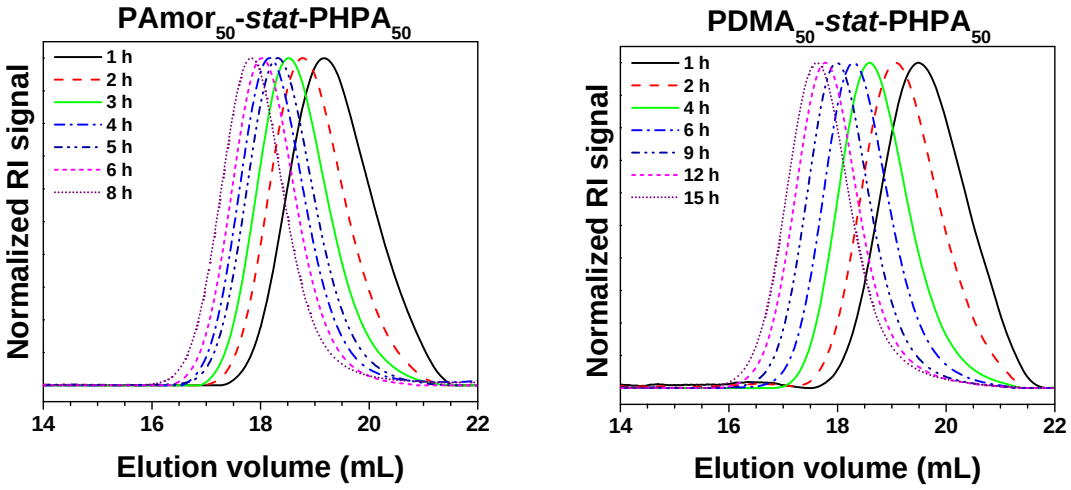

Figure 2.12. SEC traces of the obtained copolymers at different reaction times.

A reaction time of 15 hours was used for the synthesis of the PDMA–*stat*–PHPA library, which corresponds to 60% conversion in the homopolymerization of DMA and 47% conversion for HPA. The relatively low PDI values (1.20 to 1.27, Table 2.5) of the resulting polymers indicate a controlled copolymerization. The M_n of the copolymers increased with the increasing HPA content as the HPA monomer has a larger molar mass than DMA (M_{HPA} = 130.14 g/mol and M_{DMA} = 99.13 g/mol). In addition, the M_n of PHPA was also found to be

overestimated using the PMMA calibration (see Figure 2.10). The conversions of the copolymerization that were determined by GC analysis revealed an unexpected variation, which appears to represent a large error in the measurements. Interactions of this monomer combination with the glass polymer liner of the GC are thought to cause these errors. The alternative method, ^{1}H NMR spectroscopy, was not suitable for reliable conversion determination since the DMA–C*H*$_3$ groups overlap not only with the HPA–O*H* group in the ^{1}H NMR spectra, but also with broad backbone signals, which obstruct a reliable integration. Because of the large uncertainty in the GC conversion and the ^{1}H NMR spectroscopy integration, elemental analysis was used as alternative method to calculate the molecular composition of the copolymers. The molar compositions resulting from EA are within 5% of the initial monomer feed independent of the monomer ratio, indicating a random incorporation of the monomers. Table 2.5 shows the compositions calculated according to the GC conversion, the ^{1}H NMR spectroscopy and elemental analysis.

Table 2.5. Copolymerization results of the PDMA–*stat*–PHPA library.

Name [a]	**Conversion** [b] **[%] DMA / HPA**	**M_n** [c] **[g/mol]**	**PDI** [c]	**Composition NMR** [d] **[mol%] DMA/HPA**	**Composition EA [mol%] DMA/HPA**
D100	53 / 0	4,500	1.23	100 / 0	100 / 0
D90H10	60 / 93	6,800	1.20	85 / 15	88 / 12
D80H20	46 / 36	6,500	1.23	75 / 25	78 / 22
D70H30	67 / 73	8,400	1.27	69 / 31	68 / 32
D60H40	57 / 56	8,500	1.24	53 / 48	59 / 41
D50H50	66 / 53	9,800	1.27	46 / 54	50 / 50
D40H60	58 / 53	9,600	1.26	33 / 67	41 / 59
D30H70	82 / 29	10,900	1.24	28 / 72	32 / 68
D20H80	57 / 44	10,700	1.22	18 / 82	22 / 78
D10H90	71 / 48	10,500	1.20	9 / 91	12 / 88
H100	0 / 33	11,100	1.21	0 / 100	0 / 100

[a] Names indicate monomer feed: D50H50 = PDMA$_{50}$–*stat*–PHPA$_{50}$, [b] calculated by GC using monomer/DMF ratios, [c] determined by SEC in DMAc using PMMA calibration, [d] ^{1}H NMR spectra recorded in $CDCl_3$.

2.5 Glass transition temperature and LCST behavior of responsive polymers

Polymers with a lower critical solution temperature (LCST) show a reversible solubility profile in water, *i.e.* the polymers precipitate upon heating and dissolve with cooling. At temperatures below the LCST, the polymer chains are hydrated and form hydrogen bonds with water molecules (Scheme 2.4). Weakening of the hydrogen bonds at higher temperatures causes entropy driven phase transition of the polymer to a hydrophobic collapsed state. Such thermoresponsive polymers are of major interest for biotechnological applications[64] including tissue engineering,[65] biomolecule separation[66,67] and drug delivery systems,[68] but are also of interest for industrial applications in catalysis[69,70] or as membranes.[71,72] Since the phase transition temperature is directly related to the hydrophilic/hydrophobic balance in a (random co)polymer, controlling the polymer composition provides a very effective way of tuning the LCST. By creating systematical libraries of random copolymers, the relationship between monomer composition and LCST can be studied in detail.[73–75] The most widely studied thermoresponsive polymer is poly(*N*–isopropylacrylamide) (p(NIPAM)), which is known since 1956 and still attracts a lot of attention, because its LCST of 32 °C is close to physiological conditions and the phase transition shows little concentration dependence.[76,77] A surprisingly little studied polymer with LCST behavior is PHPA with a reported LCST of 16 °C at 10 wt%. Although its thermosensitivity was already reported in 1975, other appearances in literature are limited to the use of HPA as comonomer in thermoresponsive hydrogels.[78,79] Because of the low LCST of PHPA, copolymerization with a more hydrophilic monomer is expected to lead to a library that covers a broad range of transition temperatures.

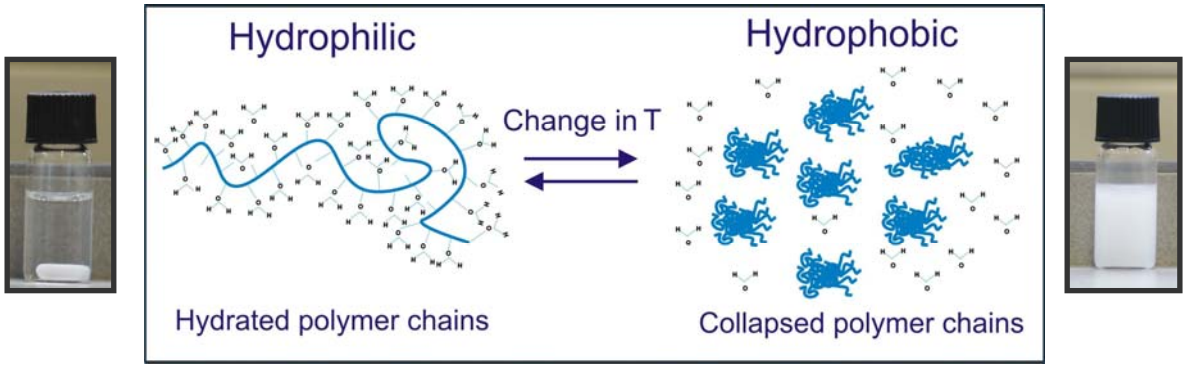

Scheme 2.4. Schematic representation of the LCST behavior of polymers below (*left*) and above (*right*) their phase transition temperature.

Initially, the thermal properties of the two copolymer libraries were investigated using differential scanning calorimetry (DSC). For both libraries, single glass transition

temperatures were observed which could be related to the monomer composition, indicating good mixing of the two polymers and/or a random monomer distribution. To further test the miscibility of the homopolymers, two blends of Amor/HPA and DMA/HPA were prepared. The blends showed a weak single glass transition that was within 10 °C of the glass transition of the corresponding copolymer with similar weight fractions of composition, demonstrating good miscibility of the homopolymers. For the thermal analysis, PHPA reacted for 15 h was used for both libraries, as the amount of isolated PHPA synthesized with 8 hours of reaction time was not sufficient for a proper analysis.

The transition temperatures for PAmor–*stat*–PHPA and PDMA–*stat*–PHPA as function of the wt% HPA are displayed in Figure 2.13. For the Amor library, glass transitions temperatures were found to be in between 147 °C (for PAmor) and 22 °C (for PHPA) as listed in Table 2.6.

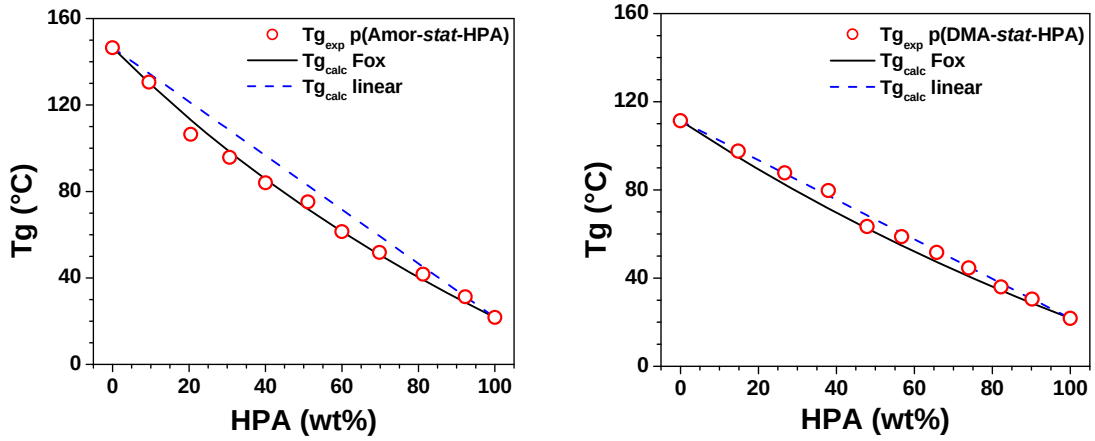

Figure 2.13. Glass transition temperature *versus* composition for the PAmor–*stat*–PHPA library (*left*) and the PDMA–*stat*–PHPA library (*right*).

The glass transition of D100 (homopolymer of DMA) was observed at 111 °C and the glass transitions for the PDMA–*stat*–PHPA copolymers, listed in Table 2.7, also revealed a relation to the wt% HPA in the temperature range of 111 °C to 22 °C. The Fox equation predicts the glass transition temperature of polymer blends or statistical copolymers *via* a reciprocal relation to the weight fraction of the composition and the transition temperature of the homopolymers.[80]

However, polymers with specific interactions such as hydrogen bonding may show glass transition temperatures with a positive deviation from the Fox equation.[81–83] For PAmor–*stat*–PHPA, the glass transition temperatures correspond well to the Fox equation (Figure 2.13). However, the glass transition temperatures of the PDMA–*stat*–PHPA

copolymers show a positive deviation with the Fox equation indicating the presence of weak hydrogen bonding of the HPA hydroxyl group with the amide group of DMA.

Table 2.6. Thermal properties and cloud points for the copolymers of the PAmor–*stat*–PHPA library.

Name	Composition [a] Amor/HPA [wt%]	Tg [b] [°C]	Cloud point [c] 0.5 wt% [°C]	Cloud point [c] 1.0 wt% [°C]
A100	100/0	146.5	soluble	soluble
A90H10	90 / 10	130.6	soluble	soluble
A80H20	80 / 20	106.4	soluble	soluble
A70H30	69 / 31	95.8	soluble	soluble
A60H40	60 / 40	84.0	soluble	88.0
A50H50	49 / 51	75.2	79.5	65.9
A40H60	40 / 60	61.4	62.7	53.0
A30H70	30 / 70	51.8	49.2	38.3
A20H80	19 / 82	41.7	41.5	30.9
A10H90	8 / 82	31.3	33.9	25.3
H100 [d]	0 / 100	21.7	26.7	21.4[d]

[a] Calculated from ^{1}H NMR spectroscopy, [b] mid–temperature, [c] 50% transmittance point in first heating curve, [d] PHPA synthesized with 15 h reaction time.

Since there are only few reports on the thermoresponsive behavior of PHPA in water, the LCST of this polymer was determined at different concentrations. Figure 2.14 shows the transmittance as function of the temperature for 0.25, 0.5, 1.0 and 1.5 wt% aqueous solutions, respectively. The 50% transmittance point in the first heating curve is taken as the cloud point, which ranges from 18.3 °C at 1.5 wt% to 33.3 °C at 0.25 wt% for PHPA. Three important observations can be made from the curves in Figure 2.14. First, the LCST decreases with increasing polymer concentration; a behavior that is also observed for other LCST polymers at concentrations below 20 wt%.[84,85] Secondly, the transition becomes more diffuse at low concentrations, in particular in the dissolution curve.

Finally, large hysteresis was observed at the lower concentrations with the redissolution occurring at higher temperatures than the precipitation. Since the size of the aggregates formed above the LCST is dependent on the concentration,[86] it appears that the intermolecular aggregation is less efficient for the lower concentrated samples. In addition, an incomplete aggregate formation could explain the higher dissolution temperature. Nevertheless, more detailed studies using FT–IR spectroscopy and/or DLS need to be performed in future work to provide a conclusive explanation for the observed behavior. It is worth noticing that the hysteresis detected is reversed from the hysteresis observed for

poly(*N*–isopropyl acrylamide) (PNIPAM), where limited diffusion of water into the hydrophobic aggregates above the LCST retards the rehydration process.[87] This might indicate fast diffusion of water into the PHPA aggregates above the LCST.

Table 2.7. Thermal properties and cloud points for the copolymers of the PDMA–*stat*–PHPA library.

Name	Composition [a] DMA/HPA [wt%]	Tg [b] [°C]	Cloud point [c] 0.5 wt% [°C]	Cloud point [c] 1.0 wt% [°C]
D100	100 / 0	111.4	soluble	soluble
D90H10	85 / 15	97.6	soluble	soluble
D80H20	73 / 27	87.7	soluble	soluble
D70H30	62 / 38	79.7	soluble	soluble
D60H40	52 / 48	63.4	soluble	soluble
D50H50	43 / 57	58.8	soluble	82.9
D40H60	34 / 66	51.6	71.6	62.3
D30H70	26 / 74	44.6	55.8	48.7
D20H80	18 / 82	36.0	46.7	38.6
D10H90	10 / 90	30.5	35.3	28.5
H100	0 / 100	21.7	26.7	21.4

[a] Calculated from elemental analysis, [b] mid–temperature, [c] 50% transmittance point in first heating curve.

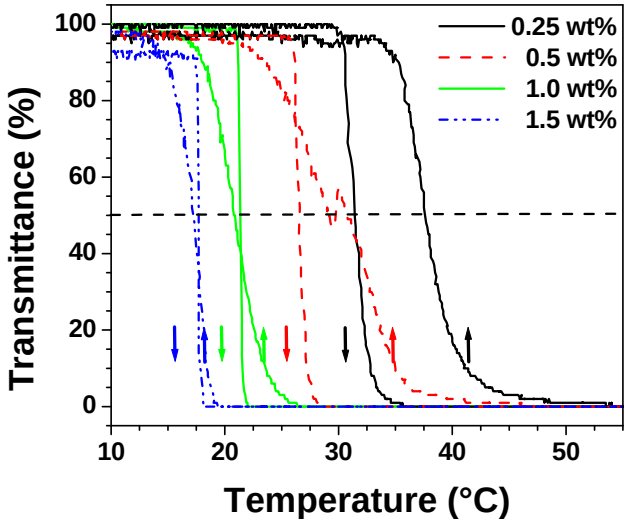

Figure 2.14. Transmittance as a function of temperature for PHPA (M_n = 11,100 g/mol, PDI = 1.21) at different concentrations.

The LCST behavior of the two copolymer libraries was studied at two different concentrations, 0.5 wt% and 1.0 wt%. The observed cloud points are listed in Table 2.6 and Table 2.7. For both libraries the cloud points could be tuned between 20 °C and 100 °C. The 50% transmittance points of the first heating curve are displayed in Figure 2.15 as function of

the wt% HPA showing a clear decrease in cloud points with increasing HPA content. The cloud point dependence on the HPA content is comparable for 0.5 wt% and 1.0 wt%, although the transitions in 0.5 wt% solutions occur approximately 10 °C higher. The PAmor–*stat*–PHPA copolymers with > 40 wt% HPA showed cloud points at 1.0 wt%, while at 0.5 wt% > 55 wt% HPA was required. The more hydrophilic DMA monomer causes a slightly sharper increase in the LCST compared to Amor. For this library, the polymers with more than 55 wt% HPA showed LCST behavior at 1.0 wt% polymer concentration while 65 wt% HPA was required to find a cloud point at 0.5 wt% polymer concentration.

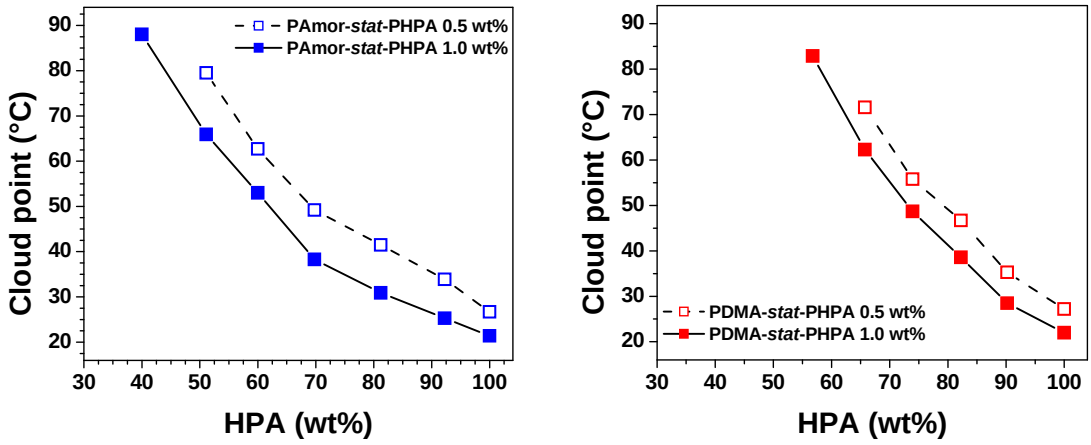

Figure 2.15. Cloud point as a function of polymer composition estimated by 50% transmittance points for the first heating curves for PAmor–*stat*–PHPA (*left*) and PDMA–*stat*–PHPA (*right*).

The transmittance drop of the first heating curve as function of the temperature is displayed in Figure 2.16. Sharp transitions are observed for the polymers with high HPA contents similar to PHPA at 1.0 wt%. The polymers with higher hydrophilic content (i.e. A60H40 and D50H50, in Figure 2.16 and Figure 2.17, respectively) show a more diffuse and incomplete transition.

Copolymers of PNIPAM with more hydrophilic monomers also exhibited more diffuse transitions, which was ascribed to an inhibited collapse and aggregate formation by the smaller amount of dissociating water molecules.[56,88] During the cooling curves, a similar increase in transition time was observed (not shown). Before the LCST measurement, A20H80 was not fully dissolved, which explains the slightly lower transmittance at lower temperatures. The transmittance of the soluble polymers slightly decreases due to a change in the sensor sensitivity at higher temperatures.[89]

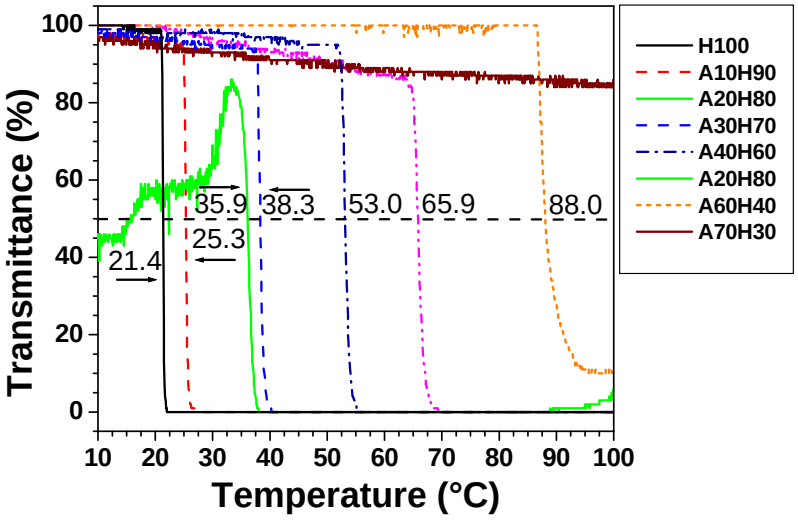

Figure 2.16. Transmittance as a function of temperature for 1.0 wt% aqueous solutions of PAmor–*stat*–PHPA.

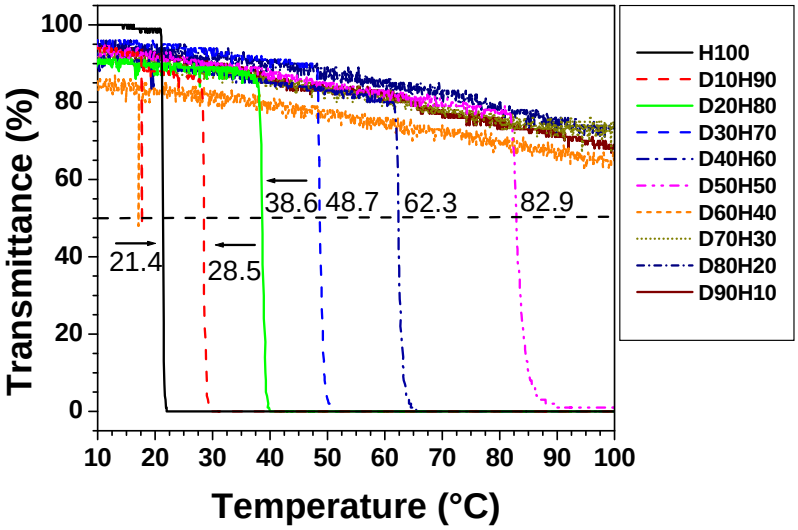

Figure 2.17. Transmittance as a function of temperature for 1.0 wt% aqueous solutions of PDMA–*stat*–PHPA.

Typical turbidity curves of two heating cycles are displayed in Figure 2.18. Although the LCST transition is known to be reversible, copolymers with high HPA contents became clear at all investigated temperatures after several heating cycles at low concentrations. Indeed, the curve of D50H50 reveals a non–complete transmittance drop in the second heating cycle.

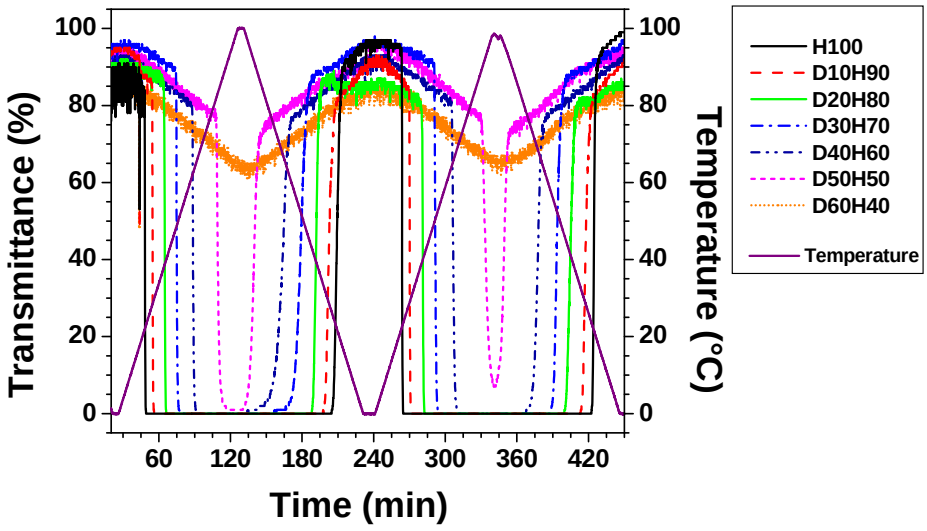

Figure 2.18. Transmittance curves as a function of time for copolymers of the PDMA–*stat*–PHPA library.

Figure 2.19 shows the 50% transmittance points for four heating and cooling cycles of different polymers from the PDMA–*stat*–PHPA library at 1.0 wt%. The increase in LCST with increasing number of heating cycles is most apparent for D50H50, which is soluble after the second heating cycle. D40H60 exhibits an increase of 8 °C in the 50% transmittance point of the heating curve. For PAmor–*stat*–PHPA, similar observations were made. The increase in the LCST for the copolymers with a high hydrophilic content became less noticeable at higher concentrations, as is shown for $PAmor_{40}$–*stat*–$PHPA_{60}$ in Figure 2.20. The temperature difference between precipitation and rehydration also decreases with increasing HPA content or increasing concentration.

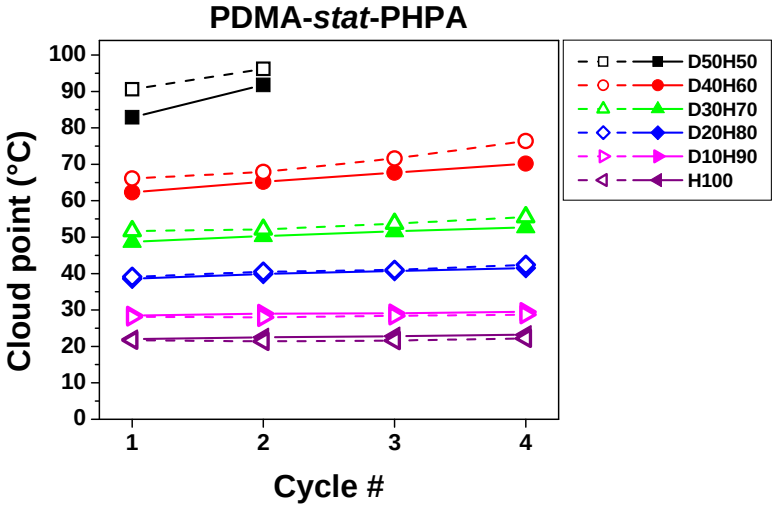

Figure 2.19. Cycle effect on the cloud points determined at 50% transmittance points in the heating curves (closed symbols) and the cooling curves (open symbols) for different compositions of PDMA–*stat*–PHPA at 1.0 wt% concentration.

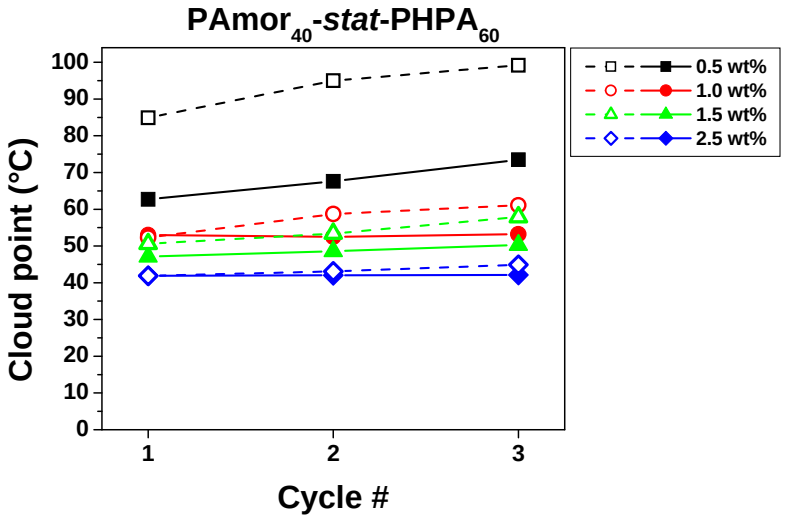

Figure 2.20. Cycle effect on the cloud points determined at 50% transmittance points in the heating curves (closed symbols) and the cooling curves (open symbols) for different compositions of $PAmor_{40}$–*stat*–$PHPA_{60}$ at different concentrations.

The increase of the LCST and hysteresis depends on the concentration as well as the hydrophilic content in the copolymer. Therefore, there seems to be a relation of the observed hysteresis to the size and composition of the aggregates above the LCST. These aggregates decrease in size at lower concentrations and become less dense and contain more water if more hydrophilic monomers are incorporated. Possibly, the size of the aggregates formed by hydrophobic interchain interactions decreases in size with repeating heating cycles and becomes too small to be detected with turbidimetry. Alternatively, the ester bond of HPA can be subject to hydrolysis causing increased hydrophilicity. As test, copolymers, that were heated to 100 °C for 10 hours and became transparent, were freeze dried and analyzed with ^{1}H NMR spectroscopy in DMSO–d_6. However, no acidic groups could be detected at ~12.4 ppm, indicating that no significant hydrolysis occurred. Further investigations on the specific hydrogen bonding interactions and aggregate size may help to identify the cause for this cycle effect.

2.6 Conclusions

The systematic kinetic screening of two important parameters for the NMP of St and *t*BA, namely the polymerization temperature and the concentration of free nitroxide, were investigated by using an automated parallel synthesizer platform. The utilized Chemspeed Accelerator provided fast, reliable and comparable results for the optimization of the nitroxide mediated radical polymerization conditions. The polymerization temperature has the greatest effect on the rate of the polymerization. Therefore, the optimization of the polymerization

temperature of St and *t*BA was conducted at several different temperatures. It was shown that the control over the polydispersity index was lost by increasing the polymerization temperature above 120 °C for the polymerization of both monomers. The optimum polymerization temperatures for the NMP of St and *t*BA were determined as 120 and 115 °C, respectively.

Morerover, the effect of introducing a slight excess of free nitroxide was investigated. In the case of St polymerization no significant influence was observed on the polymerization rates and even on the molar mass distributions. However, the polymerization rate of *t*BA was decreased by introducing a slight excess of free nitroxide to the polymerization medium. It can be concluded that addition of 5 to 6% free nitroxide regarding to the initiator improved the control over the polydispersity indices of the final polymers with reasonable reaction times. Based on the optimum conditions obtained from the optimization reactions, PS and P*t*BA macroinitiators were synthesized with different chain lengths and narrow molar mass distributions. These macroinitiators were used for the preparation of block copolymers consisting of St and *t*BA.

In the second part of this chapter, the nitroxide mediated copolymerization of HPA with Amor or DMA was investigated using Bloc Builder™ alkoxyamine initiator and additional SG1. Different reaction conditions, such as the concentration of additional SG1, were tested to optimize the homopolymerizations using a Chemspeed ASW2000 automated parallel synthesizer. Best control for the homopolymerizations (PDI values of 1.2 to 1.3) of all three monomers was achieved using 20% additional SG1 (relative to the initiator) at a reaction temperature of 110 °C for 2 M solutions in DMF and a monomer/initiator ratio of 100/1. Libraries of PAmor–*stat*–PHPA and PDMA–*stat*–PHPA were synthesized with 0 to 100 mol% HPA with 10 mol% increments using the optimized conditions obtained for the homopolymerizations. The resulting polymers had narrow molar mass distributions and their compositions, determined using ^{1}H NMR spectroscopy and elemental analysis, were found to be close to the theoretical compositions. In addition, single glass transition temperatures were observed for all copolymers of both libraries and the transition temperatures decreased from the T_g of PAmor (147 °C) and PDMA (111 °C) to the T_g of PHPA (22 °C) with increasing HPA content. The LCST behavior of PHPA showed concentration dependence as well as a concentration dependent hysteresis. The cloud points of aqueous solutions of the copolymer libraries could be tuned from 21.4 °C to 88.0 °C and to 82.9 °C for PAmor–*stat*–PHPA and PDMA–*stat*–PHPA, respectively, at a concentration of 1 wt%. LCST behavior was observed for copolymers with >40 wt% HPA in PAmor–*stat*–PHPA and >55 wt% HPA in the PDMA–*stat*–PHPA library. In conclusion, we could systematically study the thermal transitions and

LCST properties as function of copolymer composition of two newly synthesized HPA containing copolymer libraries. As such, HPA might be added to the rather limited number of monomers that can be used to prepare well–defined copolymers with a tunable LCST in aqueous solution.

2.7 Experimental part

Materials

Styrene, *tert*–butyl acrylate and anisole were bought from Aldrich and purified over neutral alumina oxide column prior to use. *N*,*N*–Dimethylacrylamide (99% Aldrich), *N*–acryloyl morpholine (97% Aldrich) and 2–hydroxypropyl acrylate (mixture of isomers, 95%, Aldrich) were filtered over a neutral alumina oxide column and stored in the fridge. All solvents were obtained from Biosolve and used as received. *N*–*tert*–Butyl–*N*–(1'–diethylphosphono–2,2'–dimethylpropyl)–*O*–(2–carboxyl–prop–2–yl) alkoxyamine initiator (Bloc Builder™) and SG1 (85%) free nitroxide were kindly provided by Arkema and used as received.

Instruments

NMP of St and *t*BA were carried out in a Chemspeed Accelerator™ SLT106 automated synthesizer. This synthesizer was equipped with a four needle head, a solid dosing unit, a double jacket heated reaction block and an individual heater reactor block. The individually heater reactor block consists of 16 parallel 13 mL reactors that all have a ceramic heating mantel, which can be individually heated from ambient temperature to 230 ± 1 °C. The double jacket heated block is connected to a Huber Unistat Tango (–40 to 145 ± 1 °C) to provide the heating. All reaction vessels were equipped with cold–finger reflux condensers that could be cooled or heated from –5 °C to 50 °C. An inert atmosphere was maintained by applying a 1.1 bar argon flow over the reactors and a 1.5 bar argon flow through the hood of the automated synthesizer.

NMP of HPA, Amor and DMA were performed in a Chemspeed ASW2000 automated parallel synthesizer.[90] The used reactor block consists of 16 parallel 13 mL vessels, each equipped with a cold finger reflux condenser controlled by a Huber Ministat in a temperature range from –5 °C to 45 °C. The reaction temperature was regulated through a heating jacket connected to a Huber Unistat 390 W cryostat with a temperature range from –90 °C to 150 °C. Agitation of the vessels was achieved by a vortex movement of the reactor block at 500 rpm. Two separately controlled argon flows were applied to flush the hood of the

synthesizer robot and to maintain an argon atmosphere in the reactor block and over the stock solutions.

Size exclusion chromatography (SEC) was performed on a Shimadzu system with a SCL–10A system controller, a LC–10AD pump, a RID–10A refractive index detector and a PSS gram 30 and PSS gram 1000 column in series at 60 °C. A solution of *N,N*–dimethylacetamide (DMAc) containing 2.1 g LiCl/L was used as an eluent at a flow rate of 1 mL/min. The average molar masses were calculated against PMMA calibration standards for the polymers of HPA, DMA and Amor. A different SEC system was utilized for the characterization of St and *t*BA containing polymers, which was a Shimadzu system equipped with a SCL–10A system controller, a LC–10AD pump, a RID–10A refractive index detector and a PL–gel 5mm Mixed–D column utilizing a chloroform:triethylamine:isopropanol (94:4:2) mixture as eluent at a flow rate of 1 mL/min and a column temperature of 50 °C. The molar masses were calculated against polystyrene standards (from 3,420 Da to 246 kDa).

Gas chromatography (GC) was used to calculate the monomer conversion through the decreasing monomer/solvent ratio in the samples. Measurements were performed on an Interscience Trace GC equipped with a PAL autosampler, a special liner for injecting polymers and a Trace Column RTX–5.

Composition and purity of the polymers were determined using ^{1}H NMR spectroscopy. Spectra were recorded on a Varian Mercury 400 MHz spectrometer in $CDCl_3$. The residual protonated solvent signals were used as reference. Elemental analysis (EA) was performed on a Hekatech EA3000 EuroVector CHNS analyzer. The determined wt% N was used to calculate the molar content of DMA monomer and Bloc Builder™ initiator (which was approximated as $1/DP_{DMA}$ from the GC conversion; the attributed nitrogen content from the added SG1 was neglected). The remaining carbon content was ascribed to the HPA monomer, leading to the HPA wt% in the copolymers. Using this method, the combined wt% of DMA, Bloc Builder™ initiator and HPA was 100% ± 6% and the calculated wt% H was within 0.1% of the measured value.

Thermal transitions were determined by differential scanning calorimetry (DSC) using a DSC 204 F1 Phoenix by Netzsch. Each measurement consisted of two heating cycles to 200 °C under a nitrogen flow. In the first cycle, heating to 200 °C and subsequent cooling to –100 °C occurred at a rate of 40 °C. The second cycle was used to determine the transition temperatures and was performed at a heating rate of 20 °C/min.

The cloud points were determined by turbidity measurements in a Crystal 16^{TM} by Avantium Technologies. Four blocks of four parallel temperature controlled sample holders are connected to a Julabo FP40 cryostat allowing 16 simultaneous measurements. Turbidity of

the solutions was measured by the transmission of a red light through the sample vial as a function of the temperature. Solutions of the polymers were prepared in deionized water (Laborpure, Behr Labor Technik) and were stirred at room temperature until the polymer was dissolved or dispersed completely. Three or four heating cycles were applied from 0 °C to 100 °C at 1 °C/min with hold steps of 5 min at the extreme temperatures. The cloud points are given as the 50% transmittance point during the heating ramp.

Optimization of the polymerization temperature for St and tBA

Two different stock solutions were prepared for St and *t*BA. The stock solution for the polymerization of styrene was prepared by adding styrene (7.33 mL, 64.0 mmol), Bloc Builder™ (244.0 mg, 0.64 mmol) and anisole (24.66 mL) together. A volume of 4 mL was transferred from the stock solution to seven reaction vessels to investigate the effect of temperature. The reaction vessels were heated to different temperatures: 90, 100, 110, 115, 120, 125, and 130 °C during the polymerization of styrene. The second stock solution was prepared by adding *t*BA (5.81 mL, 40 mmol), Bloc Builder™ (153.0 mg, 0.4 mmol) and anisole (14.19 mL) together. The volume of 4 mL was transferred from the second stock solution to four reaction vessels. These reaction vessels were heated to 90, 100, 120, and 130 °C during the polymerization of *t*BA. The reaction vessels were vortexed for 10 minutes at 20 °C, after the liquid transfers from the stock solutions to the vessels were complete. First samples of the reactions (150 μL) were transferred to 2 mL vials and 1.5 mL of chloroform mixture was added to each of them. After this first sampling, the reactors were heated to the desired temperatures. The reaction vessels were continuously vortexed at 600 rpm during the polymerization with the reflux condensers set to –5 °C. During this time, samples were taken automatically into 2 mL vials in different time intervals. All vials were characterized by GC and SEC after all the polymerizations were completed.

Optimization of the free nitroxide concentration for St and tBA

Five different stock solutions were prepared to investigate the effect of the free nitroxide concentration for St and *t*BA. The first three stock solution vials contained anisole (8.48 mL), styrene (7.33 mL, 64.0 mmol) or *t*BA (9.29 mL, 64.0 mmol). Bloc Builder™ (512.6 mg, 1.28 mmol) and SG1 (17.8 mg, 0.06 mmol) were dissolved or diluted in anisole (20 mL and 14 mL) for the preparation of the fourth and fifth stock solutions, respectively. St or *t*BA, Bloc Builder™, SG1 and anisole were added into the vessels with different SG1 ratios: 1, 2, 4, 5, 6, 8 and 10 mole percent of the initiator. The reaction vessels were vortexed for 10 minutes at 20 °C, after completing liquid transfers from the stock solutions to the vessels. First samples of the reactions (150 μL) were transferred to 2 mL vials and 1.5 mL of chloroform mixture

was added. Subsequently, the reaction vessels were heated to 110 °C for the polymerization of both monomers. The reaction vessels were continuously vortexed at 600 rpm during polymerization with the reflux condensers set to –5 °C. Samples were taken automatically into 2 mL vials in different time intervals. Subsequently, all samples were characterized by measuring GC and SEC.

Synthesis of PS and PtBA macroinitiators

PS macroinitiators with 50, 78, and 120 repeating units were synthesized in large scales according to the results obtained from the optimization reactions. Schlenk tubes were charged with St (15.0 mL, 131.0 mmol), anisole (3 mL) and different amounts of Bloc Builder™ (0.996 g, 2.61 mmol, 0,600 g, 1.57 mmol, and 0,500 g, 1.31 mmol) weighed in flasks. The resulting mixtures were bubbled with argon for 30 minutes and placed into the oil bath at 120 °C. The reactions were stopped after 5.5, 6 and 6.5 hours and the formed polymers were precipitated into methanol after cooling to room temperature. A fine white powder was obtained after drying in the vacuum oven (40 °C) overnight. Conversions were determined gravimetrically and number average molar masses were measured by SEC. Gravimetrical yields were 70%, 67% and 70% with number average molar masses of 5,200, 8,200 and 12,500 g/mol and polydispersity indices of 1.08, 1.13 and 1.11 for polystyrene macroinitiators with repeating units of 50, 78 and 120, respectively.

A P*t*BA macroinitiator with 65 repeating units was synthesized in a large scale by adding *t*BA (10 mL, 68.9 mmol), SG1 (0.012 g, 0.041 mmol), Bloc Builder™ (0.263 g, 0.689 mmol), and anisole (10 mL). The polymerization mixture was bubbled with argon for 30 minutes and immersed into an oil bath at 110 °C. After 12 hours of polymerization time the mixture was precipitated into a water/methanol (50/50) mixture in order to remove the residual monomer. The precipitate was dried in a vacuum oven at 40 °C overnight. The gravimetrical yield was calculated as 50% and the number average molar mass was found to be 8,300 g/mol with a polydispersity index of 1.25 by measuring SEC.

Synthesis of PS–b–PtBA and PtBA–b–PS block copolymers

A set of experiments was performed in the automated parallel synthesizer to investigate the kinetics of PS–*b*–P*t*BA block copolymerizations initiated with different PS macroinitiators. Three different PS macroinitiators with repeating units of 50, 78, and 120 were dissolved in anisole. In addition, *t*BA and a SG1 stock solution in anisole were prepared and all solutions were bubbled with argon for 60 minutes. Three different mole ratios of *t*BA to macroinitiators were added into the vessels, namely 50:1, 100:1 and 150:1. Additionally, 6% of SG1 regarding to the initiator was added to all vessels in order to improve the control

over the *t*BA polymerization. The reactions were carried out at 110 °C for 20 h and samples were taken in different time intervals.

A P*t*BA–*b*–PS block copolymerization was also investigated in the automated synthesizer. A stock solution consisting of P*t*BA as a macroinitiator, styrene and anisole was prepared and bubbled with argon for 60 minutes. The polymerization was conducted at 110 °C for 35 hours and samples were withdrawn at different time intervals. Monomer conversions and number average molar masses for all samples were determined by GC and SEC.

Homopolymerizations of HPA, Amor, and DMA

An inert atmosphere in the Chemspeed ASW2000 hood was achieved by a 45 minute flushing step with a 1.5 bar argon flow. The reaction vessels were heated to 120 °C and subjected to vacuum–argon cycles (0.1 bar to 1.1 bar) for 3 min, which were repeated 3 times to create an inert atmosphere. The monomer, *N*,*N*–dimethylformamide (DMF) and stock solutions of the Bloc Builder™ initiator and free SG1 in DMF were degassed prior to the reaction by bubbling with argon for at least 25 minutes. The monomer, stock solutions and solvent were automatically transferred to the reaction vessels in the predefined volumes leading to a total reaction volume of 4 mL. The monomer concentration was 2 M and the monomer/initiator ratio was 100/1 with variable amounts of additional SG1 free nitroxide. The reactor block was heated to 110 or 120 °C, respectively, for the predefined reaction time. After the temperature was reached, 100 μL samples were transferred to empty sample vials at set time intervals, after which 0.8 mL chloroform was added to dilute the sample. The samples were analyzed with GC and SEC to determine the reaction kinetics. For manual precipitation of the final polymers, the reaction mixtures were diluted with 4 mL $CHCl_3$ and added drop–wise to a vigorously stirred 10–fold excess of diethyl ether. p(DMA) and p(Amor) were isolated by filtration while p(HPA) was left to settle followed by decantation. The polymers were dried in a vacuum oven at 40 °C until no residual solvent was observed with ^{1}H NMR spectroscopy.

Copolymerizations of HPA, Amor, and DMA

The copolymerizations were performed using the same set–up as the homopolymerizations. The two monomers were added in different ratios resulting in monomer mixtures ranging from 0 to 100 mol% HPA with 10 mol% increments. The total monomer concentration was 2 M and the monomer/initiator/SG–1 ratio was 100/1/0.2. The reaction temperature was set to 110 °C and the reaction times were chosen to reach ~60% monomer conversion. 100 μL zero time and end samples were automatically transferred to

empty vials and diluted with 0.8 mL $CHCl_3$ to determine the monomer conversion with GC. Precipitation of the copolymers was achieved following the same procedure as for the homopolymers. A second precipitation was applied, if necessary, to remove residual DMF and monomer. The final polymers were analyzed by SEC, ^1H NMR spectroscopy and elemental analysis.

2.8 References

(1) J. S. Wang, K. Matyjaszewski, *Macromolecules* **1995**, *28*, 7901–7910.
(2) M. Kamigaito, T. Ando, M. Sawamoto, *Chem. Rev.* **2001**, *101*, 3689–3746.
(3) R. P. N. Veregin, M. K. Georges, G. K. Hamer, P. M. Kazmaier, *Macromolecules* **1995**, *28*, 4391–4398.
(4) T. Fukuda, T. Terauchi, A. Goto, K. Ohno, Y. Tsujii, T. Miyamoto, S. Kobatake, B. Yamada, *Macromolecules* **1996**, *29*, 6393–6398.
(5) J. Chiefari, Y. K. Chong, F. Ercole, J. Krstina, J. Jeffery, T. P. T. Le, R. T. A. Mayadunne, G. F. Meijs, C. L. Moad, G. Moad, E. Rizzardo, S. H. Thang, *Macromolecules* **1998**, *31*, 5559–5562.
(6) J. Qui, B. Charleux, K. Matyjaszewski, *Prog. Polym. Sci.* **2001**, *10*, 2083–2134.
(7) T. Fukuda, Yoshikawa C., Y. Kwak, A. Goto, Y. Tsujii, *In Controlled/Living Radical Polymerization*, K. Matyjaszewski, *ACS Symp. Ser. 854*, American Chemical Society: Washington, DC, **2003**, p. 24.
(8) H. Fischer, *Macromolecules* **1997**, *30*, 5666–5672.
(9) D. A. Shipp, K. Matyjaszewski, *Macromolecules* **1999**, *32*, 2948–2955.
(10) C. J. Hawker, A. W. Bosman, E. Harth, *Chem. Rev.* **2001**, *12*, 3661–3688.
(11) C. J. Hawker, G. G. Barclay, A. Orellana, J. Dao, W. Devonport, *Macromolecules* **1996**, *29*, 5245–5254.
(12) S. Marque, Le C. Mercier, P. Tordo, H. Fischer, *Macromolecules* **2000**, *33*, 4403–4410.
(13) J. M. Catala, F. Bubel, S. O. Hammouch, *Macromolecules* **1995**, *28*, 8441–8443.
(14) L. Couvreur, B. Charleux, O. Guerret, S. Magnet, *Macromol. Chem. Phys.* **2003**, *204*, 2055–2063.
(15) C. Farcet, M. Lansalot, B. Charleux, R. Pirri, J. P. Vairon, *Macromolecules* **2000**, *33*, 8559–8570.
(16) J. F. Lutz, P. L. Desmazes, B. Boutevin, *Macromol. Chem. Phys.* **2001**, *22*, 189–193.
(17) J. Nicolas, B. Charleux, O. Guerret, S. Magnet, *Macromolecules* **2005**, *38*, 9963–9973.
(18) D. Benoit, V. Chaplinski, R. Braslau, C. J. Hawker, *J. Am. Chem. Soc.* **1999**, *121*, 3904–3920.
(19) P. L. Desmazes, J. F. Lutz, B. Boutevin, *Macromol. Chem. Phys.* **2000**, *201*, 662–669.
(20) A. Goto, T. Fukuda, *Macromolecules* **1999**, *32*, 618–623.
(21) T. Diaz, A. Fischer, A. Jonquieres, A. Brembilla, P. Lochon, *Macromolecules* **2003**, *36*, 2235–2241.
(22) L. Couvreur, C. Lefay, J. Belleney, B. Charleux, O. Guerret, S. Magnet, *Macromolecules* **2003**, *36*, 8260–8267.
(23) S. Robin, O. Guerret, J. L. Couturier, Y. Gnanou, *Macromolecules* **2002**, *35*, 2481–2486.
(24) H. Zhang, V. Marin, M. W. M. Fijten, U. S. Schubert, *J. Polym. Sci.: Part A: Polym. Chem.* **2004**, *42*, 1876–1885.
(25) R. Hoogenboom, M. A. R. Meier, U. S. Schubert, *Macromol. Rapid. Commun.* **2003**, *24*, 15–32.
(26) R. Hoogenboom, M. W. M. Fijten, M. A. R. Meier, U. S. Schubert, *Macromol. Rapid Commun.* **2003**, *24*, 92–97.
(27) C. Guerro Sanchez, R. M. Paulus, M. W. M. Fijten, M. J. De La Mar, R. Hoogenboom, U. S. Schubert, *Appl. Surf. Sci.* **2006**, *252*, 2555–2561.
(28) V. Sciannamea, C. Guerrero Sanchez, U. S. Schubert, J.–M. Catala, R. Jérôme, C. Detrembleur, *Polymer* **2005**, *46*, 9632–9641.
(29) M. Leenen, F. Wiesbrock, R. Hoogenboom, U. S. Schubert, *e–polymers* **2005**, *71*, 1–9.
(30) D. Benoit, S. Grimaldi, S. Robin, J. P. Finet, P. Tordo, Y. Gnanou, *J. Am. Chem. Soc.* **2000**, *122*, 5929–5939.
(31) T. Schulte, C. A. Knoop, A. Studer, *J. Polym. Sci. Part A: Polym. Chem.* **2004**, *42*, 3342–3351.
(32) M. Yin, T. Krause, M. Messerschmidt, W. D. Habicher, B. Voit, *J. Polym. Sci. Part A: Polym Chem.* **2005**, *43*, 1873–1882.
(33) H. Mori, H. Iwaya, A. Nagai, T. Endo, *Chem. Commun.* **2005**, 4872–4874.
(34) W. A. Braunecker, K. Matyjaszewski, *Progr. Polym. Sci.* **2007**, *32*, 93–146.
(35) S. Grimaldi, F. Le Moigne, J.–P. Finet, P. Tordo, P. Nicol, M. Plechot, *PCT WO 96/24620*, August 15, **1996**.
(36) S. Grimaldi, J.–P. Finet, F. Le Moigne, A. Zeghdaoui, P. Tordo, D. Benoit, M. Fontanille, Y. Gnanou, *Macromolecules* **2000**, *33*, 1141–1147.
(37) D. Gigmes, D. Bertin, O. Guerret, S. R. A. Marque, P. Tordo, F. Chauvin, J.–L. Couturier, P.–E. Dufils, *PCT WO 2004/014926*, February 13, **2004**.
(38) C. Le Mercier, S. Acerbis, D. Bertin, F. Chauvin, D. Gigmes, O. Guerret, M. Lansalot, S. Marque, F. Le Moigne, H. Fischer, P. Tordo, *Macromol. Symp.* **2002**, *182*, 225–247.
(39) F. Chauvin, P.–E. Dufils, D. Gigmes, Y. Guilaneuf, S. R. A. Marque, P. Tordo, D. Bertin, *Macromolecules* **2006**, *39*, 5238–5250.
(40) J. Nicolas, B. Charleux, O. Guerret, S. Magnet, *Angew. Chem. Int. Ed.* **2004**, *43*, 6186–6189.
(41) P. Lacroix–Desmazes, J.–P. Lutz, F. Chauvin, R. Severac, B. Boutevin, *Macromolecules* **2001**, *34*, 8866–8871.
(42) L. D. Taylor, L. D. Cerankowski, *J. Polym. Sci.* **1975**, *13*, 2551–2570.

(43) M. W. M. Fijten, J. M. Kranenburg, H. M. L. Thijs, R. M. Paulus, B. M. van Lankvelkt, J. de Hullu, M. Springintveld, D. J. G. Thielen, C. A. Tweedie, R. Hoogenboom, U. S. Schubert, *Macromolecules* **2007**, *40*, 5879–5886.
(44) C.–D. Vo, J. Rosselgong, S. P. Armes, *Macromolecules* **2007**, *40*, 7119–7125.
(45) J. R. Lizotte, T. E. Long, *Macromol. Chem. Phys.* **2004**, *205*, 692–698.
(46) K. Bian, M. F. Cunningham, *Macromolecules* **2005**, *38*, 695–701.
(47) F. Eeckman, A. J. Moës, K. Amighi, *Eur. Polym. J.* **2004**, *40*, 873–881.
(48) A. Favier, M.–T. Charreyre, P. Chaumont, C. Pichot, *Macromolecules* **2002**, *35*, 8271–8280.
(49) A. Favier, M.–T. Charreyre, C. Pichot, *Polymer* **2004**, *45*, 8661–8674.
(50) B. De Lambert, M.–T. Charreyre, C. Chaix, C. Pichot, *Polymer* **2007**, *48*, 437–447.
(51) M. Appelt, G. Schmidt–Naake, *Macromol. Chem. Phys.* **2004**, *205*, 637–644.
(52) K. F. Mueller, *Polymer*, **1992**, *33*, 3470–3478.
(53) K. Karaky, L. Billon, C. Pouchan, J. Desbrières, *Macromolecules* **2007**, *40*, 458–464.
(54) M. Nichifor, X. X. Zhu, *Polymer* **2003**, *44*, 3053–3060.
(55) H. Y. Liu, X. X. Zhu, *Polymer* **1999**, *40*, 6985–6990.
(56) I. C. Barker, J. M. G. Cowie, T. N. Huckerby, D. A. Shaw, I. Soutar, L. Swanson, *Macromolecules* **2003**, *36*, 7765–7770.
(57) Y. Cao, X. X. Zhu, J. Luo, H. Liu, *Macromolecules* **2007**, *40*, 6418–6488.
(58) A. W. Bosman, R. Vestberg, A. Heumann, J. M. J. Fréchet, C. J. Hawker, *J. Am. Chem. Soc.* **2003**, *125*, 715–728.
(59) T. Diaz, A. Fischer, A. Jonquières, A. Brembilla, P. Lochon, *Macromolecules* **2003**, *36*, 2235–2241.
(60) K. Schierholz, M. Givenchi, P. Fabre, F. Nallet, E. Papon, O. Guerret, Y. Gnanou, *Macromolecules* **2003**, *35*, 5995–5999.
(61) T. N. T. Phan, S. Maiez–Tribut, J.–P. Pascault, A. Bonnet, P. Gerard, O. Guerret, D. Bertion, *Macromolecules* **2007**, *40*, 4516–4523.
(62) C. R. Becer, R. M. Paulus, R. Hoogenboom, U. S. Schubert, *J. Polym. Sci., Part A: Polym. Chem.* **2006**, *44*, 6202–6213.
(63) K. Bian, M. F. Cunningham, *J. Polym. Sci. Part A: Polym. Chem.* **2006**, *44*, 414–426.
(64) C. De las Heras Alarcón, S. Pennadam, C. Alexander, *Chem. Soc. Rev.* **2004**, *34*, 276–285.
(65) I. Lynch, I. A. Blute, B. Zhmud, P. Macartain, M. Tosetto, L. T. Allen, H. J. Byrne, G. F. Farrell, A. K. Keenan, W. M. Gallagher, K. A. Dawson, *Chem. Mater.* **2005**, *17*, 3889–3898.
(66) M. D. Costioli, I. Fisch, F. Garret–Flaudy, F. Hilbrig, R. Freitag, *Biotechnol. Bioeng.* **2003**, *81*, 535–545.
(67) A. Kikichi, T. Okano, *Progr. Polym. Sci.* **2002** *27*, 1165–1193.
(68) D. Schmaljohann, *Adv. Drug Deliv. Rev.* **2006**, *58*, 1655–1670.
(69) D. E. Bergbreiter, B. L. Case, Y.–S. Liu, J. W. Caraway, *Macromolecules* **1998**, *31*, 6053–6062.
(70) I. M. Okhapkin, A. A. Makhaeva, A. R. Khokhlov, *Adv. Polym. Sci.* **2006**, *195*, 177,
(71) I. Lokuge, X. Wang, P. Bohn, *Langmuir* **2007**, *23*, 305–311.
(72) G. Wu, Y. Li, M. Han, X. Liu, *J. Membrane Sci.* **2006**, *283*, 13–20.
(73) D. Fournier, R. Hoogenboom, H. M. L. Thijs, R. M. Paulus, U. S. Schubert, *Macromolecules* **2007**, *40*, 915–920.
(74) S. Jana, S. P. Rannard, A. I. Cooper, *Chem. Commun.* **2007**, 2962–2964.
(75) J. C. Meredith, E. J. Amis, *Macromol. Chem. Phys.* **2000**, *201*, 733–739.
(76) H. G. Schild, *Prog. Polym. Sci.* **1992**, *17*, 163–249.
(77) S. Aoshima, S. Kanaoka, *Adv. Polym. Sci.* **2008**, *210*, 169–208.
(78) D. Christova, R. Velichkova, W. Loos, E. J. Goethals, F. Du Prez, *Polymer* **2003**, *44*, 2255–2261.
(79) D. I. Perera, R. A. Shanks, *Polym. Int.* **1995**, *37*, 133–139.
(80) T. G. Fox, *Bull. Am. Phys. Soc.* **1956**, *1*, 123–124.
(81) R. J. Young, P. A. Lovell, *Introduction to polymers* 2nd Edition, London: Chapman & Hall, **1991**, p.298.
(82) S. O. Kyeremateng, E. Amado, J. Kressler, *Eur. Polym. J.* **2007**, *43*, 3380–3391.
(83) S.–W. Kuo, W.–P. Liu, F.–C. Chang, *Macromolecules* **2003**, *36*, 5165–5173.
(84) I. Idziak, D. Avoce, D. Lessard, D. Gravel, X. X. Zhu, *Macromolecules* **1999**, *32*, 1260–1263.
(85) Z. Tong, F. Zeng, X. Zheng, *Macromolecules* **1999**, *32*, 4488–4490.
(86) V. Aseyev, S. Hietala, A. Laukkanen, M. Nuopponen, O. Confortini, F. Du Prez, H. Tehnu, *Polymer* **2005**, *46*, 7118–7131.
(87) X. Wang, X. Qiu, C. Wu, *Macromolecules* **1998**, *31*, 2972–2976.
(88) T. Maeda, K. Yamamato, T. Aoyagi, *J. Coll. Interf. Sci.* **2006**, *302*, 467–474.
(89) R. Hoogenboom, H. M. L. Thijs, D. Wouters, S. Hoeppener, U. S. Schubert, *Soft Matter* **2008**, *4*, 103–107.
(90) R. Hoogenboom, U. S. Schubert, *J. Polym. Sci., Part A: Polym. Chem.* **2003**, *41*, 2425–2434.

Chapter 3

Reversible addition fragmentation chain transfer polymerization

Abstract

The RAFT polymerization technique was used in this chapter to prepare libraries of well–defined polymers. The prepared polymers exhibited lower critical solution temperature behavior and a systematic investigation was conducted to screen the effect of polymer composition on the phase transition behavior. Besides, we have focused on the moisture uptake of thermo-responsive polymers, super absorbers and also hydrophilic polymers. The effect of chemical structures of the monomers, chain lengths and the measurement temperature on the moisture uptake properties were examined for these classes of polymers. Based on our experience on the automated synthesis platforms and controlled radical polymerizations, we report a universal protocol for the automated kinetic optimization of the RAFT polymerization of various monomers.

Parts of this chapter have been published: C. R. Becer, S. Hahn, M. W. M. Fijten, H. M. L. Thijs, R. Hoogenboom, U. S. Schubert, *J. Polym. Sci., Part A: Polym. Chem.* **2008***, 46,* 7138–7147; H. M. L. Thijs, C. R. Becer, C. Guerrero-Sanchez, D. Fournier, R. Hoogenboom, U. S. Schubert, *J. Mater. Chem.* **2007**, *17*, 4867–4871; C. R. Becer, A. M. Groth, R. Hoogenboom, R. M. Paulus, U. S. Schubert, *QSAR Comb. Sci.* **2008**, *8*, 977–983.

3.1 Introduction

Reversible addition–fragmentation chain transfer (RAFT) polymerization has developed into one of the leading controlled/living radical polymerization techniques since its invention by the CSIRO group in 1998. It is arguably the most versatile controlled polymerization process with respect to the types of monomers and the reaction conditions that enables the formation of polymers with controlled molar mass, low polydispersity index, and complex polymeric microstructure with relative ease. The success of this powerful technique is demonstrated by a constantly growing body of work that deals with various RAFT processes leading to advanced polymeric materials.

As illustrated in Scheme 3.1, unsaturated compounds of the general structure **1** can act as transfer agents by a two-step addition-fragmentation mechanism. Such transfer agents possess a C=X double bond that is reactive toward radical addition, groups A and X that are most often CH_2 or S, a substituent Z that is chosen to give the transfer agent an appropriate reactivity toward propagating radicals and provides appropriate stability to the intermediate radicals **2**, and a group R that is a homolytic leaving group and such that R• is capable of efficiently re-initiating the polymerization. Reversible chain transfer requires that both **1** and **3** are active transfer agents under the polymerization conditions. This means that the groups A and X should be the same (both CH_2 or both S) and R must have similar or better hemolytic leaving group ability than the propagating radical.

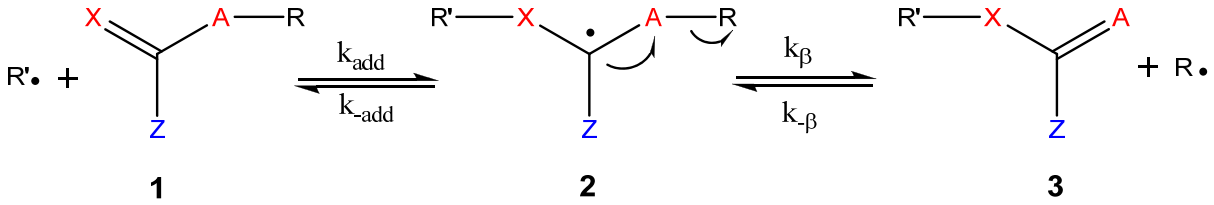

Scheme 3.1. Schematic representation of the mechanism for addition-fragmentation chain transfer.

In this chapter, we have focused on the application of RAFT polymerization for the preparation of well-defined polymer libraries using various monomers. In particular, we have investigated the lower critical solution temperature (LCST) behavior of responsive polymers. Therefore, oligo(ethylene glycol) methacrylate (OEGMA) monomers were polymerized via the RAFT polymerization method. Moreover, random copolymer libraries of OEGMA and methacrylic acid were prepared at different compositions to elucidate their structure–property relationships. The polymerizations were performed in an automated parallel synthesizer and the phase transition temperatures were measured in parallel in the Crystal16 turbidimeter. The typical copolymerization scheme is depicted in Scheme 3.2.

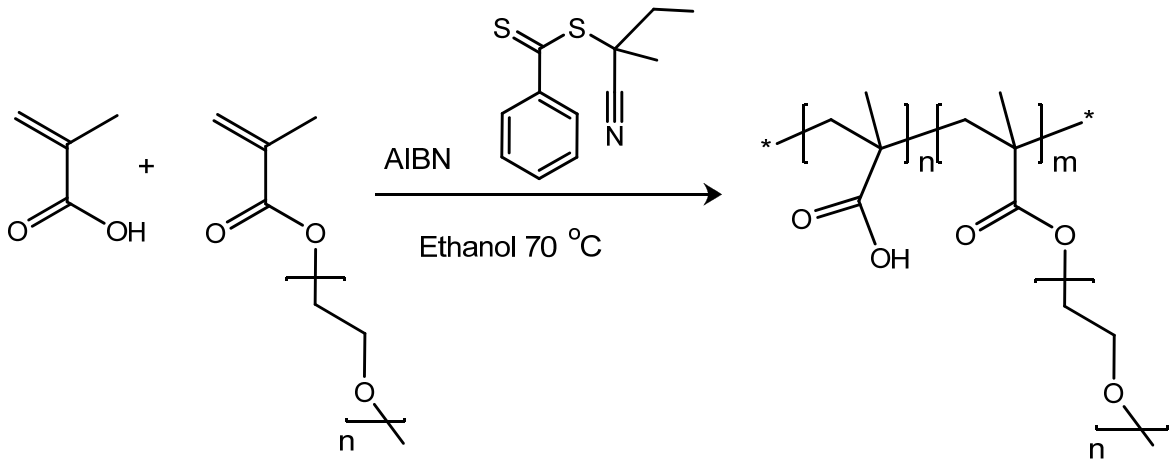

Scheme 3.2. Schematic representation of the RAFT polymerization of MAA and OEGMA derivatives.

Hydrophilic polymers contain hydrogen donor or acceptor groups that provide the close interaction with water molecules. Superhydrophilic polymers are known as superabsorbers and are used in several applications, such as diapers and gels. These polymers can absorb large amounts of water in comparison to their weight when they have direct contact with water. We have investigated the moisture uptake behavior from the air of different classes of polymers in an automated fashion and in relatively short measurement periods. Besides, thermoresponsive polymers that can change from a hydrophilic to a hydrophobic structure are definitely of interest due to several potential applications. In particular, these polymers are capable of absorbing water molecules below their LCST, whereas the water is released above their phase transition temperature.

In the final part we describe a standard protocol for the parallel optimization of RAFT polymerization conditions using an automated synthesizer. Each step of the high-throughput experimentation cycle is discussed in this protocol starting from design of experiments. The critical points of utilizing an automated parallel synthesizer for the RAFT polymerization is explained step by step including the preparation of stock solutions, inertization of the reactors and the synthesizer environment, liquid transfers to or from the reactor vessels including sampling as well as termination of the polymerization. Moreover, automated characterization techniques for the determination of monomer conversion and the molar mass distribution of the polymers are discussed.

3.2 Synthesis of oligo(ethyleneglycol) methacrylate containing copolymer libraries

Responsive polymeric structures with well–defined macromolecular composition, functionalities and topology, so-called “smart” materials, have become the interest of many

researchers.[1-4] Intelligence of these "smart" materials is mostly based on their response to the environmental changes or external stimulation. Small organic compounds as well as polymeric structures in solution can exhibit a phase transition when the polymer precipitates upon heating. This phenomenon is called lower critical solution temperature (LCST) behavior and is simply based on the existence of hydrogen bonding between the water molecules and the polymer chain. The polymers with LCST behavior show a sudden and reversible change from hydrophilic to hydrophobic behavior that makes them attractive for usage as 'smart' switchable materials in applications ranging from, *i.e.* drug delivery systems, soft actuators or valves, coatings to textile materials.[5-9]

Controlled/"living" radical polymerization techniques had a rapid development in the last decade since they allow the straight-forward synthesis of well–defined polymers.[10-13] The phase transition sharpness and the reproducibility of the LCST transitions can be tailored by utilizing living and controlled polymerization techniques, such as anionic,[14-16] radical[17-19] and cationic[20,21] polymerizations. These techniques have enabled the synthesis of advanced structures with a targeted length of the polymer. Moreover, the architecture as well as the desired monomer composition and distribution along the backbone can be controlled in an excellent manner. The RAFT polymerization mechanism is one of the most successful controlled radical polymerization techniques because of its tolerance to various functionalities and ease of application.[22-25]

The challenges to obtain a material for a specific application might be overcome by mapping the structure-property relationships of a wide range of polymeric structures that allows a subsequent prediction of polymer properties and a targeted design of materials with desired properties. Such an approach requires the preparation of libraries of well-defined polymers having systematical changes in, *e.g.*, polymer molar mass, length and/or architecture to be able to determine quantitative structure-property relationships.[26,27] The synthesis and screening of such polymer libraries can be accelerated by the use of high-throughput synthesis and screening equipment.[29] In addition, the use of automated parallel synthesis platforms increases the comparability of the different copolymers based on the elimination of handling errors.[30]

Poly(*N*-isopropyl acrylamide) (PNIPAM) is the most widely investigated thermoresponsive polymer because its LCST is close to the body temperature under physiological conditions while the thermal transition is not affected by variations in concentration or ionic strength.[31-33] Alternatively, POEGMA based polymers have attracted great attention in the last couple of years due to their tunable LCST behavior.[34-39] Polymerization of the commercially available OEGMA type of monomers yields comb

shaped polymers that can be used for many biomedical purposes, *e.g.* PEGylation of proteins.[40] These comb-shaped polymers have several advantages over linear PEG for *in vivo* applications. For instance, the excretion of linear PEG (with an M_n above 20,000 Da) from the body is much harder in comparison to comb-shaped PEG (with an M_n of 300 to 2,000 Da per "teeth") since it is linked to the backbone with a cleavable ester bond.[41]

In this section we describe the synthesis and characterization as well as cloud point determination of mono-, di- and oligo(ethyleneglycol) methacrylate (OEGMA) homopolymers with various degree of polymerization. Furthermore, the investigation of random copolymers of OEGMAs with the pH sensitive monomer, methacrylic acid (MAA), will be discussed, resulting in double responsive copolymers. The structures of the monomers used in this study are shown in Scheme 3.3.

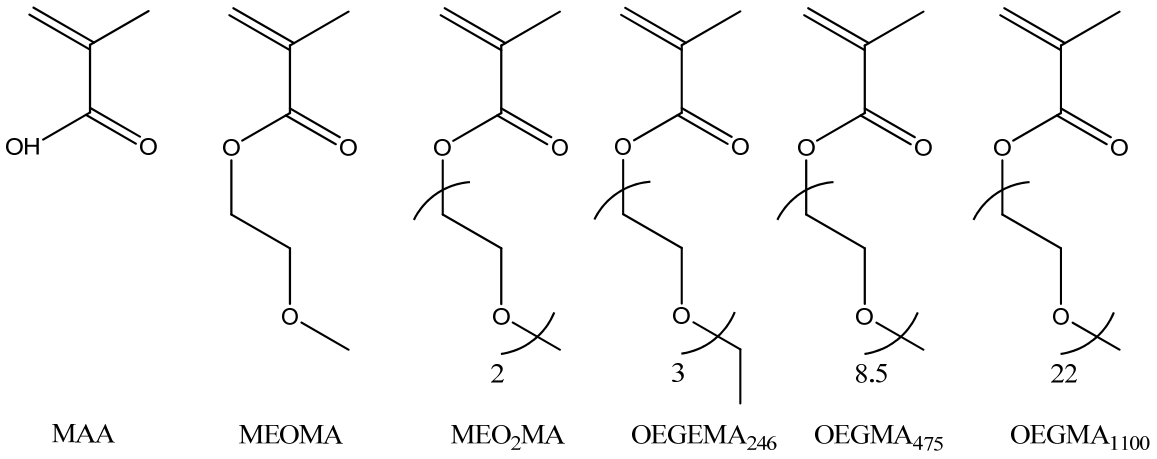

Scheme 3.3. Schematic representation of the monomers described in this study.

The homopolymer libraries of MAA, MEO_2MA, $OEGMA_{475}$ and $OEGEMA_{246}$ were synthesized by varying the monomer to chain transfer agent (CTA) ratios from 10:1 up to 100:1 (in total 10 polymers in each library). In order to accelerate the synthesis of the materials, an automated parallel synthesizer (Chemspeed Accelerator SLT106™) was used for the preparation of the libraries.

The monomer conversions were determined by gas chromatography (GC) or ^{1}H-NMR spectroscopy, whereas the molar masses and the polydispersity indices of the obtained polymers were determined by size exclusion chromatography (SEC). All synthesized polymers exhibited monomodal molar mass distributions with polydispersity indices below 1.3 in the SEC measurements, as depicted in Figure 3.1. These results clearly demonstrate that by just changing the initial monomer to CTA ratio, homopolymers of MAA, MEO_2MA, $OEGMA_{475}$ and $OEGEMA_{246}$ can be prepared with different molar masses.

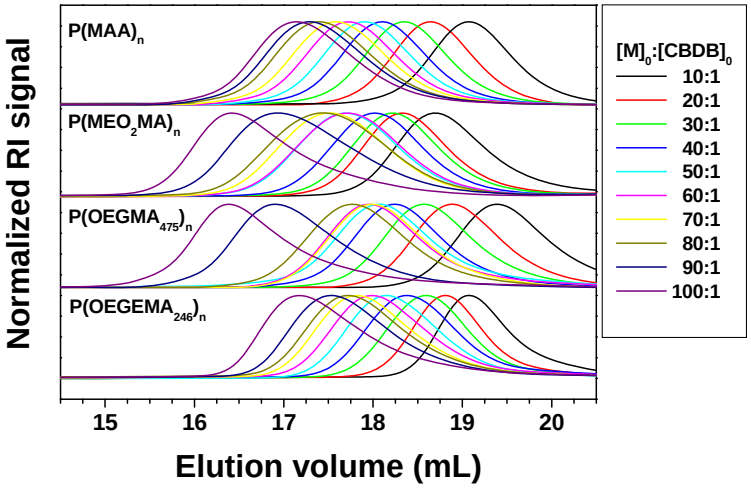

Figure 3.1. SEC traces of the obtained polymers for MAA, MEO_2MA, $OEGMA_{475}$ and $OEGEMA_{246}$.

Based on these SEC traces, the number average molar masses and polydispersity indices of the polymers were calculated using PMMA calibration standards. The obtained values for $PMAA$, $PMEO_2MA$, $POEGMA_{475}$ and $POEGEMA_{246}$ homopolymers are illustrated in Figure 3.2.

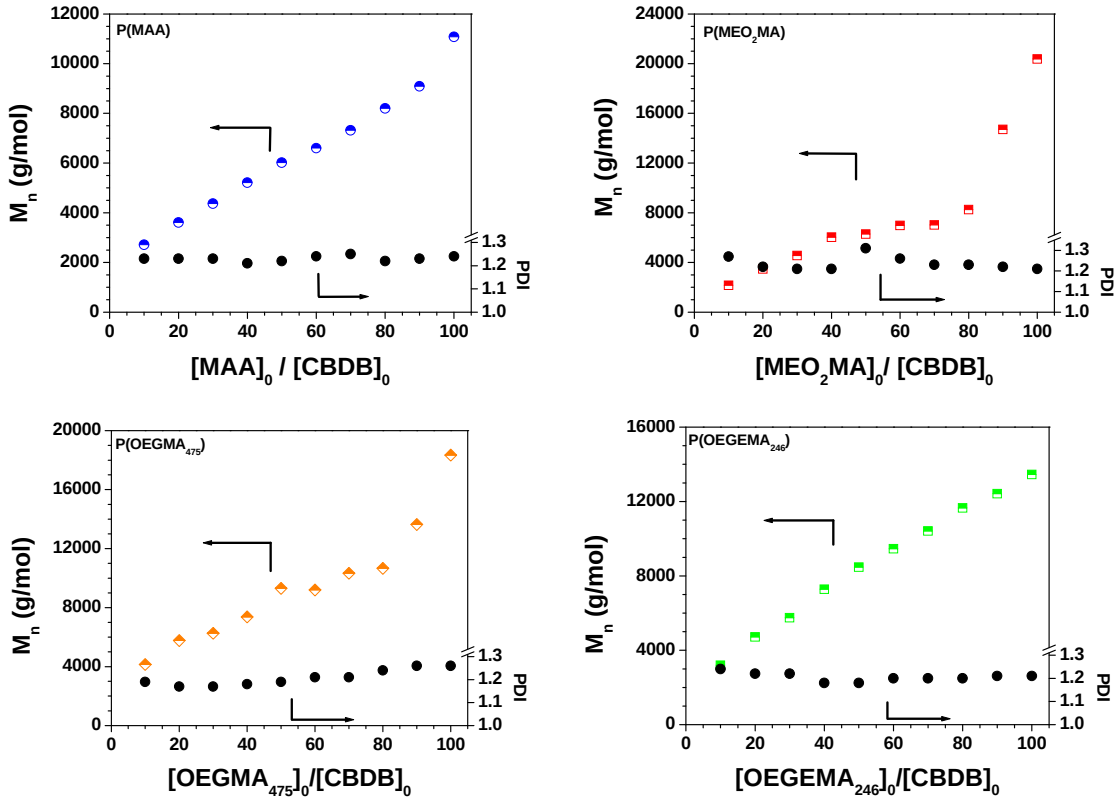

Figure 3.2. $M_{n,SEC}$ and PDI values as function of monomer to CTA ratio for the homopolymerizations of MAA, MEO_2MA, $OEGMA_{475}$ and $OEGEMA_{246}$ with different monomer to CTA feed ratios changing from 10:1 to 100:1 with steps of 10.

Besides this initial screening, the homopolymers of MAA, MEOMA, MEO_2MA, $OEGMA_{475}$, $OEGMA_{1100}$, and $OEGEMA_{246}$ with monomer to CTA ratios of 50 and 100 were manually prepared to investigate the LCST behavior. The structural characterization of these homopolymers is listed in Table 3.1. The cloud points of the purified homopolymers were determined in a parallel turbidimeter (Crystal16 from Avantium) at a polymer concentration of 5 mg/mL at pH 4, 7, and 10. There is no cloud point observed for the homopolymers of PMAA, PMEOMA, $POEGMA_{1100}$ in the range from 0 to 100 °C. In the case of PMEOMA the polymer is not soluble in water since the single ethyleneglycol unit is insufficient to solubilize the hydrophobic polymer backbone. As shown in Table 3.1, $PMEO_2MA$ and $POEGMA_{246}$ homopolymers exhibited cloud points close to room temperature (20 to 29 °C) at pH 4, 7, and 10, whereas $PMEO_2MA$ could not be dissolved at the acidic pH. It is obvious that the number of ethyleneglycol units on each repeating unit has an effect on the cloud point of the polymer. $OEGMA_{246}$ has in average three repeating units of ethyleneglycol, whereas MEO_2MA has only two. The possible reason for their similar cloud points might be due to the difference in their end groups of the ethyleneglycol repeating units, which is methyl in case of MEO_2MA and ethyl for $OEGMA_{246}$. These results indicate that the number of ethyleneglycol units is increasing the cloud point while the additional aliphatic units cause a decrease.

Table 3.1. Structural characterization data and cloud points of the homopolymers.

Code	Monomer	$[M]_0/[CBDB]_0$	$M_{n,SEC}$ [a] [g/mol]	PDI	Yield [b] [%]	CP [c] [°C] pH 4	CP [c] [°C] pH 7	CP [c] [°C] pH 10
H1	MAA	50:1	6,020	1.22	86	-	-	-
H1	MAA	100:1	11,080	1.24	67	-	-	-
H2	MEOMA	50:1	7,480	1.19	n.d.	n.s.	n.s.	n.s.
H3	ME_2OMA	50:1	6,280	1.31	56	n.s.	20.6	21.6
H4	ME_2OMA	100:1	20,380	1.21	37	n.s.	21.8	23.1
H5	$OEGMA_{475}$	50:1	9,310	1.19	35	97.0	93.7	96.6
H6	$OEGMA_{475}$	100:1	18,340	1.26	19	93.2	89.8	92.8
H7	$OEGMA_{1100}$	50:1	14,560	1.19	50	-	-	-
H8	$OEGEMA_{246}$	50:1	8,470	1.18	49	28.3	20.0	21.3
H9	$OEGEMA_{246}$	100:1	13,450	1.21	44	27.6	21.6	22.8

[a] Number average molar masses were calculated according to polystyrene standards. [b] Gravimetric yield calculated from the mass of the polymer after purification. [c] Cloud points were determined at 5 mg/mL in the range of 0 to 100 °C; n.s. = not soluble

The homopolymers of PMAA were soluble in water because of the hydrophilicity of the carboxylic acid groups that form hydrogen bonds with the surrounding water molecules.

As a consequence, there is no LCST behavior observed for PMAA up to 105 °C. $POEGMA_{1100}$ has a very similar structure to linear PEG since each methacrylate repeating unit bears 22 ethyleneglycol units in average. These side chains are sufficiently long to shield the methacrylate backbone from water making the polymer fully soluble in aqueous solution. The ratio of the ether groups to the methacrylate backbone is lower in $POEGMA_{475}$ in comparison to $POEGMA_{1100}$ homopolymers. As a result, the hydrophilicity of the $POEGMA_{475}$ homopolymers is lower and a cloud point is observed close to 100 °C.

Furthermore, the effect of the chain length on the LCST behavior of $POEGMA_{475}$ and $PMEO_2MA$ homopolymers was investigated and polymers with different chain lengths exhibited cloud points in the range of 80 to 98 °C and 15 to 25 °C, respectively. The measured cloud points are depicted in Figure 3.3. There is no strong influence of the chain length on the LCST behavior for this class of polymers. Even though these monomers are not pH-responsive, the turbidimetry measurements were performed in buffer solutions at four different pH values, which are 2, 4, 7 and 10, to allow a detailed comparison to their corresponding double responsive copolymers with methacrylic acid.

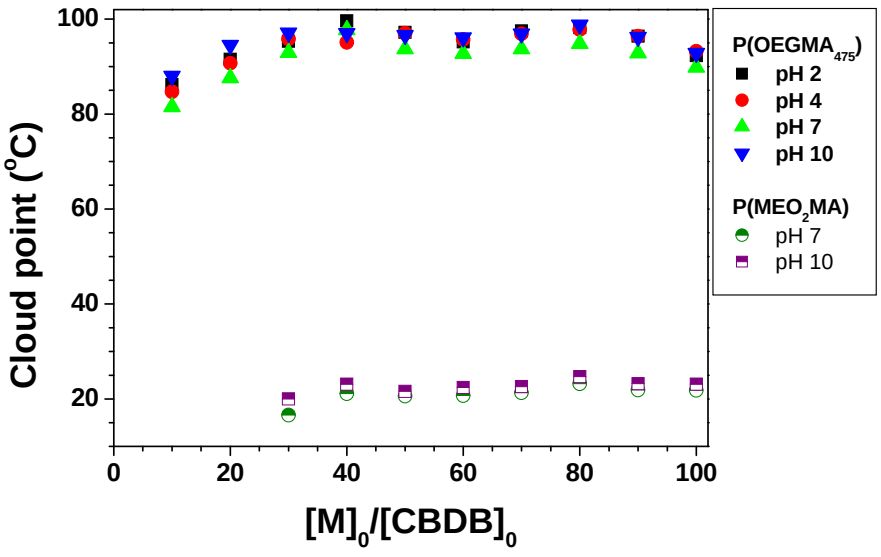

Figure 3.3. Cloud points of $p(OEGMA_{475})$ and $p(MEO_2MA)$ homopolymers as a function of monomer to CTA feed ratio at different pH values.

It is also known from the literature that there is an influence of the end group on the cloud point of the polymers, which becomes more distinct at lower molar masses.[42] Indeed, there is a slight increase in the cloud point of $POEGMA_{475}$ for the shortest chain lengths ([M]/[I] = 10 to 40), which may be attributed to the hydrophobic character of the chain transfer agent attached to the chain end. There is no strong difference in the cloud point for different pH values. Nevertheless, the cloud points are 1 to 2 °C lower at pH 7 in comparison

to acidic or basic solutions, which is most likely due to slightly stronger interactions between the PEG chains and hydroxide ions or hydronium protons compared to water. A similar behavior was observed for the homopolymers of MEO_2MA at pH values of 7 and 10. However, the CPs of $PMEO_2MA$ were found in the range from 15 to 25 °C, which is far below the CPs of $POEGMA_{475}$. This is caused by the changed hydrophilic/hydrophobic balance, which is shifted to more hydrophobic. By taking advantage of this behavior, it is possible to tune the LCST of the polymers by simply altering the MEO_2MA and $OEGMA_{475}$ content, as was previously demonstrated by Lutz *et al.*[43]

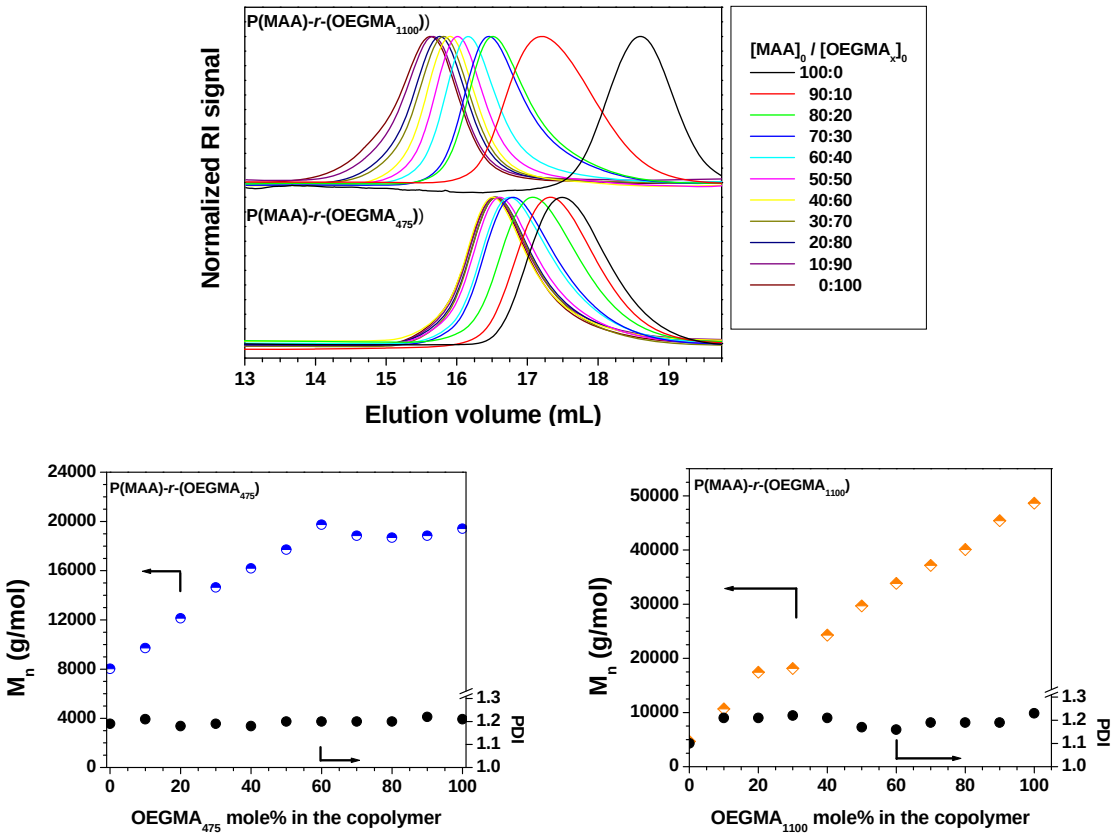

Figure 3.4. Size exclusion chromatography traces for the copolymerizations of MAA and $OEGMA_{475}$ or $OEGMA_{1100}$ with different monomer ratios changing from 0:100 to 100:0 and the corresponding $M_{n,SEC}$ and PDI values.

However, our interest is focused on double responsive polymers that are switchable both by temperature and pH. This can be achieved by the incorporation of an acidic or a basic monomeric unit. Therefore, copolymers of MAA and $OEGMA_{475}$ or $OEGMA_{1100}$ were prepared with a systematic variation of the monomer content in the polymers. The content of MAA in the copolymer was varied from 0% to 100% with steps of 10%. The molar mass and the polydispersity indices of the polymers were determined by SEC. As shown in Figure 3.4, the obtained SEC traces exhibited monomodal distribution for all polymers. Besides, the

molar masses increased linearly with the increasing content of $OEGMA_{1100}$ in the copolymer, whereas the polydispersity indices remained below 1.3.

Furthermore, the copolymers were characterized with ^{1}H-NMR spectroscopy in order to determine the incorporated monomer contents, as depicted in Figure 3.5. The content of $OEGMA_x$ was found to be slightly higher than the theoretical ratios (diagonal line), which indicates that $OEGMA_x$ has a slightly higher reactivity than MAA in the RAFT polymerization. Nevertheless, all copolymers were found to be well–defined consisting of monomer compositions close to the desired composition.

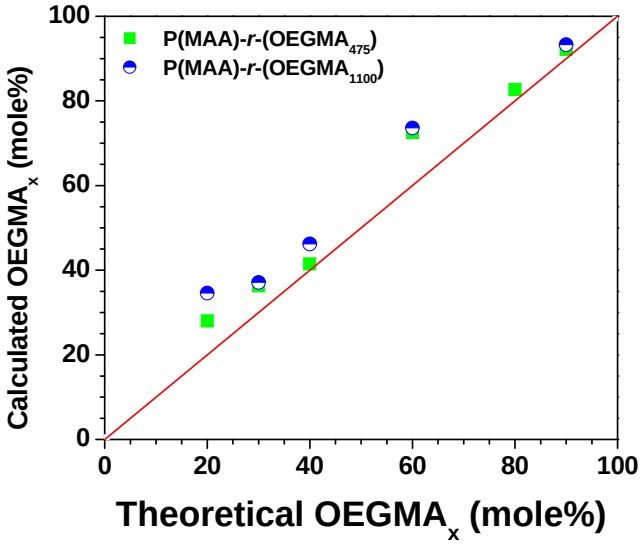

Figure 3.5. Theoretical composition *versus* the calculated composition of the MAA and $OEGMA_{475}$ or $OEGMA_{1100}$ copolymers.

The LCST behavior of the copolymer libraries with MAA and $OEGMA_{475}$ or $OEGMA_{1100}$ was investigated at pH 2, 4, 7, and 10, respectively. The copolymer library of MAA and $OEGMA_{475}$ revealed LCST behavior in a relatively wide range between 20 to 90 °C, whereby the pure PMAA and $P(MAA)_{0.1}$-*r*-$(OEGMA_{1100})_{0.9}$ did not show cloud points. Surprisingly, the cloud point of $POEGMA_{475}$ is lowered by the incorporation of the more hydrophilic MAA (Figure 3.6). It should be noted that these copolymers are double responsive showing an LCST transition at pH 2 and 4 while they are fully soluble at pH 7 and 10. As mentioned previously in this chapter, homopolymers of MAA and also $OEGMA_{1100}$ did not show any cloud point in the range from 0 to 100 °C at pH 2, 4, 7, and 10, respectively. However, the copolymers of these two monomers at certain ratios of MAA to $OEGMA_{1100}$ (90:10, 80:20, 70:30 and 60:40) also show double responsive behavior. These polymers are found to be both thermo-responsive and pH-responsive. A possible explanation for this unexpected LCST behavior might be the intramolecular interactions between the ether groups

and the carboxylic acid groups. The higher amount of ethyleneglycol units per macromolecule provided the relatively highest cloud point. For instance, the copolymer of MAA:OEGMA$_{1100}$ with a content of 90:10 revealed a cloud point at 24.1 °C in a buffer solution at pH 2 and at 37.8 °C at neutral pH, while it is fully soluble at pH 10. This type of behavior might be beneficial for the development of drug delivery applications and biocompatible contrast agents for magnetic resonance imaging (MRI).[44]

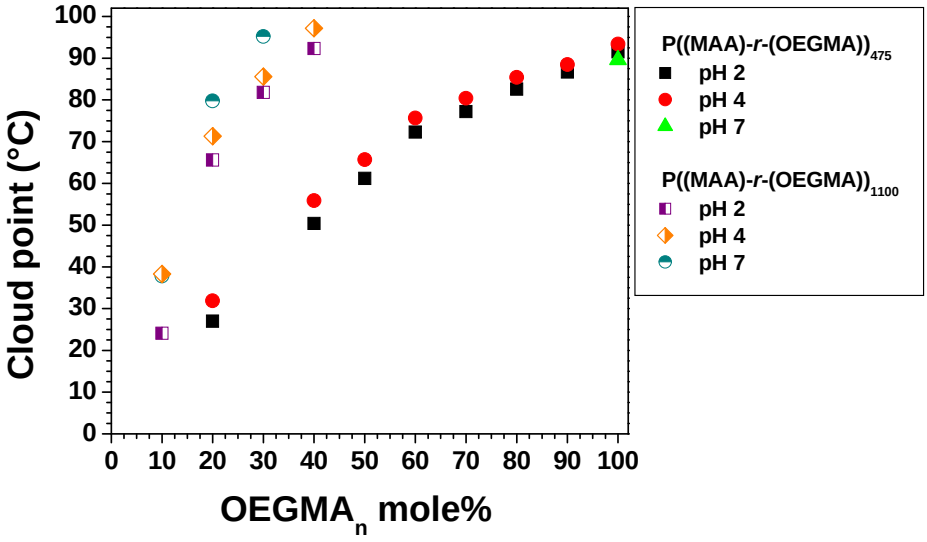

Figure 3.6. Cloud points of P(MAA)-*r*-(OEGMA$_{475}$) and P(MAA)-*r*-(OEGMA$_{1100}$) copolymers as a function of OEGMA$_n$ mole percentage at different pH values estimated by 50% transmittance points of the first heating curves.

3.3 Water uptake behavior of hydrophilic polymers

As of many decades, polymers have attracted great attention because of their advantageous material properties. Nowadays, polymers are used in a wide range of applications, *e.g.* in automotive, construction, electronic, cosmetic and pharmaceutical industries. Polymeric materials can be prepared by various polymerization techniques, including anionic, cationic, or radical[45- 48] processes, and their properties, such as mechanical, thermal and structural properties, can be analyzed by a variety of characterization tools, allowing for the determination of structure-property relationships.[49] Today, advanced characterization tools such as size exclusion chromatography (SEC), nuclear magnetic resonance (NMR) spectroscopy, nanoindentation, thermo gravimetric analysis or contact angle measurements are routinely used for the determination of selected polymer properties. One important polymer characteristic that can play a crucial role in the fields of personal care products, coatings, composite materials, membranes or biomedical applications is the

moisture uptake of the investigated material. This property can be measured directly from water or from a humid atmosphere.

There are many known polymers with a variety of structures and/or functionalities that show interesting as well as industrially important water uptake characteristics. For instance, hydrogels represent an important class of materials that are generally formed by crosslinked networks and have an ability to absorb considerable amounts of water. One of the most commonly used methods for the determination of the amount of water absorbed in crosslinked systems is a swelling test which requires the network to be in direct contact with water.[50] However, this technique is not applicable for non-crosslinked systems such as linear or star-shaped hydrophilic polymers since these are often powders or liquids and would therefore dissolve in the water. The water sorption of polymer films from air can be determined by using electro-micro balances.[51] Gavara *et al.* investigated the sorption and transport properties of water through films of Nylon-6 with this technique. Other instruments that measure the water uptake of materials from air are permeation analyzers,[52] dynamic vapor sorption instruments,[53] infrared near-field scanning optical microscopes,[54] stress analyzers,[55] and quartz crystal microbalances.[56] Alongside these techniques, certain research groups have used desiccators conditioned at specific humidities in which the samples were weighed at specific time intervals in order to determine the water uptake ability of the polymers.[57,58] The main drawbacks of these methods include their extensive measurement periods, difficulties in controlling the temperature and related handling errors.

We have investigated the water uptake behavior of several classes of polymers by using a thermal gravimetric analyzer equipped with a controlled humidity chamber. The main advantage of this type of measurement setup was that only a small amount of sample (2 to 3 mg) was required thus allowing the material to equilibrate more rapidly at various relative humidities and, consequently, significantly shortening the measuring time. The temperature was controlled by Peltier elements and could therefore be easily varied.

The main interest was to investigate the water uptake ability of different classes of hydrophilic polymers at various humidities by using a thermal gravimetric analysis (TGA-HC) system. The study was focused on the effect of certain functional groups on the water uptake of the polymers. A range of hydrophilic polymers with different functionalities, such as acid functions (PAA) or hydroxy groups (PHEMA) were investigated. Other common water soluble polymers were also examined, including poly(vinyl imidazole) (PVIM) and poly(ethylene glycol) (PEG). These investigations were followed by the determination of the effect of the chain length on the water uptake ability of poly(2-methyl-2-oxazoline) (PMeOx) and poly(2-ethyl-2-oxazoline) (PEtOx), which are known as hygroscopic polymers. Finally,

the water uptake ability of polymers with an LCST behavior, *e.g.* poly(*N*-isopropyl acrylamide) (PNIPAM) and poly(*N,N*-dimethyl acrylamide) (PDMAEMA), were also investigated. These measurements were carried out both below and above the specific LCST of each polymer.

The water uptake measurements of the polymers were investigated on a Q5000 SA thermo gravimetric analyzer from TA Instruments containing a microbalance in which the sample and the reference pans were enclosed in a humidity and temperature controlled chamber. The temperature in the Q5000 SA was controlled by Peltier elements. Dried N_2 gas flow (200 mL/min) was split into two parts, of which one part was wet by passing it through a water-saturated chamber. The desired relative humidity (RH) for the measurements could subsequently be obtained by mixing proper proportions (regulated by mass flow controllers) of dry and wet stream. A schematic representation of the instrumental setup is shown in Scheme 3.4.

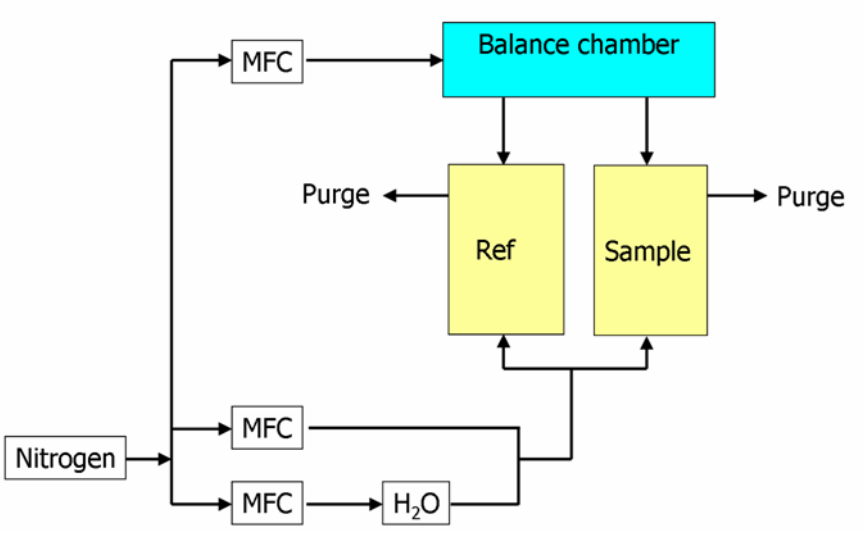

Scheme 3.4. The experimental setup for the thermal gravimetric analysis with a controlled humidity chamber. A pre-dried nitrogen flow was split into two parts. One part of the gas stream was wet and the desired relative humidity could be achieved by regulating proper proportions of the dry and wet streams with mass flow controllers.

Prior to the measurements on the polymer samples, a calibration of the humidity control chamber of the TGA was carried out by measuring the deliquescence point for a standard material. Specific salts (such as sodium bromide or lithium chloride) absorb very little amounts of water during an increase in humidity until the humidity reaches a 'critical' (deliquescence) point. At this exact relative humidity and temperature, the material starts to absorb moisture from the environment. During the calibration measurement, the humidity was raised above the onset of deliquescence and then stepped down.[59] The maximum point in the negative weight percent change is known as the deliquescence point. For sodium bromide,

this value has been reported as 57.6 ± 2% RH at 25 °C.[59] As displayed in Figure 3.7, the maximum change in weight percentage corresponds to a humidity of 58% RH which is within the error range of the reported value and thus proves the accuracy of the system.

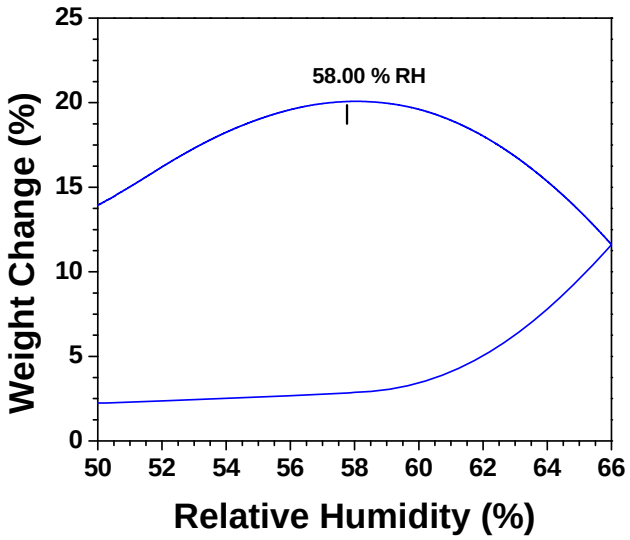

Figure 3.7. A measurement of the deliquescence point of sodium bromide in order to determine the accuracy of the TGA-HC system. The maximum point in the weight change is considered to be the deliquescence point.

The main point of interest of this study was the determination of the water uptake for various commercially as well as scientifically interesting polymers at varying humidities and at a certain temperature. For this purpose the drying process of the samples prior to the measurement was a critical step. During the drying, the polymer was heated to 60 °C at 0% RH until the weight change was smaller than 0.05% during a time period of 60 minutes. Thereafter, the temperature was set to the desired value and the humidity was increased in steps of 10 or 20% RH up to a maximum of 90% RH. Such a procedure yielded a complete isotherm at a specific temperature and provided water uptake values at all different RH's. A typical plot obtained for such a measurement on silica is illustrated in Figure 3.8.

This figure can be divided into five zones, A, B, C, D and E, which will be used for further explanation of the measurements. The first section of the graph (zone A) corresponds to the drying step at 60 °C and 0% RH. Initially, the weight of the sample decreased slightly and the weight remaining after 200 min was used to calibrate the weight change. In the next step (zone B) the temperature and the relative humidity were adjusted to 30 °C and 10%, respectively. Consequently, the weight of the sample increased up to its saturation at these specific conditions. Subsequently, if the weight change was smaller than 0.05% for 60 minutes, the humidity was increased further in steps of 20% RH up to a maximum relative humidity of 90% (zone C). The humidity was then decreased in steps of 20% RH to a final

humidity of 10% RH (zone D). In order to finalize the isotherm, an additional drying step (zone E) was included to validate the measurement by comparing the initial and final sample weights. From these plots, the equilibrated weight percent changes were extracted at different RH's and were used to plot the sorption isotherms (Figure 3.9).

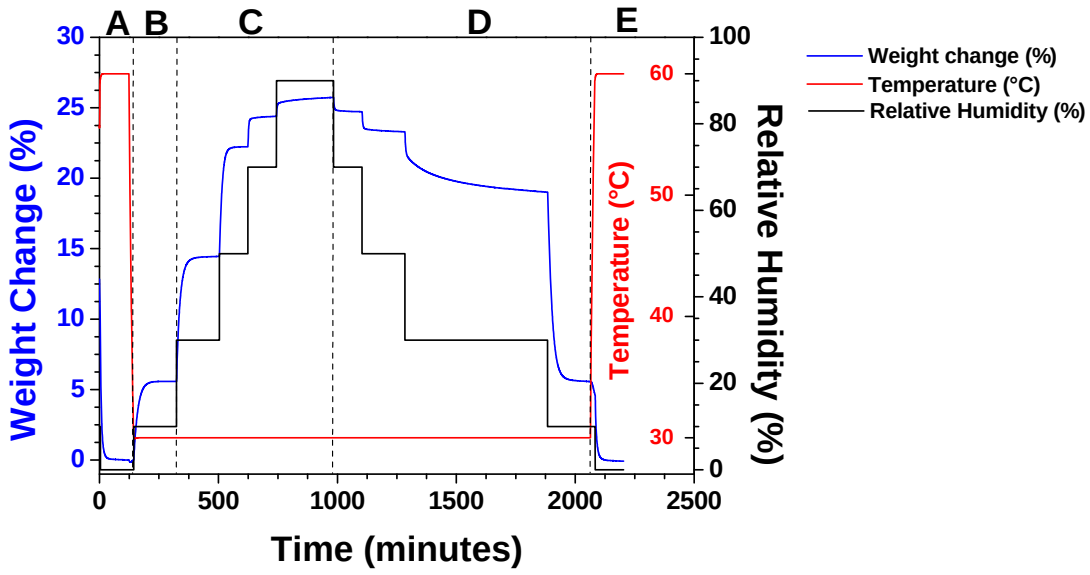

Figure 3.8. An isothermal measurement of silica in the TGA-HC system. The first step involves a drying process at 60 °C and 0% RH (A) until the weight change was stabilized. Subsequently, the humidity was increased from 20% up to 90% RH (in steps of 20% RH) (C). In the next step (D), the RH was reduced from 90 to 10% RH in steps of 20% RH. The final procedure involved drying in order to achieve the initial weight (E).

Poly(acrylic acid) sodium salt, poly(ethylene glycol) and silica are known as "super absorbers" and are used in *e.g.* diapers, personal care products or as drying agents. More specifically, as a super absorbing polymer, the PAA sodium salt has the ability to absorb up to 500 g of water per gram of polymer.[60] They thus reveal a remarkable capability to bind water molecules when immersed in water (*e.g.* in direct contact with the liquid). The standard measurement procedure was therefore applied for these materials in order to investigate their water uptake behavior when they were in a humid atmosphere as opposed to in direct contact with water. The obtained weight percent change of the materials at different RH values (sorption isotherm) is plotted in Figure 3.9. The PAANa exhibited the highest water uptake at 90% RH (88%) as compared to poly(ethylene glycol) (73%) and silica (26%). However, P(AA) sodium salt and poly(ethylene glycol) displayed smaller weight changes than silica at low humidity levels. The weight change of silica increased in a relatively linear fashion until it reached its maximum sorption level. In the case of poly(ethylene glycol), the material did not absorb any significant amounts of water until the humidity level reached 80% RH, but at

90% RH, the weight change was recorded as high as 73% after stabilization. The observed non-linear uptake behavior of the polymers can be explained by the difficulty in the formation of a first hydration shell that extends the polymer coils. To overcome this negative entropy effect a certain amount of favorable polymer-water hydrogen bonds (hydration shell) needs to be formed. The subsequent hydration shells are more easily formed due to a smaller entropy effect and, thus, a steep increase in water uptake is observed at high RH values.[61] Silica, however, did not display this effect since it is not a polymer, and thus becomes saturated much faster at higher humidities as compared with the other materials. In summary, these results demonstrated that super absorbers behave very differently when exposed to liquid water as opposed to humid atmospheres.

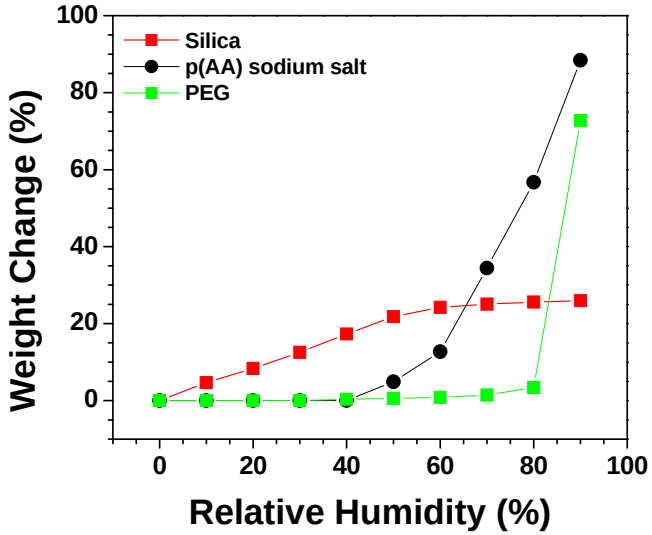

Figure 3.9. Water uptake measurements of PAANa, PEG and silica, demonstrating the weight change (%) as a function of the relative humidity (%) for each sample (sorption isotherm).

In addition to the analysis on the super absorbers, a set of water-soluble polymers (*e.g.* PAA, PHEMA and PVIM) with various functionalities was analyzed. PMMA was also included in this set of polymers to confirm that no significant amount of water was adsorbed in the sample pan and to demonstrate the poor interaction between water molecules and this hydrophobic polymer. The obtained sorption isotherms are displayed in Figure 3.10. As expected, PMMA revealed a weight change of less than 0.1% during the complete measurement cycle. The maximum measured weight percent change, *e.g.* that of the PAANa (88%), was more than twice that of PAA (34%). The sorption isotherms of PAA and PHEMA were found to be very similar with maximum water uptake values of 34% and 31% at 90% RH, respectively. In contrast, the PVIM showed higher water uptake values at all humidities

(except when compared with the PAANa), whereby the mass increased linearly up to 70% RH. The similar water uptake behavior of PAA and PHEMA could be rationalized by the presence of hydroxy and acid groups in the polymer backbone. These groups are able to act as hydrogen bond donors for water, while the acid group of the PAA and the ester group of the PHEMA are known as hydrogen bond acceptors. As such, both polymers display similar interactions with water, which might result in the formation of similar hydration shells and, thus, a similar water uptake behavior. PVIM has stronger hydrogen bond accepting groups with respect to the carboxylic acid and the ester groups as donor groups. Hence, it can be concluded that the presence of hydrogen bond accepting groups has a stronger effect on the water uptake than hydrogen bond donor groups, which again might be ascribed to the formation of more favorable hydration shells.

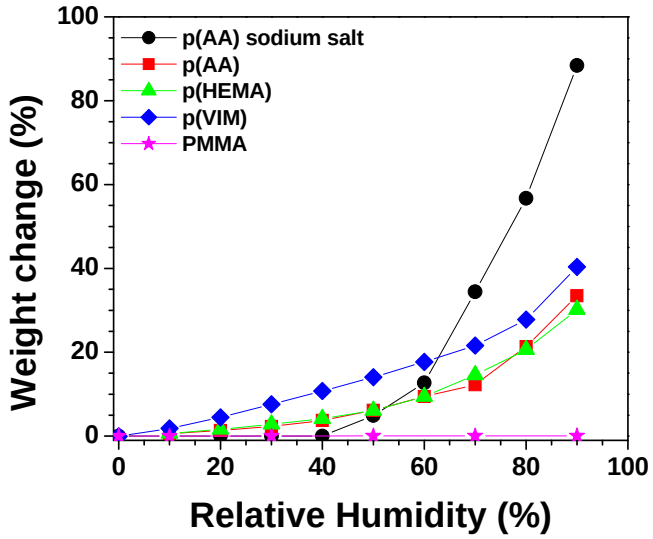

Figure 3.10. Water uptake measurements of P(AA), P(HEMA), P(VIM) and PMMA demonstrating the weight change (%) as a function of the relative humidity (%) for each sample.

The TGA-HC investigation was also carried out on two poly(2-oxazolines), namely PMeOx and PEtOx. These polymers contain amide groups with a carbonyl group in the side chain and a nitrogen group in the backbone. PMeOx and PEtOx are both water soluble. The water uptake values in both cases were measured for samples with a relatively low degree of polymerization (30 units), so that the alkyl group of the oxazolines (methyl or ethyl) should be directly responsible for any observed difference. The resulting sorption isotherms are depicted in Figure 3.11. It can be seen that the PMeOx has the ability to absorb 60% of water at 90% RH, while the PEtOx absorbs only 35% under equivalent conditions. Both polymers contain hydrogen bond accepting groups, which explains their relatively high water uptake

values. The smaller fraction of hydrophobic side chains in PMeOx rendered it more hydrophilic and PMeOx could therefore absorb more water at high humidities than PEtOx. In addition, the effect of the chain length on the water uptake was also investigated for these polymers. For this purpose, PMeOx and PEtOx polymers with 100 repeating units were used. As displayed in Figure 6, the PMeOx with 100 repeating units showed a water uptake ratio that was only slightly higher than for its counterpart with only 30 repeating units. A similar effect was observed for PEtOx. These results indicate that the effect of the chain length and the influence of the end group on the water uptake of the polymers were practically negligible in the investigated cases.

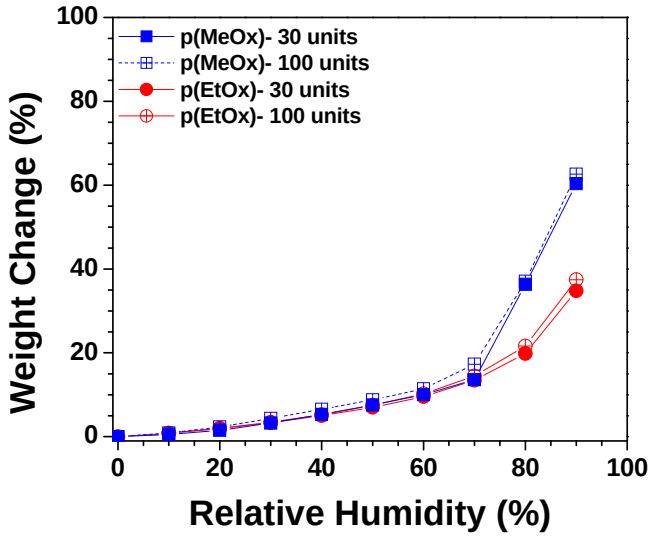

Figure 3.11. Water uptake measurements of PMeOx and PEtOx with varying chain lengths, demonstrating the weight change (%) as a function of the relative humidity (%) for each sample.

The LCST behavior is related to a delicate balance of hydrogen bonds that are formed between the polymer chain and water molecules. Below the LCST, the polymer chains are fully hydrated and the polymer exhibits a hydrophilic structure. The polymer is therefore soluble in water. However, above the LCST the hydrogen bonds between the water molecules and the polymer chains are broken and the hydration shell around the polymer is destroyed, thus giving rise to a hydrophobic structure. This, in turn, results in the chains collapsing in solution and the polymer precipitating. The water uptake behavior of LCST polymers is also of great interest since such materials are expected to display different trends below and above their specific LCSTs. As a result, it should be possible to alter the water uptake behavior by changing the temperature. PNIPAM and PDMAEMA homopolymers have been reported to display LCST values in water of 32 ºC and 46 ºC, respectively. Consequently, water uptake

measurements were performed at 20 ºC and 40 ºC for PNIPAM and at 30 ºC and 80 ºC for PDMAEMA. The isotherm measurement of PNIPAM at 20 ºC (shown in Figure 3.12) exhibited a linear increase in the change in weight percentage and a maximum water uptake of 8% was recorded. This demonstrates the ability of the polymer to attract water molecules from the environment at temperatures below its LCST. The same measurement was performed at 40 ºC. At this temperature, which was above the LCST of PNIPAM, the polymer did not absorb any water molecules. On the contrary, a slight negative weight change was observed rendering apparently the increased hydrophobicity of the polymer chain with increasing RH. A similar behavior was also observed for PDMAEMA. The slight decrease in weight upon increasing the RH above the LCST is not understood at the moment and will be the focus of future investigations. Furthermore, the obtained change in weight percentage for PDMAEMA was 22% and thus higher than for PNIPAM. The higher water uptake of PDMAEMA as compared to PNIPAM can be explained by the fact that PDMAEMA was a better hydrogen bond acceptor due to its nitrogen and carbonyl groups, which are believed to improve the formation of a hydration shell around the polymer. The reversibility of the water uptake at a constant temperature was clearly seen in the case of PDMAEMA. The PNIPAM showed a slight hysteresis during the desorption measurement, which might be related to interchain hydrogen bonding that also causes hysteresis in the LCST transition of aqueous pNIPAM solutions.

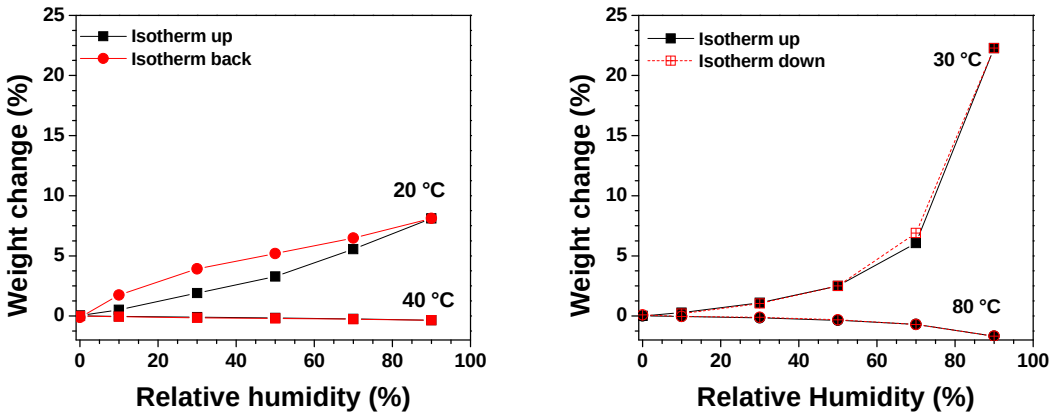

Figure 3.12. Water uptake measurements of PNIPAM (*left*) and PDMAEMA (*right*) below and above their respective LCSTs, demonstrating the weight change (%) as a function of the relative humidity (%) for each sample.

All corresponding molar masses and polydispersity indices of the materials are listed in Table 3.2. In addition, the weight changes in percentage for the samples measured at 90% relative humidity at 30 °C are also listed.

Table 3.2. Selected properties of the studied polymers.

Name	M_n [g/mol]	PDI	Weight change [%] 90% RH @ 30 °C
PAANa			88
Silica			26
PEG	2,800	1.09	73
PAA	1,800		33
PHEMA	20,600	1.31	30
PVIM	100,000		40
PMMA	4,000	1.06	0.06
PMeOx	2,975	1.12	60
	11,100	1.19	63
PEtOx	3,000	1.14	35
	10,000	1.16	37
PNIPAM	50,100	1.72	8 (@ 20°C)
PDMAEMA	9,500	1.11	20

3.4 Standard protocol for a kinetic study on RAFT polymerizations in a synthesizer

Successful synthesis of macromolecules with desired compositions, topologies and functionalities has been a source of great interest and curiosity to polymer researchers for many decades. Numerous heterogeneous or homogeneous reaction mechanisms have been reported by employing specially designed catalysts for the polymerization of a variety of monomers.[62] The efficiencies of those catalysts or chain transfer agents[63,64] (CTAs) to sustain control over the polymerization are often limited to a certain class of monomers or to specific reaction conditions. Each catalyst requires the specific selection of polymerization parameters including, *e.g.* type of monomer,[65] initiator, co-catalyst, solvent, polymerization temperature, reaction time and stirring speed. The list of important parameters may be extensive and their effect on the polymerization has to be investigated in order to produce well–defined polymers. It is possible to select some relatively important reaction parameters and to investigate their effect with a limited number of experiments. However, this classical approach provides only a narrow window to evaluate the actual effect of a certain parameter on the reaction. The combination of modern tools and HTE methodologies can provide a better understanding based on numerous automated parallel experiments all performed under the exact same conditions and in the absence of any handling errors.

Automated synthesis platforms have been used in various fields of chemistry because of their advantages over classical methodologies such as faster, unattended and more reliable experimentation. These platforms are not only used in materials science for research and development of polymers or catalysts but are also extensively used for pharmaceuticals, agrochemicals, and specialty chemicals. Nevertheless, our main interest was creating a universal protocol for the application of controlled/"living" polymerization reactions on one of the most advanced automated synthesis platforms commercially available.

Atom transfer radical polymerization (ATRP), nitroxide mediated radical polymerization (NMP) and RAFT[66] polymerization have attracted great attention since they provide well–defined polymers under certain reaction conditions without the need for a stringent purification of monomers and solvents. Therefore, many research groups conducted kinetic studies by using different monomers, initiators,[67,68] catalysts,[69,70] solvents,[71] polymerization temperatures and reaction times to understand the effect of those parameters. On the other hand, the evaluation and comparison of the results obtained by independent laboratories can not be compared easily because of the unavoidable differences in experimentation procedures and judging styles of different researchers. A fair comparison of the experimental results can only be performed by following the same procedures and under the same conditions using the same purity of reagents. To minimize and overcome these unavoidable variations in manual experiments, the use of automated parallel synthesizer platforms might be beneficial. Combinatorial synthesis and evaluation provides the researcher a possibility to obtain a better overview and deeper understanding of the effect of any parameter on the experiment.[72,73] This is possible in a timely fashion by using high–throughput experimentation and characterization tools that provide rapid screening of several parameters in parallel.[74-78]

In this section, we describe an experimental protocol for the high-throughput investigation of the RAFT polymerization kinetics for acrylates, acrylamides and styrenics. This protocol is a step by step standard program that is applicable in the automated parallel synthesizer platform. The parallel synthesis and fast characterization techniques for the determination of monomer conversion and molar mass distribution will be discussed in order to calculate the important kinetic parameters of the polymerization procedure that are required to evaluate the control over and the rate of the polymerizations. This automatic synthetic protocol was already successfully applied for optimizing the RAFT polymerization of various acrylates and methacrylates using 2-cyanobutyl dithiobenzoate as chain transfer agent (CTA).[79,80] In addition, we have demonstrated that the resulting optimized polymerization

procedure can be applied for the synthesis of copolymers[81] and that it can be directly scaled to a ten times larger volume using mechanically stirred reactors.[76]

3.4.1. Instrumentation for automated synthesis and characterization

The polymerizations reported in this protocol were performed in a Chemspeed Accelerator™ SLT106 automated synthesis platform. The schematic overview of the platform is shown in Scheme 3.5 and each unit will be explained in detail below. The platform is equipped with a glass reactor block which consists of 16 reaction vessels each with a volume of 13 mL. The reaction vessels are equipped with a heating jacket for sufficient heating. These heating jackets are connected to a Huber Unistat Tango (–5 °C to 145 °C). Besides, all reaction vessels are equipped with finger type reflux condensers to prevent evaporation during the reactions, in particular during the liquid transfers from the reactor block to the vials. Reflux condensers are connected to a Huber Ministat (–5 °C to 40 °C). Agitation was performed by vortex mixing at a rate of 600 rpm. The reactor platform is also equipped with a stock solution rack with 10 flask attachment positions and connected to an argon line to keep the stock solutions under an inert atmosphere. It is also possible to use a solid dosing unit (SDU) that has accuracy within 0.1 mg; however, it was not necessary to use that tool for the RAFT polymerizations that are discussed in this report. Furthermore, two sample vial racks with 147 positions in each of them were placed in the platform to store the polymerization samples that were used to study the polymerization kinetics. Liquid transfers were handled by using the 4-needle head (4-NH), which is capable of transferring 4 samples from 4 different reactor vessels to 4 sample vials simultaneously. The 4-NH is connected to a reservoir solvent bottle to rinse the needles after each liquid transfer step. Three separate Teflon rinsing stations are available in different positions within the synthesizer hood. The number of reactor blocks, sample vial racks, solid bottles, and stock solution racks can be altered according to the need in this flexible synthesis platform. A step by step program is prepared in the Application Editor module (Product version 1.8.2.18) of the Chemspeed software and the completed program was run in the Application Executer module. Optionally, a webcam can be mounted adjacent to the platform to monitor the experiments online with conventional web browsing software on any computer. It is also crucial that high-throughput experimentation (HTE) should be followed by high-throughput characterization (HTC), which can be performed by online monitoring[82-84] or using autosamplers on offline characterization tools.

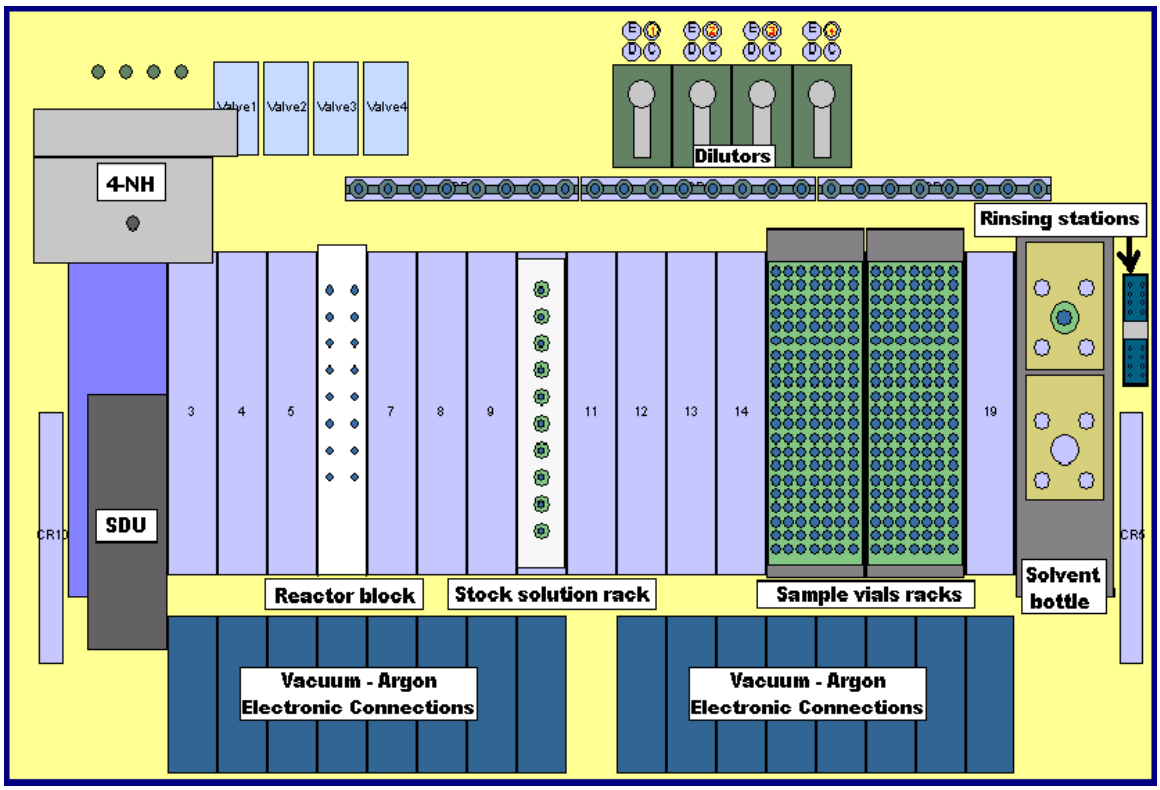

Scheme 3.5. Schematic representation of the layout of the automated synthesis platform.

Monomer conversions were determined by Gas Chromatography (GC). An Interscience Trace GC instrument with a Trace Column RTX–5 connected to a PAL autosampler was used. For the injection of polymerization samples, a special Interscience injector liner with additional glass wool was used.

Size exclusion chromatography (SEC) was measured on two different Shimadzu systems with different configurations and eluents. One system, which has chloroform:triethylamine:isopropanol (94:4:2) as eluent at a flow rate of 1 mL.min^{-1}, is equipped with an SCL-10A system controller, an LC-10AD pump, an RID-10A refractive index detector and a PLgel 5-mm mixed-D; the column oven was set to 50 ºC. Each measurement on this system takes 15 minutes per sample which is a relatively short measuring time in comparison to other SEC systems. The other system, which has *N,N*-dimethylacetamide with 5 mmol LiCl mixture as eluent at a flow rate of 1 mL.min^{-1}, is equipped with a SCL-10A system controller, a LC-10AD pump, a RID-10A refractive index detector, a SPD-10A UV detector and both a PSS Gram30 and a PSS Gram1000 column in series and the column oven was set to 60 ºC. The SEC measurement using this system takes approximately 35 minutes for each injection.

3.4.2 Typical polymerization protocol in the automated synthesizer platform

Design of experiments is the first and most important step of the any HTE protocol and must be done carefully. In this study, experiments are designed to study the polymerization kinetics of eight different monomers using two different chain transfer agents (CTA) which will result in 16 experiments in one explorative automated synthesis run. Eight different stock solutions of the monomers acrylic acid (AA), *N*-isopropyl acrylamide (NIPAM), hydroxyethyl acrylate (HEA), hydroxypropyl acrylate (HPA), *N*,*N*-dimethyl acrylamide (DMAc), *n*-butyl acrylate (*n*-BA), octadecyl acrylate (ODA) and *p*-methyl styrene (*p*-MS) in appropriate solvents and also two stock solutions for two different CTAs and, in addition, a stock solution with initiator (AIBN) in the solvent (preferably in the same solvent used for the monomer) have to be prepared. The chemical structures of the used monomers, CTAs and initiators are depicted in Scheme 3.6. The required amounts of the relevant stock solutions of monomer, initiator, CTA and solvent should be prepared at least 10% in excess. This slight excess is required to ensure that only liquid is drawn into the needle during aspiration since the end of the needle is cut on an angle and may also aspirate gas from within the stock solution flask at low solution levels. The prepared stock solutions should be bubbled with argon to remove the oxygen, not less than 30 minutes, either in a fume hood or in the synthesizer platform by using needles connected to the argon line of the robot with specifically designed tubing.

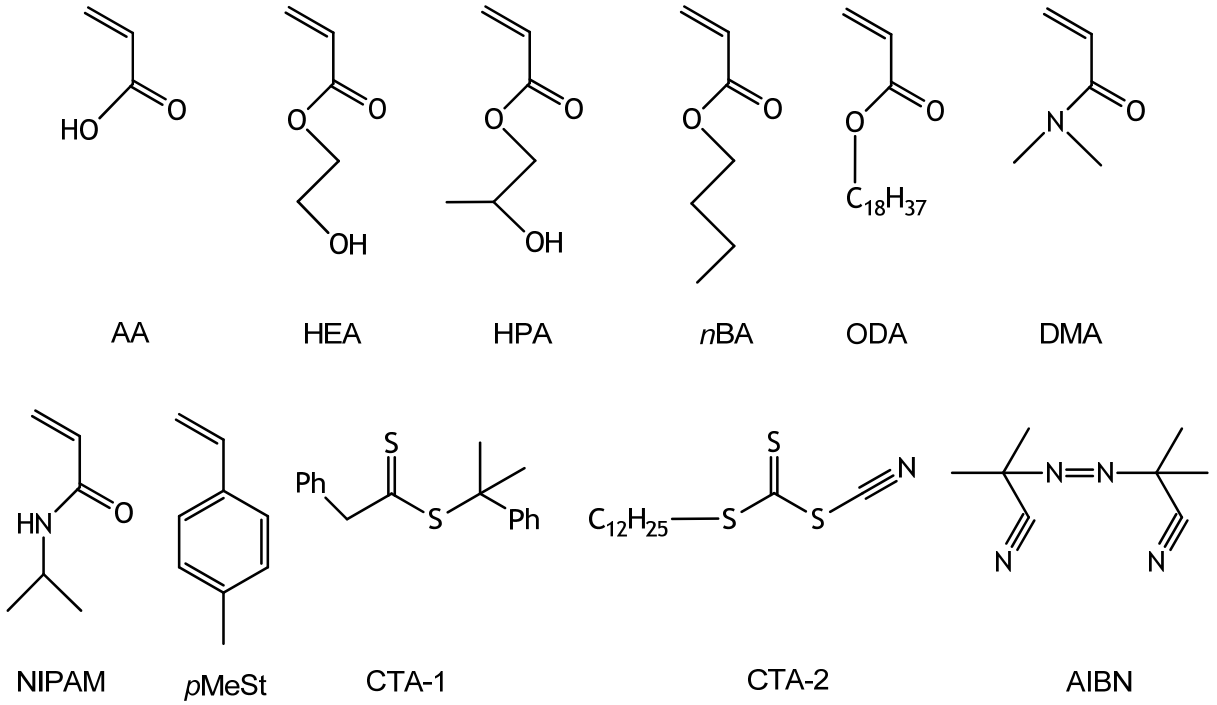

Scheme 3.6. Schematic representation of the chemical structures of the utilized CTAs, monomers and initiator.

A total reaction volume of 4 mL and a monomer concentration of 2 M (with the exception of NIPAM due to the limited solubility) were used for each of the reaction vessels when the 16×13 mL double jacket reactor block was utilized. The ratio [CTA]:[monomer]:[AIBN] can be varied to optimize the RAFT polymerization conditions. The experiment was programmed to transfer samples with a volume of 100 μL from each reactor vessel at predefined times to study the monomer conversion, molar mass and polydispersity indices in time. The transferred samples were also diluted with 1 mL of an appropriate solvent prior to the injection to gas chromatography (GC) or gel permeation chromatography (SEC) instruments. To ensure sufficient space for the sample vials, two sample vial racks each with 147 positions were placed in the platform.

Before starting the automated synthesis run, the reactor block has to be mounted in the robot system and a sufficiently large solvent reservoir has to be placed in the robot followed by flushing the tubing extensively to remove gas bubbles. Subsequently, the stock solution vials should be placed in the stock solution rack, the labeled sample vials are positioned in the sample racks, the hood of the platform is closed and the robot is flushed with argon for at least 60 minutes to create an inert atmosphere in the robot system. It should be mentioned that argon is preferred over the use of nitrogen based on the higher density of argon in combination with the loss of inert gas through the opening connections of the hood for, *e.g.*, the waste lines. During this flushing period, the program to run the robot can be prepared in the Application Editor Software module of the Chemspeed system. Note that less experienced users might want to prepare the program in advance to make sure it is ready to use when the hardware is ready. All available tasks, *e.g.* transfer liquid, transfer solid, wait, heat or cool, reflux, vacuum, etc. in the programming software are on the left side of the window and they can be added to the program by dragging and dropping to the right side. After adding a generic step to the program, the necessary settings have to be adjusted, *e.g.* the amount of liquid or solid that is to be transferred, the period of waiting time, the required temperature for the heater or cooler.

The first three steps of the program are the common ones which should be performed prior to any experiment in this platform. First, a liquid transfer from the valve ports to the waste is required to fill and rinse all the tubing prior to any liquid transfers and to remove air bubbles from the tubing to ensure accurate volume transfers. The following step is another wait step, 60 minutes, to develop a positive pressure of argon to maintain an inert atmosphere in the hood. When the robot system is equipped with a glove-box hood, the positive pressure can be directly seen by the upward positioning of the gloves. The last step of the three is possibly the most important step in the program and is labelled as ‘inertization’. This step is a

macro task and consists of numerous steps and even sub-macro-tasks. Each step of the inertization macro task is listed in Table 3.3. The macro-task starts with heating the reactor block and reflux condensers to 140 °C and 40 °C, respectively. As soon as the set temperature is reached it continues with the next sub macro-task which is applying vacuum to the reactor vessels for 2 minutes and flushing them with argon for 1 minute and repeating this cycle for 10 times while vortexing. After the completion of this sub macro task the reactor block is cooled to 20 °C and the reflux condensers to 0 °C, respectively. By finalizing this macro task, an inert atmosphere is prepared in the hood and also in the reaction vessels.

Table 3.3. Steps of the inertization macro task.

Step	Substep	Task	Description
1		Wait	Wait 1 minute
2		Vortex	Agitation ON (600 rpm) on zone reactors
3		Heating / Cooling	Thermostat ON (140 °C) on zone reactors
4		Reflux	Reflux temperature ON (40 °C) on zone reactors
5		Macro Task	Loop 10 times
	5.1	Set drawer reaction block	Closed under vacuum on zone reactors
	5.2	Vacuum	Vacuum ON on zone reactors
	5.3	Wait	Wait 2 minutes
	5.4	Set drawer reaction block	Closed under inert gas (Ar) on zone reactors
	5.5	Wait	Wait 1 minute
6		Set drawer reaction block	Open under inert gas (Ar) on zone reactors
7		Heating / Cooling	Thermostat ON (20 °C) on zone reactors
8		Reflux	Reflux temperature ON (0 °C) on zone reactors
9		Heating / Cooling	Thermostat ON (20 °C.) on zone reactors
10		Vortex	Agitation OFF on zone reactors
11		Vacuum	Vacuum OFF on zone reactors

The following steps of the program with short descriptions are listed in Table 3.4 and the detailed explanation is as follows. Subsequent to cooling the reactor block and reflux condensers, the robotic arm picks up the 4-needle head (4-NH) and starts transferring liquids from the stock solution vials to the reactor vessels with the predefined values while vortex mixing is continuously preformed. Subsequent to the addition of all necessary stock solutions to the reactors, there is a one minute waiting step to ensure the homogeneity of the reaction mixtures before transferring the initial (t_0) samples of the polymerizations to the GC vials. Following the first sampling step, the drawer valve position is set to closed under argon and heating the reactor blocks is started to the set reaction temperature (in this case 70 °C) while maintaining the reflux condensers at 0 °C. The next step after reaching the desired reaction

temperature is called 'set timer' which will be accepted as the beginning time of the reaction. The exact times for sampling will be calculated according to this initial timing step. The rest of the program consists of several waiting and sampling steps until the last step which is a shut down macro task. Importantly, after each liquid transfer from the reactor vessels to the sample vials the 4-NH will rinse the inside and also the outside of the four needles by transferring 2 mL of solvent from the reservoir to the waste. The final shut down procedure cools down the reactors, warms up the reflux condensers to room temperature and stops vortex mixing, vacuum pump, thermostat and cryostat.

Table 3.4. Step-by-step protocol for the RAFT polymerization in the automated platform.

Step	Task	Description
1	Liquid Transfer	From reservoir to waste port
2	Wait	1 hour (filling hood with Argon)
3	Inertization	Macro task
4	Liquid Transfer	From reservoir to waste port
5	Liquid Transfer	From AA stock to reactors
6	Liquid Transfer	From NIPAM stock to reactors
7	Liquid Transfer	From HPA stock to reactors
8	Liquid Transfer	From DMA stock to reactors
9	Liquid Transfer	From BuA stock to reactors
10	Liquid Transfer	From HEA stock to reactors
11	Liquid Transfer	From ODA stock to reactors
12	Liquid Transfer	From MeSty stock to reactors
13	Liquid Transfer	From CTA1 + AIBN stock to reactors
14	Liquid Transfer	From CTA2 + AIBN stock to reactors
15	Liquid Transfer	From solvent stock to reactors
16	Vortex	Agitation ON (600 rpm) on zone reactors
17	Wait	1 minute (mixing the reactors)
18	Liquid Transfer	From reactors to t-zero sample vials
19	Liquid Transfer	From solvent bottle to t-zero sample vials
20	Reflux	Reflux temperature ON (0 °C) on zone reactors
21	Heating / Cooling	Thermostat ON (70 °C) on zone reactors
22	Set Timer	Set timer = 0
23	Wait	Wait 1 hour after timer = 0
24	Liquid Transfer	From reactors to t-1 hour sample vials
25	Liquid Transfer	From solvent bottle to t-1 hour sample vials
#	Repetition of step 23-25 with different waiting times	
39	Shut down	Macro task
		Shut down thermostat, cryostat and vortex

When the program writing phase is complete, it is advised to double check each step and value in order to minimize human errors in the programming. It is also advisable to run a simulation in the Application Executor Software module (which is also the application that actually runs this program). After running the automated parallel polymerizations, the hood of the synthesis robot has to be air-extracted for at least 1 hour to remove the volatile monomers and solvent. After this extraction period, the robot system can be opened and the sample vials as well as the final polymers from the parallel reactors can be collected for analysis.

3.4.2. Automated characterization techniques for parallel kinetic experiments

Following the successful completion of 16 parallel polymerizations and transferring all samples for the kinetic studies, the monomer conversion in each sample vial is measured by using gas chromatography (GC) (or other analytical technique as necessary). The chromatograms thus obtained will yield the ratio between the monomer and reference solvent peaks (which is normally the reaction solvent – hence a different solvent to the reaction solvent must be used for diluting the GC samples). The conversion will be calculated by comparing these ratios with the initial ratio from the t_0 sample of each reaction. Depending on the oven program of the GC, each measurement takes around 10 to 30 minutes (including cooling) by using a GC equipped with an auto sampler. The accuracy of the calculation of the monomer conversion is dependent on the peak shape of the monomer and solvent in the GC trace. For instance, the AA monomer has a broad peak in GC and ODA shows no peak in GC. Therefore, the monomer conversions for AA and ODA may have to be determined by using NMR or SEC, respectively. All the other monomers that are used in this study result in narrow peak shapes with good separation providing accurate results. Semi-logarithmic kinetic plots can be drawn by using the data obtained from GC. The results of four monomers, namely *n*-BA, DMAc, HPA and *p*-MS are shown in Figure 3.13 as a representative first order kinetic plot. The slopes of each set of data in the kinetic plot divided by the CTA concentration gives the apparent propagation rates of the monomers with units of $L \times mol^{-1} \times s^{-1}$. The apparent rate constants (k_p^{app}) calculated for *n*-BA, DMAc, HPA and *p*-MS are 0.98×10^{-4} s^{-1}, 2.32×10^{-4} s^{-1}, 1.89×10^{-4} s^{-1}, 0.17×10^{-4} s^{-1}, respectively.

Besides the determination of the monomer conversion, the molar masses and polydispersity indices of the polymers represent highly important data for such a kinetic study. Therefore, SEC can be used as a rapid and efficient characterization tool to obtain the molar mass data of the polymers. Relatively short measurement times per sample can be achieved by using shorter or less serial chromatography columns. On the other hand this may reduce the accuracy of the obtained results depending on the molar mass range of the column.

After the GC measurements, the same samples are placed into the autosampler of the SEC systems and are analyzed under the appropriate conditions. Number average molar masses and polydispersity indices of the polymers *versus* monomer conversion plots can be drawn by using the data obtained from GC and SEC, as shown in Figure 3.13. It is also possible to compare the theoretical and the obtained molar masses of the polymers at certain monomer conversion. This typical plot provides crucial information about the control over the polymerization.

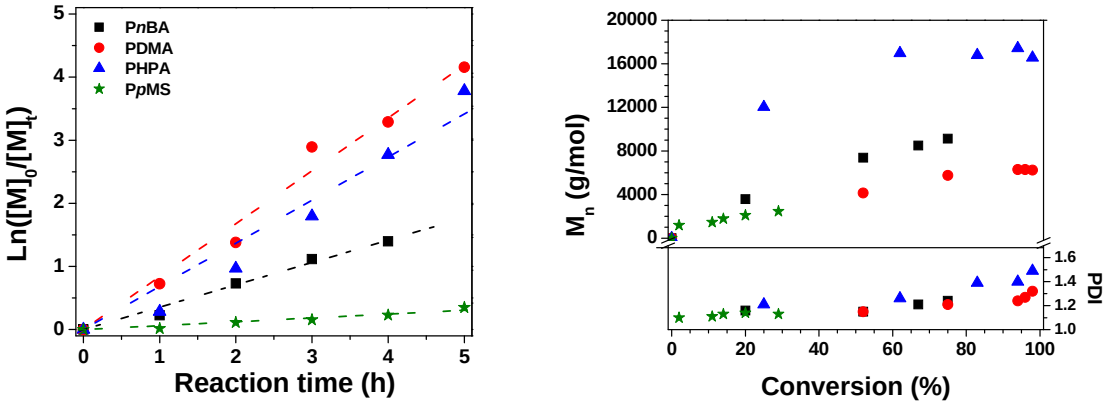

Figure 3.13 *Left:* Semi-logarithmic first order kinetic plot of *n*-BA(■), DMAc(●), HPA(▲) and *p*-MS(★). *Right:* Molar mass and polydispersity index *versus* monomer conversion plot of *n*-BA(■), DMAc(●), HPA(▲) and *p*-MS(★).

3.5 Conclusions

In this chapter, the systematic and parallel polymerization of various $OEGMA_x$ monomers and MAA with the RAFT polymerization technique is described. Libraries of well–defined homopolymers (in total 60 polymers) were prepared and investigated regarding their LCST behavior. The homopolymers with different degree of polymerization showed a slight effect on the LCST behavior, whereas the number of ethylene glycol units attached to each repeating unit revealed a strong decreasing trend with decreasing number of ethyleneglycol units. Furthermore, replacing the methoxy end group with ethoxy also significantly reduced the cloud points due to the higher hydrophobicity. In addition, well–defined copolymers of $OEGMA_x$'s and methacrylic acid were synthesized with varying the monomer contents using RAFT. In the case of p(MAA)-*r*-($OEGMA_{475}$) the cloud point could be even tuned in the range from 20 to 90 °C. Surprisingly, p(MAA)-*r*-($OEGMA_{1100}$) copolymers showed an LCST behavior at a certain composition, although their homopolymers did not reveal any LCST behavior. Such unexpected properties are more likely to be identified

by a library screening approach. A possible explanation for this unexpected behavior could be based on intramolecular hydrogen bonding interactions between the acid groups and the ethyleneglycol chains which is an additional driving force to collapse the polymer chains. Besides, the MAA-*r*-$OEGMA_{1100}$ copolymers exhibit a double responsive behavior, namely thermo- and pH-response. We believe that this systematic screening of LCST materials synthesized by controlled radical polymerization techniques represents a crucial step in order to identify structure-property relationships that will allow in the future the development and the selection of the best suited material for a desired application.

Furthermore, we have investigated the water uptake abilities of a number of materials by TGA-HC at various humidities. The feasibility of the well–defined, precisely controlled and now commercially available setup for these measurements was demonstrated on polymeric materials regardless of their physical form (liquid, powder or crosslinked systems). The various classes of polymers were analyzed for their water uptake behavior under reproducible and automated conditions. At first, the water uptake of superabsorbers, more specifically PAANa, PEG and silica, was determined. PAANa and PEG showed lower water uptake values at low humidities and higher water uptake values at high humidities compared to silica. The steep increase in water uptake at high RH conditions is believed to be related to a certain difficulty in the formation of a first hydration shell after which additional hydration shells could form more easily. Furthermore, other hydrophilic polymers, *e.g.* PAA, PHEMA, and PVIM, as well as a hydrophobic polymer, PMMA, were studied and the results were compared with those obtaine for the PAA sodium salt. In general, a material with hydrogen bond accepting groups was more prone to displaying high water uptake values than a material with hydrogen bond donor groups. This is most likely due to the facilitated formation of hydration shells around the polymer. In addition, PMeOx and PEtOx were also investigated with the TGA-HC. Although both polymers had hydrogen bond accepting groups, the PMeOx was found to absorb more water at higher humidities because of its slightly more hydrophilic structure. In addition, the effect of the length of the polymeric chain revealed almost no influence on the water uptake ability of these materials. Finally, polymers with an LCST behavior were examined and were found to reveal different trends below and above their LCSTs. PDMAEMA absorbed more water in comparison to PNIPAM at temperatures below their specific LCSTs, and a further weight loss was observed for both materials when increasing the RH above the critical temperature.

In the last part of this chapter, we reported a standard protocol for the kinetic investigation of RAFT polymerizations of various monomers that can be performed in an automated parallel synthesis platform. This standard protocol is practical in obtaining

comparable kinetic data all over the world independent of the research group, technician or student. We believe that HTE and characterization methods will be more efficient as well as eliminate errors and variability due to different researchers or laboratory conditions by employing reported standard protocols.

3.6 Experimental part

Materials

Methacrylic acid (MAA, Aldrich) and acrylic acid (AA, Aldrich 99%) were purified by treating the monomer with inhibitor-remover (Aldrich). Mono(ethyleneglycol) methyl ether methacrylate (MEOMA, Aldrich), di(ethylene glycol) methyl ether methacrylate (MEO_2MA, Aldrich), oligo(ethyleneglycol) methyl ether methacrylate ($OEGMA_{475}$, $M_n \sim 475$ g/mol, Aldrich) and oligo(ethyleneglycol) ethyl ether methacrylate ($OEGEMA_{246}$, $M_n = 246$ g/mol, Aldrich), hydroxyethyl acrylate (HEA, Aldrich 96%), hydroxypropyl acrylate (HPA, Aldrich 95%, mixture of isomers), *n*-butyl acrylate (*n*-BA, Aldrich 99+%), octadecyl acrylate (ODA, Aldrich 97%), *N*,*N*-dimethyl acrylamide (DMAc, Aldrich 99%), *N*-isopropyl acrylamide (NIPAM, Aldrich 99%) and *p*-methyl styrene (*p*-MS, Aldrich 96%) were purified by passing over a neutral aluminum oxide column. Oligo(ethyleneglycol) methyl ether methacrylate ($OEGMA_{1100}$, $M_n \sim 1100$ g/mol, Aldrich) was dissolved in dichloromethane, passed over a neutral aluminum oxide column and dried under vacuum. Azobis(isobutyronitrile) (AIBN, Aldrich) was recrystallized from methanol. 2-Cyano-2-butyl dithiobenzoate (CBDB, chain transfer agent) was kindly provided by AGFA. Cumyl phenyldithioacetate (CTA-1) and *S*-dodecyl-*S*′-cyanomethyl trithiocarbonate (CTA-2) were synthesized according to a procedure described elsewhere.[85,86] *N,N*-Dimethylformamide (DMF), *N,N*-dimethylacetamide (DMAc), and all other solvents were purchased from Biosolve Ltd.

PAANa (particle size <1,000 μm), PAA and silica (particle size from 2 to 5 mm) were purchased from Aldrich, PMMA and PEG polymer standards were obtained from PSS, and PDMAEMA and PNIPAM were synthesized via the RAFT polymerization technique as reported elsewhere.[24,31] PHEMA was synthesized via RAFT polymerization and the RAFT agent was cleaved by using *n*-hexylamine after the polymerization. PMeOx and PEtOx were prepared by a living cationic ring opening polymerization as previously reported.[87] PVIM was synthesized by free radical polymerization according to the procedure described by Tan.[88] All corresponding molar masses and polydispersity indices are listed in Table 3.2. Distilled water was used for the humidity chamber.

Instruments

GC measurements were performed on an Interscience Trace GC used with a Trace Column RTX-5 connected to a PAL autosampler. SEC measurements were performed on a Shimadzu system equipped with a SCK-10A system controller, a LC-10A pump, a RID-10A refractive index detector, and a PL gel 5 μm Mixed-D column at 50 °C, using a mixture of chloroform, triethylamine and isopropanol (94:4:2) as eluent at a flow rate of 1 $mL \cdot min^{-1}$. Turbidimetry measurements were performed in a Crystal 16 from Avantium Technologies. Four blocks of parallel temperature-controlled sample holders were connected to a Julabo FP40 cryostat, allowing 16 simultaneous measurements. Turbidity of the solutions at a concentration of 5 mg/mL was measured by the transmission of red light through the sample vial as a function of the temperature. Solutions of the polymers were prepared in deionized water (Laborpure, Behr Labor Technik) and were stirred at room temperature until all polymeric material was dissolved or dispersed. Two heating cycles were applied from 0 to 100 C at 1 °C/min with hold steps of 5 min at the most extreme temperatures. The cloud points are given as the 50% transmittance point during the first heating ramp of the aqueous polymer solutions.

The water uptake measurements of the polymers were investigated on a Q5000 SA thermo gravimetric analyzer from TA Instruments containing a microbalance in which the sample and reference pans were enclosed in a humidity and temperature controlled chamber. The temperature in the Q5000 SA was controlled by Peltier elements. Dried N_2 gas flow (200 mL/min) was split into two parts, of which one part was wet by passing it through a water-saturated chamber. The desired relative humidity (RH) for the measurements could subsequently be obtained by mixing proper proportions (regulated by mass flow controllers) of dry and wet stream.

Synthesis of the OEGMA polymer libraries

The synthesis of the polymer libraries was performed in a Chemspeed Accelerator™ SLT106 automated synthesizer. The robot was equipped with a four needle head and an array of 16 parallel 13 mL glass reactors. All reactors were connected to a Huber Unistat Tango (heating range: –40 °C to 145 °C) and were equipped with a cold-finger reflux condenser in which the temperature can be controlled from –5 °C to 40 °C. A double inert atmosphere was maintained by applying a 1.1 bar flow over the reactors and a 1.5 bar argon flow through the hood of the Accelerator™. The inert atmosphere in the hood of the Accelerator™ SLT106 was obtained by flushing with argon for at least 90 minutes prior to the experiments. In addition, the reaction vessels were heated to 120 °C, evacuated for 15 minutes, and then filled

with argon. This procedure was repeated three times to be able to perform the reactions under inert atmosphere. Different amounts of the RAFT agent (CBDB in ethanol), AIBN (in ethanol) and the desired monomers were transferred into the reaction vessels. The ratio of RAFT to AIBN was 1:0.25. The reaction was performed in ethanol and the total volume of each reaction was 4 mL. The kind of monomers, the ratio of monomers and the monomer to CBDB ratio were varied in the experiments. The polymerization mixtures were heated to 70 °C and vortexed at 600 rpm. After 10 hours stirring at 70 ºC, the reaction vessels were cooled to room temperature. The products were purified by precipitating into an appropriate non-solvent, i.e. *n*-hexane or diisopropylether, whereas chloroform was used in the case of the poly(methacrylic acid) homopolymers. After removal of the solvents and residual monomers, the polymers were dried in a vacuum oven at 40 °C overnight prior to analysis. Some polymerization experiments were performed in the oil bath using the same reagent ratios and experimental conditions as in the automated synthesis platform. Initial aliquots from each reactor and the final aliquots were withdrawn into small vials in order to determine the monomer conversion and the molar mass data.

3.7 References

(1) A. M. Mathur, B. Drescher, A. B. Scranton, J. Klier, *Nature* **1998**, *392*, 367−370.
(2) L. Zhang, R. Guo, M. Yang, J. Xiqun, B. Liu, *Adv. Mater.* **2007**, *19*, 2988−2992.
(3) Y. Z. You, Q. H. Zhou, D. S. Manickam, L. Wan, G. Z. Mao, D. Oupicky, *Macromolecules* **2007**, *40*, 8617−8624.
(4) I. Dimitrov, B. Trzebicka, A. H. E. Mueller, A. Dworak, C. B. Tsvetanov, *Prog. Polym. Sci.* **2007**, *32*, 1275−1343.
(5) M. E. Harmon, M. Tang, C. W. Frank, *Polymer* **2003**, *44*, 4547−4556.
(6) D. Schmaljohann, *e−Polymers* **2005**, *21*, 1−17.
(7) D. Schmaljohann, *Adv. Drug Delivery Rev.* **2006**, *58,* 1655−1193.
(8) E. Gil, S. Hudson, *Prog. Polym. Sci.* **2004**, *29*, 1173−1222.
(9) D. Crespy, R. M. Rossi, *Polym. Int.* **2007**, *56*, 1141−1468.
(10) J. Chiefari, Y. K. Chong, F. Ercole, J. Krstina, J. Jeffery, T. P. T. Le, R. T. A. Mayadunne, G. F. Meijs, C. L. Moad, G. Moad, E. Rizzardo, S. H. Thang, *Macromolecules* **1998**, *31*, 5559−5562.
(11) M. Kato, M. Kamigaito, M. Sawamoto, T. Higashimura, *Macromolecules* **1995**, *28*, 1721−1723.
(12) J. Wang, K. Matyjaszewski, *J. Am. Chem. Soc.* **1995**, *117*, 5614−5615.
(13) C. J. Hawker, G. G. Barclay, A. Orellana, J. Dao, W. Devonport, *Macromolecules* **1996**, *29*, 5245−5254.
(14) N. Hadjichristidis, M. Pitsikalis, S. Pispas, H. Iatrou, *Chem. Rev.* **2001**, *101*, 3747−3792.
(15) T. Ishizone, A. Seki, M. Hagiwara, S. Han, H. Yokoyama, A. Oyane, A. Deffieux, S. Carlotti, *Macromolecules* **2008**, *41*, 2963−2967.
(16) S. Han, M. Hagiwara, T. Ishizone, *Macromolecules* **2003**, *36*, 8312−8319.
(17) X. S. Wang, S. P. Armes, *Macromolecules* **2000**, *33*, 6640−6647.
(18) S. I. Yamamoto, J. Pietrasik, K. Matyjaszewski, *J. Polym. Sci., Part A: Polym. Chem.* **2008**, *46*, 194−202.
(19) M. M. Ali, H. D. H. Stoever, *Macromolecules* **2004**, *37*, 5219−5227.
(20) O. W. Webster, *Science* **1991**, *496*, 887−893.
(21) E. J. Goethals, M. Dubreuil, Y. Wang, I. De Witte, D. Christova, S. Verbrugghe, N. Yanul, L. Tanghe, G. Mynarczuk, F. Du Prez, *Macromol. Symp.* **2000**, *153*, 209−216.
(22) Y. K. Chong, T. P. T. Le, G. Moad, E. Rizzardo, S. H. Thang, *Macromolecules* **1999**, *32*, 2071−2074.
(23) S. R. Gondi, A. P. Vogt, B. S. Sumerlin, *Macromolecules* **2007**, *40*, 474−481.
(24) D. Fournier, R. Hoogenboom, H. M. L. Thijs, R. M. Paulus, U. S. Schubert, *Macromolecules* **2007**, *40*, 915−920.
(25) A. B. Lowe, C. L. McCormick, *Prog. Polym. Sci.* **2007**, *32*, 283−351.
(26) R. Hoogenboom, *Macromol. Chem. Phys.* **2007**, *208*, 18−25.
(27) M. W. M. Fijten, J. M. Kranenburg, H. M. L. Thijs, R. M. Paulus, B. M. van Lankvelkt, J. de Hullu, M. Springintveld, D. J. G. Thielen, C. A. Tweedie, R. Hoogenboom, U. S. Schubert, *Macromolecules* **2007**, *40*, 5879−5886.
(28) R. Hoogenboom, M. W. M. Fijten, S. Wijnans, A. M. J. van den Berg, H. M. L. Thijs, U. S. Schubert, *J. Comb. Chem.* **2006**, *8*, 145−148.
(29) A. Ekin, D. C. Webster, *J. Polym. Sci., Part A: Polym. Chem.* **2006**, *44*, 4880−4894.
(30) R. Hoogenboom, U. S. Schubert, *J. Polym. Sci., Part A: Polym. Chem.* **2003**, *41*, 2425−2434.
(31) H. G. Schild, *Prog. Polym. Sci.* **1992**, 17*,* 163−249.
(32) S. Aoshima, S. Kanaoka, *Adv. Polym. Sci.* **2008**, *210*, 169−208.
(33) Y. Xia, N. A. D. Burke, H. D. H. Stoever, *Macromolecules* **2006**, *39*, 2275−2283.
(34) D. Neugebauer, *Polym. Int.* **2007**, *56*, 1469−1498.
(35) D. N. Robinson, N. A. Peppas, *Macromolecules* **2002**, *35*, 3668−3674.
(36) J. F. Lutz, K. Weichenhan, O. Akdemir, A. Hoth, *Macromolecules* **2007**, *40*, 2503−2508.
(37) J. A. Jones, N. Novo, K. Flagler, C. D. Pagnucco, S. Carew, C. Cheong, X. Z. Kong, N. A. D. Burke, H. D. Stoever, *J. Polym. Sci., Part A: Polym. Chem.* **2005**, *43*, 6095−6104.
(38) J. F. Lutz, J. Andrieu, S. Uzgun, C. Rudolph, S. Agarwal, *Macromolecules* **2007**, *40*, 8540−8543.
(39) E. C. C. Goh, H. Stoever, *Macromolecules* **2002**, *35*, 9983−9989.
(40) G. Mantovani, F. Lecolley, L. Tao, D. M. Haddleton, J. Clerx, J. J. L. M. Cornelissen, K. Velonia, *J. Am. Chem. Soc.* **2005**, *127*, 2966−2973.
(41) www.warwickeffectpolymers.co.uk (last accessed March 20th, 2009).
(42) S. Jana, S. P. Rannard, A. I. Cooper, *Chem. Commun.* **2007**, 2962−2964.
(43) J. F. Lutz, O. Akdemir, A. Hoth, *J. Am. Chem. Soc.* **2006**, *128*, 13046−13047.
(44) J. F. Lutz, *J. Polym. Sci., Part A: Polym. Chem.* **2008**, *46*, 3459−3470.
(45) K. A. Davis, K. Matyjaszewski, *Adv. Polym. Sci.* **2002**, *159*, 2−166.
(46) K. Matyjaszewski, J. Xia, *Chem. Rev.* **2001**, *101*, 2921−2990.
(47) C. J. Hawker, A. W. Bosman, E. Harth, *Chem. Rev.* **2001**, *101*, 3661−3688.

(48) S. Perrier, P. Takolpuckdee, *J. Polym. Sci., Part A: Polym. Chem.* **2005**, *43*, 5347−5393.
(49) D. Tyagid, J. L. Hedrick, D. C. Webster, J. E. Mcgrath, G. L. Wilkes, *Polymer* **1988**, *29*, 883−844.
(50) D. J. T. Hill, N. G. Moss, P. J. Pomery, A. K. Whittaker, *Polymer* **2000**, *41*, 1287−1296.
(51) R. J. Hernandez, R. Gavara, *J. Polym. Sci., Part B*: *Polym. Phys.* **1994**, *32*, 2367−2374.
(52) E. Sacher, J. R. Susko, *J. Appl. Polym. Sci.* **1981**, *26*, 679−686.
(53) S. J. Kim, S. R. Shin, S. M. Lee, I. Y. Kim, S. I. Kim, *J. Appl. Polym. Sci.* **2003**, *88*, 2721−2724.
(54) L. A. McDonough, B. Dragnea, J. Preusser, S. R. Leone, *J. Phys. Chem B.* **2003**, *107*, 4951−4954.
(55) M. Ree, S. Swanson, W. Volksen, *Polymer* **1993**, *34*, 1423−1430.
(56) P. A. Taririsa, D. W. Hess,.*Macromolecules* **2006**, *39*, 7092−7097.
(57) M. Gáspár, Zs. Benkó, G. Dogossy, K. Réczey, T. Czigány, *Polym. Degrad. Stab.* **2005**, *90*, 563−569.
(58) B. De'Neve, M. E. R. Shanahan, *Polymer* **1993**, *34*, 5099−5105.
(59) Application note TA Instruments, Moisture Sorption Analysis of Pharmaceuticals**,** Hassel, R. L. *www.TAinstruments.com* (Last accessed on March 20th, 2009).
(60) Website Sigma−Aldrich *http://www.sigmaaldrich.com/catalog/search/ProductDetail/ALDRICH/436364*, (Last accessed on March 20th, 2009).
(61) R. Kjellander, E. Florin, *J. Chem. Soc.* **1981**, *77*, 2053−2077.
(62) M. Kamigaito, T. Ando, M. Sawamoto, *Chem. Rev.* **2001**, *101*, 3689–3745.
(63) R. T. A. Mayadunne, E. Rizzardo, J. Chiefari, Y. K. Chong, G. Moad, S. H. Thang, *Macromolecules* **1999**, *32*, 6977–6980.
(64) R. T. A. Mayadunne, E. Rizzardo, J. Chiefari, J. Krstina, G. Moad, A. Postma, S. H. Thang, *Macromolecules* **2000**, *33*, 243–245.
(65) A. Goto, K. Sato, Y. Tsuji, T. Fukuda, G. Moad, E. Rizzardo, S. H. Thang, *Macromolecules* **2001**, *34*, 402–408.
(66) G. Moad, J. Chiefari, Y. K. Chong, J. Krstina, R. T. A. Mayadunne, A. Postma, E. Rizzardo, S. H. Thang, *Polym. Int.* **2000**, *49*, 993–1001.
(67) D. Benoit, V. Chaplinski, R. Braslau, C. J. Hawker, *J. Am. Chem. Soc*. **1999**, *121*, 3904–3920.
(68) S. Angot, K. S. Murthy, D. Taton, Y. Gnanou, *Macromolecules* **1998**, *31*, 7218–7225.
(69) A. K. Nanda, K. Matyjaszewski, *Macromolecules* **2003**, *36*, 599–604.
(70) K. Matyjaszewski, B. Goebelt, H. J. Paik, C. P. Horwitz, *Macromolecules* **2001**, *34*, 430–440.
(71) I. Y. Ma, E. J. Lobb, N. C. Billingham, S. P. Armes, A. L. Lewis, A. W. Lloyd, J. Salvage, *Macromolecules* **2002**, *35*, 9306–9314.
(72) M. A. R. Meier, U. S. Schubert, *J. Comb. Sci.* **2005**, *7*, 356–359.
(73) M. A. R. Meier, J.−F. Gohy, C. A. Fustin, U. S. Schubert, *J. Am. Chem. Soc.* **2004**, *126*, 11517–11521.
(74) S. Schmatloch, M. A. R. Meier, U. S. Schubert, *Macromol. Rapid Commun.* **2003**, *24*, 33–46.
(75) R. Hoogenboom, M. A. R. Meier, U. S. Schubert, *Macromol. Rapid Commun.* **2003**, *24*, 15–32.
(76) R. M. Paulus, M. W. M. Fijten, M. J. de la Mar, R. Hoogenboom, U. S. Schubert, *QSAR* **2005**, *24*, 863–867.
(77) M. W. M. Fijten, R. M. Paulus, U. S. Schubert, *J. Polym. Sci., Part A: Polym. Chem.* **2005**, *43*, 3831–3839.
(78) C. R. Becer, R. M. Paulus, R. Hoogenboom, U. S. Schubert, *J. Polym. Sci., Part A: Polym. Chem.* **2006**, *44*, 6202–6213.
(79) M. W. M. Fijten, M. A. R. Meier, R. Hoogenboom, U. S. Schubert, *J. Polym. Sci., Part A: Polym. Chem.* **2004**, *42*, 5775–5783.
(80) R. Hoogenboom, W. Van Camp, F. E. Du Prez, U. S. Schubert, *Macromolecules* **2005**, *38*, 7653–7659.
(81) R. Hoogenboom, M. W. M. Fijten, R. M. Paulus, U. S. Schubert, *ACS Symp. Ser.* **2006**, *944*, 473–485.
(82) E. Mignard, J.−F. Lutz, T. Leblanc, K. Matyjaszewski, O. Guerret, W. F. Reed, *Macromolecules* **2005**, *38*, 9556–9563.
(83) R. Hoogenboom, M. W. M. Fijten, C. H. Abeln, U. S. Schubert, *Macromol. Rapid Commun.* **2004**, *25*, 237–242.
(84) A. Giz, A. O. Koc, H. Giz, A. Alb, W. F. Reed, *Macromolecules* **2002**, *35*, 6557–6571.
(85) S. W. Prescott, M. J. Ballard, E. Rizzardo, R. G. Gilbert, *Macromolecules* **2002**, *35,* 5417–5425.
(86) Y. K. Chong, G. Moad, E. Rizzardo, S. H. Thang, *Macromolecules* **2007**, *40*, 4446–4455.
(87) R. Hoogenboom, R. M. Paulus, M. W. M. Fijten, U. S. Schubert, *J. Polym. Sci., Part A: Polym. Chem.* **2005**, *49*, 1487–1497.
(88) J. S. Tan, A. R. Sochor, *Macromolecules* **1981**, *14*, 1700–1706.

Chapter 4

Atom transfer radical polymerization

Abstract

Atom transfer radical polymerization (ATRP) is the most widely applied controlled/"living" radical polymerization technique. Various types of initiators, metal salts and ligands have been tested to successfully polymerize different classes of monomers. We have investigated the use of a nitrogen based tetradentate ligand with long pendant oligo(ethylene glycol) groups. ATRP of methyl methacrylate was performed using this ligand at different polymerization temperatures and catalyst concentrations to obtain the optimum conditions. Moreover, ATRP of styrene was initiated from a chemically active patterned surface. For this purpose, polystyrene brushes were grafted from the patterned surface and subsequently a second block of tert-butyl acrylate could be polymerized as a result of the end-functionality of the polystyrene chains.

Parts of this chapter have been published: C. R. Becer, R. Hoogenboom, D. Fournier, U. S. Schubert, *Macromol. Rapid Commun.* **2007***, 28*, 1161–1166; C. R. Becer, C. Haensch, S. Hoeppener, U. S. Schubert, *Small* **2007**, *3*, 220–225.

4.1 Introduction

One of the most widely studied controlled radical polymerization techniques is atom transfer radical polymerization (ATRP). ATRP has been thoroughly investigated since it was developed independently by Matyjaszewski and Wang[1,2] as well as Sawamoto *et al.*[3] in 1995. It was developed based on earlier work on redox catalyzed telomerization reactions[4,5] as well as from atom transfer radical addition (ATRA).[6] ATRA is a modification of the Kharasch addition reaction, in which a transition metal catalyst acts as a carrier of the halogen atom in a reversible redox process.[7,8] ATRP has proven to be a powerful tool in the synthesis of polymers with narrow polydispersity indices and controlled molar masses.[9] The reaction is termed controlled/"living" since termination reactions can not be completely avoided.[10]

All ATRP systems are composed of monomer, initiator and catalyst (a transition metal and a suitable ligand). Various vinyl monomers, such as styrenes,[11-13] (meth)acrylates,[14-18] acrylonitriles,[19,20] and (meth)acrylamides[21,22] can be homopolymerized with ATRP. The initiator is typically an alkyl halide (RX). The halide is usually bromide or chloride, although iodide based initiators have been reported too.[23] Examples of halogenated compounds that have been used as initiators in ATRP are carbon tetrachloride and chloroform, benzyl halides and α–halo esters.[24] The only requirement is that the initiator must have a halogen attached to an atom containing radical stabilizing substituents. Also, the initiation rate must be faster than or equal to the propagation rate to obtain a controlled polymerization.[25] Several transition metals have been used in ATRP. Copper is by far the most common metal, due to its versatility and relatively low cost. However, other metals such as iron,[26,27] ruthenium,[28] nickel,[29] molybdenum,[30,31] rhenium,[23] rhodium[32] and palladium[33] have also proven successful for various monomers. The metal ions are used in conjunction with a large variety of ligands.

In ATRP, the active species is formed when the halogen in the alkyl halide is abstracted by the metal complex in a reversible redox process. The bond between the alkyl and the halide is cleaved homolytically and a carbon–centered radical is formed on the alkyl. In this process the deactivation rate must be higher than the activation rate in order to create a low concentration of propagating radicals. Thus, the equilibrium between active and dormant species must be greatly shifted towards the dormant species. If deactivation is very slow or non–existent the polymerization becomes uncontrolled. The overall rate of the reaction is highly dependent on the redox potential of the metal complexes. The general opinion is that ATRP involves chain propagation via free radicals and that the homolytically cleaved halide is in no way associated with the formed free radical on the chain–end. However, it has been

shown that polar solvents, such as water, greatly affect the rate of the polymerization.[34,35] Haddleton *et al.* have suggested that the mechanism of the propagation step in Cu(I) mediated ATRP is different to that of a free radical due to association between the chain–end radical and the metal complex.[36] Independent of the nature of the propagating species, the polymerization takes place in two steps: initiation and propagation. In Scheme 4.1 the mechanism is exemplified with copper(I) as catalyst. Termination reactions also occur, but no more than a few percentages of the growing chains undergo termination in ATRP.

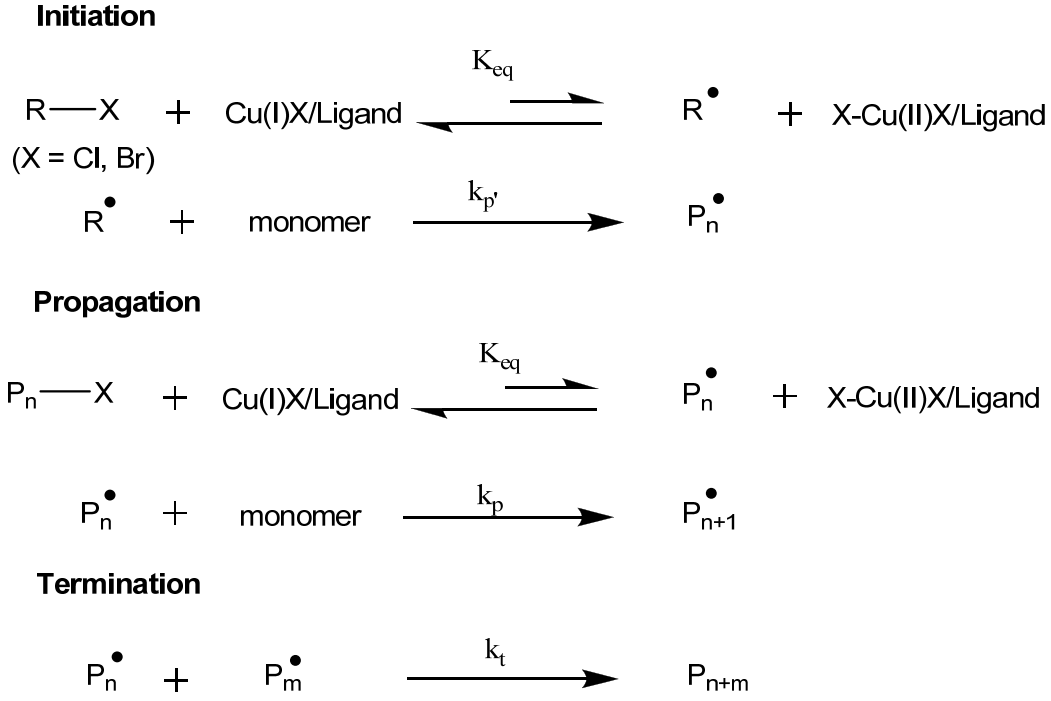

Scheme 4.1. Schematic representation of the mechanism of ATRP.

The ligands are an important part of the ATRP system and its role is three–fold. Firstly, the ligands solubilize the metal ion in the organic media. Secondly, they control selectivity by steric and electronic effects. Finally, by their electronic effects, they also affect the redox chemistry of the final metal complex.[37] The ligands are usually nitrogen[38-40] or phosphine–based.[26] As the importance of the ligands in ATRP is obvious, we have conducted research on finding alternative catalyst systems. Therefore, a new ligand bearing oligo(ethylene glycol) side chains was examined for the optimum ATRP conditions of MMA. Besides, this ligand has been further used for the surface initiated polymerization of styrene, which will be discussed in detail in the last part of this chapter.

4.2 ATRP of methyl methacrylate using an oligo(ethylene glycol) functionalized ligand

ATRP comprises a halide functionalized initiator, a transition metal ion and a ligand which forms a complex with the metal ion. The transition metal complex plays a crucial role in the formation of a fast and reversible halogen transfer between the active radical and the dormant species. The amount of catalyst required for ATRP is ranging from 0.1 to 1 mol% with respect to the monomer and has to be removed from the final polymer. The most important challenge that stimulated the investigation of new ATRP systems was the elimination or reduction of the required amount of metal content. Several studies were also conducted on removing and recycling the catalyst efficiently by using different methods i.e. extraction, immobilization, precipitation, and biphasic systems.[41 -44]

Several different techniques, *i.e.* reverse ATRP,[45] simultaneous normal and reverse initiation (SR&NI) ATRP,[46] activators generated by electron transfer (AGET),[47] activators regenerated by electron transfer (ARGET),[48] single electron transfer living radical polymerization (SET-LRP)[49] were successfully developed by Matyjaszewski *et al.*, Percec *et al.*, and Haddleton *et al.* mostly with the aim of reducing the metal catalyst concentration, or using air stable catalysts at their higher oxidation state as well as for the preparation of high molar mass polymers at ambient temperature. All of these systems are based on metal mediated LRP, whereby different initiation mechanisms have been examined in detail by changing the polymerization parameters,[50,51] *i.e.* initiator, transition metal ion and ligand.[52]

It is possible to reduce the required concentration of metal ion and ligand complex to as low as a few ppm by using the ARGET process. However, the use of an appropriate ligand is still of major importance to provide an efficient halogen-exchange reaction between the dormant and the active species.[53] Most of the research that was conducted on ATRP has been focused on the synthesis and investigation of nitrogen-based ligands[54 -57] since sulfur, oxygen, or phosphorus ligands are often more expensive and less effective due to inappropriate electronic effects or unfavorable binding constants.

In the current work, a new tetradentate amine ligand bearing *N,N,N,N′,N″,N‴,N‴′*-hexaoligo(ethylene-glycol) triethylenetetramine (HOEGTETA) pendant groups has been investigated for the ATRP of methyl methacrylate (MMA). The ATRP of MMA was conducted at three different polymerization temperatures in order to determine the most effective temperature. Subsequently, the effect of the Cu(I) to Cu(II) ratio on the control over the polymerization was investigated and comparison reactions were done by using *N,N,N′,N″,N″*-pentamethyldiethylenetriamine (PMDETA) as ligand. Due to the fact that, the

higher oxidation state of the metal ion is less expensive and also air stable, a special attention was given to the ATRP system which was conducted with only Cu(II) in the absence of any reducing agent or free radical initiator.

The ATRP of MMA was performed in anisole at three different temperatures (60, 80 and 90 ºC) by using ethyl-2-bromoisobutyrate (EB*i*B) as initiator. Cu(I)Br and HOEGTETA were used as a homogenous catalytic system in the polymerization medium and the ratio of MMA:EBiB:CuBr:HOEGTETA was 200:1:1:1. As depicted in Figure 4.1, a linear increase in the semi–logarithmic kinetic plot was observed for the reactions at 80 and 90 °C and higher apparent rate constants were obtained at elevated temperatures, as expected. However, the monomer conversion was rather limited for the polymerization at 60 °C. The calculated apparent rate constants, which are listed in Table 4.1 (entry 1, 2, and 3) were found as 4.4×10^{-5}, 1.20×10^{-4}, and 2.42×10^{-4} s^{-1} for the polymerization temperatures of 60, 80 and 90 ºC, respectively. Besides, the polymerization temperature has a crucial role to maintain the delicate balance of the activation/deactivation process of the ligand/metal complex. By taking in to account the apparent rate constants, the obtained molar mass as well as the polydispersity indices the optimum polymerization temperature was determined as 90 °C; as a consequence all further reactions were conducted at this temperature.

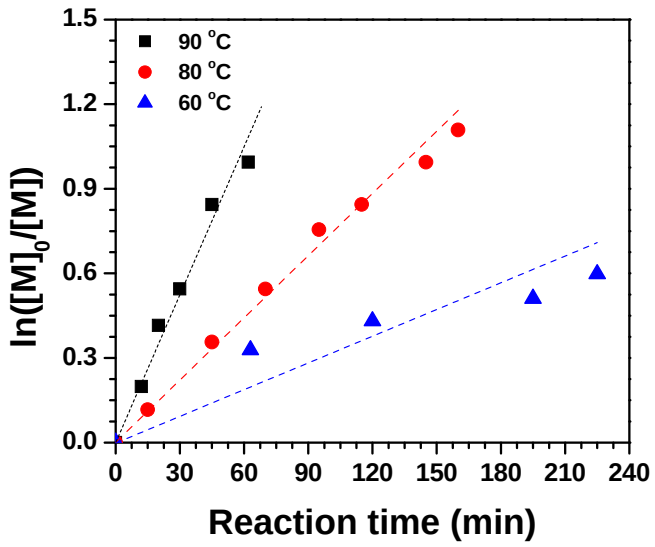

Figure 4.1. Semi-logaritmic kinetic plots for the ATRP of MMA at (▲) 60 °C, (●) 80 °C, and (■) 90 °C. $[MMA]_0 = 2.0$ M, $[EBiB]_0 = [CuBr]_0 = [HOEGTETA]_0 = 1.0 \times 10^{-2}$ M. Anisole was used as a solvent (50 v/v %).

The molar mass distributions of the synthesized polymers were found to be rather broad (Table 4.1, entries 1, 2 and 3), which is an evidence of inadequate control over the polymerization process. In addition, the observed molar masses were higher than the

theoretical values, in particular at the beginning of the reaction. One reason for the poor control over the molar mass increase might be a steric hindrance of the bulky pendant groups of the ligand which limit the accessibility of the amine core. Although these pendant groups provide the formation of a homogeneous metal/ligand complex in the polymerization medium, they also reduce the accessibility of the copper ions and thus the efficiency of the halogen exchange equilibrium. Another reason for the loss of control that should be considered is the low amount of deactivator (copper(II)bromide) at the initial state of the polymerization. Therefore, the activation reaction is fast but the radical deactivation reaction is slow at the early stage of the polymerization, which results in a high radical concentration. As a consequence of these effects, irreversible radical terminations can occur at the beginning of the polymerization, which causes a decrease in initiation efficiency and polymerization rate.

Table 4.1. Polymerization of MMA under different conditions.

Entry	Temp [°C]	Reac time [min]	Conv [%]	$M_{n,theo}$ [g/mol]	$M_{n,SEC}$ [g/mol]	PDI [M_w/M_n]	k_{app} [$10^{-4}/s^{-1}$]
1[a]	90	62	63	12,800	15,000	1.46	2.88
2[a]	80	160	67	13,600	15,000	1.63	1.20
3[a]	60	275	47	9,600	13,600	1.44	0.44
4[b]	90	100	85	17,200	26,000	1.34	3.25
5[c]	90	85	72	14,600	22,100	1.27	2.47
6[d]	90	190	86	17,400	27,100	1.32	1.66
7[e]	90	125	44	9,000	11,000	1.15	0.77
8[f]	90	125	46	9,400	10,800	1.15	0.75

[a] [MMA] : [EB*i*B] : [Cu(I)] : [Cu(II)] : [HOEGTETA] = 200:1:1:–:1
[b] [MMA] : [EB*i*B] : [Cu(I)] : [Cu(II)] : [HOEGTETA] = 200:1:0.9:0.1:1
[c] [MMA] : [EB*i*B] : [Cu(I)] : [Cu(II)] : [HOEGTETA] = 200:1:0.5:0.5:1
[d] [MMA] : [EB*i*B] : [Cu(I)] : [Cu(II)] : [HOEGTETA] = 200:1:–:1:1
[e] [MMA] : [EB*i*B] : [Cu(I)] : [Cu(II)] : [PMDETA] = 200:1:–:1:1
[f] [MMA] : [EB*i*B] : [Cu(I)] : [Cu(II)] : [PMDETA] : [PEG_{300}] = 200:1:–:1:1:1
All reactions were performed in anisole (50 vol.-%).

To analyze the effect of the amount of the deactivator in the ATRP of MMA, different amounts of Cu(II) were added to the polymerization medium. For the first attempt the ratio of [Cu(I)]:[Cu(II)] was changed from 1:0 to 0.9:0.1 (Table 4.1, entries 1 and 4) and a very slow propagation was expected. Surprisingly, the apparent rate of polymerization was found to be higher when 10% Cu(II) (with respect to the total amount of copper species) was added to the system, and at the same range when 50% Cu(II) was present, as shown in Figure 4.2. Besides, the polydispersity indices of the resulting polymers were decreased and an improved control over the molar masses was achieved. This might be due to the complexation of Cu(II) ions with the oligo(ethylene glycol) chains, which may result in an improved activation–deactivation rate. In order to better understand this effect, the ratio of Cu(I) to Cu(II) was

altered from 0.9:0.1 to 0.5:0.5 and to 0:1.0. The apparent rates of polymerization decreased when the amount of Cu(II) was increased. Although there is a difference between the theoretical molar masses and the obtained molar masses, monomer conversions of more than 70% were achieved with polydispersity indices around 1.3, as listed in Table 4.1 (entries 4, 5, and 6). However, the results obtained for the polymerization of MMA starting from 100% Cu(II), *i.e.* a controlled polymerization, lead us to consider possible reducing agents or radical sources. According to the normal ATRP procedure it should not be possible to initiate the polymerization reaction without any reducing agent or radical source.

When considering the reverse ATRP or AGET mechanism, a free radical source or a reducing agent is required to generate the lower oxidation state of the transition metal complex, respectively. Since there is no free radical initiator in the present system, we searched for possible reducing agents. Different reducing agents such as phenols,[58] thiophenols,[59] monosaccharides,[60] triethylamine[61] and ascorbic acid[62] were examined in detail by various research groups and they successfully conducted reverse ATRP or AGET by the use of these compounds. However, the present optimization reactions reported in this study were carried out in the absence of any of these reducing agents.

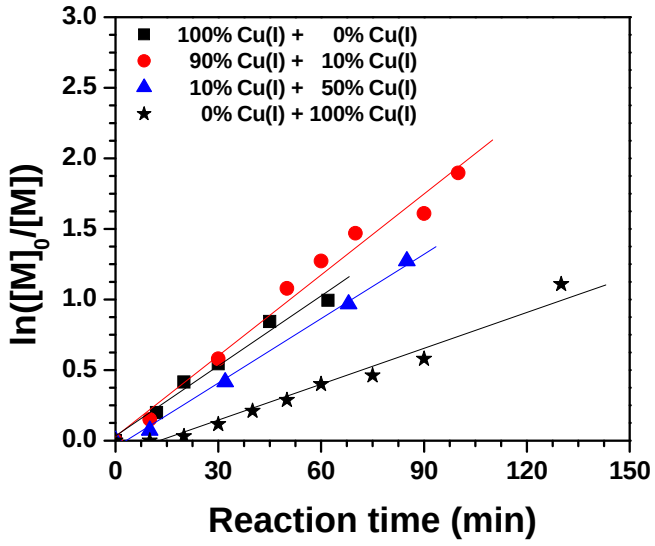

Figure 4.2. Semi-logarithmic kinetic plots for the polymerization of MMA at 90 °C with different concentrations of Cu(I) and Cu(II). $[MMA]_0 = 2.0$ M, $[EBiB]_0 = [HOEGTETA]_0 = 1.0 \times 10^{-2}$ M, (★) $[Cu(II)]_0 = 1.0 \times 10^{-2}$ M, (▲) $[Cu(II)]_0 = 0.9 \times 10^{-2}$ M and $[Cu(I)]_0 = 0.1 \times 10^{-2}$ M, (●) $[Cu(II)]_0 = 0.5 \times 10^{-2}$ M and $[Cu(I)]_0 = 0.5 \times 10^{-2}$ M, (■) $[Cu(I)]_0 = 1.0 \times 10^{-2}$ M. Anisole was used as a solvent (50 vol.-%).

Mathias *et al.* reported a study on an air-induced ATRP of methacrylates in the absence of an initiator using $CuCl_2$/PMDETA as a catalyst complex.[63] They showed the possibility of synthesizing polymers with low polydispersity indices by using a transition

metal ion at its higher oxidation state. On the other hand, the polymerization conditions did not allow the quantification of the effects of individual components such as the ratio of monomer to initiator. Moreover, the molar masses of the resulting polymers were unpredictable. However, when we performed the polymerization of MMA in the absence of initiator we did not observe any polymer formation which shows that there is no air induced initiation in our system. Matyjaszewski *et al.* provided a deeper insight into the oxygen initiated mechanism by performing kinetic studies on the synthesis of high molar mass polymers.[64] Furthermore, the authors investigated the addition reaction of $CuBr_2$ and MMA that resulted in a reduction of Cu(II) to Cu(I) and the formation of 1,2-dibromoisobutyrate. This indirect generation of Cu(I) species allows a halogen-exchange mechanism, possibly combined with an induction period at the beginning of the polymerization. We also observed an induction period as seen in Figure 4.2, in particular when more Cu(II) was used in comparison to Cu(I). Therefore, we propose that the here observed polymerization with Cu(II) proceeds via a kind of AGET mechanism, whereby the MMA reduces the Cu(II) ion to Cu(I) by an addition reaction[64] which is shown in Scheme 4.2. Alternatively, it could also be considered that the amine core of the ligand is capable of reducing Cu(II) ions to Cu(I).

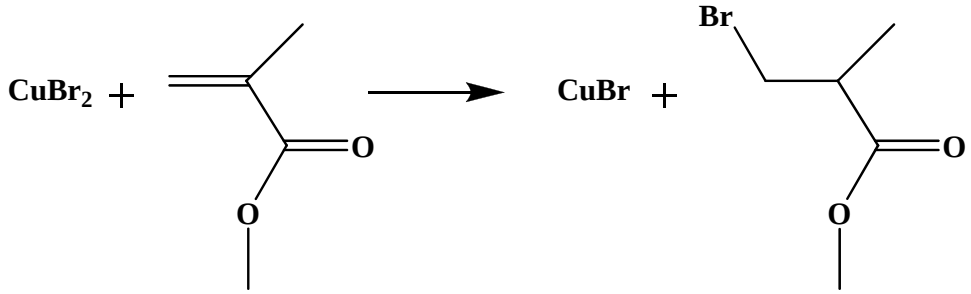

Scheme 4.2. Schematic representation of the addition reaction between MMA and $CuBr_2$.

Figure 4.3 shows the SEC results of the MMA polymerization when only Cu(II) is added at the beginning of the reaction. The molar masses of the obtained PMMA increased and the polydispersity indices remained relatively low as the MMA conversion progressed. In addition, the SEC traces of the resulting polymers shifted to high molar masses as illustrated in Figure 4.3 right as well. The reason for the difference between the measured molar masses and the theoretical values can be found in slow exchange reactions which result in low initiation efficiencies as previously discussed for the Cu(I) catalyzed polymerization.

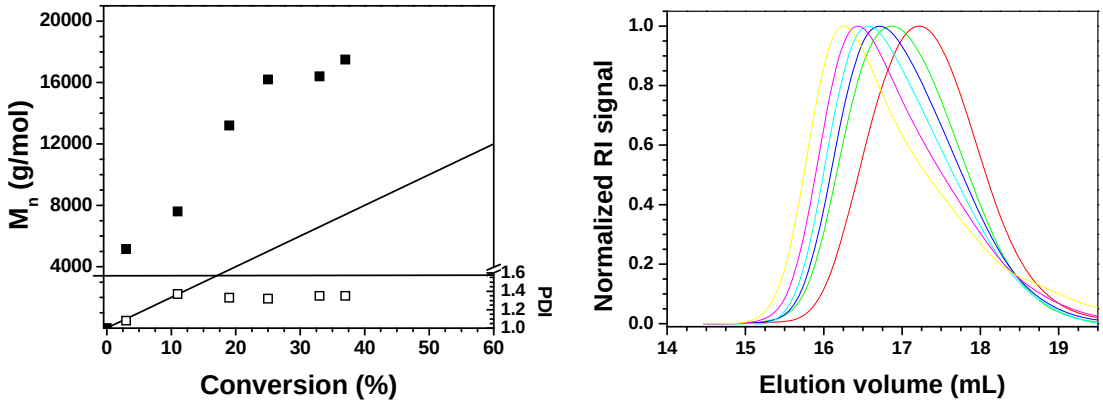

Figure 4.3. Dependence of the $M_{n,SEC}$ and the PDI of PMMA on the monomer conversion (*left*) at a polymerization temperature of 90 °C and $[MMA]_0 = 2.0$ M, $[EBiB]_0 = [HOEGTETA]_0 = [Cu(II)]_0 = 1.0 \times 10^{-2}$ M. SEC traces of the prepared polymers (*right*).

The ATRP of MMA in the presence of only Cu(II) was also conducted using PMDETA as a ligand in order to compare the rate of polymerization obtained with HOEGTETA with a known ligand. PMMA was obtained with low polydispersity indices and the experimental molar masses were found to be close to the theoretical values although at low conversion a large positive deviation was observed (Figure 4.4). These results clearly demonstrate that the high molar masses obtained with HOEGTETA are due to the ligand and not the use of Cu(II). The apparent rate of the polymerization was found to be lower with PMDETA compared to HOEGTETA as a ligand (Table 4.1, entries 6 and 8). There can be two possible reasons for this. The difference in the number of dentates of ligands could affect the polymerization rate. It is known that ATRP conducted by using tetradentate amine ligands in comparison to tridentate amine ligands exhibit faster apparent rate constants.[65] Secondly, HOEGTETA forms a homogenous complex with the metal ion whereas PMDETA is only dissolving partially the metal ion. It should be taken into account that the differences in the solubility of the copper ions in the polymerization medium have a great effect on the rate of polymerization.

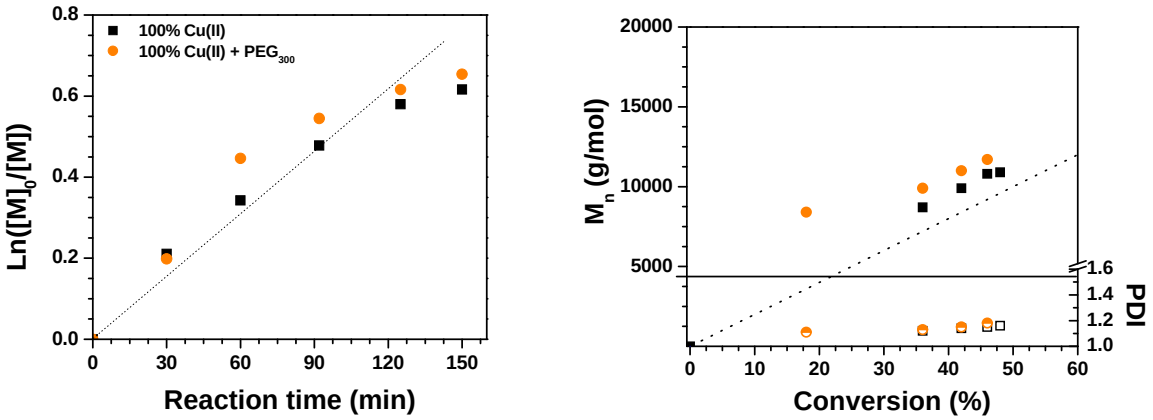

Figure 4.4. Dependence of the $M_{n,SEC}$ and the PDI of PMMA on monomer conversion (*right*) and semi-logarithmic kinetic plot (*left*) at a polymerization temperature of 90 °C with and without additional PEG_{300}. $[MMA]_0$ = 2.0 M, $[EBiB]_0 = [PMDETA]_0 = [Cu(II)]_0 = 1.0 \times 10^{-2}$ M, (●) $[PEG_{300}]_0 = 0$, (■) $[PEG_{300}]_0 = 1.0 \times 10^{-2}$ M. Anisole was used as solvent (50 vol.-%).

Haddleton *et al.* reported the effect of water on the copper mediated LRP and it was found that increasing polarity of the medium provides an enhanced polymerization rate.[35] To study the effect of the PEG chains of HOEGTETA on the ATRP of MMA, we also investigated the effect of free PEG units in the polymerization mixture. The ATRP of MMA was conducted with Cu(II), PMDETA and one equivalent of PEG_{300} (regarding to the ratio of PMDETA). As depicted in Figure 4.4, there is no significant effect of PEG_{300} on the polymerization rate of MMA and also on the molar mass distribution (Table 4.1, entries 7-8).

4.3 Surface initiated polymerization of styrene on chemically patterned surfaces[66]

The use of selectively activated surfaces to fabricate brush systems has attracted great attention as these structures can be used to combine topographical properties with the possibility to select the appropriate chemical functionality for applications in both electronic[67] and biological[68] areas. Stable, covalently-bonded polymer films provide a versatile possibility to tailor the chemical, mechanical, electrical and surface energetic properties of surfaces as well as the adhesion of *i.e.* proteins and cells. There are two main approaches to synthesize polymers attached to the surface, that are classified as "grafting to" and "grafting from" techniques. Since the "grafting to" method has some limitations[69] like limited diffusion of the bulky polymer chains to the immobilized functional groups on the surface, the "grafting from" approach is generally preferred to synthesize homopolymer or block copolymer[70,71]

brushes tethered to particles or substrates by use of different polymerization techniques such as conventional radical, controlled radical, carbocationic, anionic, ring opening metathesis and group transfer polymerization.[72,73]

The development of controlled/living polymerization systems lead to the synthesis of defined polymer or block copolymer brushes tethered covalently to the surface from one end. In particular, atom transfer radical polymerization (ATRP)[74-76] allows to grow well–defined brushes on the surface under mild conditions. In this latter technique a lower oxidation state metal complex abstracts a halogen from an alkyl halide to generate a radical center. Addition of the monomers to this active species continues until the higher oxidation state metal complex deactivates the active center and creates the dormant species. One of the main advantages of ATRP for surface initiated polymerizations is the low concentration of the active centers during the polymerization because of the high deactivation rate in comparison to the activation rate. This equilibrium allows to suppress termination reactions and to protect the living character of the brushes, which can also be used for creating block copolymers on the surface.

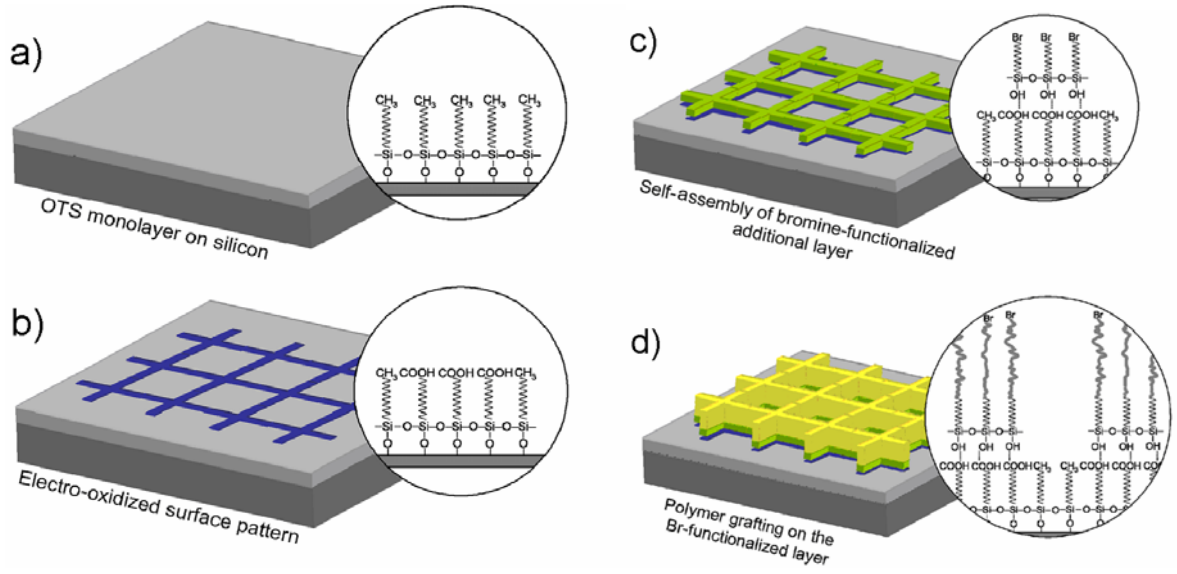

Scheme 4.3. Schematic representation of the experimental strategy to graft polymer brushes from surface templates. (a) Self-assembled monolayers of *n*-octadecyltri-chlorosilane on silicon wafers are used as substrate for the generation of chemically active surface patterns. (b) The electro-chemical oxidation of the surface terminal $–CH_3$ groups to –COOH functions is performed with the aid of a copper TEM grid. The chemical functionalization resembles a replica of the grid structure. (c) The –COOH groups are transferred into a bromine functionalized surface by the site selective self-assembly of a bromo-undecyltrichlorosilane precursor that attaches to the –COOH functions. (d) This precursor provides the alkyl bromide initiator for the subsequent ATRP polymerization of styrene on the surface template.

The polymerization propagates by starting from suitable halide groups present on the surface. Although tertiary or secondary alkyl halide functions are widely used as an initiator in the literature,[77] it is known that primary alkyl halide functions can also initiate the polymerization to some extent.[78] The patterning of these initiators offers the possibility to fabricate structured polymer brush systems, which are of special interest, *e.g.* in sensors, combinatorial arrays as well as micro- and nanofluidic devices. Approaches targeting the structuring of polymer brush films include the patterning of the initiator by micro-contact printing,[79,80] photo–[81] and electron–beam lithography,[82] or SFM tip mediated nanografting.[83] Suitable templates for the site-selective growth of such systems are also chemically active surface patterns on self-assembled monolayers of silane molecules,[84 -91] which allow the local modification of surfaces. Different chemical functionalities, tailor-made surface properties and different adhesion/binding properties of the generated patterns can be used for subsequent modification schemes applied to the templates. This technique is used here to pattern the initiator, which is employed in the "grafting on" process. In particular, the fact that chemically active surface patterns can be used not only to graft materials but also to stabilize them covalently on the surface pattern, are major advantages of chemical active surface templates.

We used a patterning technique that utilizes an electro-chemical oxidation process to locally generate carboxylic acid functions on a *n*-octadecyltrichlorosilane (OTS) coated silicon wafer. Within this process surface terminal $–CH_3$ groups of the OTS monolayer are converted into –COOH functions by sufficient voltage pulses. This oxidation process is mediated by water and the voltage is applied via a conductive SFM tip,[92] a copper TEM grid,[93] or hydrophilic stamps.[94] These methods allow the transfer of a pattern structure to the substrate from nanometer to millimeter range. With SFM tips the fabrication of structures down to 10 nm is possible; the resolution obtained for TEM grid printed structures has been demonstrated down to ~ 7 µm, limited up to now by the dimensions of the available TEM grids. While the tip inscription of chemically active surface patterns is a relative slow process, the parallel patterning of the surface is reliably fast (a grid structure of ~ 7 mm² can be oxidized in 10 seconds) and larger modified areas become accessible. The latter method is used in this approach to obtain chemically structured surface templates to graft polymers to the surface. For this purpose a suitable initiator has to be assembled on the grid structure. Due to the chemical selectivity of the printed replica of the grid, self-assembly is a suitable method to bind the initiator to the surface template. The –COOH terminated, oxidized areas, resembling the bar structure of the TEM grid, mediate the site–selective binding of an additional trichlorosilane layer. The commercially available bromo-undecyltrichlorosilane is a

suitable molecule that might act as an initiator for ATRP polymerizations. The bromo-undecyltrichlorosilane was self-assembled onto the oxidized grid structure, forming a ~2 nm high, homogeneous layer, as confirmed by SFM, via hydrogen bond formation of the hydrolyzed trichloro species of the precursor molecules and the –COOH terminated patterns of the inscribed template structure.[95] Water vapor condensation on the grid structures can be used to analyze the modification procedure qualitatively.

With this functionalized surface template, a suitable initiator to perform ATRP polymerization processes is locally attached to the surface and the grafting of the polymer is performed under mild conditions. Tests on macroscopic scale of this process on silicon wafers directly coated with bromo–undecyltrichlorosilane show the formation of polymer films, while no detectable formation of polymers was observed in the reaction vessel, as was checked by size exclusion chromatography (SEC) investigations of the polymerization solution after the surface initiated grafting process. The small amount of generated material on the surface is one of the major problems for performing a complete characterization that is usually applied to polymer systems with classical methods. Only a limited number of characterization tools are available to investigate the grown polymer films. The study of model systems is in this respect only of restricted use as the growth mechanism of polymer brushes will crucially depend on the quality of the initiator layer. Aspects like diffusion limitation and steric hindrance create a situation that makes the "grafting from surfaces" approach difficult to compare to polymer brushes synthesized in solution or grafted to silica nanoparticles.[96] Therefore the main aim of our investigations was focused on a feasibility study to create patterned polymer brushes. Besides the inspection of the films by SFM, additional FT–IR investigations have been performed to proof the chemical structure of the grown polymers. The thickness of the macroscopic layers were investigated by additional scratch tests, which locally remove the polymer film down to the silicon substrate, as confirmed by a smooth line within the line profile. This allows the determination of the film thickness. The film thickness increases linearly with the applied reaction time (Figure 4.5).

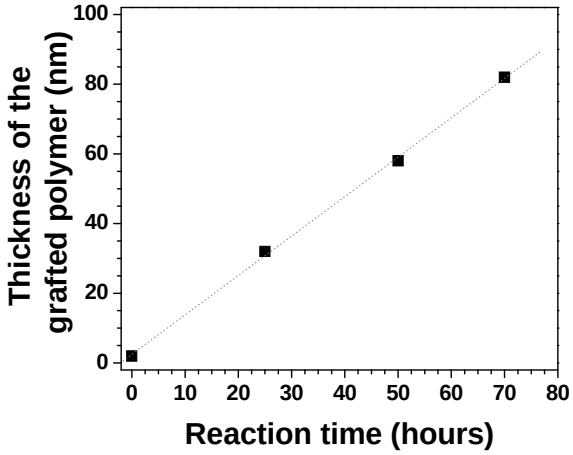

Figure 4.5. Analysis of the thickness of the polystyrene layer grafted from the bromine precursor at different polymerization times.

This surface initiated grafting process could also be performed on the previously introduced bromo-functionalized patterned surface templates. Figure 4.6 depicts optical microscopy images of films that have been grown on the patterned surface.

The grafting process produces a contrast in the optical image that resembles the bar structure of the initial surface pattern (Figure 4.6). Clear boundaries between the grafted grid replica and the unmodified OTS within the square structures of the pattern are observed, demonstrating the selectivity of the polymerization process on the bromine-functionalized surface areas. The dark contrast of the squares most likely originates from unspecifically bound catalyst that is absorbed on the OTS surface. This catalyst and other contaminations that might attach to the surface can be easily removed by cleaning with Scotch tape^{TM} tape that is attached to and removed from the surface. This process does not affect the polymer brush or the unmodified OTS area, as here hydrophobic surface properties are dominating, but significantly reduces the amount of contamination in the monolayer areas. This test shows moreover that the film is stable and well grafted to the surface. Alternatively "classical" cleaning by rinsing with a chloroform methanol mixture has been applied. After several rinsing steps comparably clean OTS areas can be found which are surrounded by polymer brushes. Differences in the film height can be identified by the different color of the film in few areas, whereas the overall film thickness is observed to be rather homogeneous across the sample. These optical micrographs have been recorded with a low magnification CCD camera system of the SFM setup. The deduction of the bar width is difficult to determine in these images due to the limited resolution of the system. Therefore SFM investigations have been performed to determine the structure and the size of the patterned polymer brushes. The patterning was performed in this case with a fine bar mesh 1000 TEM grid with a patch size of 25 μm.

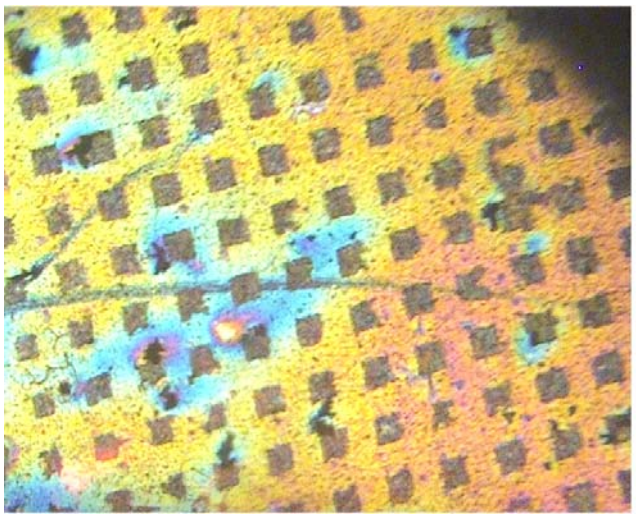

Figure 4.6. Optical micrograph of the surface templates after grafting polymer brushes to the surface.

Tapping mode images (Figure 4.7 a, b) of bromine terminated patterns on a templated OTS monolayer were recorded after the ATRP polymerization. The bars of the grid are ~ 7 μm wide, which is in good agreement with the dimensions of the copper grid that was used for the electroprinting of the surface template. The height of the polymer films is in the range of 40 to 50 nm (see line profile Figure 4.7 c). It is of interest to know if the chains of the polymer brush are still Br-terminated, as this would open the possibility to form patterned structures that consist of two different polymer blocks. For this purpose, the grid structures were used for an additional ATRP polymerization cycle with *tert*-butyl acrylate. Figure 4.7 f indicates an increase in height of the bar structure, measured close to the structures shown in Figure 4.7 a. The height of the bar features increased to 60 – 80 nm, which suggests that the bromine is still active and can be used for the grafting of additional polymer layers. However, the quality of the film appears to be poor. The structure of the bars before the second polymerization step changed after the grafting of the *tert*-butyl acrylate into a grainy structure (Figure 4.7 e), which might indicate that not all of the bromine functions are still active after the first inspection with SFM. Besides, locally dense packed polystyrene chains limit the accessibility of the chain end for the further chain growth. Different chain conformations might also limit the initiation of the number of chains. Moreover, the cleaning steps after the first polymerization might be responsible for the reduced activity of the polymer chain ends. The surface was exposed to air atmosphere during the cleaning and drying steps, which might deactivate a number of bromine end groups. More careful experimental conditions during the film preparation and characterization might be helpful to improve the film quality. Nonetheless, these preliminary studies demonstrate the potential to prepare 3–dimensional, well controlled architectures of micropatterned surface structures.

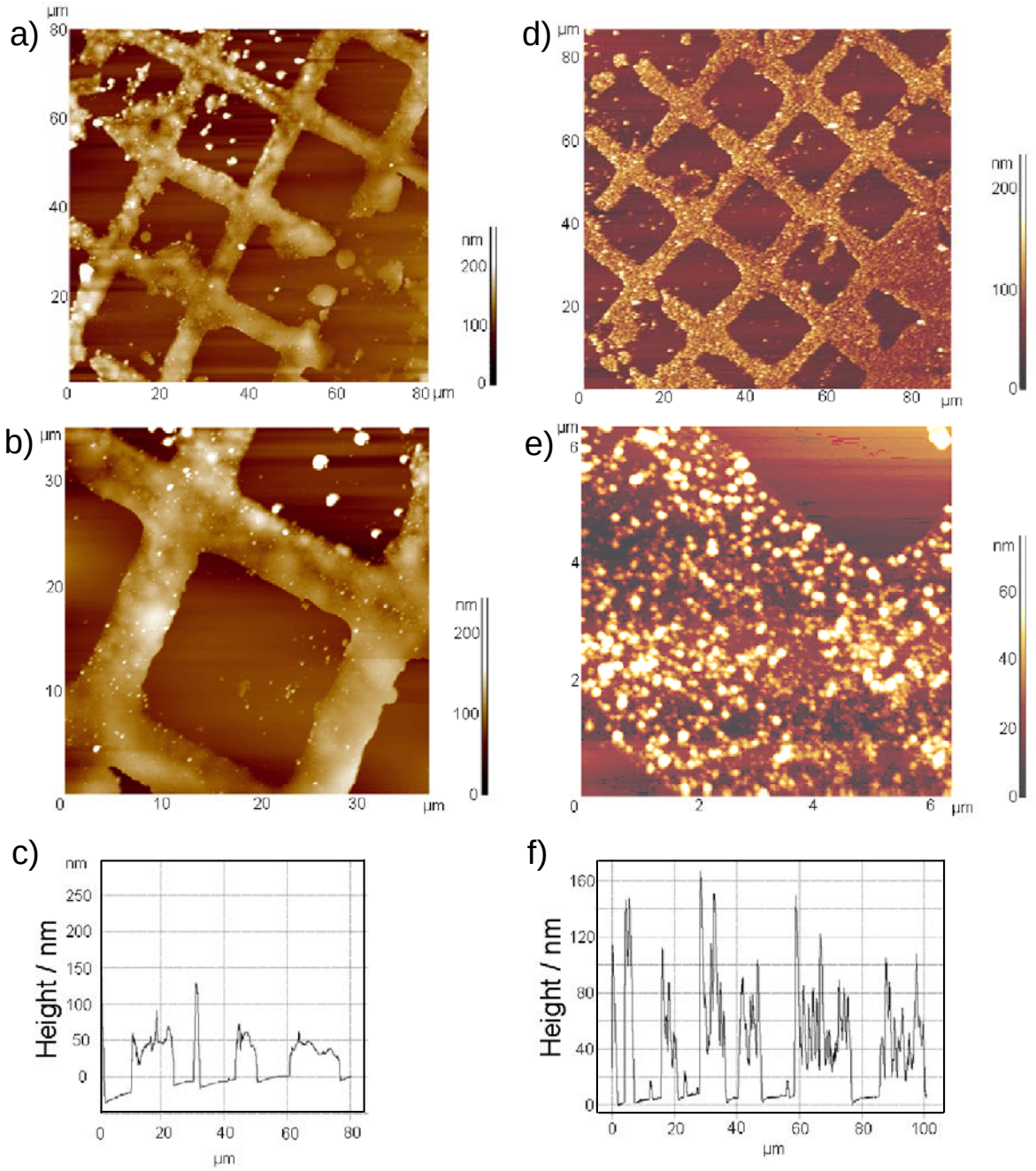

Figure 4.7. SFM tapping mode images of the polymers grafted from the surface template. a) and b): Polystyrene was grafted from the bromine functionalized bars, representing the TEM grid replica on the surface. c) Line profile of the structure. d) and e): Bar structures in the same surface area as a and b after the grafting of the second block *tert*-butyl acrylate. f) Line profile of d.

4.4 Conclusions

We have demonstrated for the first time the polymerization of MMA by using a linear tetramine ligand bearing oligo(ethylene glycol) pendant groups. The effect of polymerization temperature and Cu(I) to Cu(II) ratio on the polymerization process was investigated in detail. It was found that a controlled polymerization of MMA could be conducted by using the

transition metal ion at its higher oxidation state in the absence of any reducing agent. According to the results obtained in this study, Cu(I) species were presumably generated by an addition reaction of $CuBr_2$ and MMA. This generation of lower oxidation state metal species resulted in an initiation of the ATRP of MMA. Excess of Cu(II) provided better control over the polymerization and prevented the loss of control at the early stage of the polymerization. These conditions were also employed for the polymerization of MMA by using PMDETA, demonstrating the controlled radical polymerization with only Cu(II) species. It was also shown that a catalytic amount of PEG_{300} had no significant effect on the polymerization of MMA by using PMDETA.

Grafting polymer films from chemically active surface templates fabricated by electro-oxidative lithography provides a convenient and powerful possibility to pattern polymer brushes on the surface in a versatile fashion. Our results represent the first example of the subsequent chemical modification of TEM–grid electro-printed microstructures. As already demonstrated earlier, the combination of different patterning techniques represents a promising technique to hierarchically create structures with different feature dimension. As a consequence the whole dimensions range from millimeter down to the nanometer regime can be covered with the electro-oxidative patterning approach. Moreover, the combination of different modification schemes[97-99] represents an attractive possibility for the step-by-step assembly of more complex features. The mild reaction conditions required for the ATRP polymerization, in combination with the possibility to functionalize the surface patterns with other initiators, opens moreover the possibility to design 3-dimensional architectures, including the controlled formation of defined block copolymer systems, which offers attractive solutions to create not only a chemical contrast but also to generate a topographic contrast, a feature which is certainly interesting for biomedical applications of such surface templates.

4.5 Experimental part

Materials

MMA (99%, Aldrich), styrene (99%, Aldrich) and anisole (99.0%, Fluka) were passed over a neutral alumina oxide column prior to use. CuBr (99.999%, Aldrich), Cu(II)Br (99.999%, Aldrich), ethyl 2-bromoisobutyate (EB*i*B) (98%, Aldrich), PMDETA (99%, Aldrich), and poly(ethylene glycol) (M_n = 300 g/mol, Aldrich) were used as received. HOEGTETA ($M_{n,NMR}$ = 2,790 g/mol) was kindly provided by the BASF AG and precipitated into diethyl ether and dried under reduced pressure before use. All other solvents such as diethyl ether, chloroform,

dimethylacetamide, and methanol were purchased from Biosolve and used without further purification.

Instrumentation

Monomer conversion was determined by ^{1}H-NMR spectroscopy, which was recorded on a Varian Mercury 400 NMR in deuterated chloroform. The chemical shifts were calibrated to tetramethylsilane (TMS). Size exclusion chromatography (SEC) was measured on a Shimadzu system equipped with a SCL-10A system controller, a LC-10AD pump, a RID-10A refractive index detector, a SPD-10A UV detector and both a PSS Gram30 and a PSS Gram1000 column in series, whereby *N,N*-dimethylacetamide with 5 mmol LiCl was used as eluent at 1 mL/min flow rate and the column oven was set to 60 ºC. The molar mass and the molar mass distributions of the prepared polymers were calculated using poly(methyl methacrylate) standards.

Investigations on the patterned structures performed by tapping mode scanning force microscopy with a NTegra Aura from NT-MDT. Standard silicon tapping mode SFM tips from Digital Instruments with a typical force constant of 20 to 80 Nm^{-1} were employed within the investigation.

MMA polymerizations with HOEGTETA ligand

A typical polymerization procedure of MMA using Cu(I)Br was as follows. CuBr (36 mg, 2.5 mmol), HOEGTETA (697.5 mg, 2.5 mmol) and a stirring bar were added into a Schlenk tube and sealed with a rubber septum. The tube was flushed with argon for 15 minutes and subsequently deoxygenated anisole (5.35 mL, 50 vol.-% with respect to MMA) and MMA (5.35 mL, 50 mmol) were introduced into the tube and bubbled for additional 15 minutes with argon. EB*i*B (36.5 µL, 2.5 mmol) was added with a degassed syringe and the tube was immersed into an oil bath that was preheated to the desired temperature. At different time intervals, samples were withdrawn with a degassed syringe and each sample was divided into two portions. The first portion was diluted with deuterated chloroform for the determination of the conversion by ^{1}H-NMR spectroscopy. The second portion was precipitated into methanol to remove the catalyst prior to injection to SEC for the determination of molar mass and polydispersity index. All polymerizations and sample preparations were conducted with the same procedure unless otherwise indicated.

Preparation of patterned surfaces and ATRP of styrene

n-Octadecyltrichlorosilane OTS (Sigma) was self-assembled on clean silicon wafers (Silicon Quest International) as described elsewhere.[97] Surface patterns where generated by pressing a TEM grid (SPI Supplies) to the OTS surface and applying a bias voltage of -25 V with respect to the TEM grid for a time period of 40 to 60 seconds. Substrates were subsequently cleaned in aqueous HCl solution and rinsed with clean water (MilliQ water) before blow dried in a stream of nitrogen.

The bromo-undecyltrichlorosilane was self-assembled in dry bicyclohexyl (Fluka), which was dried over sodium from a 1 mM solution onto the grid printed patterns. Self-assembly times of 10 minutes were sufficient to obtain homogeneous films of ~2 nm thickness. Primary bromine functionalized surfaces were placed in a conical polymerization tube with a magnetic stirrer bar. Styrene monomer (35 mmol), Cu(I)Br catalyst (0.07 mmol) and hexaoligoethylene oxide substituted triethylenetetramine (HOEGTETA) (0.07 mmol) ligand were added into the tube. The reaction mixture was stirred at room temperature for 15 minutes and the solution turned into green as complex formation occurred and remained homogenous. The tube was immersed into an oil bath (60 °C) after bubbling with argon for 10 minutes and reacted for 60 hours. The wafer was dipped into methanol for a couple of times to remove the residual metal–ligand complex, which was absorbed to the surface during the polymerization and was dried with pressurized air.

4.6 References

(1) J.S. Wang, K. Matyjaszewski, *J. Am. Chem. Soc.* **1995**, *117*, 5614–5615.
(2) J. S. Wang, K. Matyjaszewski, *Macromolecules* **1995**, *28*, 7901–7910.
(3) M. Kato, M. Kamigaito, M. Sawamoto, T. Higashimura, *Macromolecules* **1995**, *28*, 1721–1723.
(4) B. Boutevin, C. Maubert, A. Mebkhout, Y. J. Pietrasanta, *J. Polym. Sci., Part A: Polym. Chem.* **1981**, *19*, 499–507.
(5) B. Boutevin, *J. Polym. Sci., Part A: Polym. Chem.* **2000**, 38, 3235–3243.
(6) D. P. Curran, *Synthesis* **1988**, 489–513.
(7) M. S. Karasch, E. V. Jensen, W. H. Urry, *Science* **1945**, *102*, 128–130.
(8) M. S. Karasch, P. S. Skell, P. Fischer, *J. Am. Chem. Soc.* **1948**, 1055–1059.
(9) T. E. Patten, J. Xia, T. Abernathy, K. Matyjaszewski, *Science* **1996**, *272*, 866–868.
(10) T. E. Patten, K. Matyjaszewski, *Adv. Mater.* **1998**, *10*, 901–915.
(11) K. Matyjaszewski, T. E. Patten, J. Xia, *J. Am. Chem. Soc.* **1997**, *119*, 674–680.
(12) V. Percec, B. Barboiu, *Macromolecules* **1995**, *28*, 7970–7972.
(13) Y. Kotani, M. Kamigaito, M. Sawamoto, *Macromolecules* **2000**, *33*, 6746–6751.
(14) T. Ando, M. Kato, M. Kamigaito, M. Sawamoto, *Macromolecules* **1996**, *29*, 1070–1072.
(15) D. M. Haddleton, A. J. Clark, M. C. Crossman, D. J. Duncalf, A. M. Heming, S. R. Morsley, A. J. Shooter, *Chem. Commun.* **1997**, 1173–1174.
(16) S. Coca, C. B. Jasieczek, K. L. Beers, K. Matyjaszewski, *J. Polym. Sci., Part A : Polym. Chem.* **1998**, *36*, 1417–1424.
(17) G. Moineau, M. Minet, P. Dubois, P. Teyssie, T. Senninger, R. Jerome, *Macromolecules* **1999**, *32*, 27–35.
(18) X. S. Wang, S. F. Lascelles, R. A. Jackson, S. P. Armes, *Chem. Commun.* **1999**, 1817–1818.
(19) K. Matyjaszewski, S. M. Jo, H. J. Paik, D. A. Shipp, *Macromolecules* **1999**, *32*, 6431–6438.
(20) K. Matyjaszewski, S. M. Jo, H. J. Paik, S. G. Gaynor, *Macromolecules* **1997**, *30*, 6398–6400.
(21) M. Senoo, Y. Kotani, M. Kamigaito, M. Sawamoto, *Macromolecules* **1999**, *32*, 8005–8009.
(22) M. Teodorescu, K. Matyjaszewski, *Macromolecules* **1999**, *32*, 4826–4831.
(23) Y. Kotani, M. Kamigaito, M. Sawamoto, *Macromolecules* **1999**, *32*, 2420–2424.
(24) K. Matyjaszewski, J. Xia, *Chem. Rev.* **2001**, *101*, 2921–2990.
(25) K. Matyjaszewski, J. L. Wang, T. Grimaud, D. A. Shipp, *Macromolecules* **1998**, *31*, 1527–1534.
(26) T. Ando, M. Kamigaito, M. Sawamoto, *Macromolecules* **1997**, *30*, 4507–4510.
(27) K. Matyjaszewski, M. Wei, J. Xia, N. E. McDermott, *Macromolecules* **1997**, *30*, 8161–8164.
(28) F. Simal, A. Demonceau, A. F. Noels, *Angew. Chem. Int. Ed.* **1999**, *38*, 538–540.
(29) H. Uegaki, Y. Kotani, M. Kamigaito, M. Sawamoto, *Macromolecules* **1997**, *30*, 2249–2253.
(30) J. A. M. Brandts, P. van de Geijn, E. E. van Faassen, J. Boersma, G. van Koten, *J. Organomet. Chem.* **1999**, *584*, 246–253.
(31) E. Le Grognec, J. Claverie, R. Poli, *J. Am. Chem. Soc.* **2001**, *123*, 9513–9524.
(32) G. Moineau, C. Granel, P. Dubois, R. Jérôme, P. Teyssié, *Macromolecules* **1998**, *31*, 542–544.
(33) P. Lecomte, I. Drapier, P. Dubois, P. Teyssié, R. Jérôme, *Macromolecules* **1997**, *30*, 7631–7633.
(34) X. S. Wang, S. P. Armes, *Macromolecules* **2000**, *33*, 6640–6647.
(35) S. Perrier, D. M. Haddleton, *Macromol. Symp.* **2002**, *182*, 261–272.
(36) S. Harrisson, J. P. Rourke, D. M. Haddleton, *Chem. Commun.* **2002**, 1470–1471.
(37) K. Matyjaszewski, *J. Macromol. Sci., Pure Appl. Chem.* **1997**, *A34*, 1785–1801.
(38) J. Xia, K. Matyjaszewski, *Macromolecules* **1997**, *30*, 7697–7700.
(39) J. Queffelec, S. G. Gaynor, K. Matyjaszewski, *Macromolecules* **2000**, *33*, 8629–8639.
(40) D. M. Haddleton, C. B. Jasieczek, M. J. Hannon, A. J. Shooter, *Macromolecules* **1997**, *30*, 2190–2193.
(41) J. Qui, B. Charleux, K. Matyjaszewski, *Prog. Polym. Sci.* **2001**, *26*, 2083–2134.
(42) D. M. Haddleton, D. Kukulj, A. P. Radigue, *Chem. Commun*. **1999**, 99–100.
(43) S. C. Hong, K. Matyjaszewski, *Macromolecules* **2002**, *35*, 7592–7605.
(44) J. Pyun, K. Matyjaszewski, T. Kowalewski, D. Savin, G. Patterson, G. Kickelbick, N. Huesing, *J. Am. Chem. Soc.* **2001**, *123*, 9445–9446.
(45) K. Matyjaszewski, *Macromolecules* **1998**, *31*, 4710–4717.
(46) M. Li, N. M. Jahed, K. Min, K. Matyjaszewski, *Macromolecules* **2004**, *37*, 2434–2441.
(47) W. Jakubowski, K. Matyjaszewski, *Macromolecules* **2005**, *38*, 4139–4146.
(48) W. Jakubowski, K. Matyjaszewski, *Angew. Chem. Int. Ed.* **2006**, *118*, 4594–4598.
(49) V. Percec, T. Guliashvili, J. S. Ladislaw, A. Wistrand, A. Stjerndahl, M. J. Sienkowska, M. J. Monteiro, S. Sahoo, *J. Am. Chem. Soc.* **2006**, *128*, 14156–14165.
(50) A. K. Nanda, K. Matyjaszewski, *Macromolecules* **2003**, *36*, 1487–1493.

(51) H. Q. Zhang, V. Marin, M. W. M. Fijten, U. S. Schubert, *J. Polym. Sci., Part A: Polym. Chem.* **2004**, *42*, 1876–1885.
(52) T. Pintauer, K. Matyjaszewski, *Coord. Chem. Rev.* **2005**, *249*, 1155–1184.
(53) H. Tang, N. Arulsamy, M. Radosz, Y. Shen, N. V. Tsarevsky, W. A. Braunecker, W. Tang, K. Matyjaszewski, *J. Am. Chem. Soc.* **2006**, *128*, 16277–16285.
(54) J. Gromada, J. Spanswick, K. Matyjaszewski, *Macromol. Chem. Phys.* **2004**, *205*, 551–566.
(55) J. Chu, J, Chen, K. Zhang, *J. Polym. Sci., Part A: Polym. Chem.* **2004**, *42*, 1963–1969.
(56) A. Mittal, S. Sivaram, *J. Polym. Sci., Part A: Polym. Chem.* **2005**, *43*, 4996–5008.
(57) M. H. Acar, C. R. Becer, H. A. Ondur, S. Inceoglu, in "Controlled/ Living Radical Polymerization: From Synthesis to Materials, *ACS Symp. Ser.* K. Matyjaszewski, Ed, Washington, DC, **2006**, *97*, p. 994.
(58) G. Hizal, U. Tunca, S. Aras, H. Mert, *J. Polym. Sci., Part A: Polym. Chem.* **2006**, *44*, 77–87.
(59) H. Mert, U. Tunca, G. Hizal, *J. Polym. Sci., Part A: Polym. Chem.* **2006**, *44*, 5923–5932.
(60) A. Vries, B. Klumperman, D. Wet–Roos, R. D. Sanderson, *Macromol. Chem. Phys.* **2001**, *202*, 1645–1648.
(61) H. Tang, Y. Shen, *Macromol. Rapid Commun.* **2006**, *27*, 1127–1131.
(62) K. Min, H. Gao, K. Matyjaszewski, *J. Am. Chem. Soc.* **2005**, *127*, 3825–3830.
(63) A. E. Acar, M. B. Yagci, L. J. Mathias, *Macromolecules* **2000**, *33*, 7700–7706.
(64) A. K. Nanda, S. C. Hong, K. Matyjaszewski, *Macromol. Chem. Phys.* **2003**, *204*, 1151–1159.
(65) W. Tang, K. Matyjaszewski, *Macromolecules* **2006**, *39*, 4953–4959.
(66) This section of will also be part of the Ph.D. thesis of C. Haensch (Eindhoven, 2009).
(67) R. C. Bailey, J. T. Hupp, *Anal. Chem.* **2003**, *75*, 2392–2398.
(68) N. Nath, A. Chilkoti, *Adv. Mater.* **2002**, *14*, 1243–1247.
(69) B. Zhao, W. J. Brittain, *Prog. Polym. Sci.* **2000**, *25*, 677–710.
(70) S. G. Boyes, W. J. Brittain, X. Weng, S. Z. D. Cheng, *Macromolecules* **2002**, *35*, 4960–4967.
(71) X. X. Kong, T. Kawai, J. Abe, T. Iyoda, *Macromolecules*, **2001**, *34*, 1837–1844.
(72) S. Edmondson, V. L. Osborne, W. T. S. Huck, *Chem. Soc. Rev.* **2004**, *33*, 14–22.
(73) M. Husseman, E.E. Malmstrom, M. McNamara, M. Mate, D. Mecerreyes, D. G. Benoit, J. L. Hedrick, P. Mansky, E. Huang, T. P. Russell, C. J. Hawker, *Macromolecules* **1999**, *32*, 1424–1431.
(74) J. S. Wang, K. Matyjaszewski, *J. Am. Chem. Soc.* **1995**, *117*, 5614–5615.
(75) J. Pyun, T. Kowalewski, K. Matyjaszewski, *Macromol. Rapid Commun.* **2003**, *24*, 1043–1059.
(76) J. B. Kim, W. X. Huang, M. D. Miller, G. L. Baker, M. L. Bruening, *J. Polym. Sci., Part A: Polym. Chem.* **2003**, *41*, 386–394.
(77) K. Matyjaszewski, J. Xia, *Chem. Rev.* **2001**, *101*, 2921–2990.
(78) M. Kato, M. Kamigaito, M. Sawamoto, T. Higashimura, *Macromolecules* **1995**, *28*, 1721–1723.
(79) Y. N. Xia, G. M. Whitesides, *Angew. Chem. Int. Ed.* **1998**, *37*, 551–575.
(80) R. R. Shah, D. Merreceyes, M. Husemann, I. Rees, N. L. Abbott, C. J. Hawker, J. L. Hedrick, *Macromolecules* **2000**, *33*, 597–605.
(81) O. Prucker, M. Schimmel, G. Tovar, W. Knoll, J. Rühe, *Adv. Mater.* **1998**, *10*, 1073–1077.
(82) Y. Tsujii, M. Ejaz, A. Yamamoto, T. Fukuda, K. Shigeto, K. Mibu, T. Shinjo, *Polymer* **2002**, *43*, 3837–3841.
(83) M. Kaholek, W.–K. Lee, B. LaMattina, K. C. Caster, S. Zauscher, *Nano Lett.* **2004**, *4*, 373–376.
(84) R. Maoz, E. Frydman, S. R. Cohen, J. Sagiv, *Adv. Mater.* **2000**, *12*, 725–731.
(85) H. Sugimura, *Int. J. Nanotechnol.* **2005**, *2*, 314–347.
(86) Y. J. Jung, Y.–H. La, H. J. Kim, T.–H. Kang, K. Ihm, K.–J. Kim, B. Kim, J. W. Park, *Langmuir* **2003**, *19*, 4512–4518.
(87) U. Schmelmer, R. Jordan, W. Geyer, W. Eck, A. Golzhauser, M. Grunze, A. Ulman, *Angew. Chem. Int. Ed.* **2003**, *42*, 559–563.
(88) R. Konradi, J. Rühe, *Langmuir* **2006**, *22*, 8571–8575.
(89) Q. He, Y. Tian, A. Kuller, M. Grunze, A. Golzhauser, J. Li, *Int. J. Nanosci.* **2006**, *6*, 1838–1841.
(90) A. Ramakrishnan, R. Dhamodharan, *J. Polym. Sci., Part A: Polym. Chem.* **2006**, *44*, 1758–1769.
(91) S. J. Ahn, M. Kaholek, W.–K. Lee, B. LaMattina, T. H. LaBean, S. Zauscher, *Adv. Mater.* **2004**, *16*, 2141–2145.
(92) R. Maoz, S. R. Cohen, J. Sagiv, *Adv. Mater*. **1999**, *11*, 55–61.
(93) S. Hoeppener, R. Maoz, J. Sagiv, *Nano Lett.* **2003**, *3*, 761–767.
(94) S. Hoeppener, R. Maoz, J. Sagiv, *Adv. Mater.* **2006**, *18,* 1286–1290.
(95) R. Maoz, J. Sagiv, D. Degenhard, H. Möhwald, P. Quint, *Supramol. Sci.* **1995**, *2*, 9–4.
(96) A. Tsuchida, M. Suda, M. Ohta, R. Zamauchi, N. Tsubokawa, *J. Polym. Sci., Part A: Polym. Chem.* **2006**, *4*, 2272–2279.
(97) S. Hoeppener, R. Maoz, S. R. Cohen, L. F. Chi, H. Fuchs, J. Sagiv, J. *Adv. Mater.* **2002**, *14*, 1036–1041.
(98) S. Liu, R. Maoz, G. Schmid, J. Sagiv, *Nano Lett.* **2004**, *4*, 845–851.
(99) D. Wouters, U. S. Schubert, *J. Mater. Chem.* **2005**, *15*, 2353–2355.

Chapter 5

Cationic ring opening polymerization of 2-ethyl-2-oxazoline and combination with ATRP of styrene

Abstract

Well–defined polymers with narrow polydispersity indices were obtained by the living cationic ring opening polymerization of 2-ethyl-2-oxazoline using four different acetyl halide initiators (acetyl chloride, acetyl bromide, acetyl iodide and α-bromo-isobutyrylbromide) at various temperatures. Relatively high molar mass poly(2-ethyl-2-oxazoline) homopolymers could be obtained with low polydispersity indices using microwave irradiation. The polymerization kinetics were investigated to determine the activation energies and the polymerization rates were found to strongly depend on the type of halide counter ion. Moreover, α-bromo-isobutyrylbromide initiated poly(2-ethy-2-oxazoline) was used as a macroinitiator for the atom transfer radical polymerization of styrene. Thus, poly(2-ethyl-2-oxazoline)-b-(styrene) amphiphilic block copolymers were obtained and their micellization behavior was investigated in detail.

Parts of this chapter have been published: R. P. Paulus, C. R. Becer, R. Hoogenboom, U. S. Schubert, *Macromol. Chem. Phys.* **2008***, 209*, 794–800; C. R. Becer, R. M. Paulus, S. Hoeppener, R. Hoogenboom, C. A. Fustin, J. F. Gohy, U. S. Schubert, *Macromolecules* **2008**, *41*, 5210–5215.

5.1 Introduction

In the last decade, significant progress has been made in the research and development of well-defined block copolymers. The discovery of controlled ionic polymerizations, and later of controlled radical polymerizations, has accelerated these developments. Traditional techniques for the preparation of block copolymers have some disadvantages. For instance, chain coupling is limited to the coupling of oligomers, whereas sequential monomer addition is only suitable for monomers that polymerize with the same mechanism and is further limited by the relative monomer reactivities. The development of mechanism transformation caused great progress, since this approach comprises the combination of different polymerization techniques.[1-5] As a consequence of this discovery, a whole range of copolymers became available that could not be prepared by coupling reactions or sequential monomer addition. The disadvantage of mechanism transformation, however, is that intermediate transformation and functionalization steps are required to transform the active center typical for one polymerization into an active center that can initiate another polymerization mechanism. To circumvent this inconvenience, dual and heterofunctional initiators have been developed, capable of initiating different polymerization mechanisms without intermediate transformation and functionalization steps.[6,7] Therefore, we have investigated the use of a heterofunctional initiator that is capable of initiating both a cationic polymerization and a radical polymerization. The mechanistic overview of the use of the dual initiator for the synthesis of amphiphilic block copolymers is shown in Scheme 5.1.

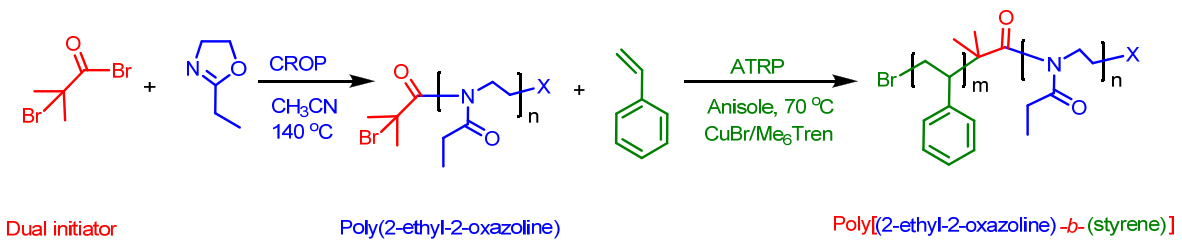

Scheme 5.1. Schematic representation for the use of a dual initiator for the CROP of EtOx and the ATRP of St.

Atom transfer radical polymerization (ATRP) is one of the most successful methods to polymerize styrenes, (meth)acrylates and a variety of other monomers in a controlled fashion, yielding polymers with molar masses predetermined by the ratio of the concentrations of consumed monomer to introduced initiator and low polydispersity indices.[8,9] Because of its radical nature, ATRP is tolerant to many functionalities in monomers providing access to polymers with functionalities along the chains. Moreover, the initiator used determines the end groups of the polymers. By using a functional initiator, functionalities such as vinyl, hydroxyl, epoxide, cyano and other groups have been incorporated at one chain end, while the

other chain end remains an alkyl halide. The polymer can be dehalogenated in a one pot process or the halogen end groups can be transformed to other functionalities using nucleophilic substitution reactions or electrophilic addition reactions. Moreover, utilizing the ability of the halogen chain end to be reactivated, radical addition reactions can be used to incorporate allyl end groups, insert one less reactive monomer unit at the chain end, or to end-cap the polymer chain. With ATRP, functionality and architecture can be combined resulting in multifunctional polymers of different compositions and shapes such as block copolymers, multiarmed star or hyperbranched polymers.

Living cationic ring-opening polymerization (CROP) of 2-ethyl-2-oxazoline (EtOx) was first described in 1966.[10,-12] Ever since, the biocompatible and hydrophilic poly(2-ethyl-2-oxazoline)s have been used for a broad range of applications.[13,14] The living character of the polymerization provides easy access to block copolymers by sequential addition of different monomers and functional end-groups by using functional initiators or terminating agents.[15] By chain extending the hydrophilic poly(2-ethyl-2-oxazoline) (PEtOx) with a hydrophobic block, amphiphilic structures can be obtained.[16 -20] The polymerization kinetics for the cationic ring-opening polymerization of 2-oxazolines with many initiators has been investigated by a number of groups.[21- 26] Most commonly, tosylate and triflate derivatives are used as initiators for the cationic ring opening polymerization of oxazolines.[27] Moreover, some research groups focused on using bifunctional and multifunctional initiators in order to combine CROP of oxazolines with nitroxide mediated radical polymerization, anionic ring opening polymerization or other living radical polymerization techniques.[28,29] The use of acetyl chloride and methacryloyl chloride as initiator for the CROP of 2-methyl-2-oxazoline and 2-phenyl-2-oxazoline was demonstrated with and without addition of silver triflate or potassium iodide to accelerate the polymerizations.[30]

The use of different acetyl halides as initiators for the CROP of 2-ethyl-2-oxazoline has been reported for the first time during this thesis. Therefore, acetyl chloride (ACl), acetyl bromide (ABr), acetyl iodide (AI) and α-bromo-isobutyrylbromide (BrEBBr) were examined as initiators for the CROP of EtOx at different temperatures using microwave irradiation. The polymerization kinetics was followed and activation energies have been calculated accordingly. Furthermore, BrEBBr initiated functional PEtOx homopolymers were used as macroinitiator for the ATRP of styrene. Thus, amphiphilic block copolymers of styrene and EtOx were obtained and their micellization behavior is also discussed in this chapter.

5.2 Screening the effect of initiator on the cationic ring opening polymerization of 2-ethyl-2-oxazoline

The simplified reaction mechanism for the acetyl halide initiated cationic ring-opening polymerization of 2-ethyl-2-oxazoline is schematically shown in Scheme 5.2. The polymerization is initiated by the electrophilic acetyl halide forming the cationic oxazolinium ring. The C-O bond in the oxazolinium ring is weakened and the polymerization propagates by nucleophilic attack of the next monomer onto this carbon atom. Block copolymers can be potentially synthesized by adding a second monomer when all initial monomer is consumed or the polymerization can be terminated by adding a nucleophile (terminating agent). If chain transfer and chain termination can be excluded, the polymerization proceeds in a living manner. In this case, the concentration of propagating species is constant and the polymerization should proceed via first order kinetics.

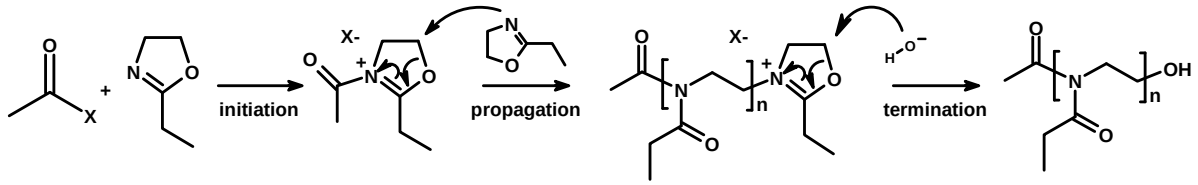

Scheme 5.2. Schematic representation of the mechanism of the living CROP of EtOx with acetyl halide as initiator (X = Cl, Br, I).

The rate of polymerization k_p (assuming all initiator molecules react instantaneously upon heating) can be expressed by Equation 5.1.

$$-\frac{d[M]}{dt} = k_p \cdot [P^*] \cdot [M] \qquad (5.1)$$

Integration of Equation 5.1 results in the velocity Equation 5.2 when it is assumed that the concentration of the propagating species is equal to the starting initiator concentration. The temperature dependence of the rate of polymerization is expressed in Equation 5.3 (Arrhenius equation).

$$\ln \frac{[M]_0}{[M]_t} = k_p \cdot [I]_0 \cdot t \qquad (5.2)$$

$$k_p = A \cdot e^{-\frac{E_a}{RT}} \qquad (5.3)$$

A major drawback of the cationic ring-opening polymerization of 2-oxazolines is the long reaction time from several hours up to several weeks.[31] However, the required

polymerization period can be reduced by performing the reaction in a closed vial under microwave irradiation.[32,33] Relatively high polymerization temperatures and pressure can be reached by using this type of reaction setup which results in acceleration of the synthesis of poly(2-oxazoline)s. Recently, Schubert *et al.* reported up-scaling possibilities for the polymerization of oxazolines under microwave irradiation.[34,35]

In this section we discuss the kinetic investigations for the polymerization of 2-ethyl-2-oxazoline (EtOx) using four different acetyl halide initiators at various polymerization temperatures. The motivation for this kinetic study with acetyl halides as initiators was their commercial availability and their potential future application for the synthesis of functionalized polymers using various acetyl halides with functional groups as initiator. Moreover, the synthesis of high molar mass poly(2-ethyl-2-oxazoline)s was investigated using these initiators.

The polymerization of EtOx in acetonitrile initiated with acetyl chloride (ACl), acetyl bromide (ABr), acetyl iodide (AI), and α-bromo-isobutyrylbromide (BrEBBr) was investigated at different temperatures (160, 180, 200 and 220 ºC for ACl; 100, 120, 140, 160 and 180 °C for ABr; 80, 90, 100, 120, 140 and 160 ºC for AI; 100, 120, 140, 160, and 180 ºC for BrEBBr) in closed reaction vials using microwave irradiation as heating source. The polymerizations in this kinetic study were performed using a 4 M initial monomer concentration and a monomer to initiator ratio of 60 for ACl, ABr, and AI, and 100 for BrEBBr.

The monomer conversions were calculated from GC measurements and the semi-logarithmic kinetic plot for the ACl initiated CROP of EtOx is depicted in Figure 5. 1 left. According to the polymerization kinetics, the polymerization rates (k_i is the initial slope of the fitted non-linear kinetic plot and k_p is the final slope of the fitted non-linear kinetic plot) increased in time at all investigated temperatures. This acceleration in k_p might be related to the increase in the concentration of cationic active centers in time: After fast initiation with the acetyl chloride, covalent chloride propagating species are formed that have a very low reactivity. With increasing reaction time, an equilibrium between the covalent and the more reactive cationic propagating species will be formed resulting in higher polymerization rates. Similar observations have been previously made for the cationic ring-opening polymerization of EtOx with benzyl chloride and benzyl bromide as initiator using *N,N*-dimethylacetamide as solvent.[36,37] The molar masses and polydispersity indices of the synthesized polymers, determined by SEC, are plotted against monomer conversion in Figure 5.1 right. An increase in the molar mass of the polymers was observed with increasing conversions and the polydispersity indices remained below 1.2 for all polymers and mostly below 1.10, which

supports the proposed fast initiation followed by a slow polymerization rate. Nonetheless, it should be noted that, in particular at low conversion, the molar mass *versus* conversion plot is deviating from the theoretical molar mass. The reason for this non-linearity might be the slow initiation behavior of the acetyl chloride.

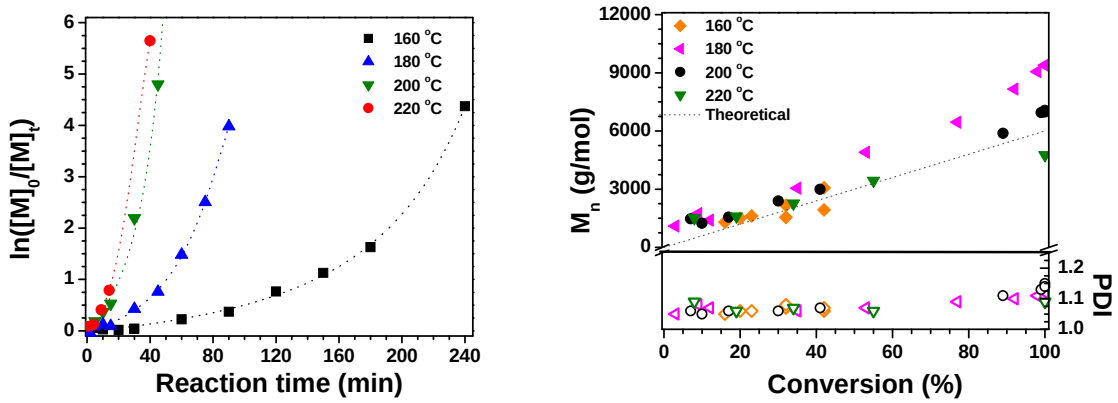

Figure 5.1. *Left*: First order kinetic plot for the acetyl chloride initiated CROP of EtOx in acetonitrile at different temperatures using 4 M monomer concentration and a monomer to initiator ratio of 60. The dotted lines are added to guide the eye. *Right*: $M_{n,SEC}$ against monomer conversion and PDI values for the acetyl chloride initiated polymerization of EtOx in acetonitrile at different temperatures.

The acetyl bromide initiated polymerization of EtOx was investigated at six different polymerization temperatures, namely 100, 120, 140, 160 and 180 °C. The resulting first order kinetic plots for these polymerizations (Figure 5.2, left) revealed linear first order kinetics for all investigated polymerization temperatures indicating fast initiation and the absence of chain termination. Moreover, the apparent rate constants increased with increasing temperatures, as expected based on the higher energy input. The molar mass and polydispersity index *versus* conversion plot is shown in Figure 5.2 right. The molar masses obtained by measuring SEC were found to be close to the theoretical molar masses proving the livingness of the polymerization, whereby the polydispersity indices remained below 1.2. To further investigate the proposed initiation mechanism, a poly(2-ethyl-2-oxazoline) was prepared using acetyl bromide as initiator and a monomer to initiator ratio of 100. The polymerization was performed up to ~ 50% to repress the possible occurrence of side reactions and the polymer was analyzed by MALDI-TOF MS. Figure 5.3 illustrates the MALDI-TOFMS spectrum with a peak spacing of 99.13 corresponding to the mass of one monomer unit. In addition, end-group analysis revealed that the major distribution corresponds to poly(2-ethyl-2-oxazoline) having the acetyl initiator group at one chain end and the bromide at the other chain end, whereby the polymer was charged by a sodium(I) ion, which proves the proposed polymerization mechanism.

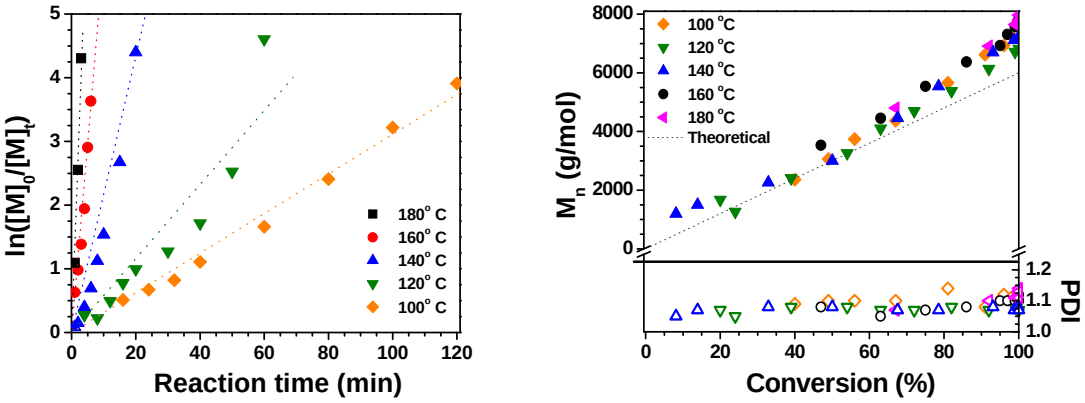

Figure 5.2. *Left*: First order kinetic plot for the acetyl bromide initiated CROP of EtOx in acetonitrile at different temperatures using 4 M monomer concentration and a monomer to initiator ratio of 60. The dotted lines are linear fits to the data. *Right*: $M_{n,SEC}$ against monomer conversion and PDI values for the acetyl bromide initiated polymerization of EtOx in acetonitrile at different temperatures.

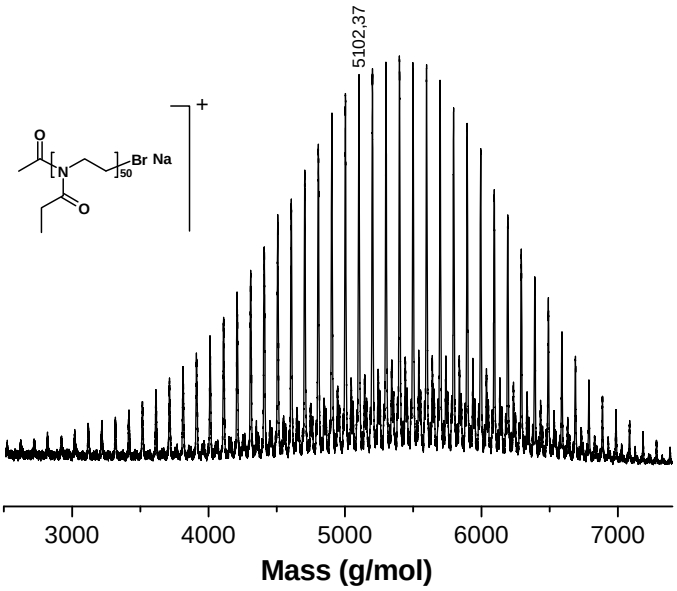

Figure 5.3. MALDI-TOF MS spectrum of the acetyl bromide initiated polymer of EtOx with the corresponding peak assignment.

The acetyl iodide is expected to result in the fastest polymerization amongst the three investigated acetyl halides. As shown in Figure 5.4 left, the acetyl iodide initiated polymerizations exhibited a linear relationship in the first order kinetic plots and increased polymerization rates were observed at elevated temperatures. Molar masses of the resulting polymers increased linearly with the increasing conversion and the polydispersity indices remained below 1.2, as depicted in Figure 5.4 right.

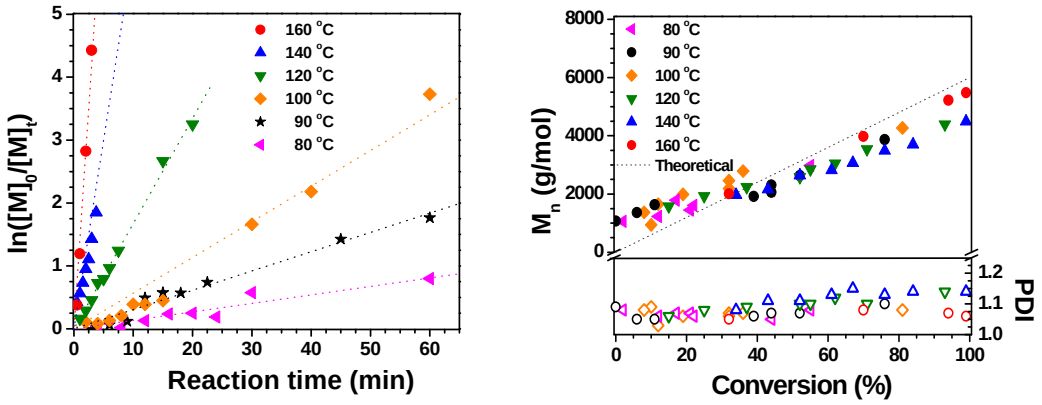

Figure 5.4. *Left*: First order kinetic plot for the acetyl iodide initiated CROP of EtOx in acetonitrile at different temperatures using 4 M monomer concentration and a monomer to initiator ratio of 60. The dotted lines are linear fits to the data. *Right*: $M_{n,SEC}$ against monomer conversion and PDI values for the acetyl iodide initiated EtOx polymerization in acetonitrile at different temperatures.

These results demonstrate that the polymerizations proceeded *via* a living polymerization mechanism with fast initiation. Nonetheless, the small deviations of the molar mass from the theoretical molar mass might be due to the used polystyrene standards for calibration and/or the occurrence of minor side reactions like chain-transfer[38] or spontaneous initiation by small traces of impurities.[39,40] As a representative example of the monomodal distributions of the resulting polymers, SEC traces obtained at different reaction times for the acetyl iodide initiated polymerization of EtOx at 140 °C are depicted in Figure 5.5.

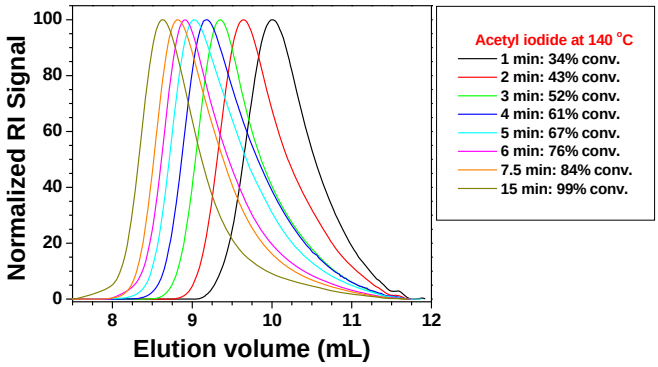

Figure 5.5. SEC traces obtained at different reaction times for the acetyl iodide initiated polymerization of EtOx in acetonitrile at 140 °C (SEC with chloroform: triethylamine: 2-propanol (94:4:2) eluent mixture).

The kinetic study for BrEBBr initiated CROP of EtOx was performed under microwave irradiation in CH_3CN as solvent. Polymerization temperatures and times were selected according to the results obtained for the acetyl bromide initiated CROP of EtOx. The resulting semi-logarithmic first order kinetic plot is depicted in Figure 5.6 left. The apparent rate constants of the polymerizations were found to be 7.92×10^{-3}, 24.9×10^{-3}, 44.6×10^{-3},

202 × 10^{-3} and 351 × 10^{-3} L·mol^{-1}·s^{-1} at 100, 120, 140, 160 and 180 °C, respectively. The apparent rate constants are in the same range as those observed for acetyl bromide initiated polymerizations. The molar masses of the obtained polymers were measured by SEC and calculated according to poly(styrene) standards. It is shown in Figure 5.6 right that the obtained molar masses are slightly above the theoretical line and the polydispersity indices are below 1.25 at all investigated temperatures.

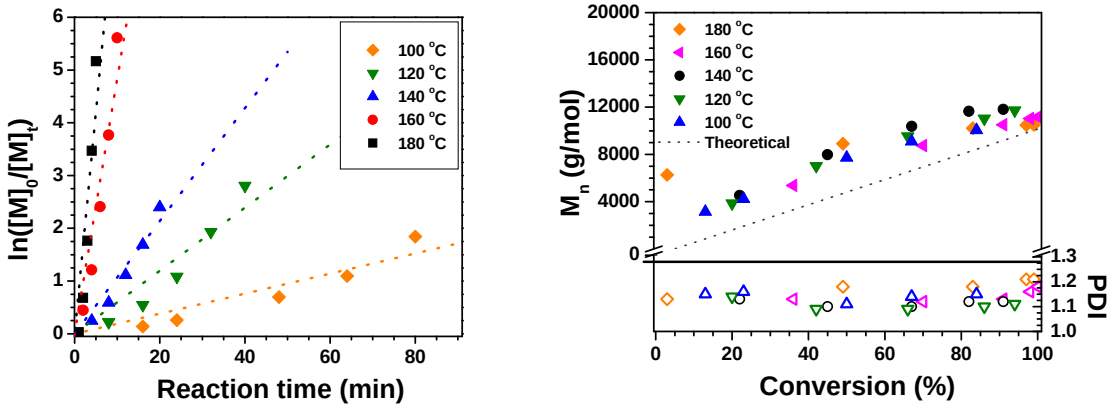

Figure 5.6. *Left*: First order kinetic plot for the BrEBBr initiated CROP of EtOx in acetonitrile at different temperatures using 4 M monomer concentration and a monomer to initiator ratio of 100. The dotted lines are linear fits to the data. *Right*: $M_{n,SEC}$ against monomer conversion and PDI values for the BrEBBr initiated EtOx polymerization in acetonitrile at different temperatures.

These plots indicate a living polymerization mechanism with relatively low polydispersity indices even at full monomer conversions. The possibility of undesired initiation by tertiary bromine was tested by using ethyl-2-bromoisobutyrate (EBBr) as an initiator. A solution of EtOx in CH_3CN was reacted in the microwave for 2 hours at 140 °C and characterized with GC, SEC and ^{1}H-NMR spectroscopy. There was no polymer found and no conversion of the monomer was detected by using EBBr as an initiator for the CROP of EtOx demonstrating that only the acid bromide group initiates the EtOx polymerization. A representative MALDI-TOF MS spectrum of a BrEBBr initiated EtOx homopolymer is displayed in Figure 5.7. The main distribution, separated by the mass of one monomer unit, could be fitted to the poly(2-ethyl-2-oxazoline) with one iodine end group and one hydroxy end group. The presence of iodine instead of bromine on the PS terminus can be explained by an exchange reaction with sodium iodide, which was used as a salt for the MALDI-analysis. The hydroxy end group of the polymer at the PEtOx end is formed since an excess amount of water is added to the polymerization mixture after microwave heating to stop the polymerization. There are two other relatively small distributions visible in the MALDI-TOF MS spectrum and they correspond to polymers with bromine end groups instead of iodine

and/or hydroxy. Besides, one distribution should belong to hydrogen initiated chains as a result of a chain transfer reaction. These chains are not capable of initiating ATRP, thus remains as contamination as shown in Figure 5.11 right.

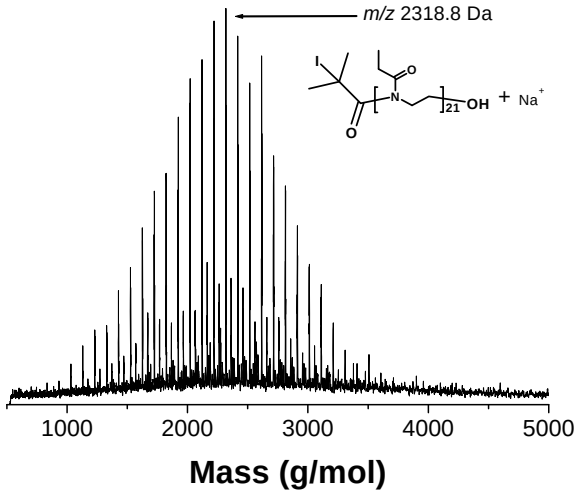

Figure 5.7. MALDI-TOF MS spectrum of BrEBBr initiated CROP of EtOx. NaI was used as a salt in the DCTB matrix.

The CROP of EtOx at a polymerization temperature of 160 ºC initiated by acetyl iodide was found to be approximately 2 and 190 times faster compared to the acetyl bromide and acetyl chloride initiated polymerizations at 160 ºC, respectively. Furthermore, the apparent rate constant values (k_p) of the acetyl bromide and iodide initiated polymerizations at different polymerization temperatures were calculated from the slopes of the regression lines in the semi-logarithmic kinetic plots. However, for the non-linear increase of the first order kinetics of all acetyl chloride initiated polymerizations the initial slope was taken as a measure for the initial polymerization rate (k_i) and the final slope as measure for k_p. The k_p's for the acetyl halide initiators at different polymerization temperatures are listed in Table 5.1 demonstrating the influence of the initiator on the polymerization rates. The standard deviation of the polymerization rates is within 10%, except for the k_p's of the acetyl chloride initiated polymerizations for which it is arbitrary how the fit the final slope of the curves. The obtained order in polymerization rate constants for the different initiators is in agreement with the general statement that the polymerization rate increases with lower basicity of the counter ion: $I^- < Br^- < Cl^-$.

The Arrhenius plots for ACl, ABr, AI, and BrEBBr initiated polymerizations were drawn using the data obtained from the corresponding kinetic plots (Figure 8). From these Arrhenius plots, the activation energies were determined to be 59.5 kJ/mol, 47.9 kJ/mol, 69.3 kJ/mol, 67.9 kJ/mol, and 73.6 kJ/mol for the ACl (k_i and k_p), ABr, BrEBBr and AI, respectively. These values are also in the same range to previously reported values for the

polymerization of 2-ethyl-2-oxazoline with various initiators (68.7, 71.1, 81.3, and 113 kJ/mol).[41 -43]

Table 5.1. Polymerization rates for the different initiators (in 10^{-3} $L \cdot mol^{-1} \cdot s^{-1}$) at different temperatures.

Initiator	80 °C	90 °C	100 °C	120 °C	140 °C	160 °C	180 °C	200 °C	220 °C
ACl (k_i)	–	–	–	–	–	1.8 ± 0.2	3.8 ± 0.3	8.3 ± 0.3	38 ± 5
ACl(k_p)	–	–	–	–	–	11.4	47.4	111.3	126.79
ABr	–	–	7.8 ± 0.1	15 ± 1	54 ± 4	149 ± 1	342 ± 18	–	–
BrEBBr	–	–	7.9 ± 0.1	25 ± 1	45 ± 4	202 ± 1	351 ± 18	–	–
AI	3.5 ± 0.3	7.7 ± 0.3	14.3 ± 0.1	42 ± 1	150 ± 9	351 ± 1	–	–	–

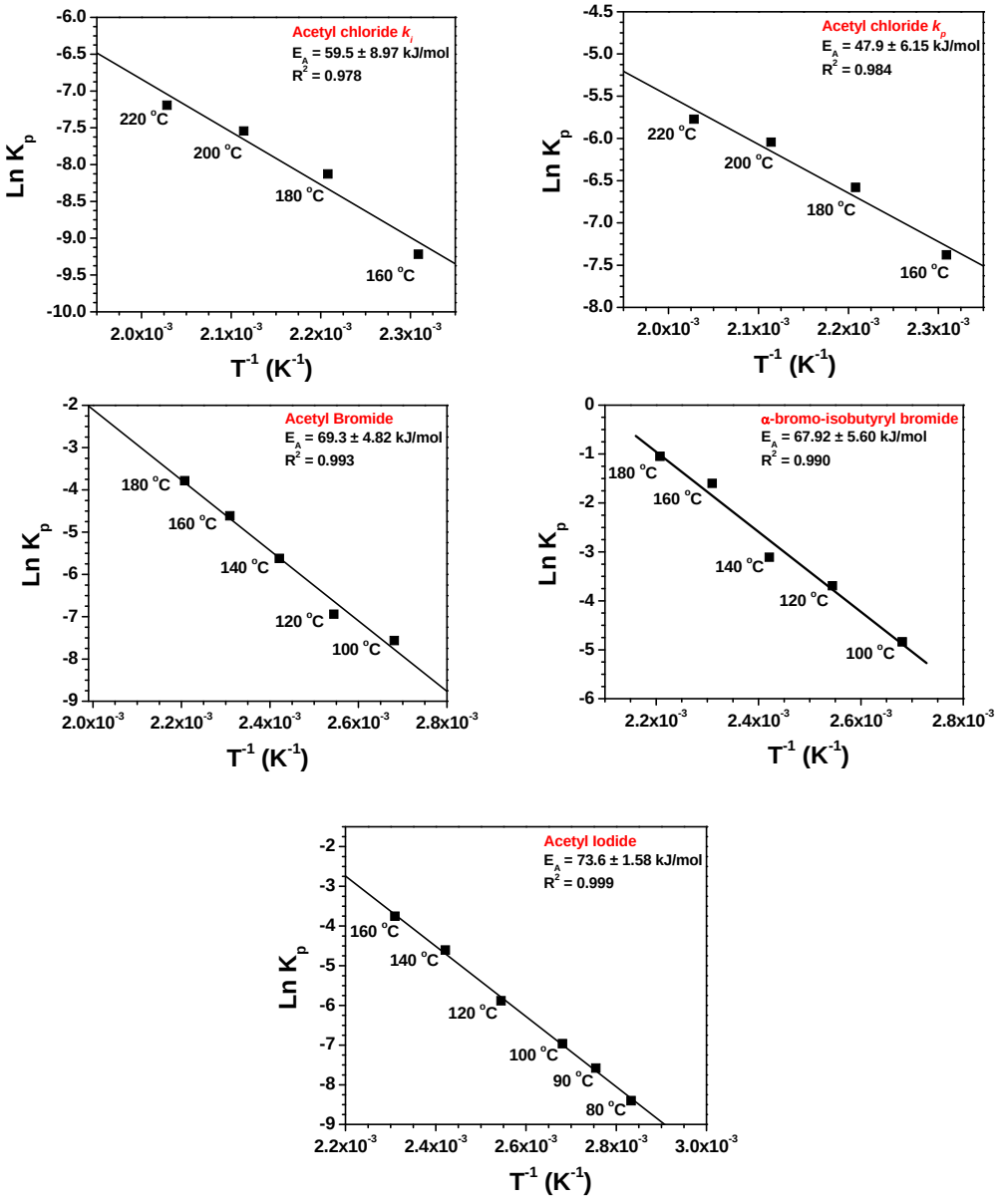

Figure 5.8. Arrhenius plots for the ACl (*top left* and *top right*, calculated from k_i and k_p, respectively), ABr, BrEBBr, and AI initiated polymerizations of EtOx in acetonitrile.

5.3 Synthesis of poly(2-ethyl-2-oxazoline) macroinitiators for ATRP

The common initiators used in CROP of oxazolines are benzyl halides, tosylate or triflate derivatives. Functional end groups can be introduced to the polymer chains using functionalized initiators, which requires additional synthesis and purification steps, or by employing post polymerization modifications. Preferably, a commercially available functional initiator is used for simplicity. We demonstrate the use of the commercially available BrEBBr as a new heterofunctional initiator for the CROP of EtOx followed by the ATRP of St in order to prepare amphiphilic diblock copolymers by combination of two distinct polymerization mechanisms without the need to perform post-polymerization modifications.

The obtained insights into the polymerization kinetics of EtOx in acetonitrile with the different acetyl halide initiators at different temperatures were applied to synthesize PEtOx with higher molar masses (M_n > 10,000 g/mol). Polymerizations were performed at a constant monomer concentration of 4 M and EtOx to ABr ratios of 100, 200 and 400 at a polymerization temperature of 140 °C. The vials were reacted for 30, 60, and 120 minutes, respectively, aiming for 50% conversion to suppress the occurrence of side reactions. As a result, PEtOx homopolymers with relatively high molar masses were obtained and the data obtained from SEC analysis are listed in Table 5.2.

Table 5.2. Molar masses of the polymers with ABr as initiator and higher monomer to initiator ratios obtained from SEC analysis calculated with PS standards.

Sample	[M]/[I]	Temperature [ºC]	Reaction time [min]	$M_{n,theo}$ [g/mol]	$M_{n,SEC}$ [g/mol]	$M_{w,SEC}$ [g/mol]	PDI
1	100	140	30	10,130	8,600	9,100	1.06
2	200	140	60	20,150	19,450	22,100	1.13
3	400	140	120	40,170	28,200	36,100	1.28

Furthermore, the obtained SEC traces for the higher molar mass PEtOx are shown in Figure 5.9. At the high molar mass region of the SEC traces, a small shoulder was observed for all the obtained polymers. The shoulders become less visible with higher monomer to initiator ratios due to a larger extend of overlap of the two peaks. In addition, the peak molar mass (M_p) of the shoulders are twice the M_p of the main peak, which points to chain coupling. Nonetheless, even with these shoulders, polymers with reasonable low PDI values (PDI < 1.3) were obtained with molar masses up to 28,000 g/mol.

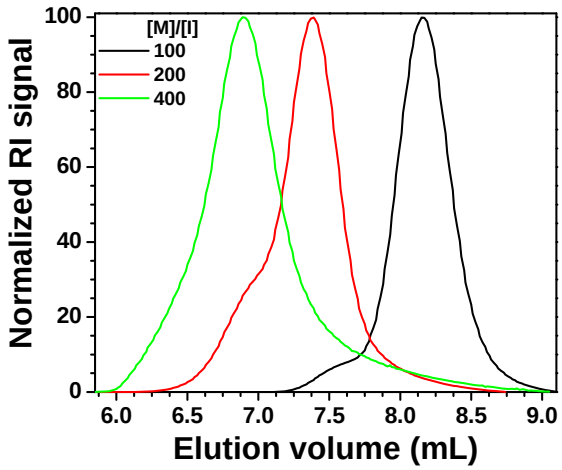

Figure 5.9. SEC traces of the PEtOx that were prepared with different monomer to initiator ratios using ABr as initiator in CH_3CN at 140 °C (SEC eluent: $CHCl_3$:NEt_3:*i*-PrOH=94:4:2).

Moreover, different EtOx to BrEBBr ratios (100, 200, 400, 1000 and 2000) were used for the CROP of EtOx. Reasonably well–defined homopolymers of PEtOx were obtained with molar masses up to 48,500 g/mol and polydispersity indices remaining below 1.3. The corresponding SEC traces of the synthesized PEtOx homopolymers are shown in Figure 5.10 (the results are summarized in Table 5.3). Polydispersity indices and deviation from the theoretical molar masses increase when the monomer to initiator ratio exceeds 1000. The number average molar masses listed in Table 5.3 are relative values that were calculated according to the PS standards. Besides, a possible reason for this observation might be the occurrence of chain transfer reactions, which are more pronounced at higher monomer conversions.

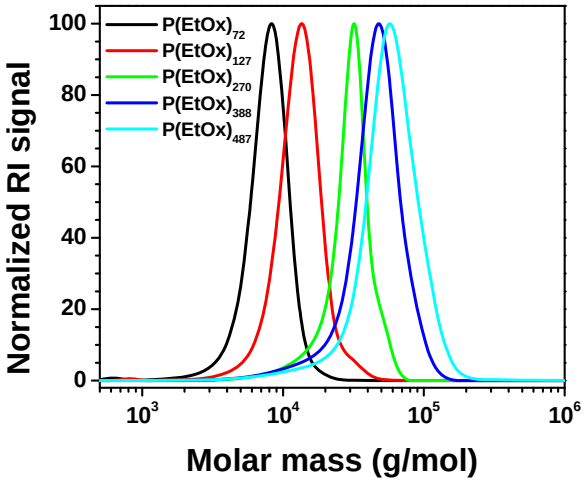

Figure 5.10. SEC traces of the PEtOx that were prepared with different monomer to initiator ratios using BrEBBr as initiator in CH_3CN at 140 °C (SEC eluent: $CHCl_3$:NEt_3:*i*-PrOH=94:4:2).

Table 5.3. Conversion and molar mass data of relatively high molar mass PEtOx homopolymers.

Sample	M/I [a]	Reaction time [min]	Conv.[b] [%]	$M_{n,theo}$[b] [g/mol]	$M_{n,SEC}$[c] [g/mol]	PDI
M1	100	8	43	4,500	7,350	1.12
M2	200	16	46	9,350	12,800	1.13
M3	400	42	65	26,000	27,000	1.15
M4	1000	104	84	83,500	38,700	1.25
M5	2000	208	100	198,500	48,500	1.29

[a] Initial monomer to initiator ratios. [b] Monomer conversions were determined by measuring GC. [c] Theoretical molar masses were calculated by this formula ($M_{n,theo}$ = 230 + (([EtOx] / [BrEBBr]) × monomer conversion × 99.13)) (SEC eluent: $CHCl_3$:NEt_3:*i*-PrOH=94:4:2).

5.4 Synthesis of amphiphilic block copolymers of styrene and 2-ethyl-2-oxazoline

In some cases, *i.e.* using dual initiators, different polymerization mechanisms can be carried out simultaneously. Dual and heterofunctional initiators allow for a wide range of combinations of monomers that polymerize according to different mechanisms, leading to a broad spectrum of accesible block copolymers. There was much evolution in the design of dual initiators during the last decades. In the early years, the synthesis of block copolymers with only controlled polymerization mechanisms was not possible. Mostly, free radical polymerization (FRP) was involved in the block copolymer formation process. There are clearly limitations associated with this approach, namely a rather limited control on the polymerization process can be exerted, and accordingly blocks of varying molar masses and polydispersity indices are produced. Moreover, the block copolymer architecture (AB, ABA, etc.) is dependent on the termination mode of the vinyl monomer involved in FRP. Although block copolymerization by free radical techniques leads to a variety of products as a result of transfer and termination reactions, it has been extensively employed due to a wide choice of monomer combinations and low sensitivity towards impurities. With the introduction of controlled radical polymerizations great progress was made, which resulted in an exponential growth of the use of dual initiators after the year 2000. Similar as for FRP, controlled radical polymerization does not require rigorous purification conditions, in contrast to controlled ionic polymerizations. The substitution of FRP by controlled radical polymerization (CRP) opened the way to the synthesis of block copolymer architectures by combination of only controlled polymerization techniques.

Advanced macromolecular structures constructed by the combination of different monomeric units have attracted great attention because of their enhanced properties for various applications such as, *e.g.*, surface modifiers, coating materials, drug delivery systems and adhesives.[46] It is now possible to obtain well–defined macromolecules with controlled molar mass, polydispersity index, architecture and terminal functionalities by employing controlled/"living" polymerization methods. These polymerizations may proceed by anionic,[47] cationic,[48] group transfer,[49] metathesis,[50] Ziegler-Natta[51] or various radical mechanisms.[52- 55]

Recently, Yagci *et al*. have reviewed the mechanistic transformations of controlled/living polymerization techniques which provide a facile route to the synthesis of block copolymers that cannot be performed by a single polymerization method.[6] Moreover, Du Prez *et al.* discussed the combination of different polymerization techniques using dual initiators to synthesize block copolymers which do not require any intermediate transformation and protection steps.[56] A dual initiator, or more general a heterofunctional initiator, contains at least two initiation sites with selective and independent initiating groups for the concurrent polymerization mechanisms. Matyjaszewski *et al.* have examined a general method for the transformation of "living" carbocationic polymerizations into "living" radical polymerizations without any modification of the initiating sites and they presented a successful synthesis of AB type block copolymers of tetrahydrofuran (THF) and styrene (St) or methyl (meth)acrylate, respectively.[57] Voit *et al.* employed a "grafting from" method for the synthesis of complex macromolecular structures consisting of *N*-isopropyl acrylamide and 2-alkyl-2-oxazolines and investigated their lower critical solution temperature behavior.[58] These reports are only a few examples that demonstrate the importance of exploiting and improving the combination of different polymerization techniques in order to obtain well–defined block copolymers combining the properties of both monomer sequences.[59- 64]

Consequently, we have studied the α–bromo isobutyrylbromine initiated CROP of EtOx and the direct use of the obtained polymers as macroinitiators for the ATRP of St without the need for post polymerization modifications to transform the mechanism from ionic to radical. According to the knowledge obtained from the kinetic investigation, a PEtOx macroinitiator was synthesized in a relatively larger scale (6.11 g) by using the BrEBBr heterofunctional initiator. The molar mass of the PEtOx macroinitiator was measured by SEC ($M_{n,SEC}$ = 3,700 g/mol, M_w/M_n = 1.09) and the monomer conversion (~100%) was determined by ^{1}H-NMR spectroscopy.

This PEtOx homopolymer was subsequently used as a macroinitiator for the ATRP of St in order to obtain well–defined PEtOx-*b*-PS diblock copolymers. Various ligands, *i.e. N, N,*

N′, N″, N‴-pentamethyldiethylenetriamine (PMDETA), 2,2-bipyridyl (BPy) and *N*-(*n*-hexyl)-2-pyridylmethanimine (NHPMI),[65,66] were tested for the ATRP of St in the presence of CuBr metal salt. However, none of these ligands provided a good initiation for the ATRP of St. Therefore, a more active ligand, Me_6Tren, was selected and in this case it was possible to initiate the ATRP of St. It was necessary to use a more active ligand since the initiation of amide initiators are more difficult in comparison to ester initiators. The overall reaction scheme of ATRP of St initiated by PEtOx is shown in Scheme 5.3.

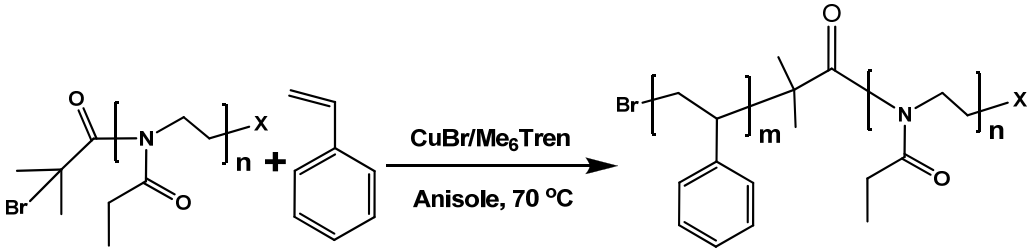

Scheme 5.3. Schematic representation of the atom transfer radical polymerization of St initiated by a PEtOx macroinitiator.

The polymerization was performed in anisole at 70 °C for 7 hours. A linear relationship was observed in the semi-logarithmic kinetic plot which indicates a controlled growth of the second block (Figure 5.11 left). The apparent rate of polymerization was calculated from this plot as 6.16×10^{-3} L·mol^{-1}·s^{-1}. The aliquots were withdrawn from the polymerization mixture in a relatively large scale (approximately. 2 mL) in order to be able to purify and further characterize the copolymers. In this way, it was possible to synthesize a set of amphihilic block copolymers with a constant length of the first PEtOx block and increasing length of the second PS block. The samples taken at different time intervals were characterized by SEC. A shift of the peak to lower elution volumes is clearly visible in Figure 5.11 right, evidencing the chain extension. On the other hand, it was observed that some amount of unreacted macroinitiator remained in the polymerization mixture. The possible explanation for this could be the presence of chain transfer initiated EtOx chains without ATRP initiator functionality.

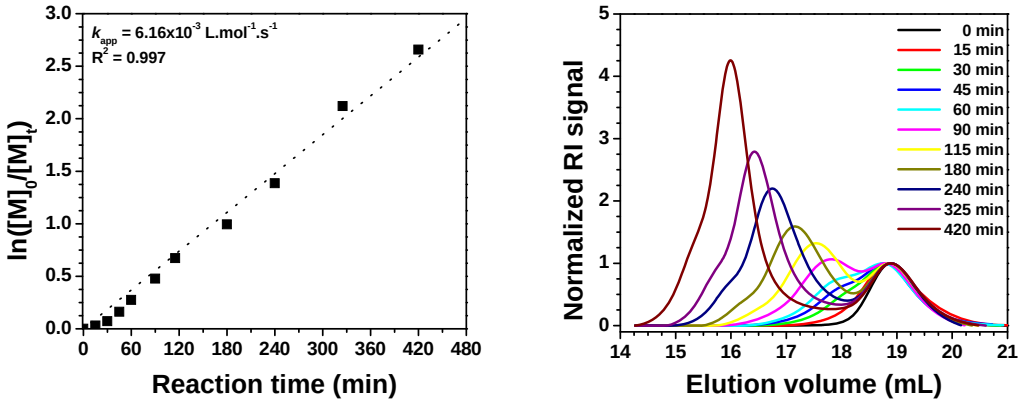

Figure 5.11. SEC traces of the samples withdrawn from the block copolymerization of St *via* ATRP initiated by the PEtOx-Br macroinitiator.

The conversion and molar mass data of the samples measured directly from the polymerization solutions are summarized in Table 5.4. Monomer conversions were measured with GC and anisole was used as an internal standard. In the SEC measurements, the peak maxima of the block copolymers were listed for a better comparison. It was observed that the peak maxima of the SEC traces for the samples taken at different reaction times were shifting to the high molar mass region; this represents a strong indication for the controlled polymerization.

Table 5.4. Conversion and molar mass data of PEtOx-*b*-PS prior to purification.

Sample	**Reaction time [min]**	**Conv.**[a] **[%]**	$M_{n,theo}$[b] **[g/mol]**	$M_{p,SEC}$[c] **[g/mol]**
P0	0	–	3,700	4,150
P1	15	3	4,320	4,150
P2	30	7	5,150	4,300
P3	45	15	6,820	6,600
P4	60	24	8,700	7,600
P5	90	38	11,610	8,700
P6	115	49	13,910	10,600
P7	180	63	16,820	14,400
P8	240	75	19,320	19,500
P9	325	88	22,030	25,000
P10	420	93	23,070	35,400

[a] Monomer conversions were determined by measuring GC. [b] Theoretical molar masses were calculated by this formula ($M_{n,theo}$ = 3700 + (([St] / [PEtOx]) × monomer conversion × 104.15)). [c] Peak maximum of the block copolymers in the corresponding SEC traces.

The block copolymers were purified by a simple precipitation into a selective non-solvent. Methanol is a non-solvent for PS, whereas it is a good solvent for PEtOx. As such, precipitation of the polymerization samples into methanol yielded pure PEtOx-*b*-PS (Figure 5.12). The molar mass data and polydispersity indices of those purified diblock copolymers are listed in Table 5.5. The average degree of polymerization (DP) for the styrene block and the corresponding experimental molar masses were calculated from ^{1}H-NMR measurements.

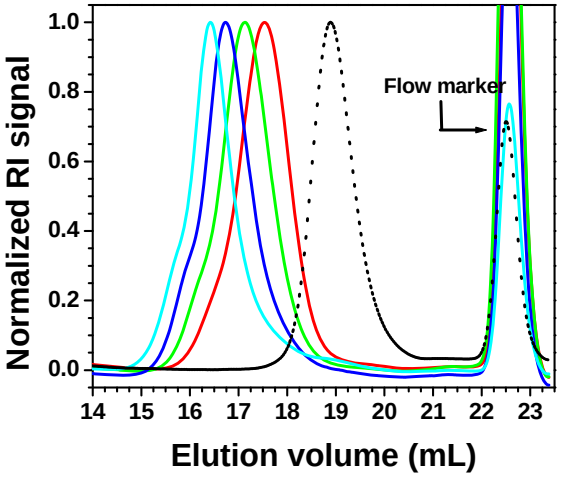

Figure 5.12. SEC traces of PEtOx-*b*-PS copolymers after precipitation. The dotted line represents the PEtOx-Br macroinitiator.

Table 5.5. Molar mass data and degree of polymerization of PEtOx-*b*-PS after purification.

Sample	$M_{n,SEC}$ [a] [g/mol]	$M_{n,NMR}$ [b] [g/mol]	PDI	$DP_{EtOx,SEC}$ [c]	$DP_{St,NMR}$ [d]
P0	3,700		1.09	35	–
P6	10,200	13,800	1.20	35	97
P7	13,100	16,600	1.24	35	124
P8	16,500	17,900	1.27	35	136
P9	22,200	21,200	1.23	35	168
P10	35,200	27,000	1.21	35	224

[a] Number average molar mass of PEtOx-*b*-PS calculated by measuring SEC. [b] Molar masses of the block copolymers calculated by the combination of SEC and ^{1}H−NMR results. [c] Degree of polymerization for the PEtOx block calculated using optimized SEC. [d] Degree of polymerization for the second block of PEtOx-*b*-PS calculated from ^{1}H-NMR measurements.

5.5 Micellization behavior of block copolymers

The micellization behavior of the different amphiphilic PEtOx-*b*-PS copolymers has been studied in water. Because of the rather short PEtOx block the copolymers are not

directly soluble in water. They have thus been first dissolved in a non–selective solvent, *i.e.* DMF, and water has been added to trigger the micellization. In a last step, DMF was removed by dialysis against water. The obtained micelles have been characterized by DLS and AFM. For all copolymers, a CONTIN analysis of the DLS data revealed a single, relatively broad, population. The DLS data did not show any significant dependence on dilution, in agreement with the formation of "frozen" micelles.[67] The hydrodynamic radii, summarized in Table 5.6, seem large considering the molar mass of the copolymers.

Table 5.6. Hydrodynamic radius (R_h) and the diameter of the core (D_c) of the block copolymers.

Sample	P6	P7	P8	P9	P10
R_h (nm)	141	93	77	114	84
D_c (nm)	19	22	24	28	35

Moreover, there is no visible correlation between the measured R_h and the composition of the copolymers. Since all copolymers have the same hydrophilic block length and a hydrophobic block length increasing from P6 to P10, a corresponding increase of R_h was expected, according to the usual trend observed for block copolymer micelles.[67] This lack of correlation could be due to the formation of aggregates of micelles in the presence of non-spherical aggregates. Even if the CONTIN histograms only show a single population, this peak accounts in fact for unresolved isolated micelles and small clusters of micelles.[68] This behavior is a common feature for micellar objects presenting only a steric stabilization from water-soluble coronal blocks, such as poly(ethylene oxide)[68,69] or PEtOx.[18,19] Moreover, the copolymers used in this study have a rather short hydrophilic block, providing thus a poor stabilization of the micelles. To help clarify the situation and to possibly observe isolated objects, the micelles have been deposited onto silicon substrates by spin-coating and were subsequently characterized in the dry state by AFM. A typical height image recorded on such a sample is shown in Figure 5.13.

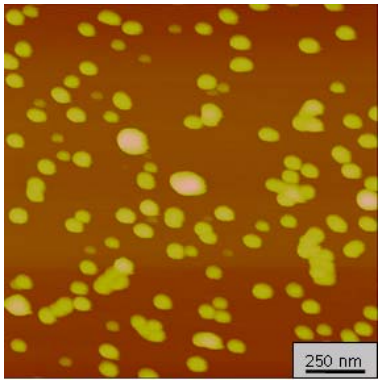

Figure 5.13. AFM height image recorded on micelles, obtained from copolymer P7, deposited on a silicon substrate.

Isolated micelles but also small clusters are clearly seen, confirming their tendency to aggregate. To avoid tip convolution effects, the height of the micelles have been measured. This height can be assimilated to the diameter of the micellar core since the coronal block is short and collapsed in the dried state. The results are reported in Table 5.5. Here, a clear correlation between the copolymer compositions and the micelle size is observed, the diameter of the core increased progressively with the length of the PS block. For classical hairy micelles the size of the core should scale linearly with the $3/5^{th}$ power of the degree of polymerization of the insoluble block.[70] Such a plot has been constructed (Figure 5.14), and the linear relationship is clearly evidenced. This shows that despite the tendency to form aggregates, well–defined, isolated micelles following the classical scaling laws can be obtained.

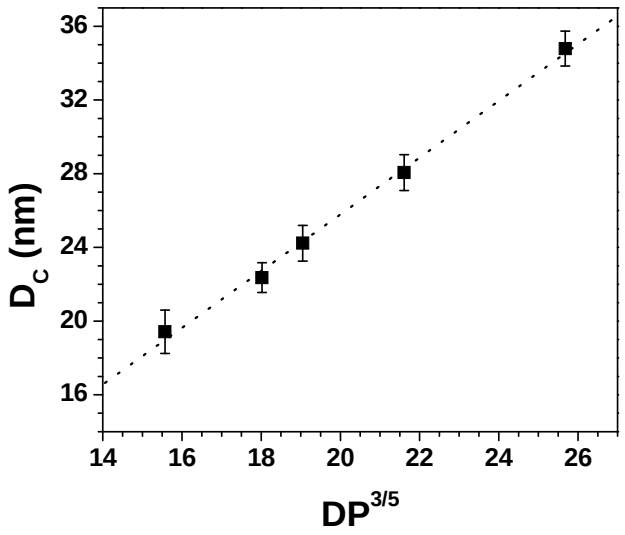

Figure 5.14. Relationship between the measured (AFM) core size of the micelles and the $3/5^{th}$ power of the degree of polymerization of the PS block. The dotted line represents a linear regression performed on those data.

5.6 Conclusions

The systematic kinetic screening of the polymerization of 2-ethyl-2-oxazoline was investigated with four different acetyl halide initiators (acetyl chloride, acetyl bromide, α-bromo-isobutyrylbromide and acetyl iodide) at different polymerization temperatures (ranging from 80 to 220 ºC) using a monomer concentration of 4 M and a monomer to initiator ratio of 60. As expected, the order in polymerization rate for the different initiators was found to increase with decreasing basicity of the halide: chloride < bromide < iodide. In addition, it was demonstrated that the polymerization rates increased at higher temperatures, and that the polymerizations were controlled at all polymerization temperatures (PDI ~ 1.10). MALDI-

TOF MS confirmed that both the acetyl group and the halide were present at the chain ends of the resulting polymers. From the first order kinetic plots, the polymerization rates and activation energies were calculated for the polymerizations with the three acetyl halide initiators.

The kinetic insights in the EtOx polymerizations with these acetyl halide initiators were used to synthesize polymers with relatively high monomer to initiator ratios of 100, 200, 400, 1000, and 2000 using ABr or BrEBBr as initiator at 140 ºC. Even though SEC analysis indicated the occurrence of some chain transfer and/or chain coupling reactions, reasonably well-defined polymers were obtained with molar masses up to 50 kDa and polydispersity indices below 1.3.

Moreover, we demonstrated the use of a commercially available heterofunctional initiator for the CROP of EtOx followed by the ATRP of St. PEtOx-*b*-PS copolymers with different PS chain length were synthesized by ATRP from the well-defined PEtOx macroinitiators. Those diblock copolymers were obtained with controlled molar masses and relatively narrow polydispersity indices.

Micellization in water of these amphihilic block copolymers was investigated by DLS and AFM measurements. The results clearly revealed a correlation between the length of the PS block and the diameter of the core of the micelles.

5.7 Experimental part

Materials

2-Ethyl-2-oxazoline (EtOx) (≥99%, Aldrich) was distilled over barium oxide and stored under argon. Styrene (St) (≥99%, Aldrich) and anisole (Biosolve Ltd.) were passed through a neutral alumina oxide column prior to use. CuBr (99.999%, Aldrich) was purified as described in the literature.[71] Acetonitrile (AN) (Biosolve Ltd.) was dried over molecular sieves (3 Å). *α*–Bromo isobutyryl bromine (BrEBBr) (98%, Aldrich) was used as received. Tris[2-(dimethylamino)ethyl]amine (Me_6Tren) was synthesized according to a synthetic procedure described in the literature.[72]

GC measurements were performed on an Interscience Trace GC used with a Trace column RTX-5 and a PAL autosampler. ^{1}H-NMR spectroscopy was performed on a Varian Mercury 400 NMR in deuterated methylene chloride. The chemical shifts were calibrated with respect to tetramethylsilane (TMS). Size exclusion chromatography (SEC) was measured on a Shimadzu system equipped with a SCL-10A system controller, a LC-10AD pump, a RID-10A refractive index detector, a SPD-10A UV detector and both a PSS Gram30 and a PSS

Gram1000 column in series. *N,N*-Dimethylacetamide with 5 mmol LiCl was used as eluent at a flow rate of 1 mL/min and the column oven was set to 60 ºC. For the kinetic investigation of the BrEBBr initiated EtOx polymerization, SEC measurements were performed on a Shimadzu system equipped with a SCL-A10 system controller, a LC-10AD pump, a RID-10A refractive index detector, a SPD-10A UV-detector at 254 nm and a PLgel 5 μm Mixed-D column at 50 ºC utilizing a chloroform: triethylamine: 2-propanol (94:4:2) mixture as eluent at a flow rate of 1 mL/min. The molar mass and the molar mass distribution of the prepared polymers were calculated using poly(styrene) standards in both SEC systems. MALDI measurements were performed on a Voyager-DE PRO Biospectrometry Workstation (Applied Biosystems, Foster City, CA) time-of-flight mass spectrometer in linear mode. The spectra were obtained in the positive ion mode. Ionization was performed with a 337-nm pulsed nitrogen laser. The sample was prepared with a multiple-layer spotting technique utilizing *t*-2-(3-(4-*t*-butyl-phenyl)-2-methyl-2-propenylidene)malononitrile (DCTB) as matrix and NaI as salt similar as described in literature.[73] Cationic ring opening polymerizations were performed using the Emrys Liberator monomode microwave synthesizer (Biotage) under temperature control utilizing an IR temperature sensor. Dynamic light scattering (DLS) experiments were performed on a Malvern CGS-3 equipped with a He-Ne laser (633 nm). The measurements have been performed at an angle of 90° and a temperature of 25 °C. The results were analyzed by the CONTIN method which is based on an inverse-Laplace transformation of the data and which gives access to a size distribution histogram for the analyzed micellar solutions. AFM images of the micelles were obtained using a Digital Instruments Nanoscope IV scanning force microscope in tapping mode using NCL type cantilevers (Si, 48 N/m, 330 kHz, Nanosensors). The samples were prepared by spin-coating a dilute solution of micelles on a silicon wafer. The micelles were prepared by first dissolving the copolymer in DMF at a concentration of 1 g/L. In a next step, a water volume equal to half the DMF volume was added under stirring by steps of 50 μL, followed by the addition of the same water volume in one shot. Afterwards the solution was dialyzed against water to remove the DMF. The final concentration was about 0.3 g/L.

Typical polymerization procedure for the kinetic investigations

In order to perform a kinetic study for each initiator at different temperatures, stock solutions were prepared with monomer, solvent and initiator (acetyl chloride, acetyl bromide, α-bromo-isobutyrylbromide or acetyl iodide) having a monomer to initiation ratio of 60 and an initial monomer concentration of 4 M. From these stock solutions, 1 mL aliquots were transferred into different microwave vials. Subsequently, 10 of these vials were heated with

different predefined reaction times for each investigated temperature. All reactions were terminated by the automated addition of 50 µL water using the liquid handling system of the microwave synthesizer. Samples were taken from the microwave reactors and diluted (100 µL crude sample + 1000 µL chloroform) for GC analysis and acetonitrile was used as internal standard to calculate the monomer conversions. A second sample was withdrawn from the reactors and diluted (100 µL crude sample + 1000 µL chloroform: triethylamine: 2-propanol (94:4:2) mixture) for SEC analysis in order to calculate the molar masses and polydispersity indices against polystyrene standards.

Upscaling of the PEtOx macroinitiator synthesis

EtOx (8 mL, 7.92 mmol), CH_3CN (12 mL) and BrEBBr (384 µL, 1.98 mmol) were added to a microwave vial, which had an inner volume of 22 mL. It was reacted in the microwave synthesizer at 140 °C for 500 seconds and a few drops of water were added to terminate the polymerization. The polymer solution was subsequently diluted by adding chloroform, and the polymer was precipitated into cold diethyl ether. The white precipitate was filtered, washed with cold diethyl ether and stored at 25 °C in a vacuum oven.

ATRP of St initiated by PEtOx macroinitiators

0.067 g (0.467 mmol) of CuBr and 124 µL (0.467 mmol) of Me_6Tren were added to a 25 mL Schlenk flask and stirred under argon. Pre-degassed anisole (10 mL) and 10.7 mL of St (93.4 mmol) were added into the flask. After bubbling with argon and stirring for at least 30 minutes, 1.73 g (0.467 mmol) of PEtOx macroinitiator dissolved in 10 mL of anisole, which was degassed in another flask, were added to the Schlenk flask via a degassed syringe. An initial sample was taken and the Schlenk flask was placed into the oil bath preheated to 70 °C, and reacted for 7 hours. At certain time intervals, aliquots (approx. 2 mL) were withdrawn and quenched with air. The sampling times, monomer conversion and molar mass data of the obtained block copolymers before precipitation are listed in Table 5.4.

5.8 References

(1) Y. Yagci, M. K. Mishra, *Macroinitiators in multi-modepolymerization.* In: Mishra MK, editor. Macromolecular design: concept and practice (macromonomers, macroinitiators, macroiniferters, macroinimers, macroiniters, and macroinifers). New York: Polymer Frontiers International; **1994,** 391–426.

(2) Y. Yagci, M. K. Mishra, *Block copolymers (by changing polymerization mechanism).* Boca Raton: CRC Press, Inc.; **1996**, 1–15.

(3) Y. Yagci, *Synthesis of block copolymers by combination of different polymerization routes.* In: H. S. Nalwa, editor. Advanced functional molecules and polymers, vol. 1. Synthesis. Singapore: Gordon & Breach Science Publishers; **2001**, 233–69.

(4) N. Hadjichristidis, S. Pispas, G. Floudas, *Block copolymers: synthetic strategies, physical properties, and applications.* Hoboken, NJ: Wiley; **2003**.

(5) N. Hadjichristidis, M. Pitsikalis, H. Iatrou, *Adv. Polym. Sci.* **2005**, *189*, 1–124.

(6) K. V. Bernaerts, F. E. Du Prez, *Prog. Polym. Sci.* **2006**, *31*, 671–722.

(7) R. Jerome, *Macromol. Symp.* **2002**, *177*, 43–57.

(8) K. Matyjaszewski, J. Xia, *Chem. Rev.* **2001**, *101*, 2921–2990.

(9) M. Kamigaito, T. Ando, M. Sawamoto, *Chem. Rev.* **2001**, *101*, 3689–3745.

(10) D. A. Tomalia, D. P. Sheetz, *J. Polym. Sci., Part A: Polym. Chem.* **1966**, *4*, 2253–2265.

(11) W. Seeliger, E. Aufderhaar, W. Diepers, R. Feinauer, R. Nehring, W. Thier, H. Hellmann, *Angew. Chem.* **1966**, *20*, 913–927; *Angew. Chem. Int. Ed. Engl.* **1966**, *5*, 875–876.

(12) T. G. Bassiri, A. Levy, M. Litt, *Polym. Lett.* **1967**, *5*, 871–879.

(13) K. Aoi, M. Okada, *Prog. Polym. Sci.* **1996**, *21*, 151–208.

(14) S. Kobayashi, H. Uyama, *J. Polym. Sci., Part A: Polym. Chem.* **2002**, *40*, 192–209.

(15) O. W. Webster, *Science* **1991**, *496*, 887–893.

(16) S. Kobayashi, T. Igarashi, Y. Moriuchi, T. Saegusa, *Macromolecules* **1986**, *19*, 535–541.

(17) R.-H. Jin, *Adv. Mater.* **2002**, *14*, 889–892.

(18) R. Hoogenboom, F. Wiesbrock, H. Huang, M. A. M. Leenen, S. F. G. M. van Nispen, M. van der Loop, C.-A. Fustin, A. M. Jonas, J.-F. Gohy, U. S. Schubert, *Macromolecules* **2006**, *39*, 4719–4725.

(19) R. Hoogenboom, F. Wiesbrock, M. A. M. Leenen, H. M. L. Thijs, H. Huang, C. A. Fustin, P. Guillet, J.-F. Gohy, U. S. Schubert, *Macromolecules* **2007**, *40*, 2837–2843.

(20) H. Huang, R. Hoogenboom, M. A. M. Leenen, P. Guillet, A. M. Jonas, U. S. Schubert, J.-F. Gohy, *J. Am. Chem. Soc.* **2006**, *128*, 3784–3788.

(21) R. Hoogenboom, M. W. M. Fijten, U. S. Schubert, *J. Polym. Sci., Part A: Polym. Chem.* **2004***, 42,* 1830–1840.

(22) T. Saegusa, H. Ikeda, *Macromolecules* **1973**, *6*, 808–811.

(23) T. Saegusa, H. Ikeda, H. Fujii, *Macromolecules* **1972**, *5*, 359–362.

(24) T. Saegusa, H. Ikeda, H. Fujii, *Macromolecules* **1973**, *6*, 315–319.

(25) Q. Lui, M. Konnas, J. S. Riffle, *Macromolecules* **1993**, *26*, 5572–5576.

(26) A. Dworak, *Macromol. Chem. Phys.* **1998**, *199*, 1843–1849.

(27) M. Einzmann, W. H. Binder, *J. Polym. Sci., Part A: Polym. Chem.* **2001**, *39*, 2821–2831.

(28) R. D. Puts, D. Y. Sogah, *Macromolecules* **1997**, *30*, 7050–7055.

(29) Y. Wang, W. J. Brittain, *Macromol. Rapid Commun.* **2007**, *28*, 811–815.

(30) A. Dworak, *Polym. Bull.* **1997**, *38*, 7–11.

(31) J.-S. Park, Y. Akiyama, F. M. Winnik, K. Kataoka, *Polymer* **2004**, *37*, 6786–6792.

(32) F. Wiesbrock, R. Hoogenboom, C. H. Abeln, U. S. Schubert, *Macromol. Rapid Commun.* **2004**, *25*, 1895–1899.

(33) F. Wiesbrock, R. Hoogenboom, M. A. M. Leenen, M. A. R. Meier, U. S. Schubert, *Macromolecules* **2005**, *38*, 5025–5034.

(34) R. Hoogenboom, R. M. Paulus, A. Pilotti, U. S. Schubert, *Macromol. Rapid Commun.* **2006**, *27*, 1556–1560.

(35) R. M. Paulus, T. Erdmenger, C. R. Becer, R. Hoogenboom, U. S. Schubert, *Macromol. Rapid Commun.* **2007**, *28*, 484–491.

(36) R. Hoogenboom, R. M. Paulus, M. W. M. Fijten, U. S. Schubert, *J. Polym. Sci., Part A: Polym. Chem*. **2005**, *43*, 1487–1497.

(37) M. W. M. Fijten, R. Hoogenboom, U. S. Schubert *J. Polym. Sci., Part A: Polym. Chem*. **2008**, *46*, 4804–4816.

(38) M. Litt, A. Levy, J. Herz, *J. Macromol. Sci. Chem.* **1975**, *5*, 703–727.

(39) B. L. Rivas, E. Sanhueza, *Polym. Bull.* **1999**, *42*, 281–286.

(40) J. Kadokawa, K. Ikuma, H. Tagaya, *Eur. Polym. J.* **2002**, *38*, 7–11.

(41) R. Hoogenboom, M. W. M. Fijten, C. Brandli, J. Schroer, U. S. Schubert, *Macromol. Rapid Commun.* **2003**, *24*, 98–103.

(42) T. Kagiya, T. Matsuda, R. Hirata, *J. Macromol. Chem. Sci.* **1972**, *6*, 451–462.

(43) T. Kagiya, T. Matsuda, *J. Macromol. Chem. Sci.* **1971**, *5*, 1265–1285.
(44) D. M. Haddleton, D. Kukulj, A. P. Radigue, *Chem. Commun*. **1999**, 99–100.
(45) S. C. Hong, K. Matyjaszewski, *Macromolecules* **2002**, *35*, 7592–7605.
(46) G. Riess, G. Hurtrez, P. Bahadur, In: H. F. Mark, N. M. Bikales, C. G. Overberger, G. Menges, J. I. Kroschwitz, Editors. *Encyclopedia of Polymer Science and Engineering*, vol. 2. New York: Wiley **1985**, p. 324.
(47) M. Szwarc, *Nature* **1956**, *178*, 1168–1169.
(48) K. Matyjaszewski, *Cationic Polymerizations, Mechanisms, Synthesis, and Applications* Marcel Dekker: New York, **1996**.
(49) O. W. Webster, W. R. Hertler, D. Y. Sogah, W. B. Farnhem, T. Rajan-Babn, V. *J. Am. Chem. Soc.* **1983**, *105*, 5706–5708.
(50) B. M. Novak, W. Risse, R. H. Grubbs, *Adv. Polym. Sci.* **1992**, *102*, 47–72.
(51) C. M. Killian, D. J. Tempel, L. K. Johnson, M. Brookhart, *J. Am. Chem. Soc.* **1996**, *118*, 11664–11670.
(52) K. Matyjaszewski, J. Xia, *Chem. Rev.* **2001**, *101*, 2921–2990.
(53) M. Kamigaito, T. Ando, M. Sawamoto, *Chem. Rev.* **2001**, *101*, 3689–3745.
(54) J. Chiefari, Y. K. Chong, F. Ercole, J. Krstina, J. Jeffery, T. P. T. Le, R. T. A. Mayadunne, G. F. Meijs, C. L. Moad, G. Moad, E. Rizzardo, S. H. Thang, *Macromolecules* **1998**, *31*, 5559–5562.
(55) C. J. Hawker, A. W. Bosman, E. Harth, *Chem. Rev.* **2001**, *101*, 3661–3688.
(56) K. V. Bernaerts, F. E. Du Prez, *Prog. Polym. Sci.* **2006**, *31*, 671–722.
(57) A. Kajiwara, K. Matyjaszewski, *Macromolecules* **1998**, *31*, 3489–3493.
(58) J. Rueda, S. Zschoche, H. Komber, D. Schmaljohann, B. Voit, *Macromolecules* **2005**, *38*, 7330–7336.
(59) I. Cianga, Y. Hepuzer, E. Serhatli, Y. Yagci, *J. Polym. Sci., Part A: Polym. Chem.* **2002**, *40*, 2199–2208.
(60) S. Q. Xu, H. Y. Zhao, T. Tang, B. T. Huang, *Chin. J. Polym. Sci.* **1999**, *17*, 145–150.
(61) D. Christova, R. Velichkova, E. J. Goethals, *Macromol. Rapid Commun.* **1997**, *18*, 1067–1073.
(62) T. Erdogan, K. V. Bernaerts, L. M. Van Renterghem, F. E. Du Prez, E. J. Goethals, *Des. Monomers Polym.* **2005**, *8*, 705–714.
(63) D. Christova, R. Velichkova, E. J. Goethals, F. E. Du Prez, *Polymer* **2002**, *43*, 4585–4590.
(64) K. V. Bernaerts, E. H. Schacht, E. J. Goethals, F. E. Du Prez, *J. Polym. Sci., Part A: Polym. Chem.* **2003**, *41*, 3206–3217.
(65) H. Zhang, U. S. Schubert, *Chem. Commun.* **2004**, 858–859.
(66) D. M. Haddleton, C. B. Jasieczek, M. J. Hannon, A. J. Shooter, *Macromolecules* **1997**, *30*, 2190–2193.
(67) J.-F. Gohy, *Adv. Polym. Sci*. **2005**, *190*, 65–136.
(68) O. Regev, J.-F. Gohy, B. G. G. Lohmeijer, S. K. Varshney, D. H. W. Hubert, P. Frederik, U. S. Schubert, *Colloid Polym. Sci.* **2004**, *282*, 407–411.
(69) A. Jada, G. Hurtrez, B. Siffert, R. Riess, *Macromol. Chem. Phys.* **1996**, *197*, 3697–3710.
(70) I. W. Hamley, *The Physics of Block Copolymers* Oxford University Press: Oxford, UK, **1998**.
(71) S. V. Arehart, K. Matyjaszewski, *Macromolecules* **1999**, *32*, 2221–2231.
(72) J. Queffelec, S. G. Gaynor, K. Matyjaszewski, *Macromolecules* **2000**, *33*, 8629–8639.
(73) Meier, M. A. R. Schubert, U. S. *Rapid Commun. Mass Spectrom.* **2003**, *17*, 713–716.

Chapter 6

Well–defined fluorinated glycopolymers *via* thiol–*para* fluoro "click" reaction

Abstract

The synthesis of glycopolymers consisting of styrene (St) and pentafluorostyrene (PFS) by a combination of nitroxide mediated radical polymerization and "click" chemistry processes have been demonstrated in this chapter. Therefore, a series of well–defined homopolymers, block and random copolymers of St and PFS have been prepared with different ratios using Bloc Builder™ as an alkoxyamine initiator. Moreover, a thiol–glycoside (2,3,4,6–tetra–O–acetyl–1–thio–β–D–gluco–pyranose) has been reacted under ambient conditions with PFS moieties on the polymeric backbone utilizing a thiol–para fluoro "click" reaction. This nucleophilic substitution reaction was performed with high yields, and the reaction kinetics was monitored online with ^{19}F–NMR spectroscopy. Finally, the deacetylation of the protected glucose moieties was carried out to yield well–defined water soluble glycopolymers that were characterized in detail by ^{1}H, ^{13}C and ^{19}F–NMR spectroscopy, size exclusion chromatography as well as MALDI–TOF mass spectrometry.

Parts of this chapter have been published: C. R. Becer, R. Hoogenboom, U. S. Schubert, *Angew. Chem. Int. Ed.* **2009***,* in press; C. R. Becer, K. Babiuch, D. Pilz, S. Hornig, T. Heinze, M. Gottschaldt, U. S. Schubert, *Macromolecules* **2009**, 42, 2387–2394.

6.1 Introduction

The synthesis of tailor–made macromolecules for advanced applications in various fields, *i.e.* drug delivery, catalysis, electronics, and nanotechnology, represents a major target of contemporary research.[1-3] For drug delivery devices, increasing attention has been paid to synthetic polymers substituted with pendant carbohydrates as biological recognition units.[4,5] Therefore, controlled and "living" polymerization techniques have been competing with other demanding polymerization techniques to provide biocompatible and economically accessible macromolecules with relatively efficient and simple synthetic procedures.[6-9]

In recent years, controlled radical polymerization (CRP) techniques have attracted more attention than ionic polymerizations for the synthesis of tailor–made complex architectures.[10-12] Although ionic polymerizations provide macromolecules with extremely good control over the molecular architecture, they are very sensitive to impurities and require sophisticated experimental setups. In particular, nitroxide mediated radical polymerization (NMP) has been attracting the attention for the synthesis of biopolymers since this technique does not require any catalyst or a metal salt to mediate the reaction, which represents a major disadvantage of many other methods.[13-19]

The "click" reaction concept, on the other hand, offers easy and robust reactions, *e.g.* for combining macromolecules and carbohydrates; as a consequence they became very popular in the last few years also in polymer science.[20-24] The "click" chemistry concept was first introduced by Sharpless and coworkers utilizing the Cu(I)–mediated Huisgen 1,3–dipolar cycloaddition reaction of azides and acetylenes.[25] However, the use of a copper salt remained questionable in terms of biocompatibility and cytotoxicity of the materials.[26] Therefore, alternative reactions that provide robust and efficient synthetic processes for complex macromolecules and fulfill the requirements of "click" chemistry have been pursued persistently.[27-29] Recently, Schlaad *et al.* reported a new type of "click" reaction for polymers, "thio click", a thiol–ene radical addition reaction.[30-32] Following to that, Hawker *et al.* employed thiol–ene "click" reactions to synthesize G4 dendrimers.[33-35] One considerable point in both thiol "click" reports is the need of a UV–light source as well as the use of a radical initiator. Moreover, very recently Lin *et al.* have synthesized tetrazole containing compounds which were further reacted with an allyl phenyl ether in just a few minutes under UV–irradiation.[36] They have called this reaction "photoclick chemistry", however, an excess of allyl phenyl ether was necessary for the cycloaddition reaction to obey first order kinetics. In addition, Schubert *et al.* have reported a synthetic procedure for the preparation of well–defined multifunctional graft copolymers using a post modification approach of

pentafluorostyrene units with amino terpyridine moieties.[37] This reaction requires relatively short reaction times (20 min); however, an excess (2.5 eq.) of the amino compound and the use of microwave irradiation at elevated temperatures were required.[38,39]

In this chapter, we describe an efficient route for the synthesis of well–defined glycopolymers by combining a controlled radical polymerization technique and a metal–free "click" reaction between thiol–glucose and pentafluorostyrene units. The overall synthetic procedure is depicted in Scheme 6.1. The initial step of this route is the preparation of St and PFS containing homo, block and random polymers using a ß–phosphonylated alkoxyamine initiator (Bloc Builder). The second step is the nucleophilic substitution reaction between the pentafluorophenyl groups and thiol-glucose. The final step is the deacetylation of the glucose units to obtain the glycopolymers with narrow polydispersity indices. Moreover, in this chapter special attention is given to provide an overview of metal–free "click" reactions to evaluate their success in fulfilling the requirements of "click" chemistry.

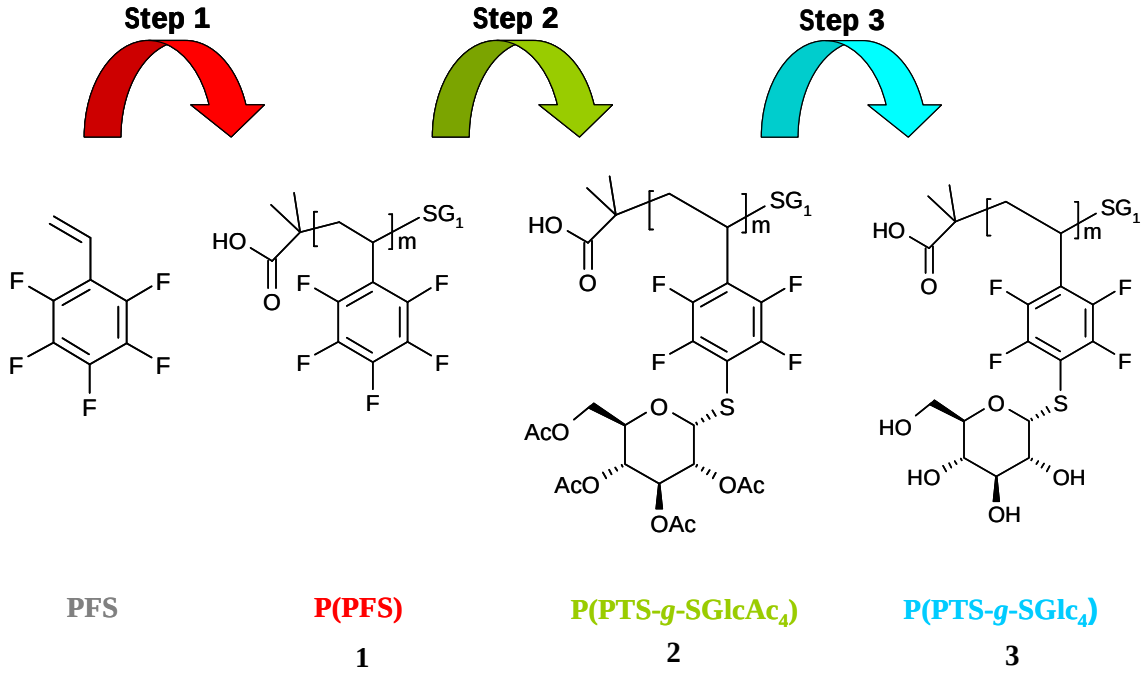

Scheme 6.1. Schematic representation of the synthesis of glycopolymers via combination of NMP and "click" chemistry techniques.

6.2 Metal catalyst–free "click" reactions

The overwhelming success of "click" chemistry encouraged researchers to investigate alternative "spring–loaded" chemical reactions to be employed in different fields of chemistry. Initially, the copper(I) catalyzed azide–alkyne cycloaddition was the sole representative of "click" chemistry. In recent years, metal–free [3+2] cycloaddition reactions, Diels–Alder reactions, and thiol–alkene radical addition reactions stepped forward as metal–

free click reactions based on their easy synthetic procedures, high yields, wide applicability as well as physiological compatibility. These and more alternative "click" reactions (Table 6.1) expand the toolbox of synthetic chemists to accomplish the synthesis of not only small organic compounds but also tailor–made macromolecules and bioconjugates.

To aid the forthcoming discussion of the different metal–free "click" reactions, the requirements for "click" chemistry that have been defined by Sharpless and his co–workers are listed as follows:[25] should be modular and wide in scope; should be highly efficient and give high yields; preferably, no or inoffensive side products; should be stereospecific; readily available starting materials and reagents; preferably, no solvent or a solvent that is benign; should require no or only simple purification techniques.

6.2.1. Copper–free [3+2] cycloaddition reactions with azides

The preparation of a wide range of azides is well–studied in organic chemistry and in recent years azides obtained increased attention due to their potential use in CuAAC "click" reactions. The easy access to azide containing compounds makes them good candidates for "click" reactions. However, in the absence of metal–catalyst they do not react easily with alkynes since they are usually poor 1,3–dipolar acceptors. Therefore, different approaches have been developed to increase the reactivity of the alkyne groups allowing metal–free azide–alkyne cycloadditions under mild conditions.

6.2.1.1 Reaction of azides and substituted cyclooctyne

Bertozzi and her co–workers have reacted azides with cyclooctyne derivatives and called this reaction strain promoted [3+2] azide alkyne cycloaddition (SPAAC).[28,40 −44] This reaction was developed from the initial work of Wittig and Krebs.[45,46] The SPAAC reactions exhibited relatively slow reaction rates with the first generation of cyclooctyne in comparison to the corresponding CuAAC reactions. Therefore, mono–fluorinated (2nd generation) and difluorinated (3rd generation) derivatives of cyclooctynes have been designed to decrease the LUMO level of the alkyne by introducing electron–withdrawing groups to its neighbor resulting in increased second order rate constants.[47] The relative second–order rate constants ($M^{-1}s^{-1}$) of cyclooctynes were improved with higher generations (see Scheme 1.5).

The SPAAC reaction fulfils many requirements of "click" chemistry. However, the demanding organic synthesis of cyclooctyne derivatives needs to be improved in order to be used not only in chemical biology but also in the other fields of chemistry. Alternatively, the commercial availability of the third generation of the cyclooctyne would significantly improve the scope and applicability of this reaction.

Table 6.1. Overview of "click" reactions that proceed in the absence of a metal–catalyst in comparison to the CuAAC (0).

	Reagent A	Reagent B	Mechanism	Notes on reaction*	Reference
0	Azide	Alkyne	Cu–catalyzed [3+2] azide–alkyne cycloaddition (CuAAC)	2 h at 60 °C in H_2O	[48]
1	Azide	Cyclooctyne	Strain promoted [3+2] azide–alkyne cyclo-addition (SPAAC)	1 h at RT	[28,40–47]
2	Azide	Activated–alkyne	[3+2] Huisgen cycloaddition	4 h at 50 °C	[49]
3	Azide	Electron deficient alkyne	[3+2] Cycloaddittion	12 h at RT in H_2O	[50]
4	Azide	Aryne	[3+2] Cycloaddittion	4 h at RT in THF with crown ether or 24 h at RT in CH_3CN	[51,52]
5	Tetrazine	Alkene	Diels–Alder Retro–[4+2] cycloaddition	40 min at 25 °C (100% yield) N_2 is the only byproduct	[80–82]
6	Tetrazole	Alkene	1,3–dipolar cycloaddition	Few min UV irradiation and then overnight at 4 °C.	[36,83]
7	Dithioester	Diene	Hetero Diels–Alder cycloaddition	10 min at RT	[87]
8	Anthracene	Maleimide	[4+2] Diels–Alder reaction	2 days at toluene reflux temperature	[84]
9	Thiol	Alkene	Radical addition (thio–click)	30 min UV (quant. conv.) or 24 h UV irradiation (>96%)	[31,33,35,56, 57,59,60]
10	Thiol	Enone	Michael addition	24 h at RT in CH_3CN	[66]
11	Thiol	Maleimide	Michael addition	1 h at 40 °C in THF or 16 h at RT in dioxane	[61–65]
12	Thiol	*para*–fluoro	Nucleophilic substitution	Overnight at RT in DMF or 60 min at 40 °C in DMF	[69]
13	Amine	*para*–fluoro	Nucleophilic substitution	20 min MW at 95 °C in NMP as solvent	[37]

[*] RT = room temperature, DMF = *N,N*–dimethylformamide, NMP = *N*–methyl pyrrolidone, THF = tetrahydrofuran, CH_3CN = Acetonitrile.

6.2.1.2. Reaction of azide and activated alkynes

Sarkar *et al.* reported a non–catalyzed "click" reaction based on the higher reactivity rates of activated alkynes.[49] The authors have prepared glass and silicon surfaces with azido functionalized self–assembled monolayers (SAM). The functional surfaces were reacted with the Fisher carbene complex **4** (phenylacetyl–enylethoxycarbene–pentacarbonyl tungsten) under argon atmosphere (stirring at 50 °C for 4 hours, Scheme 6.2). The detailed characterizations of the surfaces were performed by ellipsometry, FT–IR, ATR–IR, AFM and contact angle measurements. Moreover, the Fisher carbene "clicked" SAM was tested for a nucleophilic substitution with a pyrene based fluorescent probe.

Although this reaction needs to be investigated in more details with regard to, *e.g.*, yields and modularity, it represents a promising example for a non–catalyzed "click" reaction. However, the tungsten activation of the alkyne prevents this reaction to be classified as metal–

free "click" reaction. Even though the accessibility of the activated alkynes is easier in comparison to cyclooctyne derivatives, other activation methods have to be developed to make it suitable for application in biological systems.

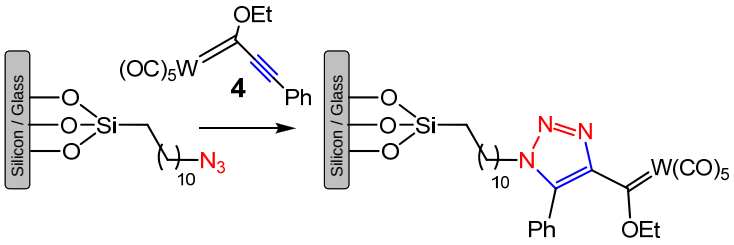

Scheme 6.2. Schematic representation of the copper–free "click" reaction between an azido SAM and an alkynyl Fisher carbene complex.

6.2.1.3. Reaction of azide and electron–deficient alkynes

As shown in the previous examples, activated alkynes can undergo cycloaddition reactions with azides in the absence of any metal catalyst. In 2004, Ju *et al.* have reported a very simple synthetic protocol for the 1,3–dipolar cycloaddition of azides with electron–deficient alkynes.[50] A series of alkynes with at least one neighboring electron–withdrawing group were investigated for the "click" reaction to 5–azidovalerate in water at room temperature (Scheme 6.3). The obtained yields were in the range of 67 to 94%. The authors have extended this "click" reaction to couple an azido–DNA molecule and successfully presented a potential method for introducing functional groups to DNA under physiological conditions

The promising results of Ju *et al.* might serve as basis to extend this metal–free "click" reaction to other fields of chemistry. However, the yields of the described "click" reaction should be improved since this represents the most critical criteria of "click" chemistry. In addition, the modularity and availability of the alkyne starting materials have to be evaluated as well as the sterospecificity.

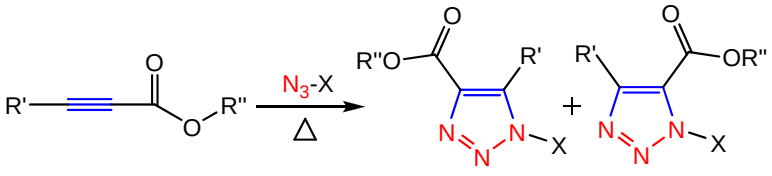

Scheme 6.3. Schematic representation of the "click" reaction between azides and electron–deficient alkynes (R` = H or CH_3 or COO(Et), R`` = Me or Et, and N_3–X = 5–azido–valerate or 5'–azido DNA).

6.2.1.4. Reaction of azides and arynes

Larock and his co–workers developed a facile, efficient and general method for the synthesis of substituted, functionalized benzotriazoles by the 1,3–dipolar cycloaddition of

benzynes with azides under very mild reaction conditions.[51] They have named this reaction "benzyne click chemistry" (Scheme 6.4). The optimized reaction conditions for benzyl azide and *o*–(trimethylsilyl)phenyl triflate **5** requires CsF as a fluoride source and acetonitrile as solvent. The reaction was performed at room temperature for 18 hours and the isolated yield was found to be 76%. The reaction scope was extended by testing various benzyne precursors and azides.

A similar study was reported by Feringa *et al.* reporting that the isolated yields of this reaction could be improved by the use of a complementary crown ether.[52] Besides, the required reaction periods were also significantly decreased from several hours to less than two hours.

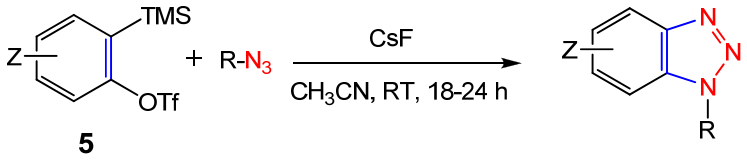

Scheme 6.4. Schematic representation for an example of "benzyne click chemistry".

The model reactions performed in both reports accomplish the main requirements of "click" chemistry. The improved reaction can be performed in short reaction times, at room temperature, under air atmosphere and results in a single product in good yields. In contrast, a limitation for this chemistry was reported that azides bearing electron–withdrawing groups directly attached to the azide moiety do not react under those conditions. Besides, a fluorine source is necessary to conduct this reaction and the availability of the required multifunctional aromatic starting materials might be questionable.

6.2.2. Thiol based "click" reactions

Thiols have been used in diverse chemical reactions for well over a century.[53,54] Initially, thiol–ene chemistry was used in the preparation of well–defined films or networks. However, there were some practical considerations regarding the utilized thiols such as odor, the storage and shelf life stability. Most of these challenges have been solved in our days by improved synthetic methods for the synthesis of the monomers; various efficient stabilizers have been developed.[55] Thus, there is a comprehensive database in the literature on the reaction pathways and kinetics of thiols. Besides, the accessibility of the wide range of thiol compounds is relatively effortless. These features enable thiols to be good candidates for "click" reactions.[34]

6.2.2.1. Radical addition reaction between thiols and alkenes

The free–radical addition of thiols onto double bonds is a highly efficient tool used for polymerizations, curing reactions, and for the modification of polymers.[35,56–58] Schlaad and his co–workers demonstrated a post–polymerization modification of a well–defined poly[2–(3–butenyl)–2–oxazoline], which was polymerized by a living cationic ring opening polymerization (CROP) process. Various mercaptans i.e. fluorinated thiols, acetylated glucose thiols and dihydroxy functionalized thiols were used as model reactions (Scheme 6.5). These "thio–click" reactions were performed under inert atmosphere and exposure to UV light for 24 hours.[31] Furthermore, Schlaad *et al.* performed the "thio–click" reaction for poly(butadiene) modification under direct sunlight, since the thiol–ene photoaddition reaction can proceed at near–visible wavelengths (λ = 365 to 405 nm).[59]

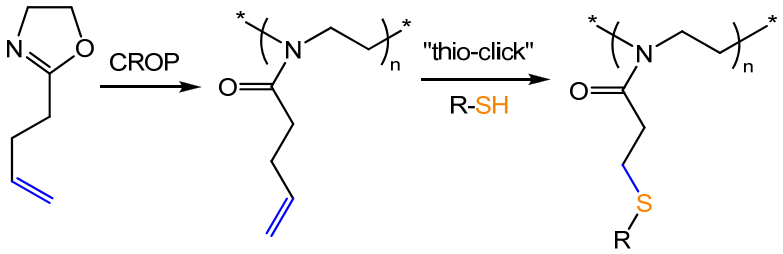

Scheme 6.5. Schematic representation of the synthesis and "thio–click" modification of poly[2–(3–butenyl)–2–oxazoline].

Hawker *et al.* reported a robust, efficient, and orthogonal synthesis of 4th generation dendrimers using thiol–ene "click" reactions.[33] The solvent free reaction between alkene **6** and thiol **7** was performed at room temperature, without deoxygenation, by irradiation for 30 min with a hand–held UV–lamp (λ = 365 nm) (Scheme 6.6). Additionally, trace amounts of photoinitiator **8** were used to increase the radical concentration and, thus, the reaction rate. The first generation of dendrimer **9** is shown in Scheme 6.5 and the further generations were synthesized in the same manner with purification by simple precipitation into diethyl ether in between each step.

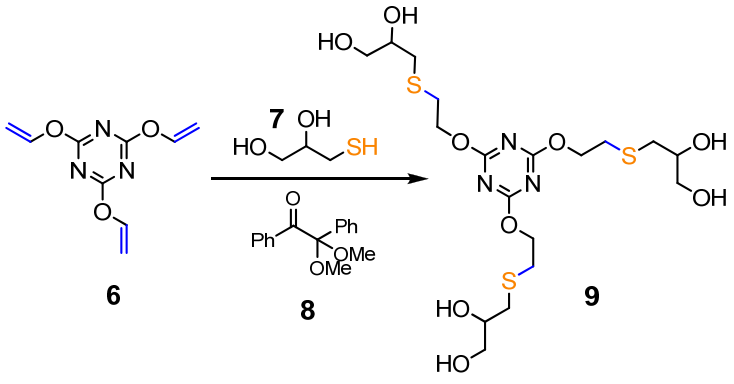

Scheme 6.6. Schematic representation of the thiol–ene "click" chemistry for the synthesis of a [G1] dendrimer.

Hoyle and Lowe *et al.* demonstrated a convergent synthesis of 3–arm star polymers by a combination of the reversible addition–fragmentation chain transfer (RAFT) polymerization and the thiol–ene "click" reaction. Terminal thiol containing polymers were synthesized by RAFT polymerization and the chains were coupled to trimethylolpropane triacrylate to form star–shaped polymers.[60]

The thiol–ene chemistry regained its deserved attention in the last two years, because of the simplicity, high reactivity, and broad variety of available reagents. Besides, the reaction can be conducted at ambient conditions in relatively short reaction times. Thiol–ene "click" reactions have indeed a bright future for the synthesis of not only tailor–made macromolecules but also small organic molecules and bioconjugates.

6.2.2.2. Michael addition reactions of thiols

Thiol–terminated polymers can be easily prepared by RAFT polymerization as mentioned in the previous section. This polymerization technique is well established and various chain transfer agents are available for most kinds of monomers to yield well–defined functional polymers.[61,62]

Dove *et al.* reported metal free thiol–maleimide "click" reactions as a mild functionalization strategy for degradable polymers.[63,64] Moreover, Sumerlin and his co–workers demonstrated a successful synthesis of block copolymers by the use of Michael additions or Diels–Alder reactions on polymers prepared by RAFT technique.[65] As illustrated in Scheme 6.7, the polymerization and following "click" reactions were all performed in the absence of any metal–catalyst. Michael addition reaction of maleimide terminated poly(*N*–isopropylacrylamide) with thiol terminated polystyrene (PS–SH) was conducted under inert atmosphere and stirred for 24 hours at room temperature. The excess of PS–SH was removed from the reaction mixture by immobilization onto an insoluble iodoacetate–functionalized support, which represents an elegant method to avoid chromatographic purification steps. These model reactions confirm the potential of this methodology to combine RAFT synthesized thiol–terminated polymers with a variety of other macromolecular thiols.

Another "click" chemistry approach was reported by Nguyen *et al.* based on the Michael addition of thiosugar to a highly reactive enone.[66] This base catalyzed reaction was conducted in 24 hours at room temperature using acetonitrile as solvent. The detailed ^{1}H–NMR characterization of the product revealed a completely stereoselective reaction with a yield of 94%.

Even though the reaction conditions employed in Michael additions do not (yet) meet the stringent criteria of "click" chemistry, these reactions provide a modular approach for the

preparation of a variety of functional telechelics and block copolymers synthesized by the RAFT technique. As such, Michael additions have the potential to become "click" reactions based on future developments.

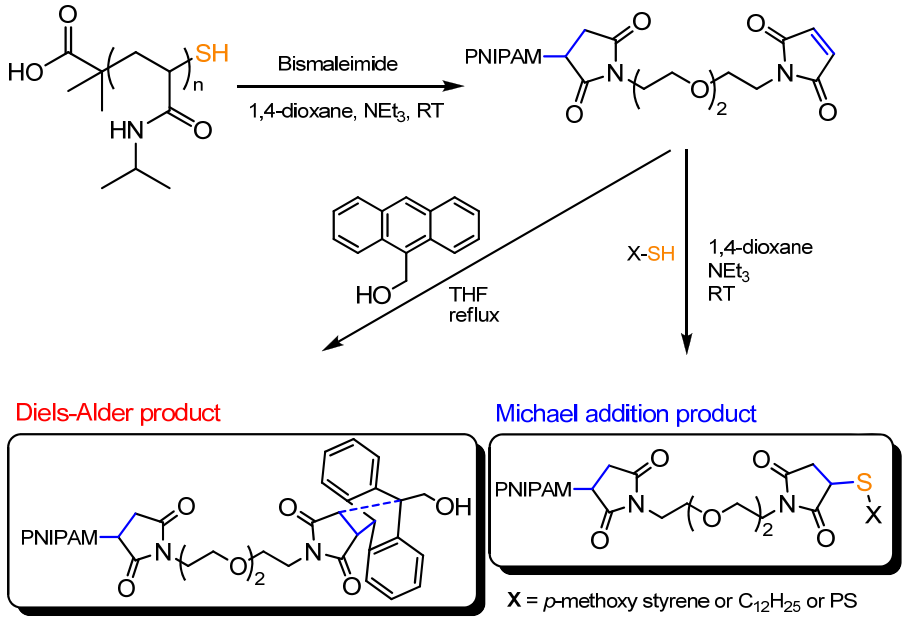

Scheme 6.7. Schematic representation of the chain end modification of PNIPAM–SH with bismaleimide and subsequent Michael addition or Diels–Alder reaction.

6.2.2.3. Nucleophilic substitution reactions of thiols and amines

It is well–known in organic chemistry that the labile para–fluorine substituents of pentafluorophenyl (C_6F_5) groups can undergo nucleophilic substitution reactions by primary amino groups and thiols.[38,39,67] Mansuy *et al.* described a procedure for the preparation of functionalized polyhalogenated porphyrins in one step and high yields by selective substitution of the para–fluoro substituents of the C_6F_5 groups of meso–*tetra*–(pentafluorophenyl)porphyrin by various nuchleophiles.[68]

Hoogenboom and Schubert *et al.* demonstrated the application of this chemistry for the functionalization of macromolecules to create well–defined multifunctional graft polymers (Scheme 6.8).[37] The reaction was performed in a microwave synthesizer using *N*–methyl pyrrolidone as solvent. The solution was reacted at 95 °C for 20 minutes using 5–amino–pentanol or α–amine–ω–hydroxy polyethyleneglycol as primary amines. This approach provides the synthesis of graft polymers by the "grafting onto" method. Besides, side chain functionalization of the polymers, *i.e.* by 5–aminopentanol, enables the synthesis of graft polymers by the "grafting from" method as was demonstrated by the ring opening polymerization of L–lactide from the hydroxyl groups that are "clicked" onto the side chain.

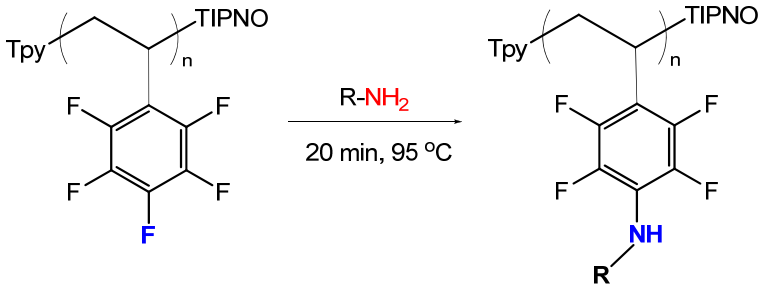

Scheme 6.8. Schematic representation of the para–fluoro–amine "click" reaction on a terpyridine funtionalized well–defined copolymer of styrene and pentafluorostyrene ($R–NH_2$ represents 5–aminopentanol or α–amine–ω–hydroxy polyethyleneglycol).

Synthesis of well–defined glycopolymers is often demanding since it requires mild reaction conditions to prevent degradation. "Grafting onto" a well–defined polymer can be preferred in case the monomeric units bear functional groups such as alkyne or C_6F_5 on which sugar moieties can be "clicked". However, the CuAAC reaction requires a copper catalyst and the purification of the glycopolymers becomes more demanding.[21,26] Therefore, metal–catalyst free "click" chemistry is a valuable tool for the synthesis of glycopolymers. As illustrated in Scheme 6.9, well–defined copolymers of styrene and pentafluorostyrene (PFS) can be functionalized by a thiol–glucose at room temperature in the presence of triethylamine as base and *N,N*–dimethylformamide as solvent. The kinetics of the substitution reaction was monitored by measuring ^{19}F–NMR spectra at 40 °C and quantitative conversions were observed in less than one hour.[69]

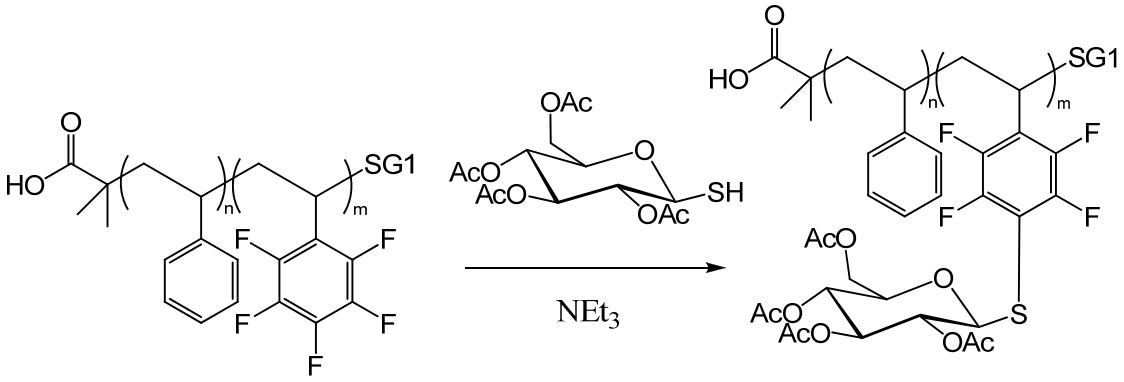

Scheme 6.9. Schematic representation of the synthesis of glycopolymers via the para–fluoro–thiol "click" reaction.

The versatility and efficiency of the amine or thiol substitution to the *para* position of C_6F_5 have been demonstrated to comply with most of the "click" chemistry requirements. In addition, a wide range of primary amines and thiols are available in the databases. However, the accessibility of C_6F_5 groups is rather limited obstructing the scope and modularity of the reaction.

6.2.3. Diels–Alder reactions

Diels–Alder reactions were first documented in 1928.[70] They are amongst the most fascinating organic reactions, both in terms of synthetic potential and reaction mechanism. Diels–Alder reactions involve the simultaneous formation and breakage of carbon–carbon bonds.[71 –74] This reaction requires very little energy, thus can be employed even below room temperature. There are several reports based on Diels–Alder "click" chemistry[75 –79] and here we highlight some recently published outstanding examples for bioconjugates and macromolecules.

6.2.3.1. Reaction of tetrazines with alkenes

Fox and his co–workers reported a bio–orthogonal reaction that proceeds with high reaction rates without the need for a catalyst.[80] The procedure involves the inverse electron demand Diels–Alder reaction of tetrazines with cyclooctynes that produces N_2 as the only byproduct upon subsequent retro–[4+2] cycloaddition. As illustrated in Scheme 6.10, trans–cyclooctyne **10** and tetrazine **11** reacted for 40 minutes at 25 °C (micromolar concentrations, 5×10^{-6} M) in quantitative yields.[81] Besides, the reaction preserves its high reactivity in organic solvents, in water and even in cell media. In addition, the synthesis of *trans*–cyclooctyne and dipyridyl–tetrazine with functional groups was demonstrated, which broadens the scope of the retro–Diels–Alder "click" reaction.

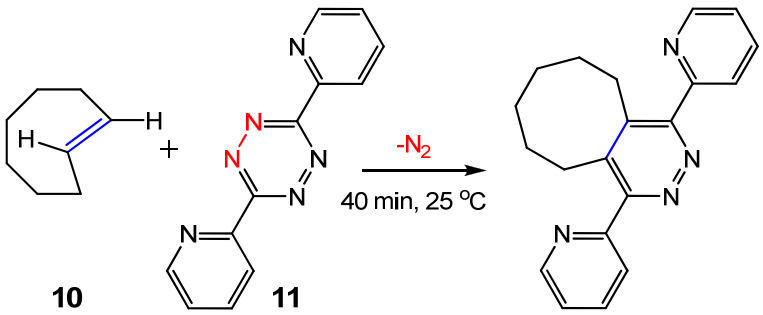

Scheme 6.10. Schematic representation of the [4+2] retro–Diels–Alder reaction of trans–cyclooctyne and tetrazine.

Shortly after this report, Hilderbrand *et al.* demonstrated tetrazine based cycloadditions for pretargeted live cell imaging.[82] The reaction of norbornene and tetrazine revealed multiple isomeric dihydropyridazines in the LC/MS chromatogram since both norbornene and tetrazine are asymmetric compounds. The overall yield was reported to be larger than 93%. A similar approach using tetrazoles has been reported by Lin *et al.*[36] As shown in Scheme 6.11 (*bottom*), a genetically encoded alkene–containing protein could be selectively functionalized using a photo–activated, nitrile imine mediated 1,3–dipolar

cycloaddition reaction in Esherichia coli. Practically, BL21(DE3) cells expressing either wt–Z or O–allyl–tyrosine containing Z–domain proteins **12** were suspended in the PBS buffer containing 5% glycerol and 100 μM tetrazole. Following the incubation at 37 °C for 30 min, the cell suspensions were irradiated with UV light at 302 nm for 4 min. The bacterial cells were incubated at 4 °C overnight to allow the cycloaddition reaction to yield pyrazoline–Z **13** in quantitative yields. Consequently, this simple, straightforward reaction is called "photoclick" chemistry and the reaction scheme is illustrated in Scheme 6.11 (*top*).[83]

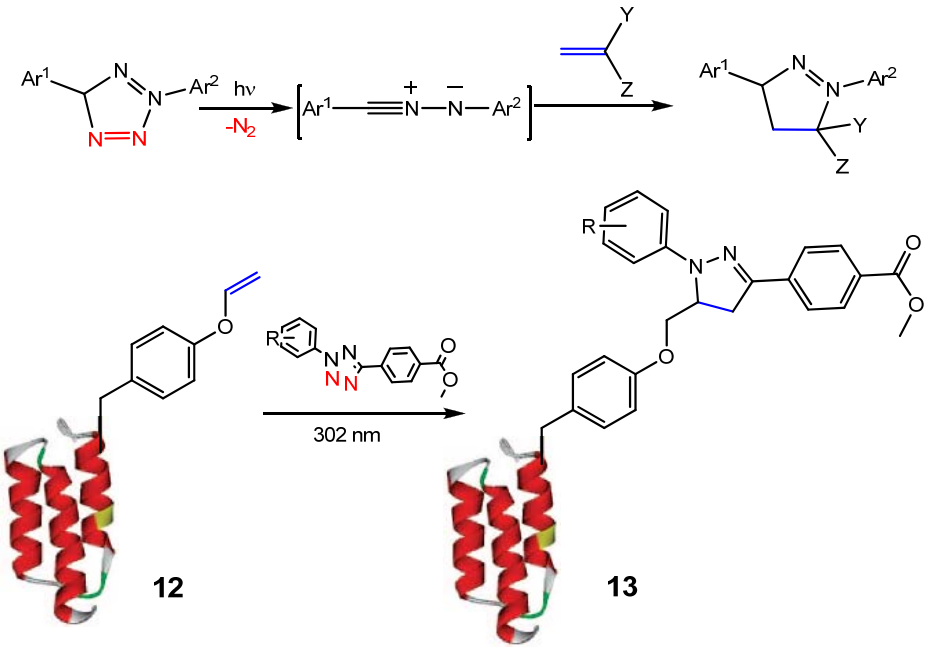

Scheme 6.11. *Top*: Schematic representation of the photoactivated 1,3–dipolar cycloaddition reaction between a 2,5–diaryl tetrazole and a substituted alkene dipolarophile. *Bottom*: Schematic representation of the selective functionalization of Z–domain protein encoding O–allyl–tyrosine via a photoclick reaction.

6.2.3.2. Reaction of anthracene and maleimide

Tunca and Hizal *et al.* demonstrated the preparation of 3–arm star polymers via Diels–Alder reactions.[84] They have used furan protected maleimide end functionalized polymers **15** (poly(ethyleneglycol), poly(methyl methacrylate), and poly(*tert*–butyl acrylate)) and the trianthracene functional coupling agent **14**. The reaction was conducted in toluene under reflux for 48 hours (Scheme 6.12). Based on the detailed SEC characterization, the Diels–Alder "click" reaction was found to be as successful as the CuAAC for the construction of star–shaped polymers by the arm–first method. The same authors demonstrated that a number of other copolymer architectures was accessible by Diels–Alder "click" chemistry, sometimes in combination with CuAAC, exemplifying the wide scope and modularity of this "click" reaction.[75–79]

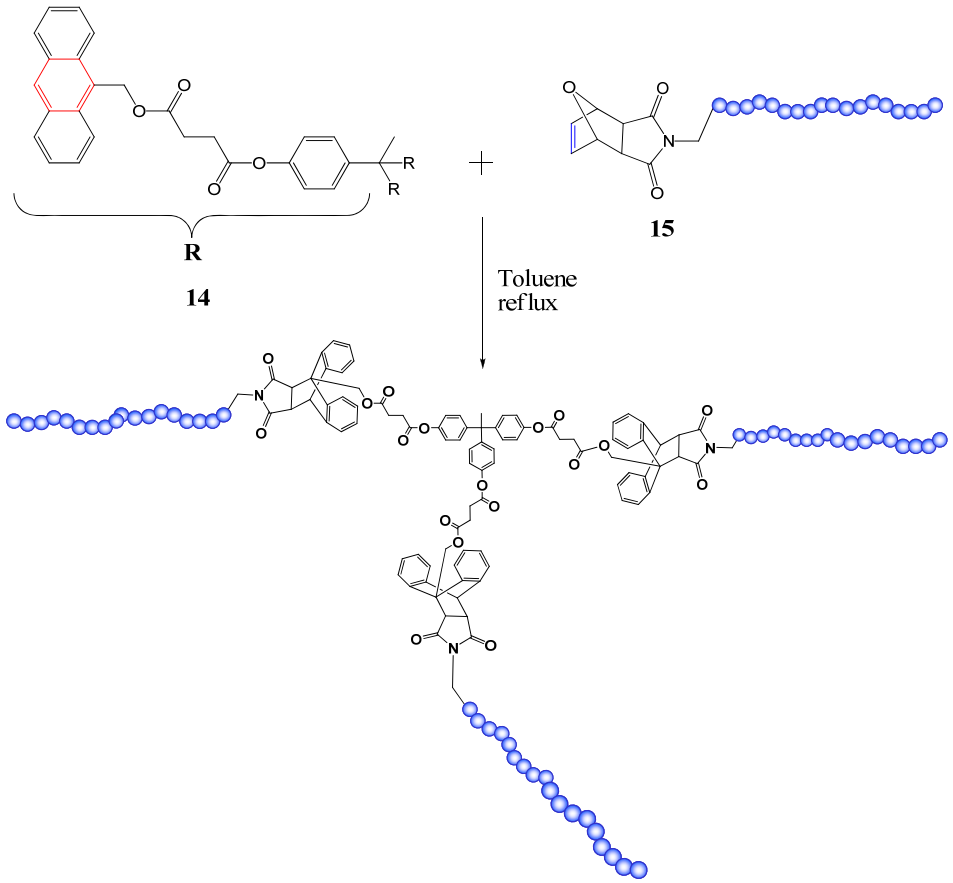

Scheme 6.12. Schematic representation of the Diels–Alder "click" reaction for the preparation of star polymers.

6.2.3.3. Reaction of dithioester and diene

Barner–Kowollik, Stenzel and their co–workers recently reported a convenient conjugation tool to access complex macromolecular systems.[85,86] Therefore, the RAFT polymerization of styrene was followed by a hetero–Diels–Alder cycloaddition reaction of the RAFT agent to yield star–shaped polymers. By using an appropriate coupling agent and TFA as catalyst, 2–arm, 3–arm and 4–arm star polymers were synthesized with yields of 91, 86, and 82%, respectively. Moreover, the complete cleavage of the arms was achieved by treating the star polymers at 160 °C for 24 hours. This approach might be the inspiration of developing "reversible click reactions" in the future. Very recently, the same authors reported ultrafast click conjugation of macromolecular building blocks at ambient temperature in just a few minutes in the absence of a catalyst by Diels-Alder reaction of the more reactive cyclopentadiene with the RAFT agent (Scheme 6.13).[87] This click reaction is extremely efficient and allows the synthesis of block copolymers by macromolecular coupling just by shaking the reaction flask at room temperature.

There is no doubt that Diels–Alder reactions easily fulfill many requirements of "click" chemistry. However, in particular for macromolecular systems, long reaction times and high reaction temperatures might be the limitation of this technique. It was noted by

Tunca and Hizal that there could be some difficulties to access high molar mass star polymers because of steric hindrance caused by already "clicked" arms, which is equally true for the copper(I) catalyzed azide–alkyne cycloadditions.[84] Nevertheless, the use of electron deficient dithioesters in combination with cyclopentadienes resulted in a dramatic reaction rate improvement in hetero–Diels–Alder reactions.[87] Therefore, this coupling procedure does qualify as "click" reaction and should be seriously considered for the preparation of not only block copolymers but also bio–conjugates.

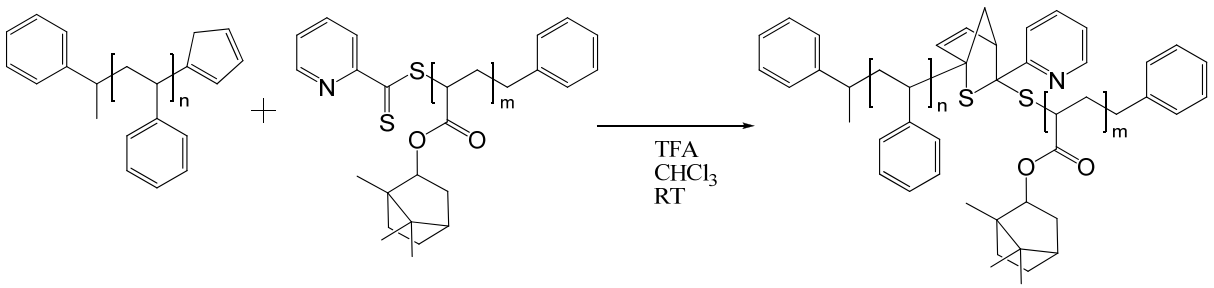

Scheme 6.13. Schematic representation of the selected example of the formation of the poly(styrene–*b*–*iso* bornyl acrylate) block copolymer by ultrafast HDA click chemistry.

6.3 Synthesis of fluorinated copolymers

The NMP conditions of St and *tert*–butyl acrylate have been optimized in our previous studies and as discussed in Chapter 2.[88] Confirming our results, Maric and coworkers have reported that there is no effect of additional free nitroxide on the control over the polymerization of St.[89] Accordingly, we have performed the polymerization of PFS without adding any free nitroxide (SG1) and used similar reaction conditions to the NMP of St. However, in this study all reactions were carried out in an oil bath instead of an automated parallel synthesizer.[90-92] The data of the synthesized homopolymers and random copolymers are listed in Table 6.2. Besides, the homopolymer of PFS was synthesized in a relatively large scale and **H1** was used further for the glycopolymer synthesis. In addition, we have prepared a series of random copolymers of St and PFS with different ratios varying from 90:10 to 50:50, respectively. According to the SEC results, all synthesized polymers exhibited narrow molar mass distributions. The monomer conversions were determined by either GC or ^{1}H–NMR spectroscopy. Moreover, the calculated experimental copolymer ratios of random copolymers were found to be very close to the feed ratios.

Even though, the measured $M_{n,SEC}$ values of the random copolymers were found to be close to the theoretical values, PFS exhibits a slightly different hydrodynamic volume than St in the SEC eluent. The solubility behavior of PFS containing polymers needs to be

investigated further with a special focus on the micellization behavior of its block copolymers.

Table 6.2. Characterization of the synthesized homopolymers and random copolymers

Run	$[St]_0$ /$[I]_0$	$[PFS]_0$ /$[I]_0$	Reac. time [h]	Conv. St [%]	Conv. PFS [%]	$M_{n,theo}$ [Da]	$M_{n,SEC}$[b] [Da]	M_w/M_n[b]	Structure[c]
H1	–	50	5	–	78	7,950	3,500	1.03	PFS_{16}
H2[a]	100	–	5.5	70	–	7,670	5,200	1.08	PS_{46}
H3[a]	200	–	6.5	70	–	14,600	12,500	1.11	PS_{116}
R1	25	25	5	51	49	3,820	3,120	1.08	PFS_{12}–*r*–PS_{12}
R2	45	5	5	36	69	2,750	3,400	1.06	PFS_3–*r*–PS_{16}
R3	50	50	5	58	58	9,000	7,800	1.07	PFS_{29}–*r*–PS_{29}
R4	75	25	5	38	59	6,200	8,650	1.09	PFS_{15}–*r*–PS_{29}
R5	90	10	5	48	74	6,300	6,450	1.09	PFS_8–*r*–PS_{44}

[a] The data of **H2** and **H3** are taken from reference 88. [b] calculated according to PS standards using chloroform:isopropanol:triethylamine (94:4:2) as eluent. [c] Calculated from the conversion.

MALDI–TOF MS has become a fundamental characterization tool not only for the detection of end groups but also for the molar mass determination of polymers.[93] However, this technique has some limitations depending on the chemical structure of the polymer. Most importantly, the molar mass of the polymers should be below a certain mass value, which differs according to the ionization and desorption capability of the macromolecules. For instance, PS is known as an easily ionizable polymer and, on the contrary, fluorinated polymers are very difficult to ionize with available matrices and salts. Another consideration is that labile end groups, *i.e.* nitroxide, dithioesters or bromo, are usually cleaved off during the MALDI–TOF MS measurement process. Several unexpected distributions in the obtained spectrum are results of this instability of the end groups under the high energy of the laser beam. Nevertheless, we have succeeded to obtain relatively good resolved spectra for the PFS containing random copolymer **R2**, as depicted in Figure 6.1. Although the baseline is rather noisy, it was possible to determine seven peaks that correspond to different ratios of St and PFS monomers in copolymer **R2**.

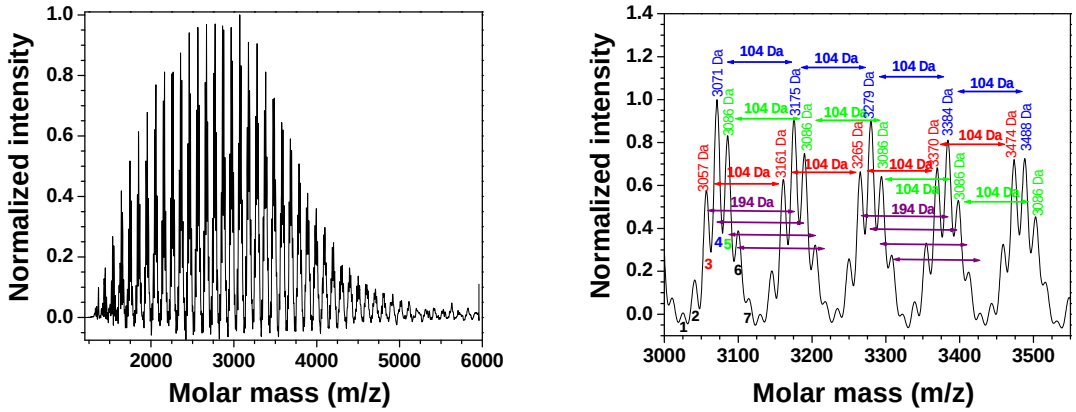

Figure 6.1. Left: MALDI–TOF–MS measurement of **R2**. Right: A zoom into the region of 3,000 to 3,550 Da.

Furthermore, we have performed a kinetic experiment for the SG1 mediated random copolymerization of St and PFS with a monomer to initiator ratio of 45 to 5, respectively. The monomer conversions were followed by GC and the molar mass values were determined by SEC in chloroform as eluent. As shown in Figure 6.2, the $M_{n,SEC}$ values increased with increasing monomer conversions, which is an indication of a "living" polymerization process. Besides, linear relationships were obtained for both monomers in the semi–logarithmic kinetic plot. Fortunately, the polydispersity index values of the polymers did not increase even at higher monomer conversions and remained below 1.15 in all cases.

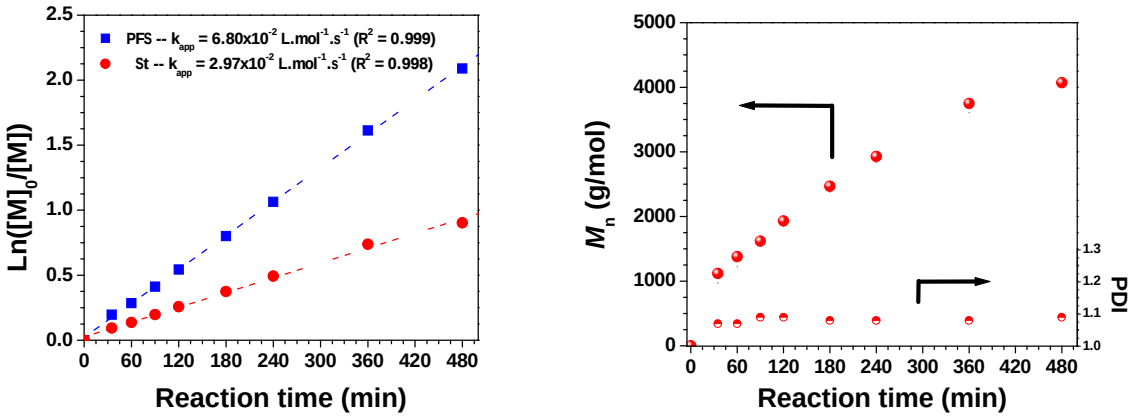

Figure 6.2. *Left*: Semi–logarithmic kinetic plot for the copolymerization of St and PFS. *Right*: $M_{n,SEC}$ and PDI values *versus* reaction time plot of the synthesized copolymers.

Moreover, block copolymers of St and PFS with different block orders could successfully be prepared. The results are listed in Table 6.3. Two different macroinitiator to monomer ratios were employed to obtain PS–*b*–PFS copolymers with different compositions. Both block copolymers, **B2** and **B3**, were obtained with relatively low PDI values. In

addition, we used **H1** as a macroinitiator to have first a PFS containing block and then a relatively long styrene block to synthesize PPFS–*b*–PS.

Table 6.3. Characterization of the synthesized block copolymers

Run	Macroini.	[M]/[MI]	Conv. [%]	$M_{n,theo}$ [Da]	$M_{n,SEC}$ [Da]	M_w/M_n	Structure
B1	$PPFS_{16}$ (**H1**)	200/1	66	17,300	17,800	1.21	PFS_{16}–*b*–PS_{137}
B2	PS_{46} (**H2**)	50/1	76	12,600	7,100	1.16	PS_{46}–*b*–PFS_{10}
B3	PS_{54}	100/1	52	16,000	12,750	1.18	PS_{54}–*b*–PFS_{35}

The characterization of these block copolymers was performed by means of SEC and MALDI–TOF MS. The obtained spectra for **B1** are shown in Figure 6.3, as a representative example. There is a clear shift observed in the SEC spectrum with a slight amount of non–functionalized macroinitiator left. Besides, there is a small shoulder appearing at the lower elution volume indicating the occurrence of chain coupling reaction, which is the most favored side reaction in the case of styrene polymerization.

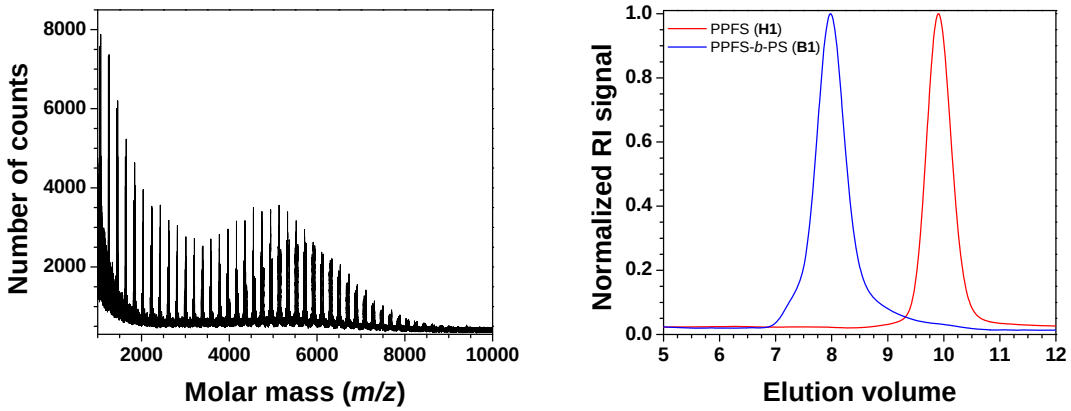

Figure 6.3. *Left*: MALDI–TOF MS spectrum of the PPFS macroinitiator **H1**. *Right*: SEC traces of macroinitiator **H1** and block copolymer **B1**.

6.4 Kinetics of thiol–*para* fluoro "click" reaction

Thiols are well–known as soft nucleophiles in comparison to primary amines or alcohols, hence displaying higher reactivity in nucleophilic substitution reactions.[67] Besides, this reaction occurs with quantitative yields under ambient conditions without any need for a metal catalyst. Therefore, we have dissolved the PPFS homopolymer **H1** (1 equivalent with respect to the PFS units) and 2,3,4,6–tetra–*O*–acetyl–1–thio–ß–D–glucopyranose (SH–$GlcAc_4$) (1.2 eq.) in DMF and reacted them at room temperature for 4 hours in the presence of

triethylamine (3 eq.) as a base. Afterwards, the solution was precipitated into methanol to result in a white precipitate with an isolated yield of 93%. ^{1}H–NMR spectra of the homopolymer **H1**, the acetylated glycopolymer (PTFS–*g*–SGlcAc$_4$) and also the deprotected glycopolymer are depicted in Figure 6.4. The substitution of glucose units to the polymer backbone is clearly seen in these spectra. Besides, the hydroxy protons of the deprotected polymer became visible following the deacetylation reaction. The deacetylation reaction was also followed by measuring ^{13}C–NMR spectra to detect the disappearance of the peaks corresponding to the acetyl carbon atoms.

In addition, we have measured ^{19}F–NMR spectra of the polymers to follow the efficiency and selectivity of the thiol–*para* fluoro "click" reaction. As illustrated in Figure 6.5, there are three peaks visible in the starting homopolymer, which correspond to fluoro atoms at the *–ortho*, *–meta* and *–para* positions. Since ^{19}F–NMR spectroscopy provides quantitative results, it was possible to calculate the conversion of the "click" reaction from the integrals of the *–para* fluoro atoms of **H1**, and, consequently, the appearing peak of the *–ortho* fluoro of the product. Besides, the top spectrum (Figure 6.5, *top*) demonstrates the stability of the formed thiol–glucose and tetrafluorostyrene bond under deacetylation conditions.

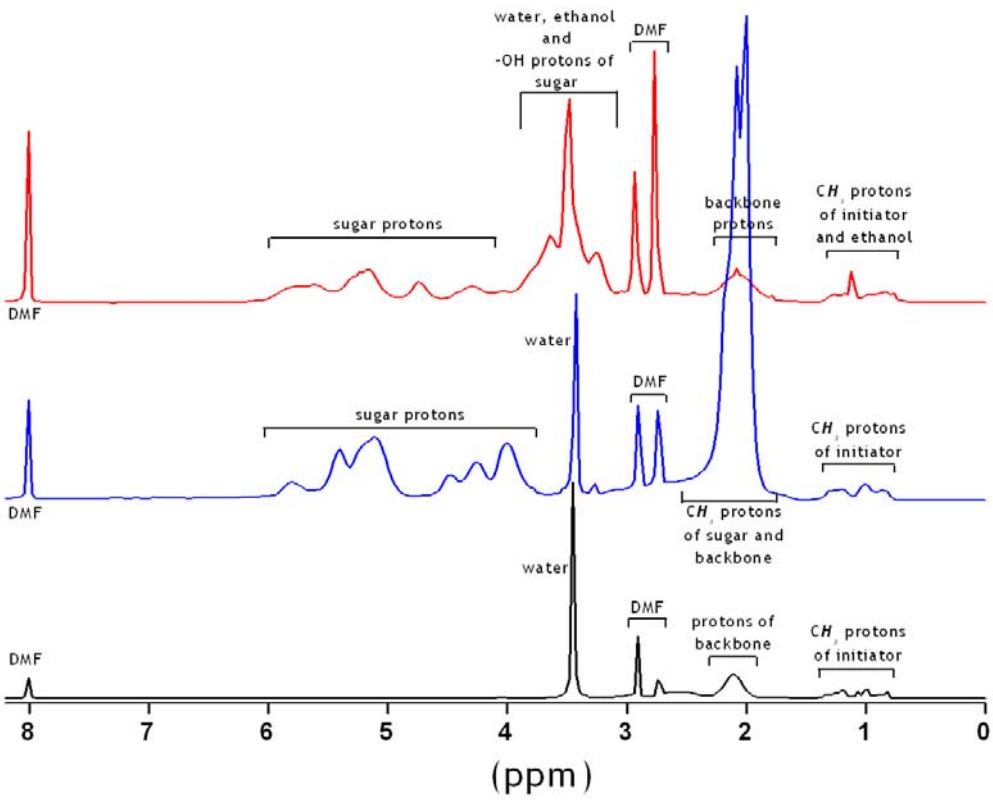

Figure 6.4. ^{1}H–NMR spectra (200 MHz, DMF–d$_7$) of P(PFS) **1** (*bottom*), protected glycopolymer P(PFS) **2** (*middle*) and glycopolymer **3** (*top*).

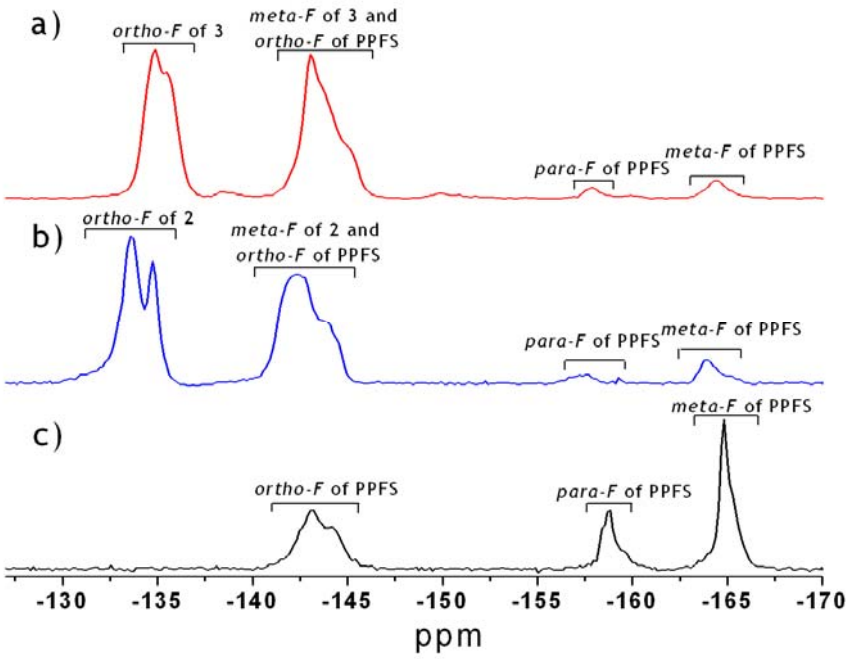

Figure 6.5. ^{19}F–NMR spectra (200 MHz, DMF–d_7) for (*top*) glycopolymer **3**, (*middle*) protected glycopolymer **2** and (*bottom*) homopolymer of PFS **1**.

Thiol–ene "click" reactions are known as highly efficient and rapid reactions.[55,94-96] Similarly, the nucleophilic substitution reaction between **1** and SH–$GlcAc_4$ also exhibited a fast reaction even at room temperature. Consequently, the kinetics of this thiol–*para* fluoro "click" reaction could be easily followed by an online kinetic experiment with ^{19}F–NMR spectroscopy. The reaction was started by adding the base into the mixture of polymer and glucose derivative (the measurement was conducted at 40 °C). A spectrum was recorded every 5 minutes for more than one hour. The calculated conversions (as explained previously) are shown in Figure 6.6. The reaction reached around 90% conversion in less than 30 minutes.

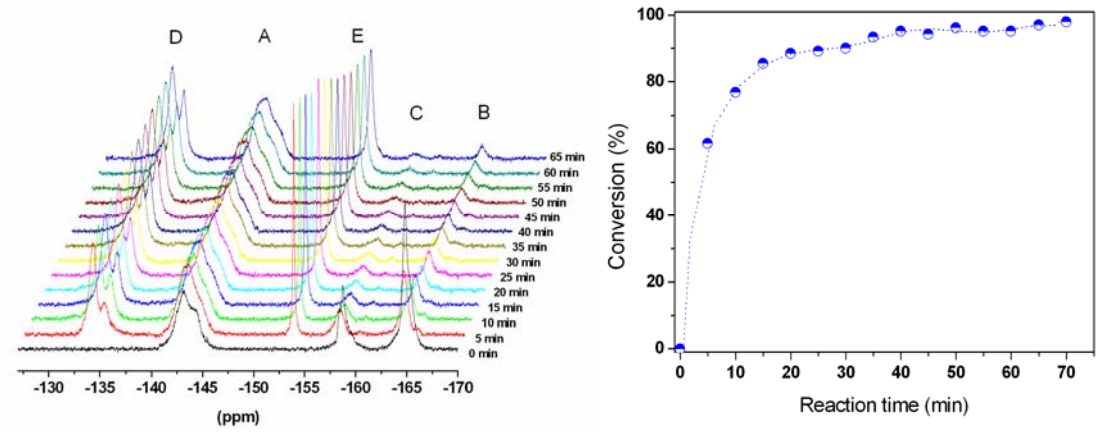

Figure 6.6. ^{19}F–NMR spectra (200 MHz, DMF–d_7) for the online measurement of the thiol–*para*–fluoro "click" reaction at 40 ºC (*left*), conversion *versus* reaction time calculated from the spectra above (*right*). A, B and C represent the *–o*, *–m* and *–p* position of **1**, respectively. D represents the *–m* position of **2**. E is the fluorine salt of triethylamine.

This "click" reaction approach was extended to the block copolymer of PS and PFS. For this purpose, PS_{46}–*b*–PFS_{12} (1.0 eq.) **B2** was reacted with SH–$GlcAc_4$ (1.2 eq.) in the presence of triethylamine (3.0 eq.). The reaction was performed in DMF at 50 °C for 12 hours. The product was precipitated into cold methanol, filtered and dried overnight. The characterization of SH–$GlcAc_4$ "clicked" block copolymer was performed by ^{1}H–NMR and ^{19}F–NMR spectroscopy as well as SEC. As shown in Figure 6.7, the reaction reached to 60% conversion under these reaction conditions. The relatively low conversion might be due to the different solubility behavior of St and PFS in DMF. Nevertheless, a clear shift in the SEC indicated that the hydrodynamic volume of the block copolymer was increased after the "click" reaction. In order to check the existence of the unreacted *para*–fluoro groups the "clicked" block copolymer (1.0 eq.) was dissolved in DMF and reacted with SH–$GlcAc_4$ (0.5 eq.) for the second time. The reaction was performed at 50 °C for 6 hours. The ^{19}F–NMR revealed an increase of the conversion to 90%. Besides, there is a slight shift observed in the SEC spectrum. These results show the possibility of performing controlled "click" reactions sequentially on the same polymer. It was clearly seen that *para*–Fluoro groups were stable under purification conditions and also provided selective reaction towards thiols. Our current studies are directed towards the preparation of copolymers with multiple sugar groups, *e.g.* thio–glucose and thio–galactose.

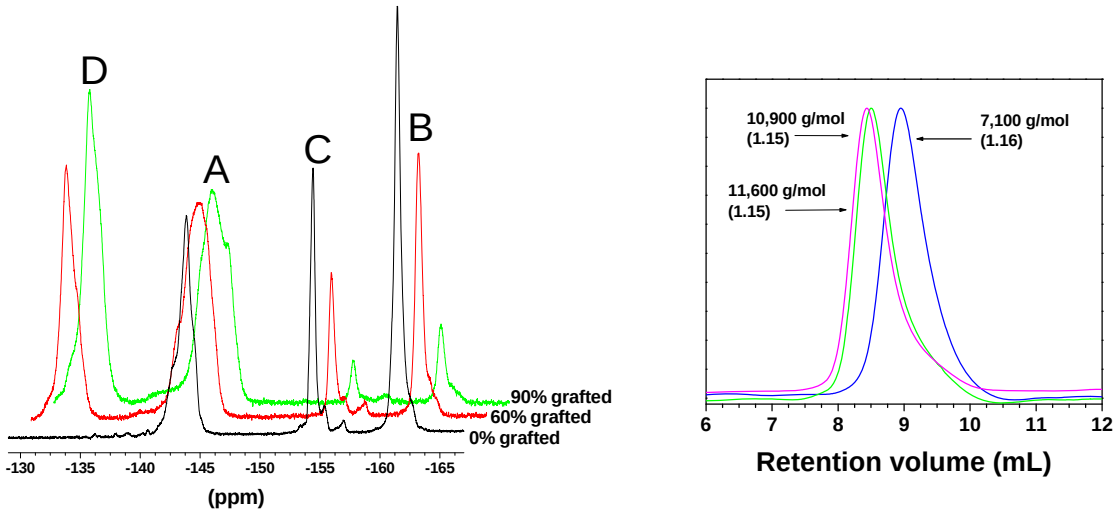

Figure 6.7. ^{19}F–NMR spectra (200 MHz, $CDCl_3$) for the thiol–*para*–fluoro "click" reaction using PS–*b*–PFS block copolymer (*left*), SEC traces of the starting material and "clicked" polymers (*right*).

As the final step of the procedure, the deacetylation of PTFS–*g*–$SGlcAc_4$ was performed. For this purpose, polymer **2** was dissolved in DMF and sodium methanolate in methanol was added. The mixture was stirred at room temperature for one hour. Subsequently, the solution was concentrated and purified by simple precipitation into cold

methanol. The disappearance of the acetyl groups was confirmed by both ^{1}H–NMR and ^{13}C–NMR spectroscopy.

Following the deacetylation, PTFS–*g*–SGlc exhibited a hydrophilic character, whereas PTFS–*g*–SGlcAc$_4$ has a hydrophobic character. This phase transition resulted in an increase in the hydrodynamic volume of the glycopolymer in *N,N*–dimethylacetamide (DMA), which was observed in SEC measurements (Figure 6.8). The molar mass and polydispersity indices of **1**, **2** and **3** were calculated, according to polystyrene standards, as 4,850 Da (M_w/M_n = 1.12), 9,200 Da (M_w/M_n = 1.11) and 19,400 Da (M_w/M_n = 1.13), respectively. Although **1** and **H1** are exactly the same polymers, they provide different molar masses (3,500 Da and 4,850 Da in $CHCl_3$ and DMA, respectively) in SEC systems running with different eluents. This behavior is caused by the different hydrodynamic volume in the different systems. We have measured SEC in DMA since it dissolves all three polymers, which are **1**, **2**, and **3**. The obtained SEC traces of these samples are depicted in Figure 6.8.

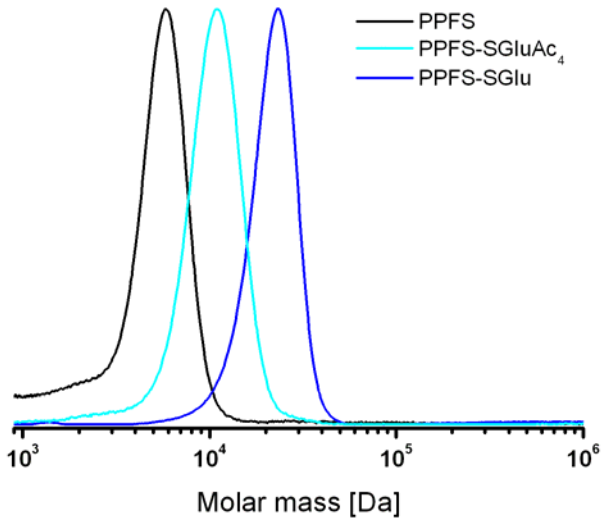

Figure 6.8. Normalized SEC traces of PPFS, PTFS-*g*-SGlcAc$_4$, and PTFS-*g*-Glc in *N,N*–dimethylacetamide as eluent with LiCl (2.1 g/L).

6.5 Conclusions

The use of the copper(I) catalyzed azide–alkyne cycloaddition flourished in all fields of chemistry following the introduction of the "click" chemistry concept by Sharpless. The need for metal–free "click" reactions, in particular for biological materials, urged the development of alternative "click" reactions. However, the beauty and popularity of azide–alkyne cycloaddition lies in the simple, readily available building blocks, whereas most of the metal–free alternative "click" reactions involve rather large complicated reactive groups such

as cyclooctyne, pentafluorostyrene, dipyridyltetrazine and anthracene. In addition, the large, when compared to 1,2,3–triazole, resulting 'coupling units' are disadvantageous for most applications. As such, it is believed that most of the hitherto reported metal free "click" reactions will remain beautiful academic examples rather than broadly applied methods.

The distinctly simpler metal free "click" reaction is the thiol–ene radical addition. The introduction of terminal alkene and thiol groups into a large variety of structures is straightforward while the resulting thio–ether bond is even smaller in size than the 1,2,3–triazole that results form azide–alkyne cycloaddition. Furthermore, the coupling procedure is even simpler than the CuAAC since no catalysts are required other than UV–light. As such, it is believed that thiol–ene "click" chemistry has the potential to become as broadly applied as CuAAC. In addition, the very recently reported dithioester–cyclopentadiene conjugation seems to be a very promising and simple method, although its broader applicability still has to be demonstrated.

Moreover, the synthesis of a series of homo, random and block copolymers of St and PFS has been demonstrated using the NMP technique. Besides, a kinetic study was performed for the random copolymerization, and the synthesized polymers were characterized using SEC, NMR spectroscopy and MALDI–TOF MS techniques. An alternative route for synthesizing glycopolymers using a nucleophilic substitution reaction of thiols to pentafluorophenyl functional groups has been established. We believe that this reaction is a good candidate to be employed as a metal–free "click" reaction. The kinetics of this reaction was investigated in detail, and well–defined polymers with a fluorinated backbone bearing glucose substituents were synthesized. Moreover, "click" reactions were performed on the block copolymers that might lead to the syntheses of heterofunctional block copolymers by sequential "click" reactions.

6.6 Experimental part

Materials

Styrene (≥99%, Aldrich), pentafluorostyrene (99%, Aldrich) and Bloc Builder^{TM} (Arkema) were used as received. 2,3,4,6–Tetra–*O*–acetyl–1–thio–*β*–D–glucopyranose (>99%) was purchased from GLYCON Biochemistry GmbH, triethylamine from Merck (for synthesis, ≥99%), *N,N*–dimethylformamide (≥99.5%) and DMA from Fluka and methanol from J.T. Baker (HPLC gradient grade, 0.008% water). Sodium methanolate was purchased from Fluka and stored under argon prior to use. All other chemicals were used as received, unless otherwise noted.

Instrumentation

For the determination of the monomer conversions, GC measurements were performed on a Shimadzu GC used with a Trace column RTX–5 and an autosampler. ^{1}H–NMR spectroscopy was recorded on a Bruker Avance 250 MHz in deuterated methylene chloride. The chemical shifts were calibrated with respect to tetramethylsilane (TMS). Size exclusion chromatography (SEC) was measured on two different systems. The first system (Shimadzu) is equipped with a SCL–10A system controller, a LC–10AD pump, a RID–10A refractive index detector, a SPD–10A UV detector and both a PSS Gram30 and a PSS Gram1000 column in series. A chloroform:isopropanol:triethylamine (94:4:2) mixture was used as eluent. The other SEC system (Agilent) is equipped with triple detectors that are diode array detector, refractive index detector and a multi angle light scattering detector. Two PSS SDV (5µ pore size) columns are placed in series. DMA with 5 mmol LiCl was used as eluent at 1 mL/min flow rate and the column oven was set to 50 ºC. The reported number average molar masses were calculated according to polystyrene standards in both systems. An Ultraflex III TOF/TOF (Bruker Daltonics, Bremen, Germany) was used for the MALDI TOF–MS analysis. The instrument is equipped with a Nd:YAG laser and a collision cell. The instrument was calibrated before every measurement with an external PMMA standard from PSS Polymer Standards Services GmbH (Mainz, Germany). MS data were processed using PolyTools 1.0 (Bruker Daltonics) and Data Explorer 4.0 (Applied Biosystems).

Synthesis of PPFS and PS homopolymers

Pentafluorostyrene (7.11 mL, 51.5 mmol) or styrene (11.8 mL, 103 mmol), Bloc Builder™ (393 mg, 1.03 mmol) and tetrahydrofuran (10 mL) were added in a 25 mL pressure resistant round bottom flask. The mixture was bubbled with argon while stirring at least for 30 minutes. Afterwards, the flask was capped and placed into an oil bath that was preheated to 110 ºC. The reaction was heated for 5 hours. After the reaction, the flask was cooled down immediately with tap water and the slightly viscous solution was precipitated into methanol to remove the residual monomer. The isolated polymers, which were white powders for both PS and PPFS, were dried in the vacuum oven for 24 hours.

Synthesis of PPFS and St containing copolymers

For the preparation of random copolymers, the required amounts of PFS, St, Bloc Builder™ and THF were added into a flask and the solution was bubbled with Argon for at least 30 minutes. Similarly, the required amount of St or PFS as monomers, PS or PPFS as macroinitiators, respectively, and THF were added into a vial for the synthesis of block copolymers. These polymerizations were carried out in 5 to 20 mL scale. The prepared vial

was immersed into a preheated oil bath at 110 ºC and the reaction was stopped after a certain reaction time. The polymerization was terminated by cooling down the vial with tap water. The obtained polymers were precipitated into methanol and dried in the vacuum oven.

"Click" reaction of 2,3,4,6–tetra–O–acetyl–1–thio–β–D–glucopyranose to $PPFS_{16}$

PPFS (433 mg, 2.23 mmol) and 2,3,4,6–tetra–*O*–acetyl–1–thio–*β*–D–glucopyranose (984 mg, 2.70 mmol) were dissolved in 15 mL of dry DMF and triethylamine (940 µL, 6.74 mmol) was added to the solution with the dissolved polymer. After stirring for 4 hours at room temperature, the reaction mixture was concentrated on a rotary evaporator to an approximate volume of 2.5 mL and precipitated into cold methanol. The white precipitate was filtered, washed twice with methanol and dried in a vacuum oven to yield 1.0 g of a white powder (93% isolated yield).

"Click" reaction of 2,3,4,6–tetra–O–acetyl–1–thio–β–D–glucopyranose to PS_{46}–b–PFS_{12}

PS_{46}–*b*–PFS_{12} (100 mg, 0.15 mmol PFS units) and 2,3,4,6–tetra–*O*–acetyl–1–thio–*β*–D–glucopyranose (67 mg, 0.18 mmol) were dissolved in 5 mL of dry DMF and triethylamine (64 µL, 0.46 mmol) was added to the solution of the polymer. After stirring for 12 hours at 50 °C, the reaction mixture was concentrated on a rotary evaporator to an approximate volume of 1 mL and precipitated into cold methanol (10 fold). The powder was filtered, washed twice with methanol and dried in a vacuum oven to yield 0.137 mg of a white powder (60% isolated yield). The isolated glycopolymer was reacted for the second time. PS_{46}–*b*–(PFS_{12}–*g*–$(SHGlcAc_4)_{7.2}$) (100 mg) and 2,3,4,6–tetra–*O*–acetyl–1–thio–*β*–D–glucopyranose (35 mg, 0.096 mmol) were dissolved in 5 mL of dry DMF and triethylamine (33 µL, 0.237 mmol) was added to the solution with the dissolved polymer. After stirring for 6 hours at 50 °C, the reaction mixture was concentrated on a rotary evaporator to an approximate volume of 1 mL and precipitated into cold methanol (10 fold). The powder was filtered, washed twice with methanol and dried in a vacuum oven (90% isolated yield).

Deacetylation of poly–p–(β–D–glycopyranosylthio)tetrafluorostyrene

Poly–*p*–(2,3,4,6–tetra–*O*–acetyl–β–D–glccopyranosylthio)tetrafluorostyrene (150 mg, 0.279 mmol) was dissolved in dry DMF (0.4 mL). Sodium methanolate (0.28 mL, 0.1 M solution in dry MeOH)) was added dropwise. After stirring for one hour at room temperature, the reaction mixture was concentrated on a rotary evaporator to a volume of 0.5 mL and precipitated into cold ethanol. The precipitate was washed with ethanol and dried to give 56 mg of the final product (55% isolated yield).

6.7 References

(1) C. J. Hawker, K. L. Wooley, *Science* **2005**, *309*, 1200−1205.
(2) S. Förster, M. Antonietti, *Adv. Mater.* **1998**, *10*, 195−217
(3) A. C. Balazs, T. Emrick, T. P. Russell, *Science* **2006**, *314*, 1107−1110
(4) K. Kobayashi, A. Tsuchida, T. Usui, T. Akaike, *Macromolecules* **1997**, *30*, 2016−2020.
(5) V. Ladmiral, E. Melia, D. M. Haddleton, *Eur. Polym. J.* **2004**, *40*, 431–449.
(6) J. Chiefari, Y. K. Chong, F. Ercole, J. Krstina, J. Jeffery, T. P. T. Le, R. T. A. Mayadunne, G. F. Meijs, C. L. Moad, G. Moad, E. Rizzardo, S. H. Thang, *Macromolecules* **1998**, *31*, 5559−5562.
(7) M. Kato, M. Kamigaito, M. Sawamoto, T. Higashimura, *Macromolecules* **1995**, *28*, 1721−1723.
(8) J. Wang, K. Matyjaszewski, *J. Am. Chem. Soc.* **1995**, *117*, 5614−5615.
(9) C. J. Hawker, G. G. Barclay, A. Orellana, J. Dao, W. Devonport, *Macromolecules* **1996**, *29*, 5245−5254.
(10) T. E. Patten, K. Matyjaszewski, *Adv. Mater.* **1998**, *10*, 901−915.
(11) G. Moad, J. Chiefari, Y. K. Chong, J. Krstina, R. T. A. Mayadunne, A. Postma, E. Rizzardo, S. H. Thang, *Polym. Int.* **2000**, *49*, 993−1001.
(12) G. Moad, E. Rizzardo, S. H. Thang, *Aust. J. Chem.* **2005**, *58*, 379−410.
(13) K. Ohno, Y. Tsujii, T. Miyamoto, T. Fukuda, M. Goto, K. Kobayashi, T. Akaike, *Macromolecules* **1998**, *31*, 1064−1069.
(14) Y. Miura, D. Koketsu, K. Kobayashi, *Polym. Adv. Technol.* **2007**, *18*, 647−651.
(15) A. Narumi, T. Matsuda, H. Kaga, T. Satoh, T. Kakuchi, *Polymer* **2002**, *43*, 4835−4840.
(16) Y. M. Chen, G. Wulff, *Macromol. Chem. Phys.* **2001**, *202*, 3426−3431.
(17) H. Gotz, E. Harth, S. M. Schiller, C. W. Frank, W. Knoll, C. J. Hawker, *J. Polym. Sci., Part A: Polym. Chem.* **2002**, *40*, 3379−3391.
(18) K. Ohno, Y. Izu, S. Yamamoto, T. Miyamoto, T. Fukuda, *Macromol. Chem. Phys.* **1999**, *200*, 1619−1625.
(19) K. Ohno, T. Fukuda, H. Kitano, *Macromol. Chem. Phys.* **1998**, *199*, 2193−2197.
(20) D. Fournier, R. Hoogenboom, U. S. Schubert, *Chem. Soc. Rev.* **2007**, *36*, 1369−1380.
(21) V. Ladmiral, G. Mantovani, G. J. Clarkson, S. Cauet, J. L. Irwin, D. M. Haddleton, *J. Am. Chem. Soc.* **2006**, *128*, 4823−4830.
(22) J. E. Moses, A. D. Moorhouse, *Chem. Soc. Rev.* **2007**, *36*, 1249−1262.
(23) J.–F. Lutz, *Angew. Chem. Int. Ed.* **2007**, *46*, 1018−1025.
(24) G. W. Goodall, W. Hayes, *Chem. Soc. Rev.* **2006**, *35*, 280−312.
(25) H. C. Kolb, M. G. Finn, K. B. Sharpless, *Angew. Chem. Int. Ed.* **2001**, *40*, 2004−2021.
(26) S. G. Spain, M. I. Gibson, N. R. Cameron, *J. Polym. Sci., Part A: Polym. Chem.* **2007**, *45*, 2059−2072.
(27) N. J. Agard, J. A. Prescher, C. R. Bertozzi, *J. Am. Chem. Soc.* **2004**, *126*, 15046−15047.
(28) S. T. Laughlin, J. M. Baskin, S. L. Amacher, C. R. Bertozzi, *Science* **2008**, *320*, 664−667.
(29) R. F. Service, *Science* **2008**, *320*, 868−869.
(30) L. You, H. Schlaad, *J. Am. Chem. Soc.* **2006**, *128*, 13336−13337.
(31) A. Gress, A. Völkel, H. Schlaad, *Macromolecules* **2007**, *40*, 7928−7933.
(32) A. Gress, B. Smarsly, H. Schlaad, *Macromol. Rapid Commun.* **2008**, *29*, 304−308.
(33) K. L. Killops, L. M. Campos, C. J. Hawker, *J. Am. Chem. Soc.* **2008**, *130*, 5062−5064.
(34) L. M. Campos, K. L. Killops, R. Sakai, J. M. J. Paulusse, D. Damiron, E. Drockenmuller, B. W. Messmore, C. J. Hawker, *Macromolecules* **2008**, *41*, 7063−7070.
(35) A. Dondoni, *Angew. Chem. Int. Ed.* **2008**, *47*, 8995−8997.
(36) W. Song, Y. Wang, J. Qu, Q. Lin, *J. Am. Chem. Soc.* **2008**, *130*, 9654−9655.
(37) C. Ott, R. Hoogenboom, U. S. Schubert, *Chem. Commun.* **2008**, 3516−3519.
(38) D. Samaroo, C. E. Soll, L. J. Todaro, C. M. Drain, *Org. Lett.* **2006**, *8*, 4985−4988.
(39) X. Chen, L. Hui, D. A. Foster, C. M. Drain, *Biochemistry* **2004**, *43*, 10918−10929.
(40) J. M. Baskin, J. A. Prescher, S. T. Laughlin, N. J. Agard, P. V. Chang, I. A. Miller, A. Lo, J. A. Codelli, C. R. Bertozzi, *Proc. Nat. Acad. Sci. U.S.A.* **2007**, *104*, 16793–16797.
(41) J. A. Johnson, J. M. Baskin, C. R. Bertozzi, J. F. Koberstein, N. J. Turro, *Chem. Commun.* **2008**, 3064–3066.
(42) J. A. Codelli, J. M. Baskin, N. J. Agard, C. R. Bertozzi, *J. Am. Chem. Soc.* **2008**, *130*, 11486–11493.
(43) E. M. Sletten, C. R. Bertozzi, *Org. Lett.* **2008**, *10*, 3097–3099.
(44) J. M. Baskin, C. R. Bertozzi, *QSAR Comb. Sci.* **2007**, *26*, 1211–1219.
(45) G. Wittig, A. Krebs, *Chem. Ber. Recl.* **1961**, *94*, 3260–3275.
(46) A. T. Blomquist, L. H. Liu, *J. Am. Chem. Soc.* **1953**, *75*, 2153–2154.
(47) D. H. Ess, G. O. Jones, K. N. Houk, *Org. Lett.* **2008**, *10*, 1633–1636.
(48) W. D. Sharpless, P. Wu, T. V. Hansen, J. G. Lindberg, *J. Chem. Edu.* **2005**, *82*, 1833–1836.
(49) S. Sawoo, P. Dutta, A. Chakraborty, R. Mukhopadhyay, O. Bouloussa, A. Sarkar, *Chem. Commun.* **2008**, 5957–5959.
(50) Z. Li, T. S. Seo, J. Ju, *Tetrahedron Lett.* **2004**, *45*, 3143–3146.

(51) F. Shi, J. P. Waldo, Y. Chen, R. C. Larock, *Org. Lett.* **2008**, *10*, 2409–2412.
(52) L. Campbell–Verdduyn, P. H. Elsinga, L. Mirfeizi, R. A. Dierckx, B. L. Feringa, *Org. Biomol. Chem.* **2008**, *6*, 3461–3463.
(53) *The chemistry of the thiol group* S. Patai, Ed.;Wiley: New York, **1974**.
(54) A. F. Jacobine, *In radiation curing in polymer science and technology III*; J. D. Fouassier, J. F. Rabek, Eds.; Elsevier: London, **1993**; *Chapter 7*, pp 219–268.
(55) C. E. Hoyle, T. Y. Lee, T. Roper, *J. Polym. Sci., Part. A: Polym. Chem.* **2008**, *42*, 5301–5338.
(56) R. L. A. David, J. A. Kornfield, *Macromolecules* **2008**, *41*, 1151–1161.
(57) C. Nilsson, N. Simpson, M. Malkoch, M. Johansson, E. Malmstrom, *J. Polym. Sci., Part A: Polym. Chem.* **2008**, *46*, 1339–1348.
(58) J. F. Lutz, H. Schlaad, *Polymer* **2008**, *49*, 817–824.
(59) N. ten Brummelhuis, C. Diehl, H. Schlaad, *Macromolecules* **2008**, *41*, 9946–9947.
(60) J. W. Chan, B. Yu, C. E. Hoyle, A. B. Lowe, *Chem. Commun.* **2008**, 4959–4961.
(61) G. Moad, E. Rizzardo, S. H. Thang, *Acc. Chem. Res.* **2008**, *41*, 1133–1142.
(62) C. Barner–Kowollik, M. Buback, B. Charleux, M. L. Coote, M. Drache, T. Fukuda, A. Goto, B. Klumperman, A. B. Lowe, J. B. McLeary, G. Moad, M. J. Monterio, R. D. Sanderson, M. P. Tonge, P. Vana, *J. Polym. Sci., Part A: Polym. Chem.* **2006**, *44*, 5809–5831.
(63) R. J. Pounder, M. J. Stanford, P. Brooks, S. P. Richards, A. P. Dove, *Chem. Commun.* **2008**, 5158–5160.
(64) M. J. Stanford, A. P. Dove, *Macromolecules* **2009**, *42*, 141–147.
(65) M. Li, P. De, S. R. Gondi, B. S. Sumerlin, *J. Polym. Sci., Part A: Polym. Chem.* **2008**, *46*, 5093–5100.
(66) Z. J. Witczak, D. Lorchak, N. Nguyen, *Carbohydr. Res.* **2007**, *342*, 1929–1933.
(67) D. Samaroo, M. Vinodu, X. Chen, C. M. Drain, *J. Comb. Chem.* **2007**, *9*, 998–1011.
(68) P. Battioni, O. Brigaud, H. Desvaux, D. Mansuy, T. G. Traylor, *Tetrahedron Lett.* **1991**, *32*, 2893–2896.
(69) C. R. Becer, K. Babiuch, K. Pilz, S. Hornig, T. Heinze, M. Gottschaldt, U. S. Schubert, *Macromolecules* **2009**, *42*, 2387-2394.
(70) Otto Paul Hermann Diels and Kurt Alder first documented the reaction in 1928 and received the Nobel Prize in Chemistry in 1950 for their work on the eponymous reaction.
(71) H. L. Holmes, R. M. Husband, C. C. Lee, P. Kawulka, *J. Am. Chem. Soc.* **1948**, *70*, 141–142.
(72) M. Lautens, W. Klute, W. Tam, *Chem. Rev.* **1996**, *96*, 49–92.
(73) K. C. Nicolaou, S. A. Snyder, T. Montagnon, G. Vassilikogiannakis, *Angew. Chem. Int. Ed.* **2002**, *41*, 1668–1698.
(74) E. J. Corey, *Angew. Chem. Int. Ed.* **2002**, *41*, 1650–1667.
(75) H. Durmaz, A. Dag, O. Altintas, T. Erdogan, G. Hizal, U. Tunca, *Macromolecules* **2007**, *40*, 191–198.
(76) H. Durmaz, A. Dag, A. Hizal, G. Hizal, U. Tunca, *J. Polym. Sci., Part A: Polym. Chem.* **2008**, *46*, 7091–7100.
(77) A. Dag, H. Durmaz, E. Demir, G. Hizal, U. Tunca, *J. Polym. Sci., Part A: Polym. Chem.* **2008**, *46*, 6969–6977.
(78) B. Gacal, H. Akat, D. K. Balta, N. Arsu, Y. Yagci, *Macromolecules* **2008**, *41*, 2401–2405.
(79) A. Dag, H. Durmaz, U. Tunca, G. Hizal, *J. Polym. Sci., Part A: Polym. Chem.* **2009**, *47*, 178–187.
(80) M. L. Blackman, M. Royzen, J. M. Fox, *J. Am. Chem. Soc.* **2008**, *130*, 13518–13519.
(81) It should be noted that *trans*–cyclooctyne is the most reactive dienophile and seven orders of magnitude more reactive than *cis*–cyclooctyne toward tetrazines.
(82) N. K. Devaraj, R. Weissleder, S. A. Hilderbrand, *Bioconjugate Chem.* **2008**, *19*, 2297–2299.
(83) W. Song, Y. Wang, J. Qu, M. M. Madden, Q. Lin, *Angew. Chem. Int. Ed.* **2008**, *47*, 2832–2835.
(84) A. Dag, H. Durmaz, G. Hizal, U. Tunca, *J. Polym. Sci., Part:A Polym. Chem.* **2008**, *46*, 302–313.
(85) A. J. Inglis, S. Sinnwell, T. P. Davis, C. Barner–Kowollik, M. H. Stenzel, *Macromolecules* **2008**, *41*, 4120–4126.
(86) S. Sinnwell, A. J. Inglis, T. P. Davis, M. H. Stenzel, C. Barner–Kowollik, *Chem. Commun.* **2008**, 2052–2054.
(87) A. J. Inglis, S. Sinwell, M. H. Stenzel, C. Barner–Kowollik, *Angew. Chem. Int. Ed.* **2009**, *48*, DOI: 10.1002/anie.200805993.
(88) C. R. Becer, R. M. Paulus, R. Hoogenboom, U. S. Schubert, *J. Polym. Sci., Part A: Polym. Chem.* **2006**, *44*, 6202−6213.
(89) B. Lessard, A. Graffe, M. Maric, *Macromolecules* **2008**, *41*, 3446−3454.
(90) T. M. Eggenhuisen, C. R. Becer, M. W. M. Fijten, R. Eckardt, R. Hoogenboom, U. S. Schubert, *Macromolecules* **2008**, *41*, 5132–5140.
(91) C. R. Becer, S. Hahn, M. W. M. Fijten, H. M. L. Thijs, R. Hoogenboom, U. S. Schubert, *J. Polym. Sci., Part A: Polym. Chem.* **2008**, *46*, 7138–7147.
(92) C. R. Becer, A. M. Groth, R. Hoogenboom, R. M. Paulus, U. S. Schubert, *QSAR Comb. Sci.* **2008**, *27*, 978–983.
(93) A. Baumgaertel, C. R. Becer, M. Gottschaldt, U. S. Schubert, *Macromol. Rapid Commun.* **2008**, *29*, 1309–1315.

(94) C. R. Morgan, F. Magnotta, A. D. Ketley, *J. Polym. Sci., Part A: Polym. Chem.* **1977**, *15*, 627−645.
(95) S. K. Reddy, R. P. Sebra, K. S. Anseth, C. N. Bowman, *J. Polym. Sci., Part A: Polym. Chem.* **2005**, *43*, 2134−2144.
(96) P. M. Johnson, J. W. Stansbury, C. N. Bowman, *J. Polym. Sci., Part A: Polym. Chem.* **2008**, *46*, 1502−1509.

Summary

In nature, complex three-dimensionally ordered macromolecular architectures, such as proteins and DNA, can be found which are dependent on a high level of structural control in order to perform their desired biological tasks. Such systems are up to now not accessible by synthetic methods; however, in the last decades tremendous progress was made in the development of advanced living and controlled polymerization techniques. Besides, several outstanding organic reactions have been discovered and perfectionated with their easy experimental conditions and resulting high yields, which are categorized as “click” reactions. These techniques allow researchers to prepare well–defined tailor–made macromolecules with before not accessible control. However, in particular living and controlled polymerization techniques require a delicate selection of the appropriate catalyst, initiator, and solvent at a certain polymerization temperature and period for each type of monomer. Therefore, high–throughput experimentation (HTE) tools and techniques are required to screen the effect of reaction parameters in relatively short times. These polymerization techniques and the application of HTE in polymer science have been reviewed in the first chapter. A major part of this thesis deal with the optimization of not only controlled radical polymerization techniques but also cationic ring opening polymerization (CROP) process.

Nitroxide mediated radical polymerization (NMP) of several monomers have been performed in an automated parallel synthesizer to obtain the most optimum reaction conditions in means of polydispersity indices, number average molar masses, monomer conversions as well as block copolymerization. We have used for this purpose a unimolecular nitroxide initiator (β-phosphonylated alkoxyamine, Bloc Builder) which has a relatively low decomposition temperature and provides good control over the polymerization progress. Some of the obtained polymer libraries were examined for their thermal properties and lower critical solution temperature behavior. The results of these experiments are discussed in detail in the second chapter.

In the third chapter, we have focused on the reversible addition fragmentation chain transfer (RAFT) polymerization technique to synthesize methacrylic acid containing thermo-responsive copolymer libraries. These polymers have been prepared using a synthesis robot and also parallel characterization techniques were

employed. Furthermore, water uptake properties of the hydrophilic polymers as well as thermo-responsive polymers have been investigated. It was demonstrated that responsive polymers behave hydrophilic below their LCST and hydrophobic above their LCST, thus exhibiting a reversible water uptake–release profile.

Atom transfer radical polymerization (ATRP) is one of the most important controlled/"living" polymerization techniques which has attracted significant attention in many fields of chemistry. We have contributed for the further development by introducing a new tetradentate nitrogen based ligand for the ATRP of methyl methacrylate and styrene. The optimization results revealed that this ligand is suitable to conduct ATRP of methyl methacrylate (MMA) in the presence of Cu(I) and Cu(II) metal ions. Besides, this ligand has been used for the ATRP of styrene initiated from functionalized surfaces. Grafting from the surface resulted in the formation of polymer brushes with controlled lengths depending on the reaction time.

Transformation of the polymerization mechanisms by post polymerization modifications or by using functional initiating/terminating agents have been of great interest to combine different classes of monomers on the same backbone. Therefore, we have employed for the first time a heterofunctional initiator for the ATRP of styrene and the CROP of 2-ethyl-2-oxazoline (EtOx) to synthesize amphiphilic block copolymers. Furthermore, we determined the optimum polymerization temperature for EtOx using acetyl halide type of initiators. These reactions have been performed systematically in a microwave synthesizer and the results have been discussed in the fifth chapter.

"Click" reactions have been employed in many fields of chemistry since 2001. These efficient reactions attracted also polymer chemists to introduce functional end groups or side groups to well–defined polymers. Several different techniques have been published in the last eight years and we discussed critically the ones which do not require a metal catalyst during the reactions in the last chapter. Besides, we have introduced a metal-free "click" reaction between thiol and pentafluorophenyl groups to synthesize glycopolymers. For this purpose, fluorinated polymers have been prepared by NMP and were further functionalized using this new "click" chemistry route.

In conclusion, this thesis provides new insights into the most important controlled radical polymerization techniques by utilizing in the automated parallel synthesis platforms and by the systematical preparation of copolymer libraries. The

detailed characterization of these libraries provided fundamental knowledge on the structure-property relationships. Moreover, a new ligand for the ATRP of MMA and styrene, a new type of heterofunctional initiator for the combination of ATRP and CROP, and a new type of “click” reaction for the synthesis of glycopolymers have been introduced during this thesis. These new compounds and routes will be employed further for the preparation of tailor-made macromolecules to be used in specific applications.

Samenvatting

In de natuur worden complexe drie-dimensionele geordende macromoleculaire architecturen aangetroffen, zoals proteines en DNA. Of deze de gewenste biologische taak kunnen vervullen, is sterk afhankelijk van de mate van controle over de structuur. Zulke systemen zijn tot op de dag van vandaag niet synthetisch te vervaardigen, terwijl er in de laatste decennia een enorme vooruitgang is geboekt in de ontwikkeling van geavanceerde "levende" en gecontroleerde polymerisatie technieken. Daarnaast zijn er verschillende uitstekende organische reacties ontdekt en geperfectioneerd, welke onder de catogorie "klik" reacties vallen. Deze zogenaamde "klik" reacties vinden plaats onder simpele experimentele condities en resulteren in hoge opbrengsten. Deze techniek maakt het de onderzoeker mogelijk om goed gedefinieerde, op maat gemaakte macromoleculen gecontroleerd te maken, wat voorheen niet mogelijk was. Maar, vooral voor "levende" en gecontroleerde polymerisatie technieken moet er een delicate selectie gemaakt worden van de juiste katalysator, initiator en oplosmiddel met de juiste polymerisatie-temperatuur en –tijd voor ieder type monomeer. Daarvoor zijn er 'high-throughput experimentation' (HTE) apparatuur en technieken nodig om het effect van de reactieparameters te screenen in een relatief korte tijd. Een groot deel van deze thesis gaat over de optimalisatie van, niet alleen gecontroleerde radicaal polymerisatietechnieken, maar ook van cationic ring-opening polymerization (CROP) processen.

Nitroxide mediated radical polymerization (NMP) van verschillende monomeren zijn gedaan in een geautomatiseerde parallel apparaat om de optimale reactiecondities te vinden in termen van polydispersiteit indices, nummer gemiddeld moleculair gewicht, monomeer conversie als mede blokcopolymerisatie. We hebben voor deze opzet een unimoleculaire nitroxide initiator (β-phosphonylated alkoxyamine, Bloc Builder) gekozen, welke een relatief lage decompositie temperatuur heeft en een goede controle biedt over de voortgang van de polymerisatie.

De thermische eigenschappen en de lower critical solution temperature (LCST) van een aantal van de verkregen polymerisatie bibliotheken zijn onderzocht. De resultaten van deze experimenten staan gedetailleerd beschreven in het tweede hoofdstuk.

In het derde hoofdstuk ligt de focus op de reversibel addition fragmentation chaintransfer (RAFT) polymerisatie techniek. Het doel was om met deze techniek een bibliotheek van copolymeren gebaseerd op methacrylzuur te synthetiseren, welke reageren op een thermische verandering. Deze polymeren zijn gemaakt met behulp van een synthese robot en ook parallelle karakterisatie technieken zijn gebruikt. Verder is onderzocht hoeveel water de hydrofiele polymeren kunnen opnemen als mede de thermische respons van de polymeren. Gedemonstreerd is dat responderende polymeren zich hydrofilisch gedragen beneden hun LCST en hydrofobisch boven hun LCST, waardoor ze een reversibele water opname-afgifte profiel laten zien.

Atom transfer radical polymerization (ATRP) is een van de belangrijkste gecontroleerde/"levende" polymerisatie technieken, welke veel aandacht getrokken heeft in diverse takken binnen de scheikunde. Wij hebben een contributie geleverd aan de verdere ontwikkeling, door een nieuwe tetradentate, een op stikstof gebaseerde ligand voor de ATRP van methyl methacrylaat en styreen, te introduceren. De resultaten voor de optimalisatie laten zien dat deze ligand geschikt is om methyl methacrylaat (MMA) in het bijzijn van de mataalionen Cu(I) en Cu(II) te polymeriseren met behulp van ATRP. Daarnaast is dit ligand gebruikt voor de ATRP van styreen geinitieerd door middel van gefunctionaliseerde oppervlakten. 'Grafting from' het oppervlak resulteerde in de vorming van polymeer 'brushes' met gecontroleerde lengtes afhankelijk van de reactietijd.

Voor de transformatie van het polymerisatiemechanisme door post polymerisatie modificaties of door het gebruik van functionele initiatie/terminatie agens is veel interesse geweest om verschillende klassen monomeren te combineren in dezelfde 'backbone'. Daarom hebben we voor de eerste keer een heterofunctionele initiator voor de ATRP van styreen en CROP van 2-ethyl-2-oxazoline (EtOx) gebruikt, om amfifiele blokcopolymeren te synthetiseren. Verder hebben we de optimale polymerisatie temperatuur voor EtOx bij gebruik van verschillende typen acetyl halide initiatoren bepaald. Deze reacties zijn systematisch uitgevoerd onder microwave condities en de resultaten staan beschreven in het vijfde hoofdstuk.

"Klik" reacties zijn gebruikt in vele takken van de scheikunde sinds 2001. Deze efficiënte reacties hebben veel aandacht getrokken van polymeerchemici om functionele eindgroepen of zijgroepen te introduceren aan goed-gedefinieerde polymeren. Verscheidende verschillende technieken zijn gepubliceerd in de laatste acht jaar en de technieken waarbij geen metaalhoudende katalysator nodig zijn tijdens

de reactie, worden kritisch besproken in het laatste hoofdstuk. Daarnaast hebben we een metaal-vrije "klik" reactie tussen thiol en pentafluorofenyl groepen geintroduceerd voor de synthese van glycopolymeren. Voor dit doel zijn gefluorideerde polymeren gemaakt met behulp van NMP en verder gefunctionaliseerd door deze nieuwe 'klik' chemie route te gebruiken.

Samengevat geeft deze thesis nieuwe inzichten in de belangrijkste gecontroleerde radicaal polymerisatie technieken door gebruik te maken van geautomatiseerde parallelle synthese platformen en door de systematische preparatie van een bibliotheek copolymeren. De gedetailleerde karakterisatie van deze bibliotheken heeft fundamentele informatie opgebracht over de structuur-eigenschappen relatie. Verder is een nieuw ligand voor de ATRP van MMA en styreen, een nieuw type heterofunctionele initiator voor de combinatie van ATRP en CROP en een nieuw type "klik" reactie voor de synthese van glycopolymeren geintroduceerd tijdens deze thesis. Deze nieuwe verbindingen en routes zullen gebruikt worden voor de preparatie van op maat gemaakte macromoleculen, te gebruiken voor specifike applicaties.

Curriculum vitae

Çağlar Remzi Becer was born in 1980 in Izmir, Turkey. After finishing high school in Izmir Turk College, he started with the Chemistry education at the Istanbul Technical University. His undergraduate research concerning the electrochromic behavior of conductive polymers was performed in the group of Prof. Dr. Sezai Sarac. After obtaining his B.Sc. degree in Chemistry, he started the Polymer Science and Technology master program in 2003 at the Istanbul Technical University. He conducted his M.Sc. project on the synthesis of nitrogen based ligands for atom transfer radical polymerization and their optimization reactions under the supervision of Prof. Dr. Metin H. Acar. In August 2005, he started his Ph.D. work under the supervision of Prof. Dr. Ulrich S. Schubert at the Eindhoven University of Technology. He spent the second half of his PhD at the Friedrich-Schiller-University Jena, Germany, as a visiting scientist, to take part in starting the Laboratory of Organic and Macromolecular Chemistry of Prof. Dr. U. S. Schubert. Recently, he has received a Marie Curie fellowship to further pursue his career as a post-doc at the laboratory of Prof. Dr. David M. Haddleton (University of Warwick, United Kingdom). His post-doc position in UK will be combined with a part-time position as a project leader at the Friedrich-Schiller-University Jena, Germany. The most important results of his PhD work are discussed in this thesis.

Refereed publications:

• this work is included in the thesis

° this work is not included in the thesis

2006

• C. R. Becer, R. M. Paulus, R. Hoogenboom, U. S. Schubert
Optimization of nitroxide mediated radical polymerization conditions for styrene and *tert*-butyl acrylate in an automated synthesizer.
J. Polym. Sci., Part A: Polym. Chem. **2006**, *44*, 6202 – 6213.

2007

• C. R. Becer, C. Haensch, S. Hoeppener, U. S. Schubert
Patterned polymer brushes grafted from bromine functionalized chemically active surface templates
Small **2007**, *3*, 220 – 225.

° R. M. Paulus, T. Erdmenger, C. R. Becer, R. Hoogenboom, U. S. Schubert
Scale-up of microwave-assisted polymerizations in a continuous-flow mode: Cationic ring-opening polymerization of 2-ethyl-2-oxazoline
Macromol. Rapid Commun. **2007**, *28*, 484 – 491.

• C. R. Becer, R. Hoogenboom, D. Fournier, U. S. Schubert
Cu(II) mediated ATRP of MMA by using a novel tetradentate amine ligand with oligo(ethylene glycol) pendant groups
Macromol. Rapid Commun. **2007**, *28*, 1161 – 1166.

• H. M. L. Thijs, C. R. Becer, D. Fournier, C. Guerrero-Sanchez, R. Hoogenboom, U. S. Schubert
Water uptake of hydrophilic polymers as determined by a thermal gravimetric analyzer with a controlled humidity chamber
J. Mater. Chem. **2007**, *17*, 4864 – 4871.

2008

• R. M. Paulus, C. R. Becer, R. Hoogenboom, U. S. Schubert
Acetyl halide initiator screening for the cationic ring opening polymerization of 2-ethyl-2-oxazoline
Macromol. Chem. Phys. **2008**, *209*, 794 – 800.

• C. R. Becer, A. M. Groth, R. Hoogenboom, R. Paulus, U. S. Schubert
Protocol for the automated kinetic investigation/optimization of the RAFT polymerization of various monomers
QSAR Comb. Sci. **2008**, *27*, 978 – 983.

• T. M. Eggenhuisen, C. R. Becer, M. W. M. Fijten, R. Eckardt, R. Hoogenboom, U. S. Schubert
Libraries of statistical hydroxypropyl acrylate containing copolymers with LCST properties prepared by NMP
Macromolecules **2008**, *41*, 5132 – 5140.

° A. Baumgaertel, C. R. Becer, M. Gottschaldt, U. S. Schubert
Matrix assisted laser desorption/ionization time-of-flight collision induced dissociation mass spectra of poly(methyl methacrylate)
Macromol. Rapid Commun. **2008**, *29*, 1309 – 1315.

• C. R. Becer, R. M. Paulus, S. Hoeppener, R. Hoogenboom, C. A. Fustin, J. F. Gohy, U. S. Schubert
Synthesis of poly(2-ethyl-2-oxazoline)-*b*-poly(styrene) copolymers via combination of cationic ring opening polymerization by using a dual initiator
Macromolecules **2008**, *41*, 5210 – 5215.

• C. R. Becer, S. Hahn, M. W. M. Fijten, H. Thijs, R. Hoogenboom, U. S. Schubert
Libraries of methacrylic acid and oligo(ethylene glycol) methacrylate copolymers with LCST behavior
J. Polym. Sci., Part A: Polym. Chem. **2008**, *46*, 7138 – 7147.

° C. Ulbricht, C. R. Becer, A. Winter, D. Veldman, U. S. Schubert
Copolymers containing phosphorescent iridium(III) complexes obtained by free and controlled radical polymerization techniques
Macromol. Rapid Commun. **2008**, *29* ,1919 – 1925.

2009

° T. Edmenger, C. R. Becer, R. Hoogenboom, U. S. Schubert
Simplifying the free-radical polymerization of styrene: Microwave assisted high-temperature auto polymerizations
Aust. J. Chem. **2009**, *62*, 58 – 63.

° A. Krieg, C. R. Becer, R. Hoogenboom, U. S. Schubert
Tailor-made macromolecules by combination of controlled radical polymerization and “click” chemistry
Macromol. Symp. **2009**, *275-276*, 73 – 81.

° C. Weber, C. R. Becer, A. Baumgaertel, R. Hoogenboom, U. S. Schubert
Preparation of methacrylate end-functionalized poly(2-ethyl-2-oxazoline) macromonomers
Des. Monomers Polym. **2009**, *12*, 149 – 165.

• C. R. Becer, K. Babiuch, D. Pilz, S. Hornig, T. Heinze, M. Gottschaldt, U. S. Schubert
Clicking pentafluorostyrene copolymers: Synthesis, nanoprecipitation and glycosylation
Macromolecules, **2009**, *42*, 2387 – 2394.

° R. M. Paulus, C. R. Becer, R. Hoogenboom, U. S. Schubert
High temperature initiator free RAFT polymerization of MMA in a microwave synthesizer
Aust. J. Chem. **2009**, *62*, 254 – 259.

° C. Weber, C. R. Becer, R. Hoogenboom, U. S. Schubert
LCST behavior of oligo(2-ethyl-2-oxazoline) containing copolymers
Macromolecules **2009**, *42*, 2965 – 2971.

• C. R. Becer, R. Hoogenboom, U. S. Schubert
"Click" chemistry beyond metal-catalyzed azide-alkyne cycloaddition
Angew. Chem. Int. Ed. **2009**, DOI: 10.1002/anie.200900755.

° S. Hornig, T. Heinze, C. R. Becer, U. S. Schubert
Synthetic polymeric nanoparticles by nanoprecipitation
J. Mater. Chem **2009**, DOI: 10.1039/b906556n.

• C. R. Becer, U. S. Schubert
Parallel optimization and high-throughput preparation of well-defined copolymer libraries using controlled/"living" polymerization methods
Adv. Polym. Sci. **2009**, in press.

Non-refereed publications:

▪ C. R. Becer, R. M. Paulus, R. Hoogenboom, U. S. Schubert
Investigation of nitroxide mediated polymerization conditions in an automated synthesizer
Polym. Prepr. **2007**, *48(1)*, 163 – 164.

▪ C. R. Becer, C. Haensch, S. Hoeppener, R. Hoogenboom, U. S. Schubert
Polymer brushes grafted from patterned chemically active surfaces via atom transfer radical polymerization
Polym. Prepr. **2007**, *48(1)*, 755 – 756.

▪ C. Ulbricht, C. R. Becer, A. Winter, U. S. Schubert
Copolymers by radical polymerization containing phosphorescent iridium(III)
Polym. Prepr. **2007**, *48(2)*, 593 – 594.

▪ R. Hoogenboom, C. R. Becer, S. Hahn, D. Fournier, U. S. Schubert
Thermo- and pH-responsive copolymers based on oligoethyleneglycol methacrylates
Polym. Prepr. **2007**, *48(2)*, 161 – 162.

▪ C. R. Becer, R. Hoogenboom, S. Hahn, U. S. Schubert
Tuning the cloud point of methacrylic acid and oligoethyleneglycol methacrylate based random copolymers
Polym. Prepr. **2008**, *49(1)*, 1095 – 1096.

▪ R. Hoogenboom, C. R. Becer, T. M. Eggenhuisen, U. S. Schubert
High-throughput optimization of nitroxide mediated radical polymerizations as basis for the synthesis of temperature-responsive copolymers
Polym. Prepr. **2008**, *49(2)*, 145 – 146.

- C. R. Becer, R. M. Paulus, R. Hoogenboom, U. S. Schubert
  Cationic ring opening polymerization of 2-ethyl-2-oxazoline with acetyl halide initiators
  Polym. Prepr. **2008**, *49(2)*, 912 – 913.

- C. R. Becer, R. M. Paulus, S. Hoeppener, R. Hoogenboom, C.-A. Fustin, J.-F. Gohy, U. S. Schubert
  A dual initiator for the synthesis of poly[(2-ethyl-2-oxazoline)-*b*-(styrene)] copolymers via combination of controlled/living polymerization techniques
  Polym. Prepr. **2008**, *49(2)*, 94 – 95.

- C. R. Becer, D. Pilz, K. Babiuch, J. Keubel, T. Jaehnert, M. Gottschaldt, U. S. Schubert
  Grafting thio glucoside onto styrene and pentafluorostyrene containing polymers prepared via nitroxide mediated polymerization
  Polym. Prepr. **2008**, *49(2)*, 141 – 142.

- C. R. Becer, A. Baumgaertel, M. Gottschaldt, U. S. Schubert
  MALDI-TOF MS/MS measurements of PMMA
  Polym. Prepr. **2008**, *49(2)*, 742 – 743.

- C. R. Becer, K. Babiuch, M. Gottschaldt, U. S. Schubert
  Synthesis of well-defined fluorinated glycopolymers
  Polym. Prepr. **2009**, submitted.

- S. Hornig, T. Heinze, C. R. Becer, U. S. Schubert
  Nanoprecipitation: An efficient technique for the preparation of versatile polymeric nanoparticles
  Polym. Prepr. **2009**, submitted.

- U. S. Schubert, S. Hornig, C. R. Becer, K. Babiuch, D. Pilz, T. Heinze, M. Gottschaldt
  Nanoparticular pentafluorostyrene copolymers
  Polym. Prepr. **2009**, submitted.

In the final pages of this thesis, I would like to acknowledge many people who helped me cherish the 4 years with good memories both in Eindhoven, Netherlands and in Jena, Germany.

First of all, I would like to thank my promoter Prof. Schubert for giving me the opportunity to work in his group with the fantastic robots, which was one of my dreams. It was a great pleasure to work in his fully equipped labs with smart co-workers around. I would like to thank you Prof. Schubert for your full support not only in Eindhoven but also in Jena. You've created the best environment for collaborations within and outside the group, which made my vision broader. Besides, I am grateful that you took care of not only me but also Ayse with great responsibility in Jena.

I would like to thank Prof. Sawamoto and Prof. Gohy for reviewing my thesis in a short period of time. Special thanks go to Dr. Richard Hoogenboom for his constructive comments during the writing period. Good luck to you in the future with your career! Besides, I am honored to have Prof. Lemstra, Prof. Küsefoğlu and Dr. Schneider in the committee. I am grateful to Prof. van Herk for accepting to be the last minute chairman.

Emma, you've always been amazing and so energetic. You've helped and supported us since the beginning. I always knew that somebody was taking care of us at the back stage. You've solved all the problems in time and took care of all SMN members.

I had the first evening outs in Eindhoven with Frank, Elisabeth and Nico. Thanks for the drinks and chatting.

I've shared the office in Eindhoven with Emine and Veronica which was mostly stressful since they were both working on their thesis in the meantime. Thanks to Martin and Renzo for helping out on the use of robots and patiently answering all my questions. It was always a pleasure to work in projects with Hanneke. Thanks for being so friendly and helpful. Caroline and Antje did not stay long after I started in SMN but thanks to Caroline for measuring AAS for my samples and Antje for ordering the chemicals and both for the nice conversations in the group. Also special thanks to Antje for showing us the best Dutch Cows and the nursery :) We've spent some nice time with Chris in front of the faculty for chatting(!) and also in the bar for table tennis or pool. Christoph, the sporty guy or candy-powered guy, likes to lift me up whenever he catches me on the corridor :) He is strong! Manuela throws a big laugh at the background as usual. I had a French guy, David, as a fume hood neighbor for some time; and it was fun and efficient to work there. He was occasionally *h*eating the polymers up. Ece became our neighbor in Vestide for the last couple of months. We had a lot of fun together with Ece and Boran; thanks for being there. Baris is a great guy, always taking care of his friends more than he does for himself. Thanks again for all your help, Turkish night organizations, laughs! I'll have some Burdur tips for you :)

I had my first lunch in Eindhoven with Daan in great expectations from the Dutch cuisine. I could have only a soup then, but Daan made us happy with the BBQ parties in the following

years. Thanks to Stephanie for measuring AFM of my samples and for her help in writing the polymer brushes paper. I will remember Claudia and Christina as the giggling girls on the corridor :) And Carlos as the most honest and open person. I wish we had more time together to work on joint projects. But I am very happy for you both and wish you good luck in Australia! Tina was talking non-stop, which was nice with beer:) Thanks for the nice conversations. I would also like to thank Jolke-my RPK mate, Hans, Tamara, Rebeca, Andreas Winter, Jürgen for providing a nice atmosphere in the group. Thanks to Beatrice for carrying our posts from Eindhoven to Jena. I would like to thank to Tamara E. and Sabine for their nice work on the responsive polymer libraries.

We've hosted Andrew Groth in our group during summer 2007 and we've learned with Renzo lots of Australian jokes, such as the map of Tazzy and the right meaning of N-M-R. Andrew had the most beautiful kids and family…

Then, on a grey, cloudy midnight, we moved to Jena with a minivan loaded with a robot, inkjet printer, a UV-vis spectrometer and our personal stuff on September 14th, 2007. That was the start of the second half.

Michael Gottschaldt exhibited an over human effort and carried our extra heavy luggage two floors up in a few minutes. Thanks for helping out for official things in the beginning. Thanks for the dinners, BBQs in your house. I enjoyed spending time with Jana and your wonderful children. Thanks for the Japan trip, moving sushi bar, Kyoto sky walk, Osaka tower and always friendly conversations. Anja Teige took care of our official things in Jena. Thanks for all your help and organization in the IOMC. It was nice to work with you, too.

I learned how to use the robot in the Netherlands and how to behave like a robot in *East* Germany. Big thanks to my driving teacher!!!

It was a great pleasure to work with Kenta Kokado. He was a hard working, social, and the funniest Japanese guy I've ever met. He was a part of our nice summer parties in Jena. Thanks for guiding me in Kyoto, Osaka and Nara.

I've met regularly with Laszlo and Bernard at the DPI meetings and special Jena events. Thanks for introducing products of Recticel to us.

In the last year of my study, I had a chance to work in Japan for a month. I would like to thank Michael, Prof. Schubert, Prof. Kakuchi and Prof. Shigenobu for the opportunity. Besides, it was a great experience and pleasure to give a lecture in Prof. Chujo's group.

We had a continuous collaboration with Innovent, namely Dr. Schnabelrauch, Dr. Wyrwa, Dr. Weissler. Thanks for all the tests you've performed on our glycopolymers and discussions on the results.

I would like to acknowledge Prof. Yağcı (Yusuf hocam) for mentoring since the beginning and sharing his great experience with me in the conferences. Thanks for showing me the best routes in this world. I wish to work in your labs one day.

I would like to thank Prof. Haddleton who has accepted me to work in his group as a post-doc and applied for the Marie Curie fellowship. This gave me the opportunity to focus better on writing my thesis and publishing more papers.

I've met with the other dimensions of safety regulations and working in a chemistry building by the help of Frau Stockmann. I would like to thank Jürgen Nowotny, Frau Arnold, Frau Bader and Frau Kuse for their help and support in Jena.

Uwe was always funny, besides we played football every Friday evening. I would also like to thank Martin, Katrin, Andreas, Justyna, Anne, Anna, Georgy, Igor, Erik for being kind and friendly. The smiley face of Andy always made me happy. Our beach volleyball evenings were a nice entertainment in Jena. Thanks to Ayse to convince the CineStar to show movies in their original language!

I was so happy to meet with Joe, Amy, Liam, Sebastian and Chicken. Thanks for the delicious food and nice conversations! Ayse and I will miss you! Keep in touch and we'll meet again one place or the other.

I thank to Nico Adams for the nice conversations during the DPI-HTE cluster meetings and to Tobias for throwing his cells on our polymers or the other way around. Luckily they did not die!

I would like to thank Joachim Kübel and Thomas Jaehnert for the synthesis of fluorinated polymers; and Krzysztof and David Pilz for their work on the synthesis of glycopolymers.

The summary of this thesis was translated by Meta. I would like to thank her not only for the summary but also for sharing Freddy with us from time to time! I wish you and Cees all the best in Jena :)

I am grateful to Kempi and Hanneke for being my paranimf for the defense. I would like to thank Christine and Kempi for sharing their lab with me and having productive scientific discussions. I want to thank to Torsten for his help in buying our *ferrari* and also for the private dance :) "Highly party motivated" Antje deserves a "BIG thank you" for spreading all her positive energy around. Thanks to Uli Mansfeld for showing how to scare a girl even in Clausthal. BAnja knows all the roads in Germany. Thanks for navigating! It was nice to play backgammon with you Thomas, thanks! I thank to Jena for being so warm and green, whereas Eindhoven for being so lively, rainy, cloudy, bikely…we wish to come back one day.

I would like to thank Stephanie Hornig for preparing nice nanoparticles and for giving nice tips about Jena. Enjoy Berkeley!

We've doubled the Turkish population in Jena by importing Aydın and Esra. Thanks for your warm friendship, conversations, dinners and nice times we shared together. I would like to thank Renzo for his stable friendship since the beginning. It was a nice summer holiday with you in Turkey and also we spent very enjoyable days in Jena together. We've jumped up on the Jena tower with Alexandra Tsotsalas (Ali) and had very nice time together. Thanks for adding fun to our lives.

Jutta and Mike have a special place for us. It was an unusual relationship we had. We came to Eindhoven and they moved to Den Bosch, now they are coming closer to Jena and we're moving to UK. We are so happy that you've shared your families, childhood memories, homes, Christmas holidays with us. It was an honor for me to be your witness Mike. Thanks for all your advice and brotherly friendship. I wish you both the best of luck in your new location, and a healthy, happy, blonde boy! We will visit often, and expect the same from you ☺

One of the best things that happened in Eindhoven was to meet Arno, Agnieszka, Prashant and Sharavati. I am so happy to have known you! You've opened your home for us whenever we visited Eindhoven. It was always a pleasure for us to spent time with you guys. Thanks for making us a part of your saddest and happiest days! This is no good bye to you because we will keep sharing memories in the future, in India, Poland, Turkey, UK and all.

Tolga, Havva, Zehra ve Talha Atay'a her Amerika ziyaretimizde bizi evlerine konuk ettikleri için çok teşekkür ederim. Bizi Eindhoven'da ziyaret eden Ilay (kafam şişti), Sirin (sıkı tutun gidiyoruz), Burçak (kutlamaya ilk sen geldin), Pelin ve Erhan'a (piknik çok güzeldi) teşekkürler. En büyük teşekkür bizi Eindhoven'da ve Jena'da yalnız bırakmayan ailelerimize. Bayram seyran yılbaşı, her fırsatta bize koşan, gelemeyenleri webcam aracılığıyla bizlerle yakınlaştıran, özlediğimiz peynirleri, börekleri, baklavaları bizlere üşenmeden taşıyan, gezmelerimize vesile olan ailelerimize… Sizin desteğiniz, moral vermeniz sayesinde 4 yılın nasıl geçtiğini anlamaya fırsatımız olmadı. Onümüzdeki 2 yıl ingiltere yılı ilan edildi. Hepinizi bekliyoruz. Ablacım sana ayrıca çok teşekkür ederim. Sen ve Ayda-Irfan-Zeynep Ergun üçlüsü en sadık misafirlerimiz oldunuz. Hangi şehirde yaşadığımıza bakmadan hep yanımızda oldunuz.

Annem ve ablam tezimi yazarken süpriz yapıp bizi ziyaret ettiğiniz icin çok teşekkür ederim. Bizi çok mutlu ettiniz ve tezimi çok daha kolay yazdım sayenizde. Hale annemden ve Metin babamdan güzel kızları Ayşe'yi uzaklaştırdığım için çok özür diler, tüm destekleri ve duaları için teşekkür ederim. Betül ablama da bizi ziyaret ettiği ve eğlendirdiği için minnettarız. Mete abiyi de inşallah Ingiltere'de görmeyi umuyoruz.

Baba bak bunu ilk defa burada açıklıyorum:) cep telefonuma yolladığın mesajlarla beni motive ettiğin ve bekleyen süprizler hakkında bilgilendirdiğin için teşekkür ederim.

Yukarıda saydığım tüm anıları, iyi ve kötü zamanları birlikte geçirdiğim, 1999 yılından beri benim yanımda olan, bu 4 yılımızın bu kadar mutlu ve güzel geçmesini sağlayan en önemli kişiye, Ayşem'e çok teşekkür ederim. Senin desteğin, verdiğin moral sayesinde bu kadar zevkle doktoramı tamamladım. Eşim olduğun için ve benimle bu yola çıktığın için çok teşekkür ederim. Ilk sayfada başladığım gibi, bu tez Ayşem'e hediyem.

Thanks to all of you.
Take care!

Remzi :)